MYCOSPHERE 16(1): 1861–2001 (2025) www.mycosphere.org ISSN 2077 7019
Doi 10.5943/mycosphere/16/1/11

ARTICLE

Microfungi associated with plant diseases on horticultural vegetation in southwestern China

Yang CL[1,2#], Li XY[1,2#], Xiang SS[1,2#], Xu XL[3*], Zeng Q[1,2], Sun QR[1,2], Liu JK[4], Maharachchikumbura SSN[4], Lv YC[1,2], Wang FH[1,2], Ji-Zuo JL[1,2], A-Niu XY[1,2], Liu YG[1,2*]

[1] *College of Forestry, Sichuan Agricultural University, Chengdu 611130, P.R. China*
[2] *Key Laboratory of National Forestry & Grassland Administration on Forest Resources Conservation and Ecological Safety in the Upper Reaches of the Yangtze River, College of Forestry, Sichuan Agricultural University, Chengdu 611130, P.R. China*
[3] *Forestry Research Institute, Chengdu Academy of Agricultural and Forestry Sciences, Chengdu 611130, P.R. China*
[4] *School of Life Science and Technology, University of Electronic Science and Technology of China, Chengdu 611731, P.R. China*

Citation – Yang CL, Li XY, Xiang SS, Xu XL, Zeng Q, Sun QR, Liu JK, Maharachchikumbura SSN, Lv YC, Wang FH, Ji-Zuo JL, A-Niu XY, Liu YG 2025 – Microfungi associated with plant diseases on horticultural vegetation in southwestern China. Mycosphere 16(1), 1861–2001, Doi 10.5943/mycosphere/16/1/11

Abstract

Horticultural plants are essential natural resources upon which human survival relies, offering diverse means of sustenance, including food, medicine, chemical raw materials, construction materials, landscaping, cultural significance, and tourism. In recent years, the widespread and increasingly harmful fungal diseases in horticultural plants have prompted this study to investigate the diversity and composition of their pathogenic fungi. Over the past six years (2019 to 2024), diseased tissues from horticultural plants in southwestern China were collected and assessed using measurements based on both morphological characteristics and phylogenetic analyses involving combined multi-locus sequence data. A total of 38 fungi were classified into two phyla, *Ascomycota* and *Basidiomycota*, and four classes: *Sordariomycetes* (*Amphisphaeriales*, *Diaporthales*, *Glomerellales*, *Hypocreales*, and *Phyllachorales*), *Dothideomycetes* (*Botryosphaeriales*, *Capnodiales*, *Cladosporiales*, *Mycosphaerellales*, *Myriangiales*, and *Pleosporales*), *Exobasidiomycetes* (*Exobasidiales*), and *Leotiomycetes* (*Helotiales*), totaling 13 orders. In this paper, we propose one new genus in *Pleosporales* (*Paramassarina*) and 13 new species, namely *Colletotrichum cymbidiumdis*, *Conidiocarpus cinnamomeus*, *Cladosporium viciae*, *Cytospora sichuanense*, *Diaporthe erythrinae*, *Exosporium rhapidis*, *Fumagospora cinnamomi*, *Neocosmospora phalaenopsidis*, *Neoscytalidium hylocereum-undulatum*, *Paramassarina euonymicola*, *Paraphoma populi*, *Phaeosphaeria phormii*, and *Pseudocercospora populina*.

Additionally, we report 19 species as new host or geographical records, 17 of which represent new host records, including *Botryosphaeria dothidea*, *Cladosporium guizhouense*, *Colletotrichum cymbidiicola*, *Col. guangyuanense*, *Col. plurivorum*, *Cytospora predappioensis*, *Diaporthe eres*, *Di. middletonii*, *Di. sojae*, *Drepanopeziza brunnea*, *Elsinoe araliae*, *Graphiola phoenicis*, *Lasiodiplodia pseudotheobromae*, *Neopestalotiopsis concentrica*, *Neop. dimorphospora*, *Neovaginatispora fuckelii*, and *Paraconiothyrium brasiliense*, and two species are new host and geographical record, namely *Pestalotiopsis oryzae* and *Phyllosticta citribrasiliensis*. Morphological illustrations, phenotypic descriptions, and phylograms are provided to elucidate the placement of the new collections in this study. These fungi, originating from infected tissues, are linked to

Submitted: 29 August 2024; **Accepted:** 17 May 2025; **Published:** 03 June 2025
[*]**Corresponding Author:** Xiu-Lan Xu – e-mail – xuxiulanxxl@126.com; Ying-Gao Liu – e-mail – lyg927@263.net
[#]Authors have equally contributed to this study
Accepted by: Kandawatte Wedaralalage Thilini Chethana

diseases either through observed symptoms or previous studies suggesting their potential pathogenicity. Further research is needed to confirm the pathogenicity of these species using Koch's postulates.

Keywords – 13 new taxa – *Ascomycota* – *Basidiomycota* – Horticultural fungi – *Blumeria* – *Botryosphaeria* – *Cladosporium* – *Colletotrichum* – *Conidiocarpus* – *Cytospora* – *Diaporthe* – *Drepanopeziza* – *Elsinoe* – *Exosporium* – *Fumagospora* – *Graphiola* – *Lasiodiplodia* – *Neocosmospora* – *Neofusicoccum* – *Neopestalotiopsis* – *Neoscytalidium* – *Neovaginatispora* – *Paraconiothyrium* – *Paramassarina* – *Paraphoma* – *Pestalotiopsis* – *Phaeosphaeria* – *Phyllachora* – *Phyllosticta* – *Pseudocercospora*

INTRODUCTION

Horticultural plants, including fruit trees, vegetables, ornamental vegetation, aromatic plants, and medicinal species, play a pivotal role to the development and prosperity of human society. These crucial economic assets have a global impact and are intimately intertwined with human existence. The symbiotic bond between horticultural plants and humans spans 10,000 years, signifying a pivotal shift from foraging to agriculture. Through cultivation, horticultural plants have served as indispensable resources for nourishment, beverages, medicine, fibers, climate regulation, shelter, and environmental enhancement (Janick & Goldman 2003, Martin & Stabler 2004, Chen et al. 2019, Lu et al. 2020, Zhu & Chen 2020). These plants have seamlessly integrated themselves into the tapestry of human civilization, leaving an indelible mark on our collective history. Horticultural plants exhibit remarkable diversity and are distributed across a wide range of taxonomic plant groups. This includes an extensive array of flowering plants, as well as a select few early-divergent land plants (Wang et al. 2017, Chen et al. 2019). Historically, horticultural plant research has primarily centered around plant applications, germplasm resources, and genetic breeding; however, the exploration of diseases and pests in this field has received comparatively less attention (Wang et al. 2016).

At the taxonomic level, horticultural plants harbor a wide range of abundant and diverse microbial resources. Among them, a significant number are pathogenic fungi, encompassing various groups such as ascomycetes, basidiomycetes, and oomycetes, especially for species of *Ascomycota* (Strange & Scott 2005, de Silva et al. 2021, Ristaino et al. 2021, Han et al. 2023, Peng et al. 2023). Fungal diseases can exert a spectrum of effects, ranging from mild symptoms to catastrophic events that result in the extensive devastation of horticultural plants cultivated for diverse purposes (Fu et al. 2019, Fan et al. 2020, Sun et al. 2023). Considerable attention is directed towards the expeditious and accurate identification of the causal organism, precise estimation of disease severity, and assessment of its impact on yield, landscape and ecological benefits (Churchill 2011, Martinelli et al. 2015). Furthermore, there is a keen interest in deciphering the virulence mechanisms, reducing pathogen inoculum, inhibiting virulence factors, and fostering genetic diversity within plant populations (Li et al. 2011a, Gullino et al. 2015, Zhan et al. 2015). Researching species definition and identification criteria of pathogenic fungi in horticultural plants remains crucial, and it serves as a fundamental basis for accurately identifying pathogenic fungi (Taylor et al. 2000, Jeewon & Hyde 2016, Aime et al. 2021). The spatiotemporal heterogeneity in the distribution of horticultural plants also indicates the potential diversity of pathogenic fungi, with the number of pathogenic species likely underestimated (Hyde et al. 2020a).

The southwestern region of China is characterized by a rich and diverse array of horticultural plants. These plants greatly contribute to the regional economy, ecology, and culture. In a study by Li et al. (2020), a total of 166 botryosphaeriaceous isolates were collected from *Eucalyptus* plantations across six regions in Yunnan Province, and 11 species were identified using a combination of morphological characteristics and DNA sequences. Fu et al. (2021) identified four fungal diseases affecting the leaves of *Paris polyphylla* var. *chinensis*, an important Chinese medicinal herb. Sun et al. (2023) also described six pathogenic pestalotoid species associated with

medicinal plants in Guizhou Province. The occurrence of fungal diseases in horticultural plants within this area is consistently documented through a wide range of reporting channels (He & Zhao 2022, Li et al. 2022a, 2023a, Xu et al. 2022, Zeng et al. 2022, Peng et al. 2023). Fungal diseases affecting horticultural plants exhibit a wide range of diversity, with fungi capable of infecting various plant parts, resulting in common diseases such as canker, shoot blight, branch blight, powdery mildew, anthracnose, leaf blight, and others (Fig. 1).

Figure 1 – Representative symptoms associated with fungi on horticultural plants in the field. a Blight of *Ficus elastica*. b Powdery mildew of *Poa annua*. c Canker of *Acer palmatum*. d Canker of *Orah mandarin*. e Branch blight of *Erythrina crista-galli*. f Twig blight of *Bougainvillea* sp. g Branch blight of *Salix* sp. h scab of *Fatsia japonica*. i Leaf blight of *Phoenix sylvestris*. j Leaf blight of *Polygonatum* sp. k Leaf spots of *Populus* × *beijingensis*. l Anthracnose of *Camellia sinensis*. m Leaf dry-rot of *Phalaenopsis aphrodite*. n Black spots on the pod of *Vicia faba*.

In this study, our team conducted a systematic survey of prevalent horticultural plants within anthropogenic environments and collected specimens exhibiting signs of disease. Through a meticulous analysis of morphological characteristics and multigene phylogeny, the following

conclusive findings were obtained: We herein introduce 38 fungal species from 26 genera, 19 families, 13 orders, and four classes within the phyla *Ascomycota* and *Basidiomycota*. This work includes one new genus and nine new species in *Dothideomycetes*, as well as four new species in *Sordariomycetes*. Detailed descriptions, complemented by illustrations of macro- and micro-morphological features alongside phylogenetic trees, have been thoroughly provided to authenticate the classification of both known and newly discovered fungal species.

MATERIALS AND METHODS

Isolates and Morphology

Sample collection, morphological study and isolation

An investigation was conducted in different places of Sichuan Province from Dec. 2019 to May 2024, including the Ngawa Tibetan & Qiang Autonomous Prefecture (Jiuzhaigou County), Chengdu City (Wenjiang District, Xindu District, Qionglai City, Chongzhou City), Leshan City (Mabian Yi Autonomous County), Liangshan Yi Autonomous Prefecture (Leibo County), Yibin City (Junlian County), Mianyang City (Zitong County), Neijiang City (Zizhong County), and Ya'an City (Tianquan County). Potential pathogenic fungi were collected from infected tissues on variously horticultural plants with 29 species from 26 host genera. Fungal isolates were established by removing a mucoid spore mass from conidiomata and/or ascomata, diffusing the suspension on the surface of potato dextrose agar (PDA) media, and incubating at 25℃ for 10 to 24 h. A single germinating conidium/ascospore was transferred to fresh PDA plates. Specimens are deposited in the Herbarium of the Sichuan Agricultural University, Sichuan, China (SICAU), and axenic cultures are maintained in the Culture Collection of the Sichuan Agricultural University (SICAUCC), Sichuan, China.

Description of the asexual and sexual morphs are based on host materials or cultural characteristics. The macro-morphological photographs were captured by a dissecting microscope NVT-GG (Shanghai Advanced Photoelectric Technology Co. Ltd, China) and photographed by a VS-800C camera (Shenzhen Weishen Times Technology Co. Ltd, China), including stromata, ostioles, conidiomata, sporodochia, and other structures. The micro-morphological characteristics were photographed using an Olympus BX43 compound microscope fitting with an Olympus DP22 digital camera (Olympus (China) Co. Ltd, China), such as asci, ascospores, paraphyses, conidia, conidiophores, conidiogenous cells, and others. Measurements were made using Tarosoft® Image Frame Work v.0.9.7 (Tarosoft (R), Nontha Buri, Thailand). Lactophenol cotton blue reagent was used to affirm the number of septa or other transparent structures, and the gelatinous appendage was observed in Black Indian ink. Faces of Fungi (FoF) numbers were recorded following the protocol outlined by Jayasiri et al. (2015), while MycoBank (MB) numbers were obtained as in MycoBank (Crous et al. 2004a). The establishment of new taxa adhered rigorously to the guidelines delineated by Chethana et al. (2021), Jayawardena et al. (2021a), Lücking et al. (2021), Maharachchikumbura et al. (2021), and Pem et al. (2021).

DNA Extraction, PCR Amplification, and Sequencing

Genomic DNA was extracted using the Fungi Genomic DNA Kit (Tiangen, China) following the manufacturer's instructions, from fungal mycelia growing on PDA, pure spore mass or fruiting bodies. Eleven loci were amplified with the respective forward and reverse primers (Table 1). PCR was conducted in 25 μL reaction volumes consisting of 22 μL Master Mix (Beijing TsingKe Biotech Co., Ltd., Beijing, China), 1 μL DNA template, 1 μL each primer (10 μM). PCR amplification conditions were conducted as described in Table 1. The PCR products were sequenced in both directions using the primers at TsingKe Biological Technology Co., Ltd. (Chengdu, China). Forward and reverse sequences were assembled to obtain a consensus sequence with BioEdit v. 7.0.5.3 (Hall 1999). Sequences generated in this paper were deposited in GenBank.

Table 1 PCR amplification procedures used in this study.

Gene	Primer	Primer sequence (5'-3')	PCR procedure	Reference
ITS	ITS1	TCCGTAGGTGAACCTGCGG	An initial denaturation step at 94°C for 3 min, followed by 35 cycles of 94°C for 30 s, 55°C for 50 s, and 72°C for 1 min and a final elongation step at 72°C for 10 min	White et al. (1990)
	ITS5	GGAAGTAAAAGTCGTAACAAGG		
	ITS4	TCCTCCGCTTATTGATATGC		
LSU	LR0R	GTACCCGCTGAACTTAAGC	94°C for 3 min, 35 cycles of 94°C for 30 s, 55°C for 50 s, and 72°C for 1 min, and 72°C for 10 min	Vilgalys & Hester (1990)
	LR5	ATCCTGAGGGAAACTTC		
	LR7	TACTACCACCAAGATCT		
SSU	NS1	GTAGTCATATGCTTGTCTC	94°C for 3 min, 35 cycles of 94°C for 30 s, 55°C for 50 s, and 72°C for 1 min, and 72°C for 10 min	White et al. (1990)
	NS4	CTTCCGTCAATTCCTTTAAG		
*tef*1-α	EF1-728F	CATCGAGAAGTTCGAGAAGG	94°C for 3 min, 35 cycles of 94°C for 30 s, 55°C for 50 s, and 72°C for 1 min, and 72°C for 10 min	O'Donnell et al. (1998), Carbone & Kohn (1999), Rehner & Buckley (2005)
	EF1-983F	GCYCCYGGHCAYCGTGAYTTYAT		
	EF1-986R	TACTTGAAGGAACCCTTACC		
	EF1-2218R	ATGACACCRACRGCRACRGTYTG		
	EF-2	GGAAGTACCAGTGATCATGTT		
act	ACT-512F	ATGTGCAAGGCCGGTTTCGC	94°C for 3 min, 35 cycles of 94°C for 30 s, 51°C for 50 s, and 72°C for 1 min, and 72°C for 10 min	Carbone & Kohn (1999)
	ACT-783R	TACGAGTCCTTCTGGCCCAT		
cal	CAL228F	GAGTTCAAGGAGGCCTTCTCCC	95°C for 4 min, 35 cycles of 94°C for 30 s, 60°C for 50 s, and 72°C for 1 min, and 72°C for 10 min	Carbone & Kohn (1999)
	CAL737R	CATCTTTCTGGCCATCATGG		
chs-1	CHS-79F	TGGGGCAAGGATGCTTGGAAGAAG	95°C for 4 min, 35 cycles of 95°C for 30 s, 58°C for 30 s, and 72°C for 45 s, and 72°C for 7 min	Carbone & Kohn (1999)
	CHS-354R	TGGAAGAACCATCTGTGAGAGTTG		

Table 1 Continued.

Gene	Primer	Primer sequence (5'-3')	PCR procedure	Reference
gapdh	GDF1	GCCGTCAACGACCCCTTCATTGA	95°C for 4 min, 35 cycles of 95°C for 30 s, 60°C for 30 s, and 72°C for 45 s, and 72°C for 7 min	Templeton et al. (1992)
	GDR1	GGGTGGAGTCGTACTTGAGCATGT		
*rpb*2	fRPB2-5f	GAYGAYMGWGATCAYTTYGG	95°C for 5 min, 35 cycles of 95°C for 1 min, 52°C for 2 min, and 72°C for 90 s, and 72°C for 10 min (for fRPB2-5f/2-7cR) 94°C for 90 s, 40 cycles of 94°C for 30 s, 55°C for 90 s, and 68°C for 2 min, and 68°C for 5 min (for RPB2-7cF/11aR/5F2)	Liu et al. (1999), Reeb et al. (2004), O'Donnell et al. (2007)
	fRPB2-7cR	CCCATRGCTTGYTTRCCCAT		
	RPB2-7cF	ATGGGYAARCAAGCYATGGG		
	RPB2-11aR	GCRTGGATCTTRTCRTCSACC		
	RPB2-5F2	GGGGWGAYCAGAAGAAGGC		
*tub*2	T1	AACATGCGTGAGATTGTAAGT	94°C for 3 min, 35 cycles of 94°C for 30 s, 51°C for 50 s, and 72°C for 1 min, and 72°C for 10 min	Glass & Donaldson (1995), O'Donnell & Cigelnik (1997), Stukenbrock et al. (2012)
	T2	TAGTGACCCTTGGCCCAGTTG		
	β-Sandy-R	GCRCGNGGVACRTACTTGTT		
	Bt2a	GGTAACCAAATCGGTGCTGCTTTC		
	Bt2b	ACCCTCAGTGTAGTGACCCTTGGC		

Abbreviations: ITS: the nuclear internal transcribed spacers, LSU: the nuclear large subunit ribosomal RNA, SSU: the nuclear ribosomal small subunit rRNA, *tef*1-α: the translation elongation factor 1-alpha, *act*: the actin, *cal*: the calmodulin, *chs*-1: the chitin synthase 1, *gapdh*: the glyceraldehyde-3-phosphate dehydrogenase, *his*3: the histone H3, *rpb*2: the second largest subunit of RNA polymerase II, *tub*2: the beta-tubulin.

Sequence alignment and phylogenetic analyses

Newly generated sequences in this study were blasted against the NCBI GenBank nucleotide database to determine the closest relatives for a taxonomic position of the studied isolates. All representative sequences used in this study were collected from GenBank and the latest publications, and alignments of different gene sequences were initially performed using MAFFT v. 7.490 online version (Katoh et al. 2019) and manually adjusted with BioEdit v. 7.0.5.3 (Hall 1999). The congruence of the overall topology was confirmed after comparing single gene sequence data, and the consensus sequences were concatenated by Mesquite v. 3.61 (build 927) (http://www.mesquiteproject.org) (Maddison & Maddison 2019) with default parameters. The evolutionary model was determined independently for each gene with MrModeltest 2.2 under the Akaike Information Criterion (AIC) (Nylander 2004). The dataset was analyzed separately in different genera or families, using maximum likelihood (ML) and Bayesian inference (BI).

Maximum likelihood analysis was performed with a randomized accelerated maximum likelihood model in RAxML v. 8.2.12 on XSEDE platform on CIPRES Science Gateway Portal (Stamatakis 2014), and relative support of internal nodes was affirmed by a rapid bootstrap with 1,000 replications. Bayesian analysis used the MrBayes v. 3.2.7a provided on CIPRES Science Gateway Portal (Stamatakis 2014) to determine posterior probabilities. The program was automatically terminated when the average standard deviation of split frequencies reached below 0.01. The phylograms were visualized in FigTree v. 1.4.4 (http://tree.bio.ed.ac.uk/software/figtree/) and edited with Adobe Illustrator CS6 (Adobe Systems Inc., United States).

The closest phylogenetic groups were identified using the Genealogical Concordance Phylogenetic Species Recognition (GCPSR) model, achieved through a pairwise homoplasy index (PHI) test (Taylor et al. 2000). The level of recombination among phylogenetically closely related species was analyzed using SplitsTree v. 4.14.6, based on multi-sequences data (Huson & Bryant 2006). The dataset exhibits significant recombination when the pairwise homoplasy index is below the 0.05 threshold ($\Phi_w < 0.05$). A split graph was employed to visualize the relationships among closely related taxa.

RESULTS

The contents in this paper to introduce new collections follow the guidelines of Chethana et al. (2021), Jayawardena et al. (2021a), Lücking et al. (2021), Maharachchikumbura et al. (2021), and Pem et al. (2021). The following paragraphs provide an introduction of the new collections, categorized alphabetically. These collections encompass a remarkable diversity, comprising 38 species in 26 genera spanning 19 families, 13 orders, and four classes within the kingdom of *Fungi*.

Phylum *Ascomycota* Caval. -Sm.

Class *Dothideomycetes* O.E. Erikss. & Winka

Botryosphaeriales C.L. Schoch, Crous & Shoemaker

Notes – The *Botryosphaeriales* order currently consists six families, including about 10 genera are classified under *Botryosphaeriales* genera *incertae sedis*, and it accommodates nearly 1,450 recorded species (Liu et al. 2012, Wijayawardene et al. 2022, Li et al. 2023a). *Botryosphaeriales* is prevalent across diverse habitats, functioning as endophytes, saprobes, and pathogens. The evolutionary emergence of this order dates back to approximately 109 million years ago, during the nascent stages of the Cretaceous period (Rathnayaka et al. 2023).

Botryosphaeriaceae Theiss. & Syd.

Notes – *Botryosphaeriaceae* was formally established by Theissen & Sydow (1918), designating *Botryosphaeria* as its prototype genus. Subsequent taxonomic evaluations by Liu et al. (2012) acknowledged the presence of 29 genera within this family. Phillips et al. (2013) endorsed 17 genera and 110 species based on cultured specimens. However, the most recent assessment by

Maharachchikumbura et al. (2022) has expanded the record to encompass 22 genera and an approximate tally of 2,140 species. *Botryosphaeriaceae* species exhibit a broad prevalence across monocotyledonous, dicotyledonous, and gymnospermous hosts, alongside their presence on lichen thalli (Mohali et al. 2007, Batista et al. 2021). These species often coexist with phytopathogenic fungi, eliciting diverse symptoms like shoot blights, stem cankers, fruit rots, root rots, die-back, and gummosis (Manawasinghe et al. 2016, Zlatković et al. 2016, Jia et al. 2023a). The divergence time of this family is estimated with a stem age of 81.1 Mya (60.9–102.1 Mya) by Rathnayaka et al. (2023).

Botryosphaeria Ces. & De Not.

Notes – *Botryosphaeria* was introduced by Cesati & Notaris (1863) to accommodate *B. dothidea* as the type species. *Botryosphaeria* species have been recorded on a wide range of hosts, and distributed throughout many geographical and climate regions (Denman et al. 2000, Phillips et al. 2013). *Botryosphaeria* species commonly inhabit a multitude of woody plants in roles ranging from endophytes and saprobes to pathogens (Úrbez-Torres et al. 2006, Liu et al. 2012, Phillips et al. 2013, Slippers et al. 2017). Some species within this genus are formidable causal agents, imparting a substantial menace to both agricultural and forest ecosystems (Marsberg et al. 2017, Yukako et al. 2021, Kenfaoui et al. 2022, Liu et al. 2023a). The primary morphological characteristics defining *Botryosphaeria* encompass hyaline to dark ascospores, multiloculate ascomata, and a diverse array of asexual morphs, generally characterized by the absence of a mucoid sheath and apical appendage (Pem et al. 2024). Currently, the Species Fungorum (https://www.speciesfungorum.org, November 2024) enumerates 242 epithets in this genus, with a limited subset having accompanying DNA sequence data available.

1. *Botryosphaeria dothidea* (Moug.) Ces. & De Not., Comm. Soc. crittog. Ital. 1(fasc. 4): 212 (1863) Fig. 2

MycoBank number: MB183247; Facesoffungi number: FoF03512

Associated with canker on stems of *Ficus elastica* Roxb. ex Hornem., symptoms appeared as dry and shriveled on the diseased tissues, and slightly raised lesions accompanied by conidia overflow. Sexual morph: Not observed. Asexual morph: *Coelomycetous*. *Conidiomata* pycnidial, embedded in the epidermis, erumpent at maturity, irregular, brown to dark brown, gathered, with white conidial mass extruding from ostiole, usually multilocular. *Conceptacle* absent. *Conidiomatal wall* consist of multi-layers of pale brown to brown, thick-walled cells of *textura angularis*. *Conidiophores* hyaline, smooth, straight or slightly sinuous, unbranched, and reduced to conidiogenous cells. *Conidiogenous cells* 11–39 × 2–4 μm ($\bar{x}$ = 20.1 × 3.4 μm, n = 30), enteroblastic, monophialidic, terminal, integrated, cylindrical, slightly tapering towards the apex. *Paraphyses* not seen. *Conidia* 21–34 × 5–7 μm ($\bar{x}$ = 26.9 × 6.4 μm, n = 50) hyaline, aseptate, sometimes uniseptate, smooth, rounded at the apex, convex to truncate at the base, guttulate.

Culture characteristics – Germinated conidia formed after 12 h, and the germinating tube grows from both ends of the spore. *Colonies* on potato dextrose agar, initially produced white dense aerial mycelia, reaching 60 mm at 6 days after inoculation, then forming dark grey colonies, which exhibited some brown to dark brown pigments in the medium.

Material examined – China, Sichuan Province, Neijiang City, Zizhong County, Huaxiang Village, 104°49′22.02″E 29°46′22.16″N, 321 m, isol. from stems of *Ficus elastica*, 4 Apr. 2021, C.L. Yang, YCL202104004 (SICAU 23-0121), culture (SICAUCC 23-0113).

GenBank numbers – SICAUCC 23-0113 = ITS: PP736364, LSU: PP732705, *tef*1-α: PP779569, *tub*2: PP782063

Notes – The morphological characteristics of the collection SICAU 23-0121 align perfectly with those of *Botryosphaeria dothidea* (Slippers et al. 2004, Hattori et al. 2021). In the multi-locus phylogenetic analysis, the phylogenetic tree closely conforms to the outcomes of prior studies (Slippers et al. 2004, Chen et al. 2020, Hattori et al. 2021, Zhang et al. 2021), with our strain forming a distinct cluster alongside the ex-epitype of *B. dothidea* (Fig. 3), and their base differences

are not significant (99% for ITS (4/500, 0 gap); 100% for LSU, *tef*1-α, and *tub*2). *Botryosphaeria dothidea* has a broad spectrum of host plants and induces diverse symptoms in various tissues (Marsberg et al. 2017, Hattori et al. 2021).

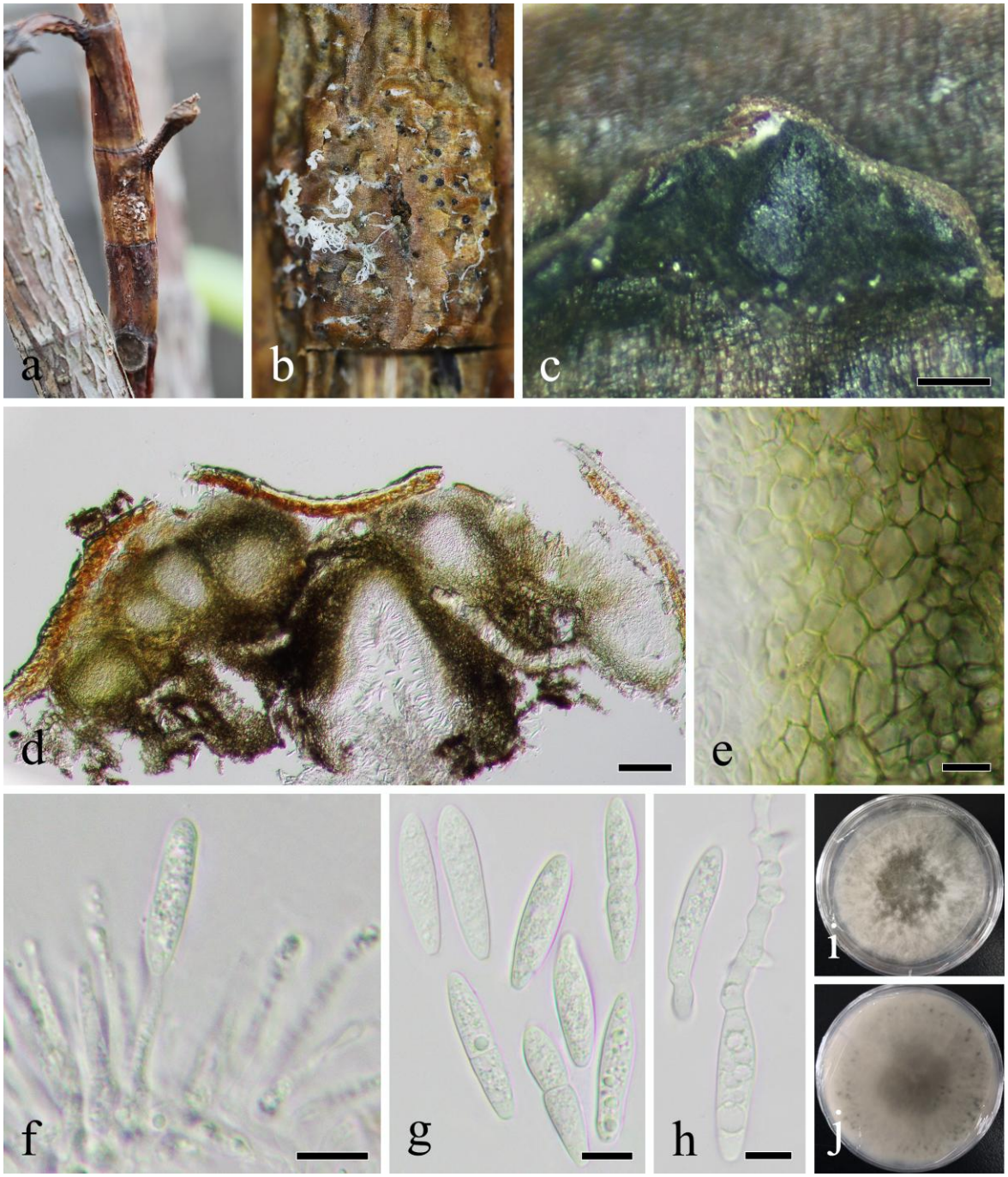

Figure 2 – *Botryosphaeria dothidea* (SICAU 23-0121). a Symptoms on the stem. b Appearance of conidiomata. c, d Cross-section of conidiomata. e Conidiomatal wall. f Conidiogenous cells with developing conidia. g Conidia. h Germinating conidia in sterilized water after 12 h. i Front view of colony on PDA. j Reverse view of colony on PDA. Scale bars: c = 200 μm, d = 100 μm, e–h = 10 μm.

Lasiodiplodia Ellis & Everh.

Notes – *Lasiodiplodia* was introduced by Ellis & Everhart (1896) with *L. theobromae* (= *L. tubericola*) as the type species (Clendenin 1896). Within subtropical and tropical regions, these

fungi, prominent among phytopathogens, are responsible for various symptoms, such as cankers, fruit rots, die-back, and shoot blights on crops or trees (Phillips et al. 2013, Huda-Shakirah et al. 2022, Hattori et al. 2023). This genus is marked by its elliptical or long ellipsoidal conidia with a single septum, varying from light brown to dark brown, often showing longitudinal striations as they mature (Phillips et al. 2013, de Silva et al. 2019). A comprehensive documentation of 90 validated species is present in the Species Fungorum (https://www.speciesfungorum.org, November 2024), showcasing its significant speciosity within the *Botryosphaeriaceae* family.

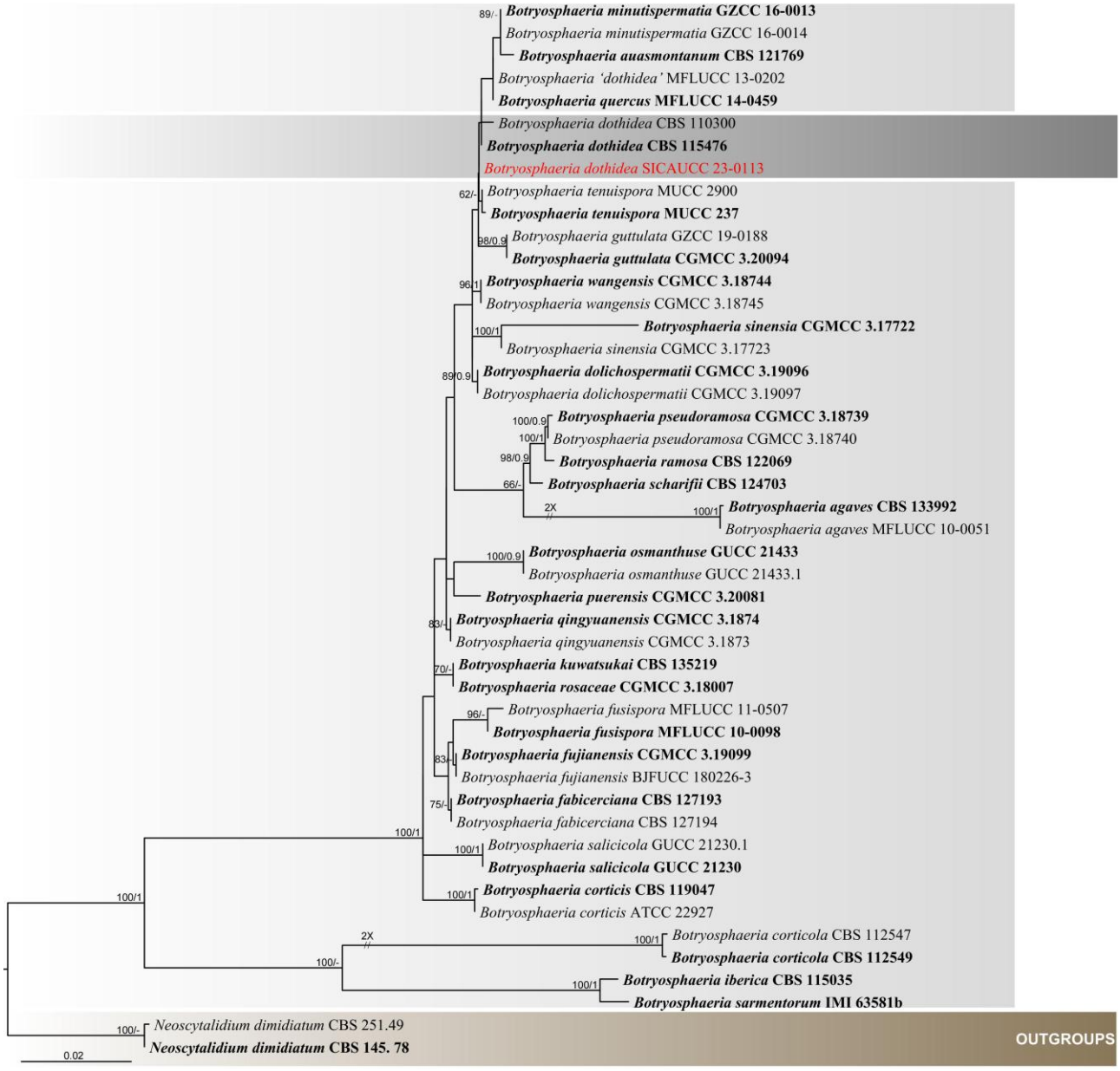

Figure 3 – Phylogram derived from maximum likelihood analyses of a combined dataset comprising ITS, LSU, *tef*1-α, *tub*2, and *rpb*2 sequences, encompassing species within the *Botryosphaeria* genus. The phylogenetic analysis included forty-seven strains and a total of 3,789 characters (ITS: 1–626, LSU: 627–1,826, *tef*1-α: 1,827–2,385, *tub*2: 2,386–2,851, *rpb*2: 2,852–3,789) after alignment. The tree is rooted to *Neoscytalidium dimidiatum* (CBS 145.78 and CBS 251.49). Single-gene analyses were conducted, resulting in similar tree topologies between the ML and BY methods, ensuring consistent comparisons of clade stability. The best-scoring RAxML tree with a final likelihood value of -9,663.238560 is presented. The matrix had 734 distinct alignment

patterns, with 50.68% of undetermined characters or gaps. Estimated base frequencies were as follows: A = 0.227819, C = 0.275213, G = 0.273288, T = 0.223680; substitution rates AC = 1.128370, AG = 1.970560, AT = 1.353334, CG = 1.162070, CT = 4.178932, GT = 1.000000. Bootstrap support values (MLBS) equal or exceeding 60%, and Bayesian posterior probabilities (BYPP) equal or exceeding 0.90 have been indicated above the nodes. The ex-type strains are in bold, and the new isolate is in red. The bar, set at 0.02, represents the estimated number of nucleotide substitution sites per branch.

2. *Lasiodiplodia pseudotheobromae* A.J.L. Phillips, A. Alves & Crous, Fungal Divers. 28: 8 (2008) Fig. 4

MycoBank number: MB510941; Facesoffungi number: FoF00166

Associated with twig blight on stems of *Acer palmatum* Thunb. Sexual morph: Not observed. Asexual morph: *Coelomycetous*. *Conidiomata* 135–230 × 80–150 μm ($\bar{x}$ = 182 × 109 μm, n = 20), pycnidial, immersed, covered with hyphae, brown to black, solitary or gregarious, globose to oblate, uniloculate. *Conidiomatal wall* 18–32 μm width, comprising 5–6 layers of thick-walled, dark brown cells of *textura angularis*, becoming thin-walled and hyaline towards the inner region. *Paraphyses* 1.0–2.5 μm width, hyaline, cylindrical. *Conidiophores* reduced to conidiogenous cells, arising from the inner cells of the conidiomata. *Conidiogenous cells* 14–26 × 12–18 μm ($\bar{x}$ = 20 × 15 μm, n = 30), holoblastic, hyaline, smooth, ampulliform or cylindrical, smooth. *Conidia* 20–29 × 10–14 μm ($\bar{x}$ = 25 × 12 μm, n = 50), oblong to ovoid, thick-walled, initially hyaline, aseptate, becoming 1-septate and pale brown to brown, with melanin deposits on the inner surface of the wall arranged longitudinally giving a striate appearance to the conidia.

Culture characteristics – Germinated conidia formed in sterilized water after 12 h. *Colonies* on PDA attaining 40–50 mm diameter in 3 days, medium sparse, circular, entire edge, white, cottony to fluffy, aerial mycelium sparse in the middle, well developed at the margin, reverse pale yellow.

Material examined – China, Sichuan Province, Chengdu City, Xindu District, 104°10′17.09″E 30°45′36.51″N, 486 m, isol. from stems of *Acer palmatum*, 4 Jun. 2021, X.L. Xu, XXL202106001 (SICAU 23-0141), culture (SICAUCC 23-0112).

GenBank numbers – SICAUCC 23-0112 = ITS: PP736374, *tub*2: PP782069, *rpb*2: PP782081

Notes – The asexual morph of *Lasiodiplodia pseudotheobromae* was initially described by Alves et al. (2008) from *Gmelina arborea*, and later, the sexual morph was described in samples from dead leaves of *Plukenetia volubilis* (Tennakoon et al. 2016). In the phylogenetic analysis, our isolate (SICAUCC 23-0112) clustered together with the type strain of *L. pseudotheobromae* with 92% MLBS / 1.00 BYPP support (Fig. 5). A comparison of ITS, *tub*2, and *rpb*2 sequence data between our strain and *L. pseudotheobromae* (CBS 116459, holotype) showed no nucleotide difference (Alves et al. 2008). Morphologically, the new isolate displays similar morphological characteristics with *L. pseudotheobromae* in having immersed conidiomata and ellipsoidal, thick-walled, 1-septate mature conidia with longitudinal striations. Therefore, we identify the new collection as *L. pseudotheobromae*, marking the first reported occurrence in *Acer palmatum*.

Neofusicoccum Crous, Slippers & A.J.L. Phillips

Notes – *Neofusicoccum* was introduced by Crous et al. (2006), with *N. parvum* as the type species. *Neofusicoccum* species, commonly cause diseases in woody plants worldwide. Several *Neofusicoccum* species were reported to be associated with shoot blight, branch cankers and bot gummosis, including *Neofusicoccum australe*, *N. luteum*, *N. mediterraneum*, *N. parvum* (Adesemoye et al. 2011, 2014, Mayorquinet et al. 2016, Vakalounakis et al. 2019). *Neofusicoccum* is characterized by fusiform to ellipsoid aseptate conidia and “dichomera-like” synanamorphs, which septate and turn brown with age, to form globose to pyriform conidia (Barber et al. 2005, Crous et al. 2006). The Species Fungorum (https://www.speciesfungorum.org, November 2024) enumerates 67 epithets in this genus.

3. *Neofusicoccum parvum* (Pennycook & Samuels) Crous, et al., Stud. Mycol. 55: 248 (2006) Fig. 6

MycoBank number: MB500879; Facesoffungi number: FoF02411

Associated with canker on stems and branches of *Citrus reticulata* Blanco (Orah mandarin). Sexual morph: Not observed. Asexual morph: *Coelomycetous*. *Conidiomata* 116–312 μm long × 87–255 μm width × 90–157 μm high ($\bar{x}$ = 175 × 149 × 129 μm, n = 30), gregarious, immersed, globose to subglobose, dark brown to black. *Peridium* 18–40 μm ($\bar{x}$ = 27 μm, n = 20) width, composed of hyaline to brown cells of *textura angularis*. *Conidiogenous cells* cylindrical, straight, colorless, and smooth. *Conidia* 13–21 × 7–10 μm ($\bar{x}$ = 16 × 8 μm, n = 50), elliptical, straight, with a rounded apex and a truncated base, hyaline, smooth-walled.

Culture characteristics – *Colonies* growing fast on PDA, reaching 8 cm in 6 days at 25°C, under 12 h light/12 h dark, circular, with even margin, floccose, white at the beginning, then became smoky gray to gray-olivaceous.

Material examined – China, Sichuan Province, Mianyang City, Zitong County, 105°9′59″E 31°37′49″N, 440 m, isol. from stems and branches of *Citrus reticulata*, 20 Oct. 2021, W.G. Cai, CWG202110001 (SICAU 23-0108), culture (SICAUCC 23-0086).

GenBank numbers – SICAUCC 23-0086 = ITS: PP133649, LSU: PP133658, *tef*1-α: PP125718, *tub*2: PP952309

Notes – The specimen in our study shared similar morphology with the description of *Neofusicoccum parvum* reported by Crous et al. (2006) and Aloi et al. (2021). The strain SICAUCC 23-0086 clustered with *N. parvum* with 93% MLBS and 0.98 BYPP bootstrap support (Fig. 7). Nucleotide comparisons of ITS, LSU, SSU, and *tef*1-α (SICAUCC 23-0086) showed high homology with the sequences of *N. parvum* (CMW9081, ex-type), similarities are 99.8% (515/516, 0 gap), 100% (609/609, 0 gap), 100% (1,012/1,012, 0 gap) and 98.9% (269/272, 0 gap), respectively.

Figure 4 – *Lasiodiplodia pseudotheobromae* (SICAU 23-0141). a Symptoms on the stem. b Appearance of conidiomata. c, d Cross-section of conidiomata. e Conidiomatal wall. f

Conidiogenous cell with developing conidium. g–j Conidia. k Germinating conidium. l Front view of colony on PDA. m Reverse view of colony on PDA. Scale bars: b = 200 µm, c = 100 µm, d = 50 µm, e = 20 µm, f = 10 µm, g–k = 20 µm.

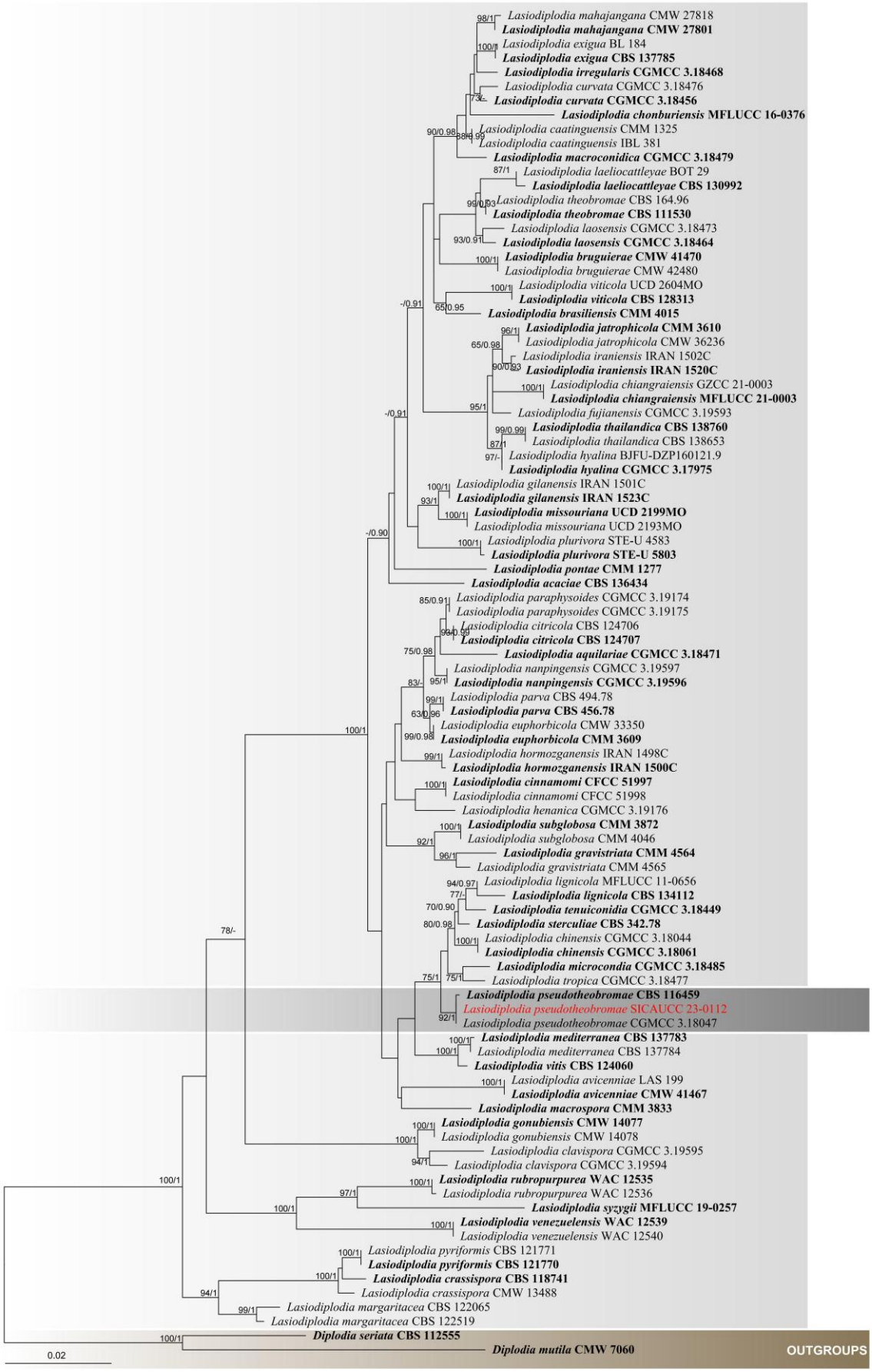

Figure 5 – Phylogram derived from maximum likelihood analyses of a combined dataset comprising ITS, *rpb*2, *tef*1-α, and *tub*2 sequences, encompassing species within the *Lasiodiplodia* genus. The phylogenetic analysis included ninety-five strains and a total of 2,902 characters (ITS: 1–619, *rpb*2: 620–1,609, *tef*1-α: 1,610–2,414, *tub*2: 2,415–2,902) after alignment. *Diplodia seriata* CBS 112555 and *Diplodia mutila* CMW 7060 were used as the outgroup taxa. Single-gene analyses were conducted, resulting in similar tree topologies between the ML and BY methods, ensuring consistent comparisons of clade stability. The best-scoring RAxML tree with a final likelihood value of -10,284.608245 is presented. The matrix had 812 distinct alignment patterns, with 44.83% of undetermined characters or gaps. Estimated base frequencies were as follows: A = 0.221943, C = 0.288622, G = 0.264014, T = 0.225421; substitution rates AC = 0.851378, AG = 3.456454, AT = 1.215356, CG = 0.882213, CT = 5.384843, GT = 1.000000. Bootstrap support values (MLBS) equal or exceeding 60%, and Bayesian posterior probabilities (BYPP) equal or exceeding 0.90 indicated at the nodes. The ex-type strains are in bold, and the new isolate is in red. Bar = 0.02 represents the estimated number of nucleotide substitution sites per branch.

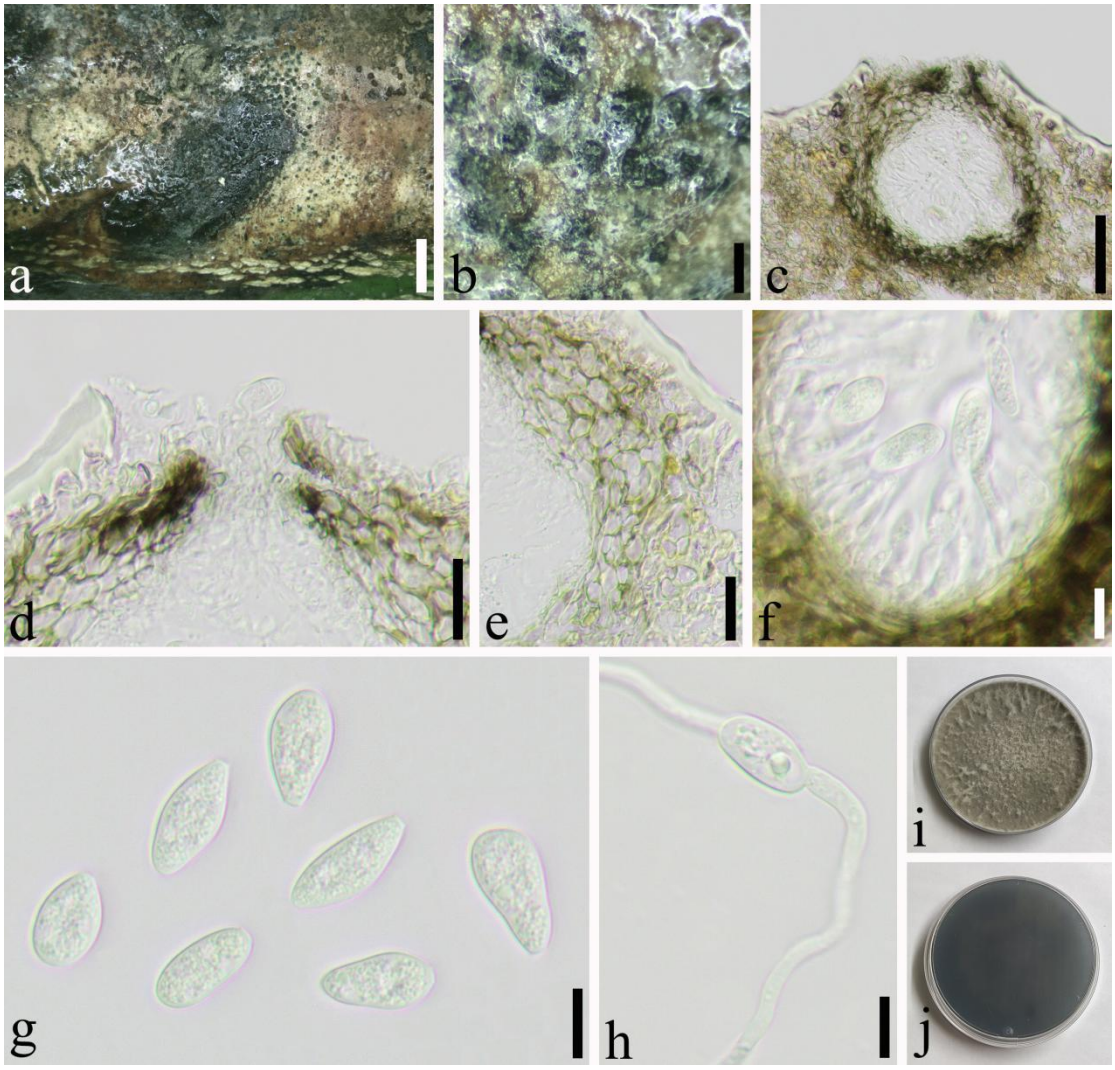

Figure 6 – *Neofusicoccum parvum* (SICAU 23-0108) a, b Appearance of conidiomata on the stem. c Cross-section of conidioma. d Ostiole with periphyses. e Peridium. f Conidiogenous cells with developing conidia. g Conidia. h Germinating conidium. i Front view of colony on PDA. j Reverse view of colony on PDA. Scale bars: a = 2 mm, b = 200 µm, c = 50 µm, d, e = 20 µm, f–h = 10 µm.

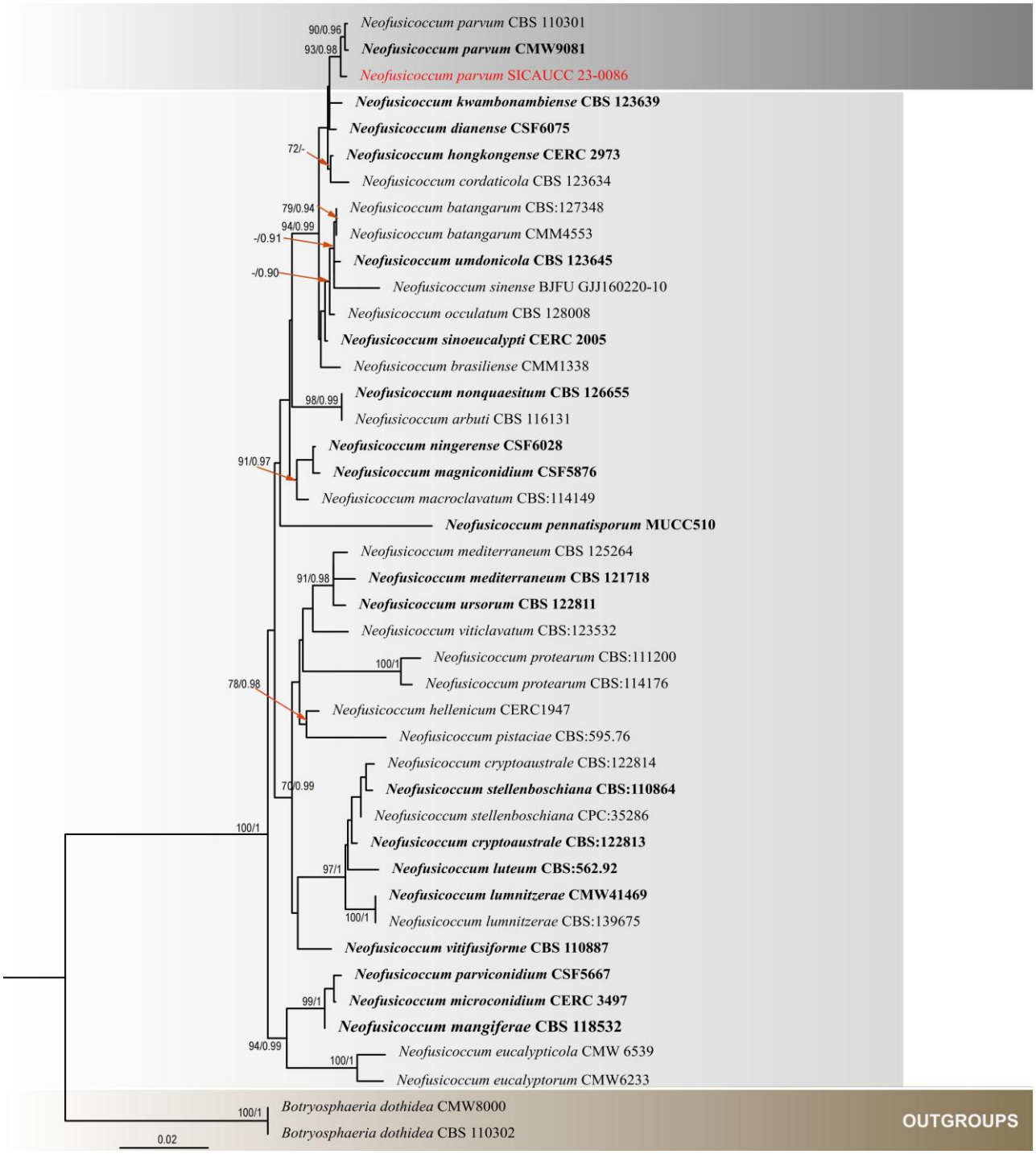

Figure 7 – Phylogram derived from maximum likelihood analyses of a combined dataset comprising ITS, LSU, *tef*1-α, and *tub*2 sequence dataset, representing the species of *Neofusicoccum*. Forty-three strains were included in the combined analyses, which comprised 2,357 characters (ITS: 1–634, LSU: 635–1,552, *tef*1-α: 1,553–1,891, *tub*2: 1,892–2,357) after alignment. Single-gene analyses were conducted, resulting in similar tree topologies between the ML and BY methods, ensuring consistent comparisons of clade stability. The best-scoring RAxML tree with a final likelihood value of -6,712.251400 is presented. The matrix had 543 distinct alignment patterns, with 28.42% of undetermined characters or gaps. Estimated base frequencies were as follows: A = 0.223444, C = 0.274508, G = 0.279918, T = 0.222130; substitution rates AC = 0.750166, AG = 4.063990, AT = 1.019792, CG = 0.940811, CT = 8.430011, GT = 1.000000. Bootstrap support values for MLBS equal or greater than 70%, and BYPP equal to or greater than 0.90 are indicated at the nodes as MLBS / BYPP. *Botryosphaeria dothidea* (CMW8000 and CBS

110302) was used as the outgroup taxa. The ex-type strains are in bold, and the new isolates of this study are in red.

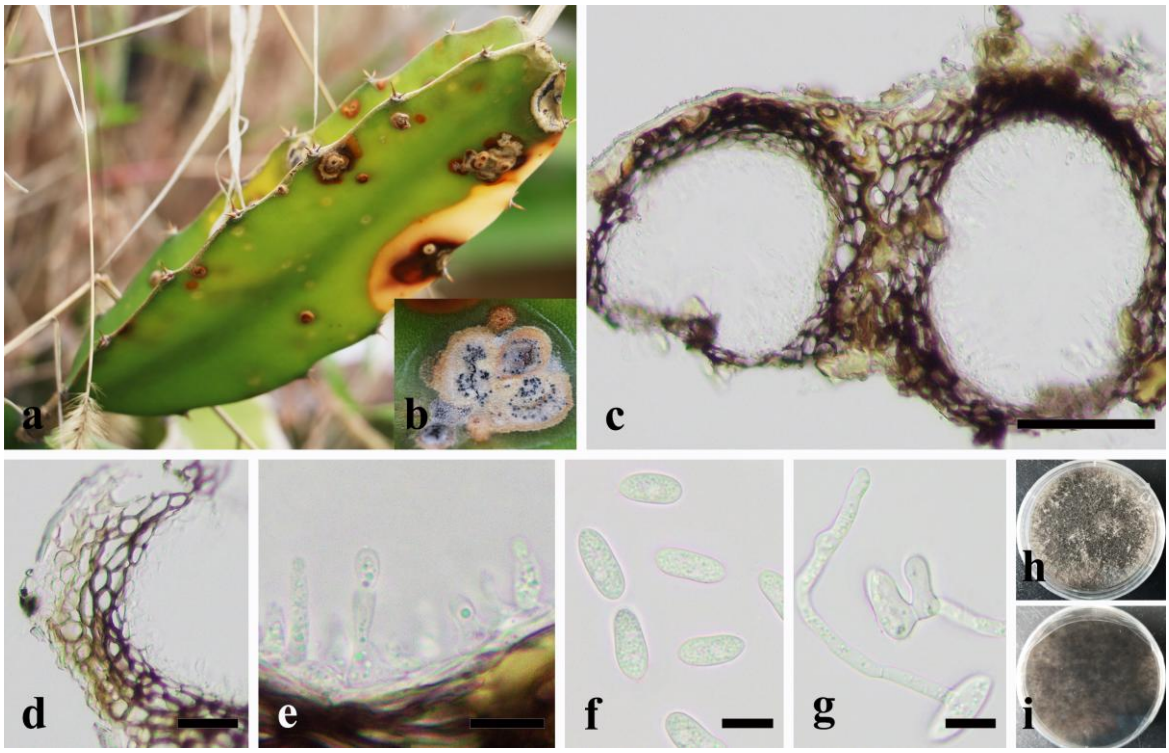

Figure 8 – *Neoscytalidium hylocereum-undulatum* (holotype, SICAU 23-0144). a, b Symptoms on the stem. c Cross-section of conidiomata. d Conidiogenous wall. e Conidiogenous cells with developing conidia. f Conidia. g Germinating conidia. h Front view of colony on PDA. i Reverse view of colony on PDA. Scale bars: c = 50 μm, d = 20 μm, e–g = 10 μm.

Neoscytalidium Crous & Slippers

Notes – *Neoscytalidium* was established by Crous et al. (2006) with *N. dimidiatum* as the type species. Crous et al. (2006) systematically determined the polyphyletic status of *Scytalidium*, prompting the establishment of the genus *Neoscytalidium* to accommodate *Scytalidium dimidiatum* as *N. dimidiatum*. *Neoscytalidium* species is characterized by conidia oblong-obtuse to doliiform, dark brown, thick-walled, 0–2-septate with a darker central cell, arthroconidia borne in dry powdery chains, oblong-obtuse to doliiform, brown and disarticulated into 0–1-septate (Crous et al. 2006, Phillips et al. 2013, Huang et al. 2016). Members of *Neoscytalidium* have generally been documented as plant pathogens, causing canker and dieback on economically important tree species (Fernández-Herrera et al. 2017, Coutinho et al. 2018, Alizadeh et al. 2022), and associated with human diseases (Bakhshizadeh et al. 2014, Calvillo-Medina et al. 2019).

4. *Neoscytalidium hylocereum-undulatum* S.S. Xiang & C.L. Yang, sp. nov. Fig. 8

MycoBank number: MB900694; Facesoffungi number: FoF16129

Etymology – The specific epithet reflects the host genus *Hylocereus*.

Holotype – SICAU 23-0144

Associated with canker on stems of *Hylocereus undatus* (Haw.) Britt. et Rose. Sexual morph: Not observed. Asexual morph: *Coelomycetous*. *Conidiomata* 95–120 × 95–180 μm ($\bar{x}$ = 102 × 123 μm, n = 10), pycnidial, immersed to partly erumpent at maturity, brown to black, solitary, scattered, uni-loculate, ellipsoid or fusiform, ostiolate, glabrous. *Conidiomatal wall* 7–34 μm width, comprising of thick-walled, pale brown to brown cells of *textura angularis*, thickening at apical zone. *Conidiophores* reduced to conidiogenous cells, arising from the inner layer cells of the conidiomata. *Conidiogenous cells* 7–18 × 2–6 μm ($\bar{x}$ = 10.2 × 3.5 μm, n = 30), hyaline,

enteroblastic, monophialidic, integrated, cylindrical to subcylindrical, tapered to the apices, straight or curved, with minute collarette, smooth-walled, collarette 0.5–3 µm long. *Conidia* 11–17(–22) × 4.5–7 µm ($\bar{x}$ = 14.4 × 5.7 µm, n = 50), hyaline, fusiform, ellipsoid, subcylindrical, straight or slightly curved, aseptate, usually with two guttules, thin-walled, smooth. *Beta-conidia* not observed.

Culture characteristics – *Colonies* on PDA attaining 60–70 mm diameter in 4 days, fast-growing, circular, fimbriat, white, filamentous aerial mycelium superficially, reverse white.

Material examined – China, Sichuan Province, Chengdu City, Wenjiang District, Schoolyard of Sichuan Agricultural University, 103°51′27.55″E 30°42′19.5″N, 550 m, isol. from stems of *Hylocereus undatus*, 10 Nov. 2020, C.L. Yang, YCL202011003 (SICAU 23-0144, holotype), ex-type culture (SICAUCC 23-0103). *ibid.* YCL202011003-2 (SICAU 23-0151), living culture SICAUCC 23-0137.

GenBank numbers – SICAUCC 23-0103 = ITS: PP781969, LSU: PP719621, SSU: PP734052, *tef*1-α: PQ005620, *tub*2: PQ005626. SICAUCC 23-0137 = ITS: PP781970, LSU: PP719626, SSU: PP734054, *tef*1-α: PQ005623, *tub*2: PQ005627

Notes – In the phylogenetic analysis, *Neoscytalidium hylocereum-undulatum* forms a well-supported subclade within *Neoscytalidium* (96% MLBS / 1.00 BYPP) and shows a close relationship with *N. hylocereum* (Fig. 9). Through pairwise nucleotide comparisons, *N. hylocereum-undulatum* exhibits distinctions from *N. hylocereum* (TSU-HP01, holotype). The ITS region shows a 98.0% similarity (496/506, 2 gaps), *tef*1-α shows 96.8% similarity (245/253, 0 gap), and *tub*2 is 100% identical (400/400, 0 gap). Morphologically, *N. hylocereum-undulatum* sets itself apart from *N. hylocereum* by having larger conidia (11–17(–22) × 4.5–7 µm vs. 9.8–13.5 × 3.7–5 µm) and a more rapid colony growth rate (15–17.5 mm/d vs. 30 mm/d). Furthermore, *N. hylocereum-undulatum* features two guttules on conidia, a characteristic absent in *N. hylocereum* (Wonglom et al. 2023). Consequently, we introduce *N. hylocereum-undulatum* as a distinct and novel species.

Phyllostictaceae Fr.

Notes – *Phyllostictaceae* (as *Phyllostictei*) was originally proposed by Fries (1849) and accepted by Hawksworth & David (1989). Seaver (1922) used the *Phyllostictales* and *Phyllostictaceae* to suit the characteristics of *Phyllosticta*. Slippers et al. (2013) and Wikee et al. (2013a) re-established *Phyllostictaceae* as an independent family within the *Botryosphaeriales* to accommodate *Phyllosticta*, a taxonomic adjustment supported by phylogenetic investigations. *Phyllostictaceae* species are generally causal agents on economic crops, and characterized by their smaller asci and ascospores compared to those of *Botryosphaeriaceae*, and their ascospores accompanied by gelatinous-capped ascospores (Liu et al. 2016). The divergence of *Phyllostictaceae* members took place in the Cretaceous epoch, subsequently giving rise to distinct genera within the Mesozoic era (66–251.90 Mya) (Rathnayaka et al. 2023).

Phyllosticta Pers.

Notes – *Phyllosticta* was introduced by Persoon (1818) with *P. convallariae* as the type species. *Phyllosticta*, initially classified in the family *Phyllostictaceae* by Fries (1849), was later moved to *Botryosphaeriaceae* based on multiple studies (Crous et al. 2006, Schoch et al. 2006, Liu et al. 2012). However, following a phylogenetic re-assessment, it was subsequently re-classified back into *Phyllostictaceae* (Slippers et al. 2013, Wikee et al. 2013). *Phyllosticta* members exhibit erumpent ascomata, 8-spored, clavate to broadly ellipsoid asci, ellipsoid to limoniform ascospores, pycnidial conidiomata with aseptate conidia enveloped by a mucoid layer, and featuring a solitary apical appendage (van der Aa 1973, van der Aa & Vanev 2002, Wikee et al. 2011). *Phyllosticta* species primarily induce leaf blight or leaf and fruit spots on various plants, with infrequent occurrences on woody substrates (Glienke et al. 2011, Guarnaccia et al. 2019, Sui et al. 2023, Wang et al. 2023a,b), and some species also display endophytic and saprobic behaviors (van der Aa & Vanev 2002, Trigiano et al. 2004, Wikee et al. 2013 b, Sui et al. 2023). The Species Fungorum

(https://www.speciesfungorum.org, November 2024) lists a comprehensive tally of 2,099 names associated with *Phyllosticta*. Nevertheless, a considerable portion of these names has been merged as synonyms, while the current consensus recognizes above 1,500 species within this genus (Bánki et al. 2023, Sui et al. 2023).

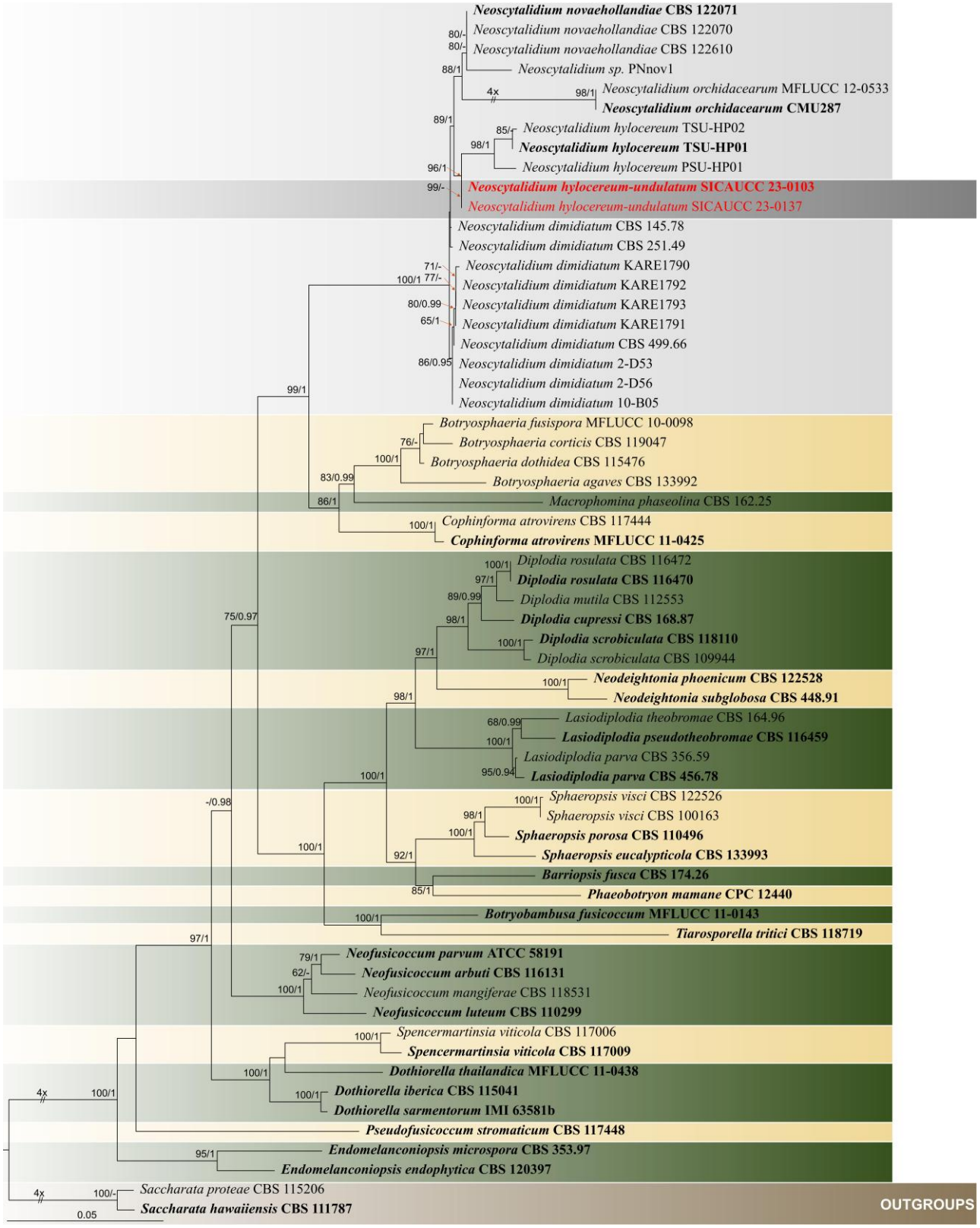

Figure 9 – Phylogram derived from maximum likelihood analyses of a combined dataset comprising ITS, LSU, SSU, *tef*1-α, and *tub*2 sequence dataset representing the species in

Botryosphaeriaceae and *Saccharataceae*. The tree is rooted to *Saccharata proteae* (CBS 115206) and *S. hawaiiensis* (CBS 111787). Sixty-two strains were included in the combined analyses, contributing to a dataset comprising 5,618 characters (ITS: 1–1,020, LSU: 1,021–2,591, SSU: 2,592–4,300, *tef*1-α: 4,301–4,966, *tub*2: 4,967–5,618) after alignment. Single-gene analyses were conducted, resulting in similar tree topologies between the ML and BY methods, ensuring consistent comparisons of clade stability. The best-scoring RAxML tree, with a final likelihood value of -22,967.039417, is presented. The matrix had 1,512 distinct alignment patterns, with 53.80% of undetermined characters or gaps. Estimated base frequencies were as follows: A = 0.235557, C = 0.256556, G = 0.274390, T = 0.233497; substitution rates AC = 1.071722, AG = 2.364299, AT = 1.019592, CG = 1.444965, CT = 4.532897, GT = 1.000000. Bootstrap support values (MLBS) ≥ 60%, and Bayesian posterior probabilities (BYPP) ≥ 0.90 are indicated at the nodes as MLBS / BYPP. The ex-type strains are bold, and the new isolates of this study are red. Bar = 0.05 represents the estimated number of nucleotide substitution sites per branch.

5. *Phyllosticta citribrasiliensis* O.L. Pereira, Glienke & Crous [as '*citribraziliensis*'], Persoonia 26: 54 (2011) Fig. 10

MycoBank number: MB172054; Facesoffungi number: FoF12964

=*Phyllosticta ericarum* Crous, Persoonia 28: 161 (2012)

Associated with black spots on leaves of *Polygonatum* sp., producing a covering on the surface of leaves, symptoms appeared as local or whole leaf blight accompanied by the formation of numerous pycnidia. Sexual morph: Not observed. Asexual morph: *Coelomycetous*. *Conidiomata* 140–230 × 100–165 μm ($\bar{x}$ = 168 × 124 μm, n = 10), pycnidial, solitary, scattered or gathered, uniloculate, subglobose to globose, semi-immersed, conspicuous on leaf surface, black. *Conidiomatal wall* 19–32 μm ($\bar{x}$ = 24.8 μm, n = 20) width, comprising brown to dark brown, 5–7 layers cells of *textura angularis*. *Ostiole* 15–20 μm ($\bar{x}$ = 17 μm, n = 10) width, central, single. *Conidiophores* reduced to conidiogenous cells. *Conidiogenous cells* 10–18 × 3–5 μm ($\bar{x}$ = 13.8 × 3.9 μm, n = 20), enteroblastic, monophialidic, integrated, cylindrical to conical, hyaline, grown from the inner layer of pycnidial wall. *Conidia* 10–14 × 8–9 μm ($\bar{x}$ = 11.7 × 8.5 μm, n = 50), hyaline, ellipsoidal to obovoid, numerous guttulate, one-celled, smooth-walled, surrounded by a mucilaginous sheath, slightly thicker on both sides, 1–3 μm ($\bar{x}$ = 2 μm, n = 20) thick, usually with a sunken area at the top, 1–3 μm ($\bar{x}$ = 2 μm, n = 10) width, thinner at apex, 0.5–1 μm ($\bar{x}$ = 1 μm, n = 10) width, with a hyaline, apical mucoid appendage. *Appendages* 11–67 × 0.5–2 μm ($\bar{x}$ = 34.5 × 1.1 μm, n = 30), unbranched, flexuous, tapering towards rounded tip.

Material examined – China, Sichuan Province, Neijiang City, Zizhong County, Huaxiang Village, 104°49′31.33″E 29°46′12.28″N, 306 m, on leaves of *Polygonatum* sp., 22 Jan. 2023, C.L. Yang, YCL202301001 (SICAU 23-0129).

GenBank numbers – SICAU 23-0129 = ITS: PP736375, LSU: PQ068882, *tef*1-α: PP779576, *act*: PP782108

Notes – *Phyllosticta citribrasiliensis* was initially documented by Glienke et al. (2011) from healthy leaves of *Citrus* sp. in Brazil. The characteristics of our collection align closely with those of *P. citribrasiliensis* (CBS 100098, holotype) in having solitary, globose pycnidia with central ostiole, and ellipsoid to obovoid, coarsely guttulate, smooth-walled conidia with mucoid apical appendage (Glienke et al. 2011). In the multi-gene phylogeny, our new collection formed a cohesive cluster with *P. citribrasiliensis*, with 85% MLBS / 0.99 BYPP support (Fig. 11). Comparison of the LSU, *act* and *tef*1-α sequence of *P. citribrasiliensis* (CBS 100098, holotype) and our strain showed 100% similarity, while the ITS showed 99.09% (544/549 bp, 2 gaps) similarity. Consequently, we accept the new collection as *P. citribrasiliensis*, which represents the first discovery of this species on *Polygonatum* sp. in China.

Capnodiales Woron.

Notes – *Capnodiales* was erected by Woronichin (1925) within *Dothideomycetes* based on phylogenetic studies (Schoch et al. 2006, 2009, Crous et al. 2009a). Within the order *Capnodiales*,

there are 10 families listed: *Aeminiaceae*, *Antennulariellaceae*, *Capnodiaceae*, *Euantennariaceae*, *Johansoniaceae*, *Metacapnodiaceae*, *Neoantennariellaceae*, *Piedraiaceae*, *Readerielliopsidaceae*, *Xenodevriesiaceae*, and *Capnodiales* genera *incertae sedis* with 10 genera (Wijayawardene et al. 2022). The divergence of the *Capnodiales* from *Myriangiales* occurred around 205 Mya (166–248), towards the end of the Triassic period (Hongsanan et al. 2016). Capnodialean species generally live on leaf as epiphytes in association with insect-generated honeydew, exhibiting roles as saprobes, leaf pathogens, usually without pseudoparaphyses in ascostromata (Hughes et al. 1976, Crous et al. 2009a, Chomnunti et al. 2011). The *Capnodiales* order predominantly comprises four families linked to sooty mold, namely *Antennulariellaceae*, *Capnodiaceae*, *Euantennariaceae*, and *Metacapnodiaceae* (Chomnunti et al. 2014).

Capnodiaceae Höhn. ex Theiss.

Notes – *Capnodiaceae* was established by Von Höhnel (1910) with *Capnodium* as its designated type genus and presently encompasses an assemblage of 11 genera and approximately 150 species (Lu et al. 2022, Wijayawardene et al. 2022). The first major monographic review of *Capnodiaceae* was undertaken by Batista & Ciferri (1963), and subsequent scholars have continued to enhance and refine our understanding of this family through the incorporation of both morphological and molecular evidence (Hughes 1976, Crous et al. 2009a, Chomnunti et al. 2011, Abdollahzadeh et al. 2020). *Capnodiaceae* represents a prolific and prevalent family within the realm of sooty molds, often found in association with honeydew secretions from insects (mainly aphids, whitefly, psyllid, and scale insects) or in coexistence with other fungicolous species (Hughes 1976, Schoch et al. 2006, Hyde et al. 2013, Hongsanan et al. 2015, Abdollahzadeh et al. 2020). Members of this family are distinguished by their black superficial mycelia with septate, dark-brown, cylindrical hyphae, asci bitunicate, and elongated pycnidia with either short or long narrow necks, where minute, unicellular, hyaline conidia formed from near the base, middle, or apex of the pycnidia (Chomnunti et al. 2011, 2014, Abdollahzadeh et al. 2020).

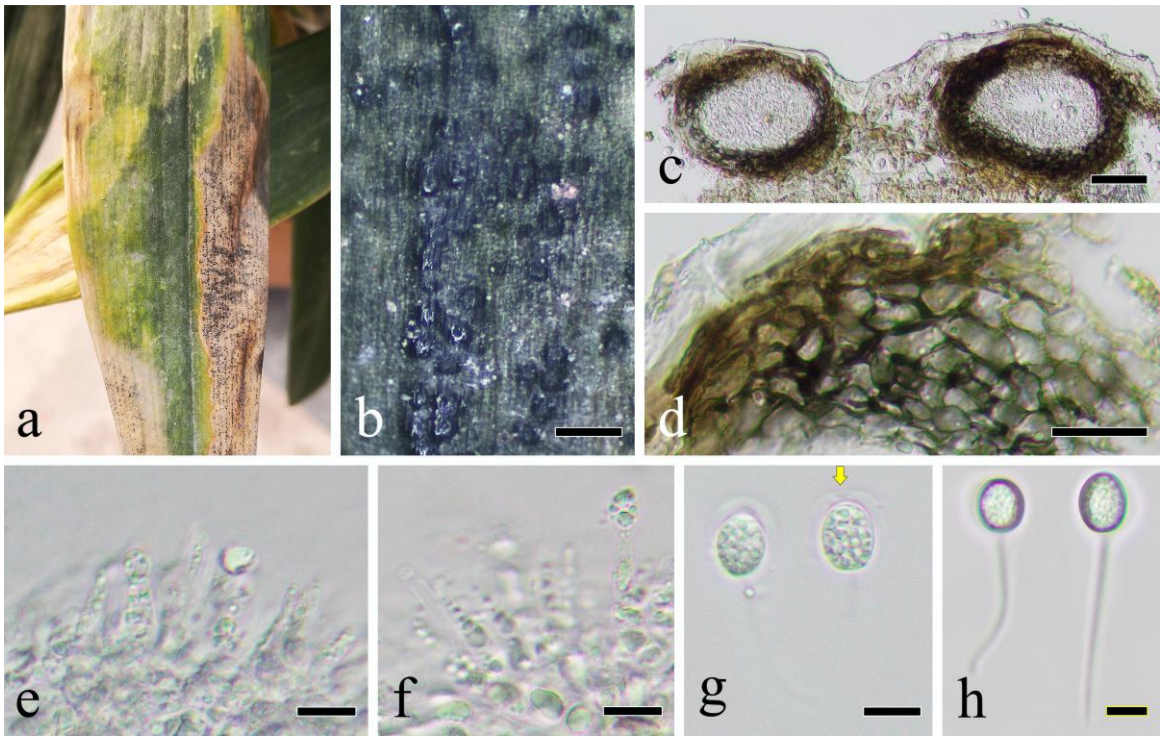

Figure 10 – *Phyllosticta citribrasiliensis* (SICAU 23-0129). a Symptoms on the leaf. b Appearance of conidiomata. c Cross-section of conidiomata. d Conidiomatal wall. e, f Conidiogenous cells with developing conidia. g, h Conidia (the arrow indicates a dimpled area at the top). Scale bars: b = 300 µm, c = 50 µm, d = 20 µm, e–h = 10 µm.

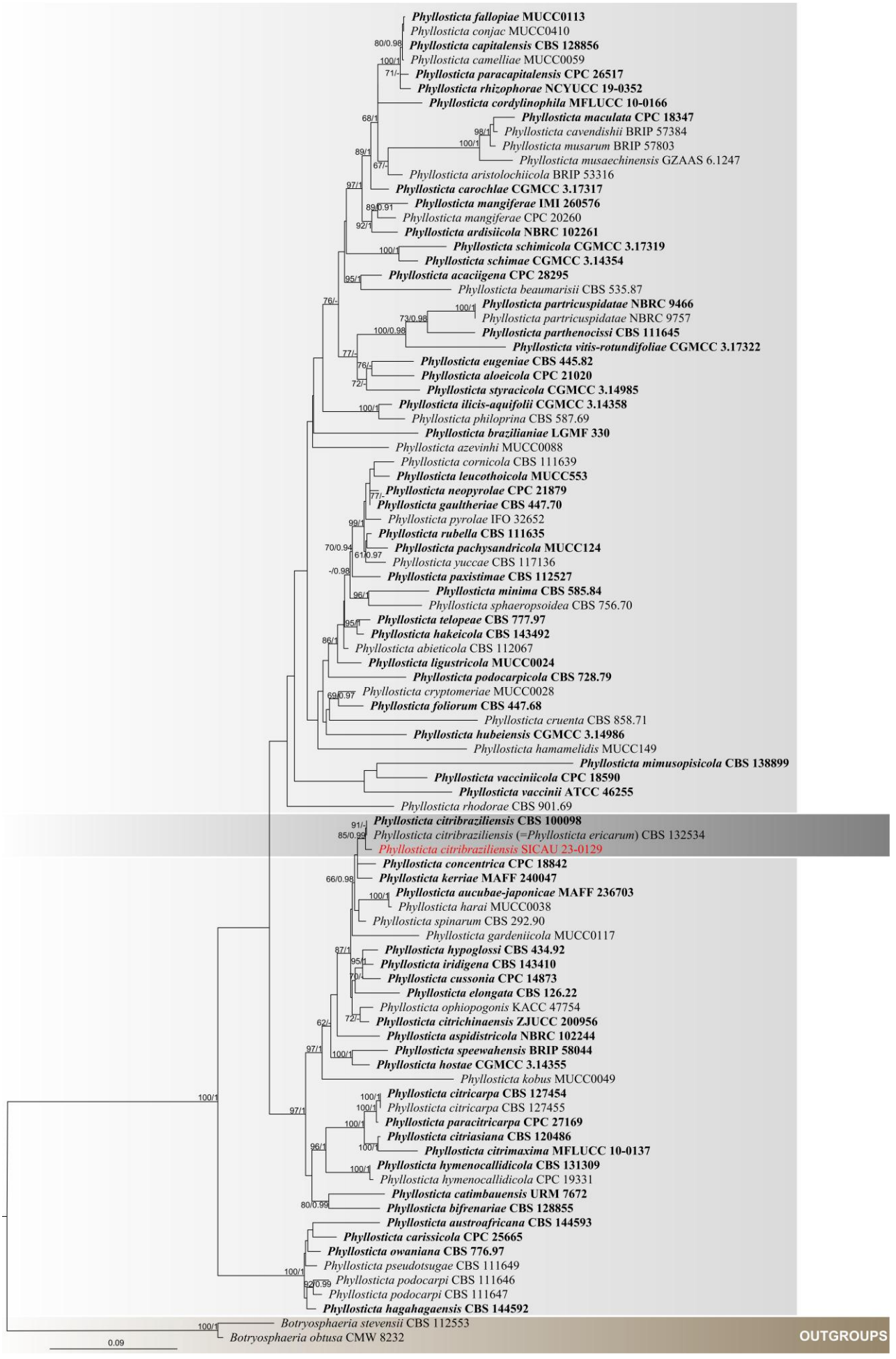
Phyllosticta fallopiae MUCC0113
Phyllosticta conjac MUCC0410
Phyllosticta capitalensis CBS 128856
Phyllosticta camelliae MUCC0059
Phyllosticta paracapitalensis CPC 26517
Phyllosticta rhizophorae NCYUCC 19-0352
Phyllosticta cordylinophila MFLUCC 10-0166
Phyllosticta maculata CPC 18347
Phyllosticta cavendishii BRIP 57384
Phyllosticta musarum BRIP 57803
Phyllosticta musaechinensis GZAAS 6.1247
Phyllosticta aristolochiicola BRIP 53316
Phyllosticta carochlae CGMCC 3.17317
Phyllosticta mangiferae IMI 260576
Phyllosticta mangiferae CPC 20260
Phyllosticta ardisiicola NBRC 102261
Phyllosticta schimicola CGMCC 3.17319
Phyllosticta schimae CGMCC 3.14354
Phyllosticta acaciigena CPC 28295
Phyllosticta beaumarisii CBS 535.87
Phyllosticta partricuspidatae NBRC 9466
Phyllosticta partricuspidatae NBRC 9757
Phyllosticta parthenocissi CBS 111645
Phyllosticta vitis-rotundifoliae CGMCC 3.17322
Phyllosticta eugeniae CBS 445.82
Phyllosticta aloeicola CPC 21020
Phyllosticta styracicola CGMCC 3.14985
Phyllosticta ilicis-aquifolii CGMCC 3.14358
Phyllosticta philoprina CBS 587.69
Phyllosticta brazilianiae LGMF 330
Phyllosticta azevinhi MUCC0088
Phyllosticta cornicola CBS 111639
Phyllosticta leucothoicola MUCC553
Phyllosticta neopyrolae CPC 21879
Phyllosticta gaultheriae CBS 447.70
Phyllosticta pyrolae IFO 32652
Phyllosticta rubella CBS 111635
Phyllosticta pachysandricola MUCC124
Phyllosticta yuccae CBS 117136
Phyllosticta paxistimae CBS 112527
Phyllosticta minima CBS 585.84
Phyllosticta sphaeropsoidea CBS 756.70
Phyllosticta telopeae CBS 777.97
Phyllosticta hakeicola CBS 143492
Phyllosticta abieticola CBS 112067
Phyllosticta ligustricola MUCC0024
Phyllosticta podocarpicola CBS 728.79
Phyllosticta cryptomeriae MUCC0028
Phyllosticta foliorum CBS 447.68
Phyllosticta cruenta CBS 858.71
Phyllosticta hubeiensis CGMCC 3.14986
Phyllosticta hamamelidis MUCC149
Phyllosticta mimusopisicola CBS 138899
Phyllosticta vacciniicola CPC 18590
Phyllosticta vaccinii ATCC 46255
Phyllosticta rhodorae CBS 901.69
Phyllosticta citribraziliensis CBS 100098
Phyllosticta citribraziliensis (=Phyllosticta ericarum) CBS 132534
Phyllosticta citribraziliensis SICAU 23-0129
Phyllosticta concentrica CPC 18842
Phyllosticta kerriae MAFF 240047
Phyllosticta aucubae-japonicae MAFF 236703
Phyllosticta harai MUCC0038
Phyllosticta spinarum CBS 292.90
Phyllosticta gardeniicola MUCC0117
Phyllosticta hypoglossi CBS 434.92
Phyllosticta iridigena CBS 143410
Phyllosticta cussonia CPC 14873
Phyllosticta elongata CBS 126.22
Phyllosticta ophiopogonis KACC 47754
Phyllosticta citrichinaensis ZJUCC 200956
Phyllosticta aspidistricola NBRC 102244
Phyllosticta speewahensis BRIP 58044
Phyllosticta hostae CGMCC 3.14355
Phyllosticta kobus MUCC0049
Phyllosticta citricarpa CBS 127454
Phyllosticta citricarpa CBS 127455
Phyllosticta paracitricarpa CPC 27169
Phyllosticta citriasiana CBS 120486
Phyllosticta citrimaxima MFLUCC 10-0137
Phyllosticta hymenocallidicola CBS 131309
Phyllosticta hymenocallidicola CPC 19331
Phyllosticta catimbauensis URM 7672
Phyllosticta bifrenariae CBS 128855
Phyllosticta austroafricana CBS 144593
Phyllosticta carissicola CPC 25665
Phyllosticta owaniana CBS 776.97
Phyllosticta pseudotsugae CBS 111649
Phyllosticta podocarpi CBS 111646
Phyllosticta podocarpi CBS 111647
Phyllosticta hagahagaensis CBS 144592
Botryosphaeria stevensii CBS 112553
Botryosphaeria obtusa CMW 8232
OUTGROUPS
0.09

Figure 11 – Phylogram derived from maximum likelihood analyses of a combined dataset comprising ITS, LSU, *tef*1-α, *act*, and *gapdh* sequence dataset representing the species of *Phyllosticta*. The phylogenetic analysis included ninety-three strains and a total of 6,847 characters (ITS: 1–2,091, LSU: 2,092–4,106, *tef*1-α: 4,107–4,900, *act*: 4,901–5,606, *gapdh*: 5,607–6,847) after alignment. The tree is rooted to *Botryosphaeria obtuse* (CMW 8232) and *Botryosphaeria stevensii* (CBS 112553). Single-gene analyses were conducted, resulting in similar tree topologies between the ML and BY methods, ensuring consistent comparisons of clade stability. The best-scoring RAxML tree with a final likelihood value of -33,904.532107 is presented. The matrix had 2,025 distinct alignment patterns, with 70.41% of undetermined characters or gaps. Estimated base frequencies were as follows: A = 0.217575, C = 0.282764, G = 0.276646, T = 0.223015; substitution rates AC = 1.234929, AG = 3.364735, AT = 1.444351, CG = 1.244741, CT = 6.889207, GT = 1.000000. Bootstrap support values (MLBS) equal to or exceeding 60%, and Bayesian posterior probabilities (BYPP) equal or exceeding 0.90 indicated at the nodes as MLBS / BYPP. The ex-type strains are in bold, and the new isolates of this study are in red. Bar = 0.07 represents the estimated number of nucleotide substitution sites per branch.

Conidiocarpus Woron.

Notes – *Conidiocarpus* was erected by Woronichin (Jaczewski 1917), with *C. caucasicus* as the type species. *Conidiocarpus* has previously been described as the asexual of *Phragmocapnias* (Hughes 1976), but subsequent research has established that the type species of *Conidiocarpus* and *Phragmocapnias* belong to two separate genera (Abdollahzadeh et al. 2020). To date, there are 14 distinct epithets associated with *Conidiocarpus* species in Species Fungorum (https://www.speciesfungorum.org, November 2024), and only four species have been recognized within this genus, namely *C. caucasicus*, *C. fici-septicae*, *C. guilanensis*, and *C. siamensis* (Abdollahzadeh et al. 2020, Khodaparast et al. 2020, Tennakoon et al. 2022a, Pem et al. 2024, Yang et al. 2024).

6. *Conidiocarpus cinnamomeus* X.Y. Li & C.L. Yang, sp. nov. Fig. 12

MycoBank number: MB900659; Facesoffungi number: FoF15926

Etymology – Refers to the host genus *Cinnamomum*, where the species collected.

Holotype – SICAU 23-0150

Associated with dark mildew on leaves of *Cinnamomum japonicum* Siebold, producing a black sooty-like covering on the surface of leaves, symptoms appeared as dark mildew accompanied by the formation of pycnidia randomly distributed throughout the leaves. *Thallus* composed of a hyphal network on leaves, consisting of cylindrical, brown, vegetative hyphae. *Superficial hyphae* 4–7 µm ($\bar{x}$ = 5.4 µm, n = 15) width, branched, septate, anastomosing. Sexual morph: Not observed. Asexual morph: *Coelomycetous*. *Conidiomata* 500–860 µm ($\bar{x}$ = 727 µm, n = 20) high, pycnidial, elongate, superficial, solitary or gregarious, sometimes accrete with two pycnidia, blackish brown, with a longstalk measuring 174–575 × 26–47 µm ($\bar{x}$ = 404 × 33 µm, n = 20), a lengthened neck, 120–250 µm ($\bar{x}$ = 197 µm, n = 20) in height, 16–26 µm ($\bar{x}$ = 21 µm, n = 20) diameter, swollen in the middle or two-thirds of the pycnidium, the swollen area producing conidia inside. *Ostiole* 4–8 µm ($\bar{x}$ = 6.3 µm, n = 10) diameter, with a fimbriate apex, 15–35 × 2.5–4 µm ($\bar{x}$ = 28.1 × 3.3 µm, n = 20). *Conidiomata in swollen part* 99–135 × 37–57 µm ($\bar{x}$ = 115 × 45 µm, n = 20), ellipsoid, bearing hyaline, continuous conidia. *Conidiomatal wall* 7–11 µm ($\bar{x}$ = 9.2 µm, n = 20), consisting of 2–4-layers of pale brown to dark brown, thick-walled cells of *textura angularis*. *Conidia* 5–6 × 2–3 µm ($\bar{x}$ = 5.5 × 2.8 µm, n = 60), hyaline, cylindrical to oblong, aseptate, ends round, smooth-walled.

Culture characteristics – Germinated conidia in water at 25–28°C for 12 h, and the germinating tube formed from both ends of the spore. *Colonies* on PDA slow growing, reaching 1.5 cm diameter after 16 days, superficial, erumpent, with entire edge, gray to gray-green, olivaceous in reverse.

Material examined – China, Sichuan Province, Chengdu City, Chongzhou City, Tianzi Mountain, 103°31′31.19″E 30°48′49.57″N, 851 m, isol. from leaves of *Cinnamomum japonicum*, 1 May 2021, C.L. Yang, YCL202105004 (SICAU 23-0150, holotype), ex-type culture (SICAUCC 23-0100). *ibid.* YCL202105004-2 (SICAU 23-0152), living culture SICAUCC 23-0135.

GenBank numbers – SICAUCC 23-0100 = LSU: PP732745, ITS: PP736390, *rpb*2: PP782090, *tef*1-α: PP779591. SICAUCC 23-0135 = LSU: PP732746, ITS: PP736391, *rpb*2: PP782091, *tef*1-α: PP779592

Notes – Phylogenetic analysis placed *Conidiocarpus cinnamomeus* as a new taxon in *Conidiocarpus*, which is closest to *C. siamensis* (MFLUCC 10-0061) and another two strains of *Conidiocarpus* sp. (CPC 20464 and CPC 20468) with 89% MLBS / 1.00 BYPP support, positioned at the basal of *Conidiocarpus* clade (Fig. 13). The comparative analysis of sequences between *C. cinnamomeus* (SICAUCC 23-0100) and *C. siamensis* (MFLUCC 10-0061) revealed a 98.1% similarity (413/421 bp, 0 gap) in the ITS and a 98.07% similarity (865/882 bp, 0 gap) in the LSU. Morphologically, *C. cinnamomeus* differs from *C. fici-septicae* (MFLUCC 19-0072, holotype) by larger conidiomata (500–860 µm vs. 240–280 µm) and larger conidia (5–6 × 2–3 µm vs. 4–5 × 1–2 µm) (Tennakoon et al. 2021). *Conidiocarpus cinnamomeus* differs from *C. caucasicus* (MFLUCC 10-0064) by the latter having smaller conidiomata (500–860 µm vs. 378–458 µm) with shorter stalks (174–575 µm vs. 22–31 µm) and larger ostiole (4–8 µm vs. 9–15 µm) (Chomnunti et al. 2011). Nevertheless, morphological comparison with *C. siamensis* (MFLUCC 10-0061) was unfeasible due to the absence of a comprehensive morphological description for this particular strain. The PHI test also showed that no significant recombination events between *C. cinnamomeus* and closely phylogenetically related species occurred (Fig. 14). Thus, taking into account its morphological characteristics, phylogenetic analysis, nucleotide polymorphism comparison, and the results of the pairwise homoplasy index ($\Phi w > 0.05$) test, *C. cinnamomeus* is described here as a new species.

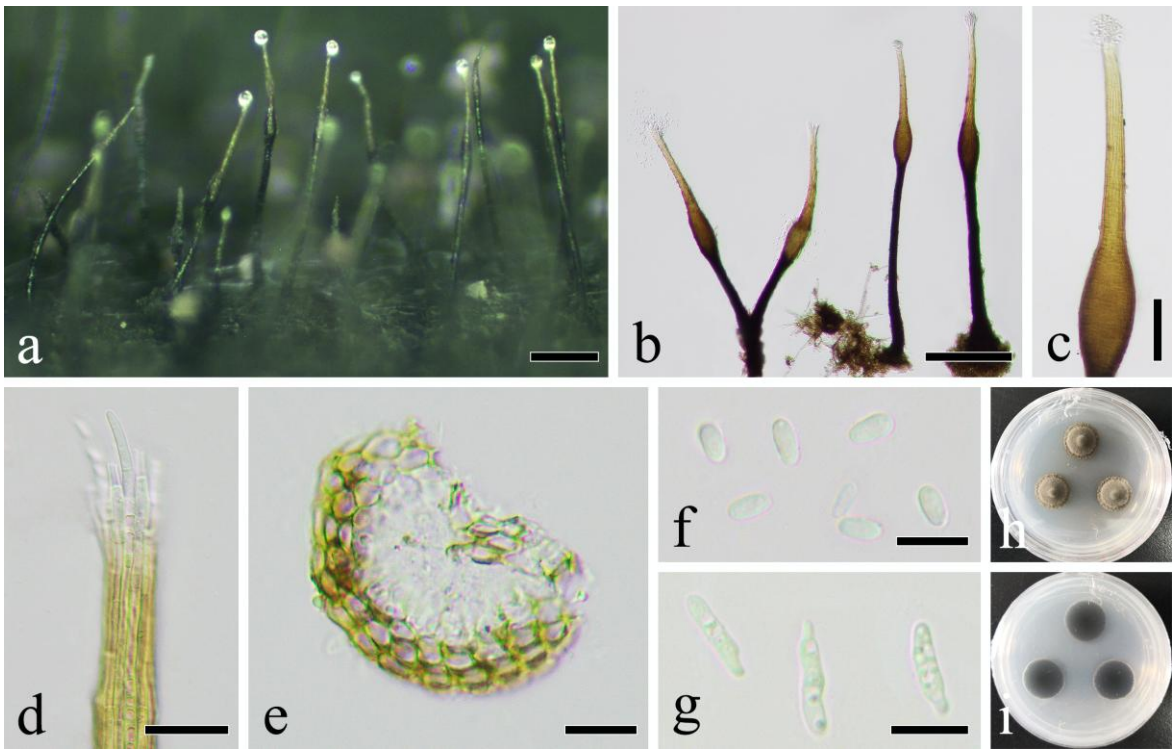

Figure 12 – *Conidiocarpus cinnamomeus* (holotype, SICAU 23-0150). a Conidiomata formed on the leaf surface. b, c Conidiomata. d Ostiolar neck. e Conidiomatal wall of swollen part. f Conidia. g Germinating conidia. h Front view of colony on PDA. i Reverse view of colony on PDA. Scale bars: a, b = 200 µm, c = 50 µm, d = 20 µm, e–g = 10 µm.

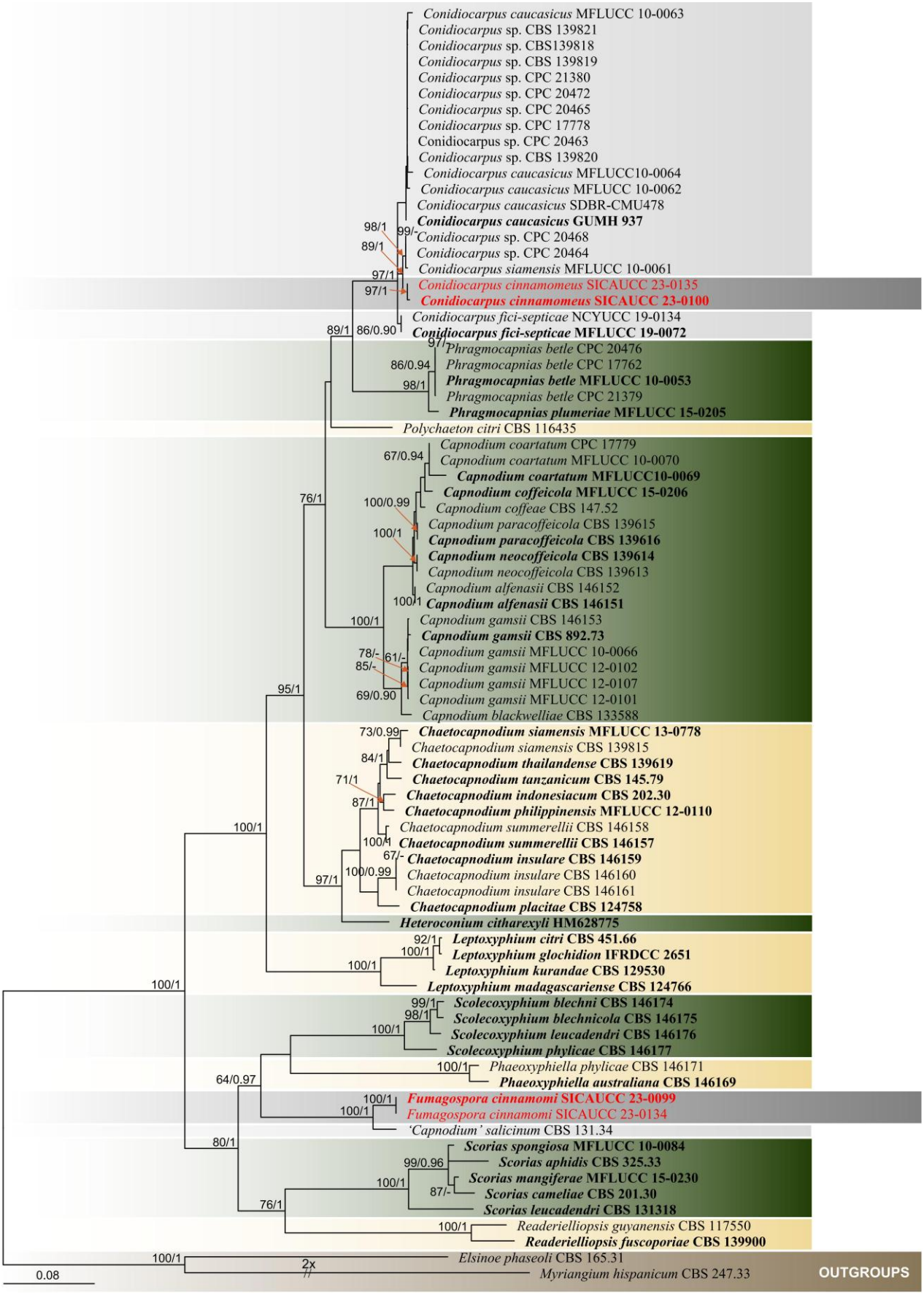

Figure 13 – Phylogram derived from maximum likelihood analyses of a combined dataset comprising LSU, ITS, *rpb*2, and *tef*1-α sequences dataset representing the species of *Capnodiaceae* and *Readerielliopsidaceae*. The phylogenetic analysis included 79 strains, which comprised 3,467

characters (LSU: 1–860, ITS: 861–1,393, *rpb*2: 1,394–2,484, *tef*1-α: 2,485–3,467) after alignment. The tree is rooted to *Elsinoe phaseoli* (CBS 165.31) and *Myriangium hispanicum* (CBS 247.33). Single-gene analyses were conducted, resulting in similar tree topologies between the ML and BY methods, ensuring consistent comparisons of clade stability. The best-scoring RAxML tree with a final likelihood value of -26,750.486737 is presented. The matrix had 1,393 distinct alignment patterns, with 21.22% of undetermined characters or gaps. Estimated base frequencies were as follows: A = 0.245237, C = 0.261262, G = 0.273510, T = 0.219991; substitution rates AC = 1.485800, AG = 4.233052, AT = 1.955834, CG = 1.276912, CT = 9.533639, GT = 1.000000. Bootstrap support values for maximum likelihood (MLBS) ≥ 60%, and Bayesian posterior probabilities (BYPP) ≥ 0.90 are indicated at the nodes, respectively. The ex-type strains are in bold, and the new isolate is in red. Bar = 0.08 estimated number of nucleotide substitutions per site per branch.

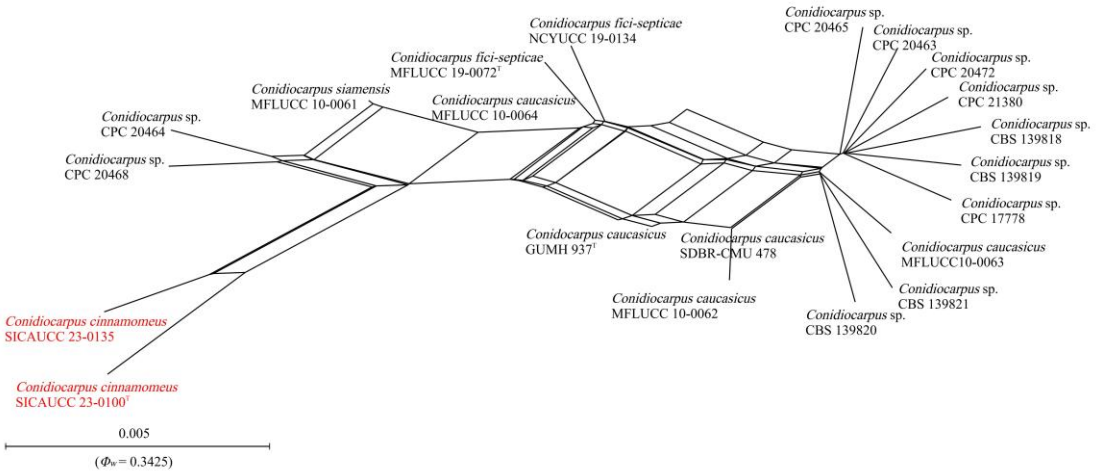

Figure 14 – The splits graph from the pairwise homoplasy index (PHI) test generated from the concatenated gene set of ITS, LSU, *rpb*2, and *tef*1-α sequence data of closely related species of *Conidiocarpus* using both LogDet transformation and splits decomposition. PHI test results (Φw) < 0.05 indicate significant recombination within the dataset. The ex-type strains are denoted by "T" and the new isolates of this study are in red.

Readerielliopsidaceae Abdollahz. & Crous

Notes – *Readerielliopsidaceae* was introduced by Abdollahzadeh et al. (2020) to accommodate *Fumagospora*, *Phaeoxyphiella*, *Readerielliopsis*, *Scolecoxyphium*, and *Scorias*, with *Readerielliopsis* as its prototype genus. Presently, 37 species from six genera viz. *Alloscorias, Fumagospora*, *Phaeoxyphiella*, *Readerielliopsis*, *Scolecoxyphium*, and *Scorias* are accepted in the family (Haituk et al. 2020, Wijayawardene et al. 2022).

Fumagospora G. Arnaud.

Notes – *Fumagospora* was introduced by Arnaud (1911) with *F. capnodioides* as the type species. *Fumagospora* is recognized as the asexual morph of certain *Capnodium* species, exemplified by *C. salicinum*, characterized by initially hyaline and continuous conidia that later become brown and transversely septate, featuring one or more longitudinally septate cells (Hughes, 1976). Abdollahzadeh et al. (2020) documented that *C. salicinum* (CBS 131.34) forms a distinct clade within *Readerielliopsidaceae*, separate from other *Capnodium* species. In a study investigating capnodiaceous sooty molds in Iran, Khodaparast et al. (2020) conducted a phylogenetic analysis using ITS sequence data, positioning isolate GUM 1315, which exhibited *Fumagospora* morphology, close to *C. salicinum* (CBS 131.34). Consequently, Abdollahzadeh et al. (2020) designated the generic name *Fumagospora* to this particular clade. In this paper, a novel

taxon *F. cinnamomi* is introduced based on the evidence of phylogenetic analysis, and constitutes the inaugural documentation of the sexual morph of *Fumagospora*.

7. *Fumagospora cinnamomi* X.Y. Li & C.L. Yang, sp. nov. Fig. 15

MycoBank number: MB900660; Facesoffungi number: FoF15925

Etymology – Refers to the host genus *Cinnamomum*, where the species collected.

Holotype – SICAU 23-0117

Associated with dark mildew on leaves of *Cinnamomum japonicum*, growing on the surface of the host's leaves, symptoms appeared as dark mildew on the leaves accompanied by the formation of ascomata randomly distributed throughout the leaves. *Thallus* thin, dark brown to black, easily removed from the leaf surface, composed of cylindrical, vegetative mycelia. *Superficial hyphae* 4–9 μm ($\bar{x}$ = 6.6 μm, n = 40) width, branched, septate, usually constricted at the septum, pale brown to brown, and the hypha often gathered into bundles with swollen cells to different degrees. Sexual morph: *Ascomata* 68–114 × 79–140 μm ($\bar{x}$ = 96 × 110 μm, n = 10), superficial, solitary, sometimes gathered, globose, dark brown to black, ostiole present at maturity with periphysis. *Ascomatal setae* absent. *Peridium* 7–20 μm ($\bar{x}$ = 13.4 μm, n = 20), consisting of 2–4-layers of pale brown, thick-walled cells of *textura angularis*. *Hamathecium* lacking pseudoparaphyses. *Asci* 54–77(–103) × 20–35 μm ($\bar{x}$ = 66 × 28 μm, n = 20), 8-spored, bitunicate, fissitunicate, subcylindrical to obovoid, short pedicellate or apedicellate, ocular chamber indistinct. *Ascospores* 19.5–32 × 8–11 μm ($\bar{x}$ = 24.8 × 9.3 μm, n = 50), hyaline, subfusiform, overlapping seriate, dictyoseptate, 5 trans-septate, the upper three cells wider than the lower cells, distinctly constricted at the third septum, guttulate, surrounded by a mucilaginous sheath, 12–27 μm ($\bar{x}$ = 18 μm, n = 30) thick in one side. Asexual morph: Not observed.

Culture characteristics – Germinated ascospores formed after 12 h, and the germinating tube grows from each cell of the spore. *Colonies* on PDA attaining 30-35 mm diameter in 30 days, dense, subcircular, crenated, coriaceous, olivaceous on the front, aerial mycelium infrequent, reverse dull green.

Material examined – China, Sichuan Province, Chengdu City, Chongzhou City, Tianzi Mountain, 103°31′31.19″E 30°48′49.57″N, 851 m, isol. from leaves of *Cinnamomum japonicum*, 1 May 2021, C.L. Yang, YCL202105003 (SICAU 23-0117, holotype), ex-type culture (SICAUCC 23-0099). *ibid.* YCL202105003-2 (SICAU 23-0153), living culture SICAUCC 23-0134.

GenBank numbers – SICAUCC 23-0099 = LSU: PP732743, ITS: PP736388, *rpb2*: PP782088, *tef*1-α: PP779589. SICAUCC 23-0134 = LSU: PP732744, ITS: PP736389, *rpb2*: PP782089, *tef*1-α: PP779590.

Notes – In the phylogenetic analyses, the new isolate *Fumagospora cinnamomi* (SICAUCC 23-0099) clustered closely with *Capnodium salicinum* (CBS 131.34), forming a distinct clade which is separate from the core *Capnodium* clade in *Capnodiaceae*, with full bootstrap support (100% MLBS / 1.00 BYPP). Abdollahzadeh et al. (2020) demonstrated that this clade, which includes *C. salicinum* (CBS 131.34) and isolates exhibiting *Fumagospora* morphology, forms a distinct lineage separate from *Capnodium sensu stricto*, leading to the designation of *Fumagospora* as a generic name for this clade. Sequence comparison between *F. cinnamomi* (SICAUCC 23-0099) and *C. salicinum* (CBS 131.34) showed 94.37% (822/871 bp, 0 gap) similarity in *rpb2*, 96.65% (893/924 bp, 0 gap) similarity in *tef*1-α, 98.25% (449/457 bp, 1 gap) similarity in ITS and 99.53% (845/849 bp, 0 gap) similarity in LSU. This genetic divergence, in conjunction with its phylogenetic placement within *Readerielliopsidaceae*, strongly supports the classification of this isolate as a novel species within *Fumagospora*. Thus, we propose *F. cinnamomi* as a new species, based on both phylogenetic analyses and sequence divergence data, and contributing the first known sexual morph for the genus.

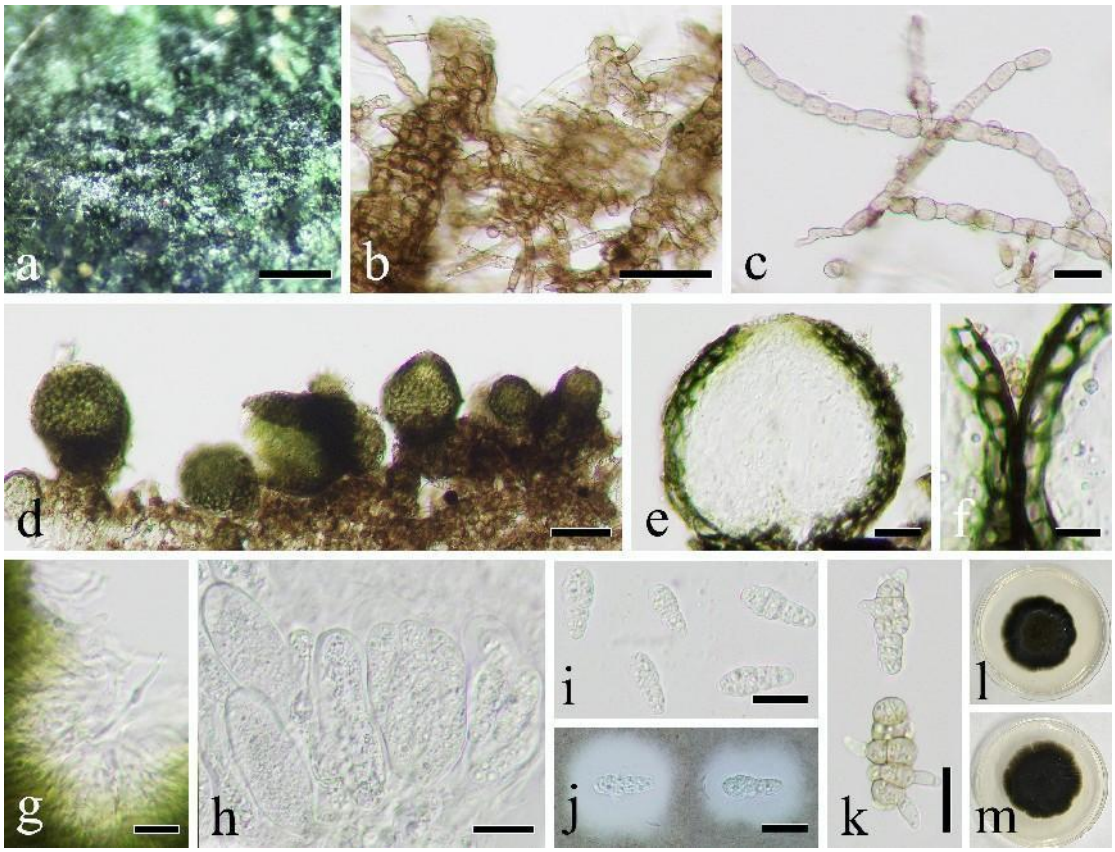

Figure 15 – *Fumagospora cinnamomi* (holotype, SICAU 23-0117). a Appearance of ascomata on the leaf. b, c Superficial hyphae. d Ascomata. e Cross-section of ascoma. f Peridium. g Hamathecium. h Asci. i Ascospores. j Ascospores with a mucilaginous sheath in ink. k Germinating ascospores in sterilized water after 12 h. l Front view of colony on PDA. m Reverse view of colony on PDA. Scale bars: a = 300 μm, b, d = 50 μm, c, e, h–k = 20 μm, f, g = 10 μm.

Cladosporiales Abdollahz. & Crous

Notes – *Cladosporiales* was established by Abdollahzadeh et al. (2020) through phylogenetic analyses, to incorporate the *Cladosporiaceae* family. This monophyletic order exhibits many lifestyles, such as saprobic, endophytic, fungicolous, lichenicolous, human, and plant pathogens (Bensch et al. 2012, Abdollahzadeh et al. 2020).

Cladosporiaceae Chalm. & R.G. Archibald

Notes – *Cladosporiaceae* is a monophyletic family in *Cladosporiales*, with *Cladosporium* as the type genus. Originally, *Cladosporiaceae* was classified within *Capnodiales* (Schoch et al. 2006). However, subsequent phylogenetic studies have consistently identified members of *Cladosporiaceae* as a separate, distinct clade, separate from *Capnodiaceae*, *Mycosphaerellaceae*, and related families (Crous et al. 2009b, Schoch et al. 2009, Suetrong et al. 2009, Hyde et al. 2013, Videira et al. 2017, Abdollahzadeh et al. 2020). *Cladosporiaceae* species are primarily saprobic and endophytic, with some species that exhibit fungicolous, lichenicolous, aquatic, or pathogenic lifestyles (Heuchert et al. 2005, Sandoval-Denis et al. 2016, Marin-Felix et al. 2017, Lee et al. 2023). The *Cladosporiaceae* family currently comprises eight genera with around 300 species, namely *Acroconidiella*, *Cladosporium*, *Davidiellomyces*, *Graphiopsis*, *Neocladosporium*, *Rachicladosporium*, *Toxicocladosporium*, and *Verrucocladosporium* (Wijayawardene et al. 2022).

Cladosporium Link

Notes – *Cladosporium* was established by Link (1816) with *C. herbarum* as the type species. *Cladosporium* is considered as one of the largest genera among dematiaceous hyphomycetes,

characterized by the typical formation of conidia in branched chains, facilitating their effortless dispersion in the environment (Abdollahzadeh et al. 2020). *Cladosporium* species exhibit a widespread global distribution, having been isolated from diverse substrates, including the atmosphere, marine, soil, dung, plants, food, debris, textiles, paint, and other materials (Temperini et al. 2018, Chung et al. 2019, Iturrieta-González et al. 2023, Lee et al. 2023, Yang et al. 2023). Members of *Cladosporium* inhabit diverse ecological niches, encompassing roles as saprophytes, endophytes, hydrophytes, phytopathogens, animal pathogens, and hyperparasites (Hamayun et al. 2009, Sandoval-Denis et al. 2015, Zambelli et al. 2015, Anderson et al. 2016, Marin-Felix et al. 2017, Iturrieta-González et al. 2021). *Cladosporium* is a monophyletic genus in *Cladosporiaceae*, whose species are distinguished by their specialized conidiophores producing acropetal chains of conidia from mono- or polyblastic conidiogenous cells. Both the conidiogenous cells and conidia display conidiogenous loci (scars) with a unique coronate structure, characterized by a central convex dome surrounded by a raised periclinal rim, usually thickened, refractive and dark (David 1997, Iturrieta-González et al. 2021).

8. *Cladosporium guizhouense* S.Y. Wang, Yong Wang bis & Yan Li, MycoKeys 91: 160 (2021) Fig. 16

MycoBank number: MB842407; Facesoffungi number: FoF15881

Associated with leaf blight on leaves of *Euonymus* sp. Sexual morph: Not observed. Asexual morph: *Hyphomycetous*. *Mycelium* sparse, mainly immerse, often forming leaf spots with abundant sporulation on the reverse. *Conidiophores* 65–340 × 4–8.9 μm ($\bar{x}$ = 160.7 × 6.4 μm, n = 50), usually gathered, sometimes scattered, macronematous, mainly arising from swollen hyphal cells, erect, straight or flexuous, cylindrical-oblong, slightly shorter in diameter towards the apex, non-nodulose, rarely branched, 3–12-septate, without constricted at septa, olivaceous or olivaceous brown, more or less thickened walled, especially towards the base of conidiophores. *Conidiogenous cells* 10.5–27 × 4–7 μm ($\bar{x}$ = 16.5 × 5 μm, n = 30), integrated, terminal or pleurogenous, cylindrical-oblong, 0-3-septate, non-nodulose, with 1–3 apically crowed loci, conspicuous, 0.5–3 μm diameter, thickened and somewhat darkened conidiogenous loci. *Ramoconidia* 7.5–16 × 4–6 μm ($\bar{x}$ = 11.7 × 4.6 μm, n = 20), cylindrical-oblong, 0–1-septate, pale olivaceous, smooth, base truncate. *Conidia* numerous, catenate, forming short branched chains in all directions, 0–1-septate. *Small terminal conidia* 4–9 × 3–5 μm ($\bar{x}$ = 6.1 × 3.7 μm, n = 50), globose, subglobose or ovoid to obovoid, apex rounded or somewhat attenuated. *Intercalary conidia* 7–11 × 4–5 μm ($\bar{x}$ = 7.9 × 4.3 μm, n = 20), limoniform to ellipsoid, 0–1-septate, with 1–2 (–3) distal hila. *Secondary ramoconidia* sparsely forming. *Hila* conspicuous, 1–2 μm diameter. *Microcyclic conidiogenesis* occasionally occurring.

Culture characteristics – *Colonies* on PDA attaining 25–35 mm diameter in a week, greyish white to grey, colony slightly wrinkled, powdery to fluffy, sporulation profuse, without prominent exudates, reverse olivaceous to olivaceous brown, pale green to greyish white towards margins, deep radially fissures. *Colonies* on MEA reaching 30–40 mm diameter after a week, greyish white, white towards margins, colony wrinkled and folded, radially furrowed, sporulation profuse, without prominent exudates, reverse olivaceous, margin white. *Colonies* on OA reaching 30–40 mm diameter after a week, greyish green with profuse sporulation, reverse olivaceous, without exudates. *Colonies* on SNA reaching 15–25 mm after a week, pale green, aerial mycelium scanty, loose, sporulation medium, reverse pale green, without exudates.

Material examined – China, Sichuan Province, Ya'an City, Tianquan County, Renyi Town, Lijia Village, 102°47′40.01″E 30°5′46.35″N, 820 m, isol. from leaves of *Euonymus* sp., 11 Jun. 2020, C.L. Yang, YCL202006005 (SICAU 23-0135), culture (SICAUCC 23-0114).

GenBank numbers – SICAUCC 23-0114 = ITS: PP736365, *act*: PP782106, *tef*1-α: PP779570

Notes – In the phylogenetic analysis (Fig. 17), the new strain SICAUCC 23-0114 clustered within a clade alongside *Cladosporium guizhouense* (GUCC 401.7, holotype) with 87% support in MLBS and 1.00 support in BYPP, maintaining consistency with the morphological characteristics described in the type description (Wang et al. 2022a). A comparison of the ITS, *act*, and *tef*1-α nucleotides between *C. guizhouense* and the new strain (SICAUCC 23-0114) showed no nucleotide

differences for ITS and *act*, while there were slight variations of 0.4% and 1.72% in *tef*1-α when compared to GUCC 401.8 and GUCC 401.7, respectively. The newly collected specimen is tentatively classified as a new strain of *C. guizhouense* based on both morphological characteristics and phylogenetic analysis (Chethana et al. 2021, Jayawardena et al. 2021a).

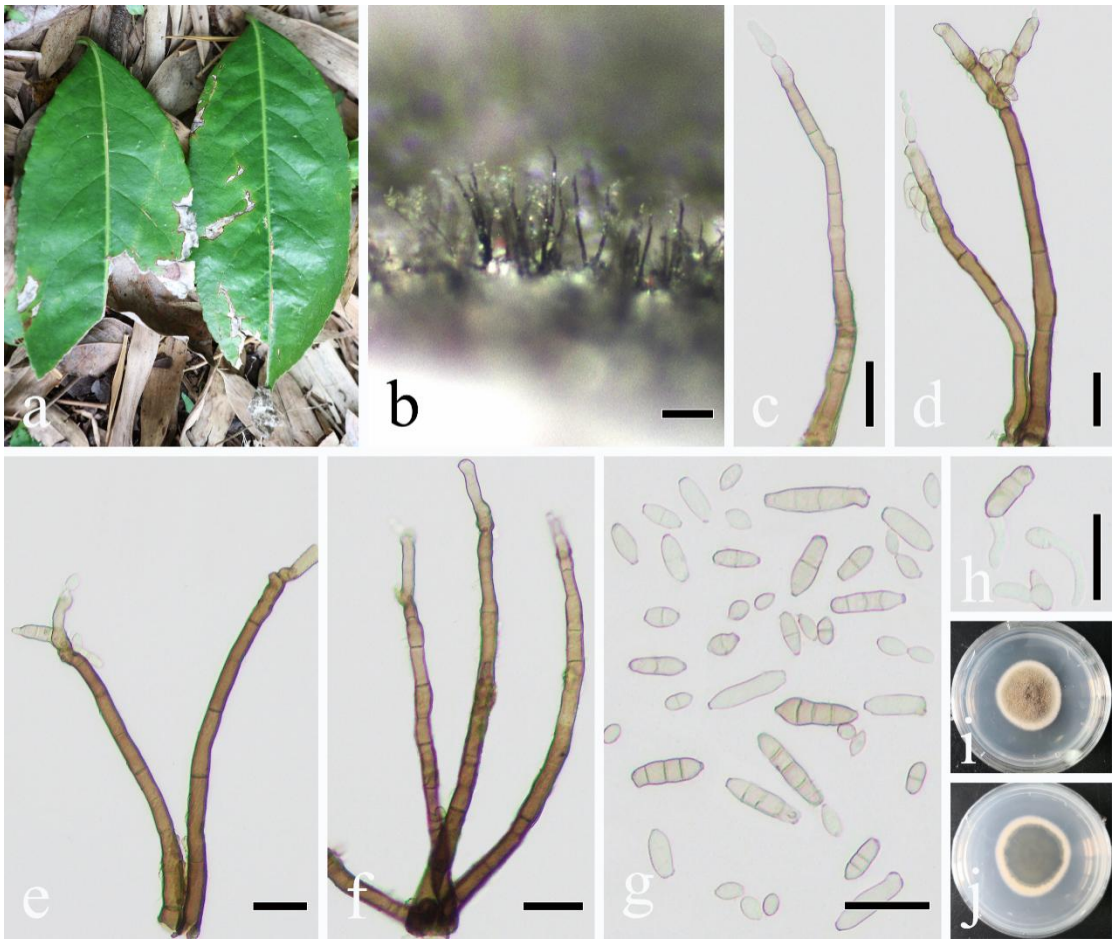

Figure 16 – *Cladosporium guizhouense* (SICAU 23-0135). a Symptoms on the leaves. b Appearance of conidiogenesis. c–f Conidiophores. g All types of conidia. h Germinating conidia in sterilized water after 12 h. i Front view of colony on PDA. j Reverse view of colony on PDA. Scale bars: b = 100 μm, c–h = 20 μm.

9. *Cladosporium viciae* X.L. Xu & C.L. Yang, sp. nov. Fig. 18

MycoBank number: MB902141; Facesoffungi number: FoF15919

Etymology – Refers to the host genus *Vicia*, where the species collected.

Holotype – SICAU 23-0134

Associated with black spots on pods of *Vicia faba* L. Sexual morph: Not observed. Asexual morph: *Hyphomycetous*. *Mycelium* scanty, superficial or immersed, pale to olivaceous brown, often forming raised, black-dark lesions on the surface with abundant sporulation. *Conidiophores* 20–440 × 2–7 μm ($\bar{x}$ = 152 × 4.1 μm, n = 30), macronematous, erect, stipes, arising terminally and laterally from hyphae or mainly from swollen hyphal cells, occasionally branched, non-nodulose, straight or medium flexuous, slightly attenuated towards the apex, 0–10-septate, pale to olivaceous brown, lighter in color towards the apex, smooth, walls unthicken to slightly thickened. *Conidiogenous cells* 7–32 × 3–6 μm ($\bar{x}$ = 14.7 × 4.7 μm, n = 30), integrated, terminal or lateral, cylindrical-oblong, 0–3-septate, with (1–) 2–4 distal conidiogenous loci, crowded at or towards the apex, sometimes slightly geniculate, conidiogenous loci conspicuous, 0.5–3 μm diameter. *Ramoconidia* 9–14 × 4–5 μm ($\bar{x}$ = 11.8 × 4.8 μm, n = 20), cylindrical-oblong, 0–1-septate, base broadly truncate. *Conidia* numerous, formed in branched chains, branching in all directions. *Small terminal conidia* 4–8 × 3–

6 µm ($\bar{x}$ = 5.6 × 4.3 µm, n = 50), obovoid or ellipsoid, apex rounded. *Intercalary conidia* 6–11 × 3–6 µm ($\bar{x}$ = 7.6 × 4.4 µm, n = 30), ellipsoid, limoniform or fusiform, 0–1-septate, with 1–2 distal hila. *Secondary ramoconidia* 7–12 × 4–7 µm ($\bar{x}$ = 9.3 × 5.2 µm, n = 20), cylindrical-oblong, 0–1-septate, with 1–3 distal hila, pale olivaceous or pale olivaceous brown, smooth. *Hila* conspicuous, 0–1 µm diameter, somewhat thickened. *Microcyclic conidiogenesis* occasionally occurs.

Culture characteristics – *Colonies* on PDA attaining 30–40 mm diameter in 1 week, olivaceous to olivaceous grey, greyish white towards margins, powdery to fluffy, sporulation profuse, without prominent exudates, reverse olivaceous, pale green to greyish white towards margins, deep radially fissures. *Colonies* on MEA reaching 40–50 mm diameter after 1 week, grey to grey olivaceous, greyish white towards margins, colony wrinkled and folded, radially furrowed, sporulation profuse, without prominent exudates, reverse olivaceous, margin white. *Colonies* on OA reaching 20–30 mm diameter after 1 week, grey olivaceous with profuse sporulation, reverse olivaceous, without exudates. *Colonies* on SNA reaching 10–15 mm after 1 week, grey olivaceous to olivaceous, aerial mycelium scanty, loose, sporulation medium, reverse olivaceous, without exudates.

Material examined – China, Sichuan Province, Neijiang City, Zizhong County, Huaxiang Village, 104°49′19.66″E 29°46′28.29″N, 316 m, isol. from pods of *Vicia faba*, 6 Apr. 2020, C.L. Yang & X.L. Xu, XXL202004001 (SICAU 23-0134, holotype), ex-type culture (SICAUCC 20-0009). *ibid.* XXL202004001-2 (SICAU 23-0154), living culture SICAUCC 23-0131.

GenBank numbers – SICAUCC 20-0009 = ITS: PP736376, *act*: PP782109, *tef*1-α: PP779577. SICAUCC 23-0131 = ITS: PP736377, *act*: PP782110, *tef*1-α: PP779578

Notes – The placement of *Cladosporium viciae* closely resembled its proximity to *C. magnoliigena* and *C. eucommiae*, forming a well-supported clade (99% MLBS / 1.00 BYPP) (Fig. 17). In comparing DNA base composition with the type strains of *C. magnoliigena* and *C. eucommiae*, no differences were found in the ITS and *act* regions (*act* data unavailable for *C. magnoliigena*), but 15/228 (6.58%) and 14/235 (5.96%) base differences were identified in the *tef*1-α region, after excluding unaligned sequences at both ends. The pairwise homoplasy index (PHI) test indicated that there was no significant evidence of recombination (Φ_w = 0.9778) between *C. viciae* (SICAUCC 20-0009 and SICAUCC 23-0131) and the related taxa, including *C. magnoliigena* (MFLUCC 18-1557 and MFLUCC 18-1559), *C. eucommiae* (GUCC 401.1), *C. yunnanense* (CGMCC 3.20622), and *C. proteacearum* (BRIP 72301a) (Fig. 19). *Cladosporium magnoliigena* is characterized by numerous small prominent exudates on MEA and uniformly colored olivaceous-brown conidiophores, whereas *C. viciae* lacks these exudates and exhibits uneven coloring with a lighter apex. *Cladosporium magnoliigena* has shorter conidiophores (50–150 × 3–4.5 µm vs. 20–440 × 2–7 µm), slightly smaller conidia (4.2–5.5 × 2–5 µm vs. 4–11 × 3–6 µm), and more septate secondary ramoconidia (0–3-septate vs. 0–1-septate) (Jayasiri et al. 2019). In comparison to *C. viciae*, *C. eucommiae* typically possesses branched conidiophores, shorter conidiophores (7–198 µm × 2.5–4.5 µm vs. 20–440 µm × 2–7 µm), and longer aseptate secondary ramoconidia (5–25 µm × 2.5–4.0 µm vs. 7–12 µm × 4–7 µm) (Wang et al. 2022a). Therefore, *C. viciae* was proposed as a novel species.

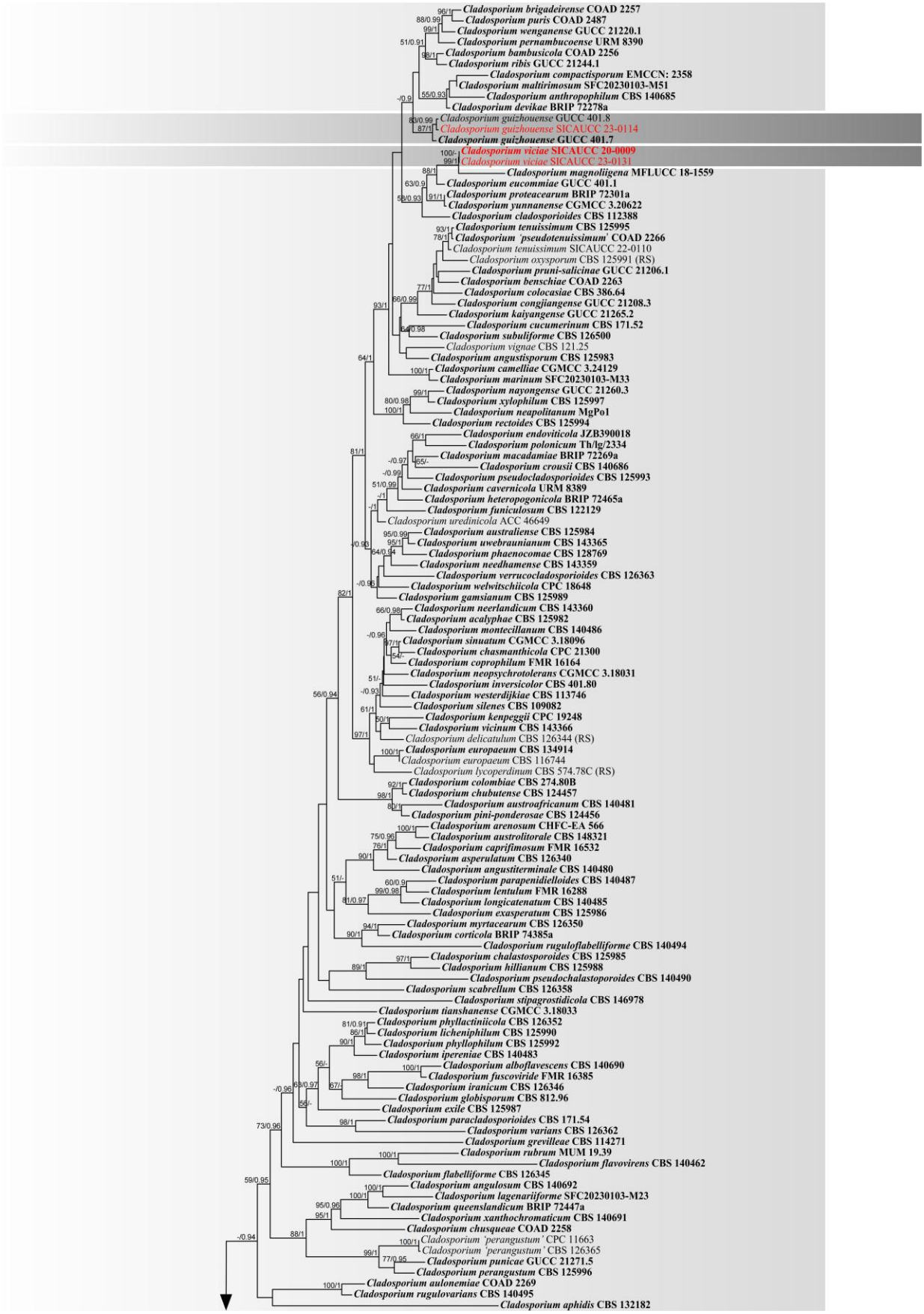

Figure 17 – Continued.

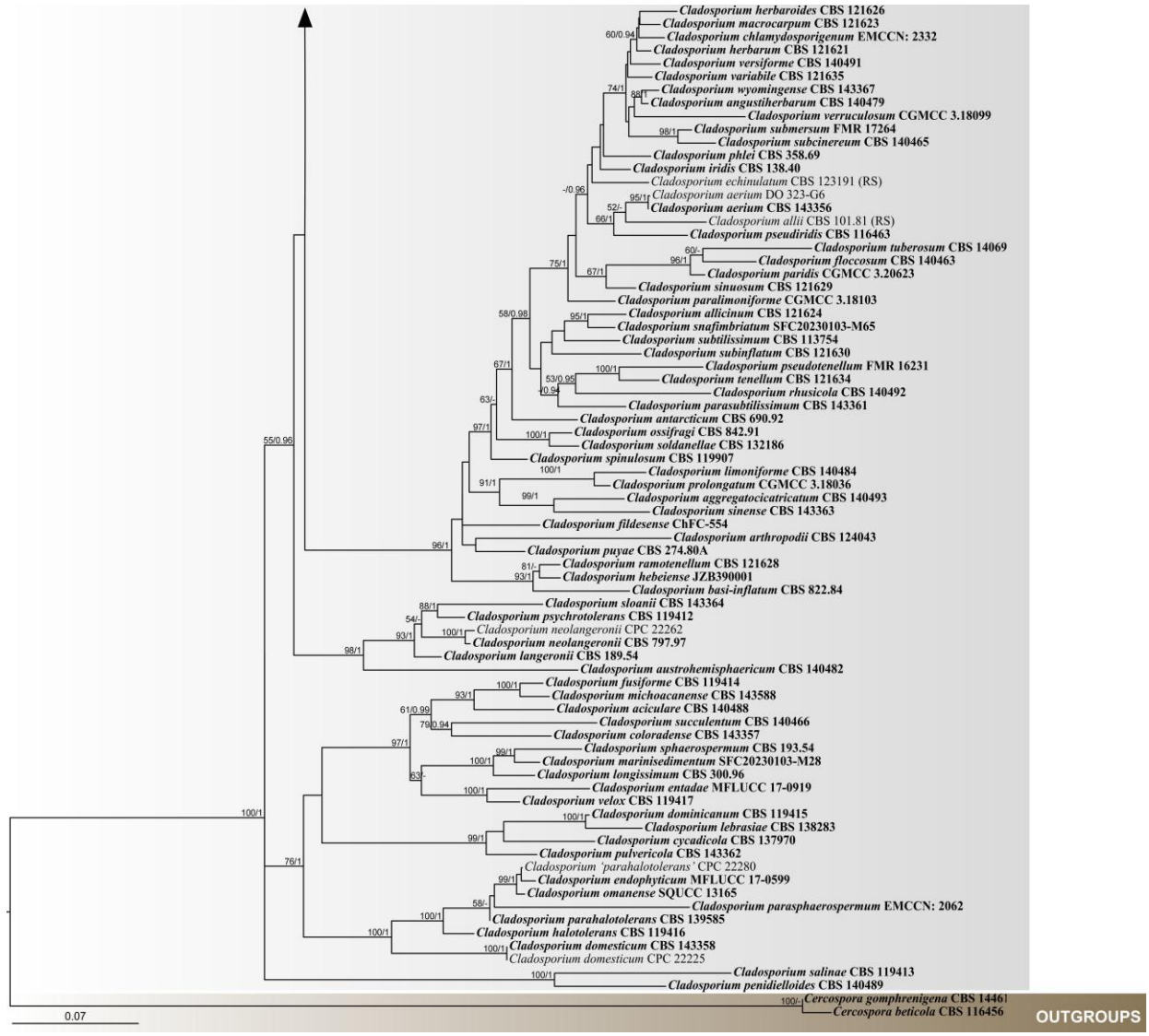

Figure 17 – Phylogram derived from maximum likelihood analyses of a combined dataset comprising ITS, *act*, and *tef*1-α sequence dataset for *Cladosporium* species. One hundred and ninety-six strains were collected in the molecular analysis, comprising 3,477 characters (ITS: 1–1,611, *act*: 1,612–2,302, *tef*1-α: 2,303–3,477) including alignment gaps. *Cercospora beticola* (CBS 116456) and *Ce. gomphrenigena* (CBS 144613) were regarded as the outgroup taxa. Single-gene analyses were performed and yielded similar tree topologies between the ML and BY methods, ensuring consistency in clade stability comparisons. The best-scoring RAxML tree with a final likelihood value of -37,935.774016 is presented. The matrix had 1,576 distinct alignment patterns, with 66.12% of undetermined characters or gaps. Estimated base frequencies were as follows: A = 0.232515, C = 0.289849, G = 0.249626, T = 0.228010; substitution rates AC = 1.819495, AG = 3.325059, AT = 1.668114, CG = 1.101089, CT = 5.579851, GT = 1.000000. ML bootstrap support equal or greater than 50%, and Bayesian posterior probabilities (BYPP) equal or greater than 0.90 are given near each branch. New isolates are highlighted in red. Strains from the holotype, epitype, and neotype are indicated in bold. "RS" means reference specimens.

Figure 18 – *Cladosporium viciae* (holotype, SICAU 23-0134). a Symptoms on the pods. b A spherical projection on the surface of pod. c Cross-section of projection in dissecting microscope. d–h Conidiophores. i All types of conidia. j Germinating conidia in sterilized water after 12 h. k Front view of colony on PDA. l Reverse view of colony on PDA. Scale bars: b, c = 500 μm, d–j = 20 μm.

Mycosphaerellales (Nannf.) P.F. Cannon

Notes – *Mycosphaerellales* originated from *Mycosphaerellineae* within *Pseudosphaeriales* and later evolved into an independent taxonomic order as confirmed by molecular analysis (Abollahzadeh et al. 2020). *Mycosphaerellales* represent a substantial assemblage within the class *Dothideomycetes*, encompassing approximately 4,500 species distributed across an impressive array of 230 genera (Wijayawardene et al. 2022). *Mycosphaerellales* species inhabit many ecological niches, including saprotrophs, ectophytes, plant pathogens, and lichen-forming fungi, showcasing their remarkable ecological diversity (Jayawardena et al. 2023).

Mycosphaerellaceae Lindau

Notes – *Mycosphaerellaceae* was erected by Lindau (1897) with *Mycosphaerella* as the type genus. This family is notably expansive, with approximately 125 accepted genera, making it one of the most extensive families in taxonomic group (Videira et al. 2017, Bakhshi & Braun 2022, Wijayawardene et al. 2022, Yadav et al. 2022, 2023). *Mycosphaerellaceae* members vary in lifestyle, *viz.* parasitic, endophytic, saprobic, epiphytic, lichenous, and fungicolous (Hyde et al. 2013, Videira et al. 2017, Kushwaha et al. 2020). Some species of *Mycosphaerellaceae* are

quarantine-regulated due to the destructive impact on crops or forest plants, such as *Lecanosticta acicola*, *Mycodiella laricis-leptolepidis*, *Pseudocercospora pini-densiflorae*, and *Sphaerulina musiva* (Quaedvlieg et al. 2012, 2013, Jeger et al. 2018, Zhao et al. 2021). The family *Mycosphaerellaceae* consistently appears polyphyletic, indicating that a more comprehensive framework and phylogeny for the family are still required.

Exosporium Link

Notes – *Exosporium* was introduced by Link (1809) with *E. tiliae* as the generic type. *Exosporium*, once considered a synonym of *Helminthosporium* due to morphology or phylogeny, exemplifies polyphyletic within the group (Fries 1832, Voglmayr & Jaklitsch 2017). *Exosporium* species are dematiaceous hyphomycetes with diverse lifestyles, including phytopathogenic, saprobic, and endophytic modes, and they exhibit a wide distribution (Zhao & Zhao 2012, Singh et al. 2015, Videira et al. 2017). There are about 42 recognized species in this genus, but additional evidence is required to clarify the status of related species, with molecular data lacking for many of them (Singh et al. 2015, Videira et al. 2017). *Exosporium* members are characterized by macronematous, mononematous, often caespitose, unbranched or branched, mid to dark brown or olivaceous brown, smooth or verruculose conidiophores, polytretic, integrated, terminal, becoming intercalary, sympodial, cylindrical or clavate, cicatrized conidiogenous cells, usually solitary, short catenate, acropleurogenous, simple conidia, with mostly obclavate, pale to dark brown or olivaceous brown, smooth, verrucose or echinulate, distoseptate, generally with a thick, dark hilum at the base (Ellis 1961, Videira et al. 2017).

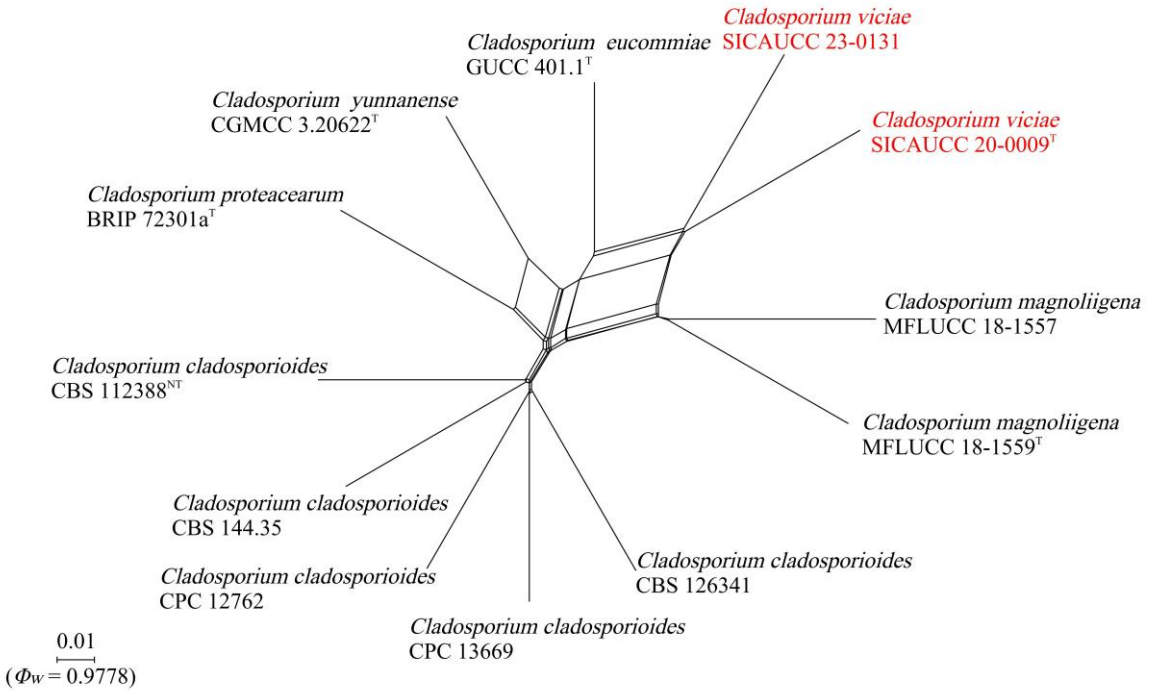

Figure 19 – The splits graph from the pairwise homoplasy index (PHI) test generated from the concatenated gene set of ITS, *act*, and *tef*1-α sequence data of closely related species of *Cladosporium viciae* using both LogDet transformation and splits decomposition. PHI test results $\Phi w \leq 0.05$ indicate significant recombination within the dataset. The ex-type strains are denoted by "T" and the new isolates of this study are in red.

10. *Exosporium rhapidis* S.S. Xiang & C.L. Yang, sp. nov. Fig. 20

MycoBank number: MB900692; Facesoffungi number: FoF16127

Etymology – The specific epithet reflects the host genus *Rhapis*.

Holotype – SICAU 23-0132

Associated with brown leaf spots on leaves of *Rhapis excelsa* (Thunb.) Henry ex Rehd., spots amphigenous, circular, oval or irregular, confluent, necrotic surrounded by a brown to dark brown margin, sometimes entire spots brown to dark brown. Sexual morph: Not observed. Asexual morph: *Hyphomycetous*. *Mycelium* sparse, mainly internal. *Stromata* semi-immersed to immersed, globose or irregular, brown to dark brown. *Conidiophores* 45–175 × 3–5 μm ($\bar{x}$ = 104 × 3.6 μm, n = 50), loose or denser fascicles, arising from stromata or hyphae, erect, straight, sometimes slightly curved, cylindrical, simple, rarely branched in the apex, regular in width, sometimes swollen cells in the base, uniformly medium brown to brown or more or less paler towards the apex, 0–7-septate, occasionally pluriseptate, smooth-walled, thickened. *Conidiogenous cells* 25–70 × 3–5 μm ($\bar{x}$ = 47.3 × 3.6 μm, n = 50), integrated, terminal, sometimes intercalary, conidiogenous loci conspicuous, 1–3 μm diameter ($\bar{x}$ = 2.1 μm, n = 50). *Conidia* 19–62 × 5–8 μm ($\bar{x}$ = 43.4 × 6.1 μm, n = 50), solitary, obclavate-cylindrical, straight to slightly curved, 2–8-distoseptate, rarely 0–1-distoseptate, pale brown, smooth-walled, apex obtuse, base gradually or short obconically truncate, with darkened hila.

Culture characteristics – *Colonies* on PDA attaining 15–25 mm diameter in 3 weeks, dense, subcircular, crenated, coriaceous, grey to dull brown in the center, orange to dark orange toward the margin, aerial mycelia infrequent, reverse pale yellowish-brown, radially furrowed.

Material examined – China, Sichuan Province, Chengdu City, Wenjiang District, Schoolyard of Sichuan Agricultural University, 103°51′33.82″E 30°42′18.52″N, 528 m, isol. from leaves of *Rhapis excelsa*, 20 Nov. 2019, C.L. Yang, YCL201911001 (SICAU 23-0132, holotype), ex-type culture (SICAUCC 23-0101). *ibid.* YCL201911001-2 (SICAU 23-0167), living culture SICAUCC 23-0136.

GenBank numbers – SICAUCC 23-0101 = ITS: PP769687, LSU: PP719617, *rpb2*: PQ005609. SICAUCC 23-0136 = ITS: PP781968, LSU: PP719618, *rpb2*: PQ005612

Notes – *Exosporium rhapidis* is phylogenetically closer to *E. livistonae* and *E. livistonicola,* as supported by both maximum likelihood and Bayesian analysis (Fig. 21). However, the sequence comparisons support them as distinct species. *Exosporium rhapidis* differs from *E. livistonicola* (MUCC 190) with a 98.3% (711/723, 0 gap) similarity in the LSU, with a 86.33% (423/490, 35 gaps) similarity in the ITS and with a 92.77% (770/830, 0 gap) similarity in the *rpb2* (Videira et al. 2017). Morphologically, *E. rhapidis* exhibits finer conidiophores cells (25–70 × 3–5 μm vs. 15–70 × 4–6 μm), smaller conidiogenous loci (1–3 μm vs. 3–4 μm), and shorter conidia (19–62 × 5–8 μm vs. 60–70 × 7–10 μm) compared to *E. livistonae* (Crous et al. 2011). Additionally, when compared to *E. livistonicola, E. rhapidis* shows variations in smaller conidiophores (45–175 × 3–5 μm vs. 40–280 × 3–6 μm) and longer conidiogenous cells (25–70 μm vs. 10–30 μm) (Braun et al. 2006, 2014). These distinctions lead us to introduce *E. rhapidis* as a new species.

Pseudocercospora Speg.

Notes – *Pseudocercospora* was established by Spegazini (1910) with *P. vitis* as the type species. *Pseudocercospora*, the second-largest genus within the cercosporoid group, exhibits a cosmopolitan distribution, colonizing a wide range of plant hosts from monocotyledons, dicotyledons, to gymnosperms, and adapting to diverse climatic conditions (Crous et al. 2013a, Videira et al. 2017, Singh et al. 2021). *Pseudocercospora* species are mainly associated with plant disease on numerous hosts that cause spots, blights, necrotic lesions, and rots (Crous et al. 2013a, Bakhshi et al. 2014, Nakashima et al. 2016), and some of them have quarantine fungi such as *P. angolensis*, *P. fijiensis*, and *P. ulei* (Zhao et al. 2021). The generic boundaries have undergone numerous revisions by various researchers, and a definitive definition remains elusive as ongoing revision efforts continue in this regard (Deighton 1976, Braun 1995, 2016, 2020, Crous et al. 2000, 2013b, Guatimosim et al. 2016).

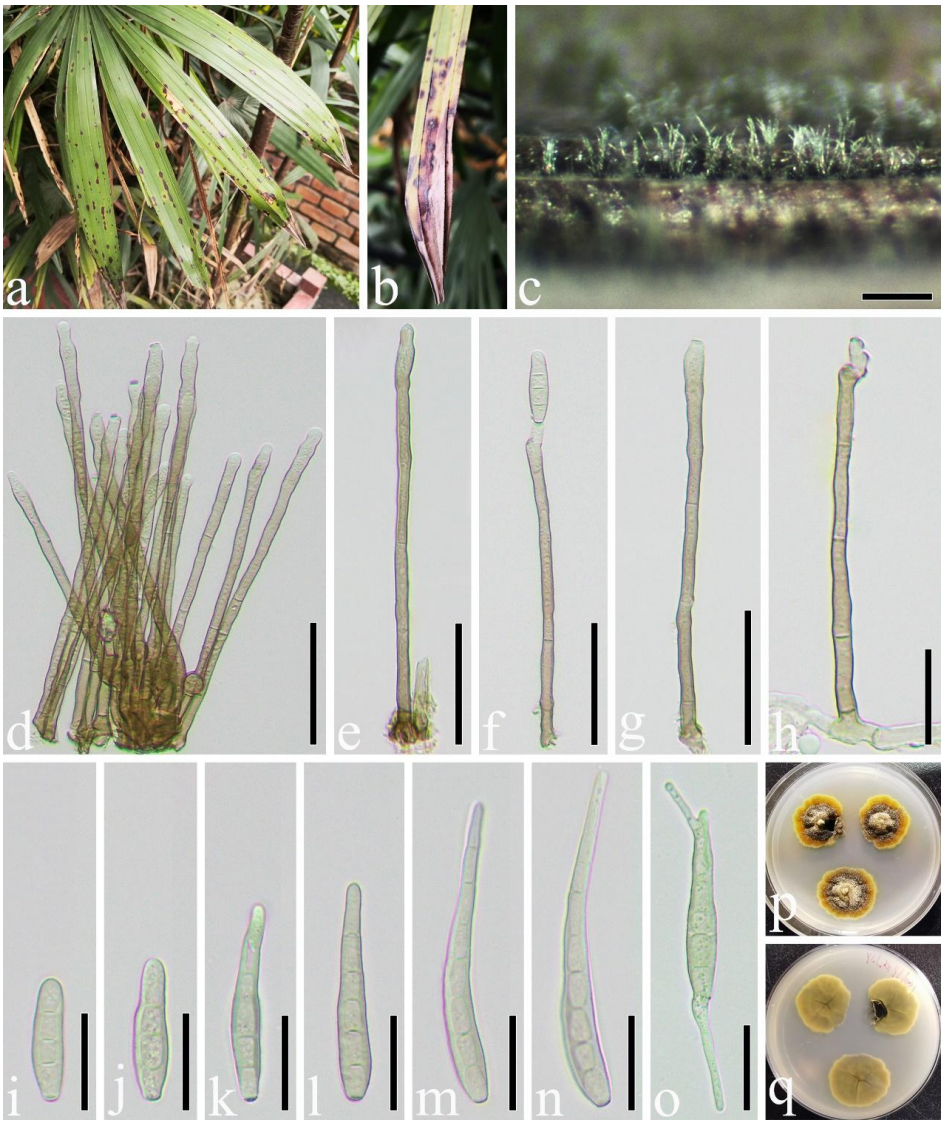

Figure 20 – *Exosporium rhapidis* (holotype, SICAU 23-0132). a, b Symptoms on the leaf. c Appearance of conidiogenesis. d Conidiophores. e–h Conidiogenous cells with developing conidia. i–n Conidia. o Germinating conidium. p Front view of colony on PDA. q Reverse view of colony on PDA. Scale bars: c = 200 μm, d–g = 40 μm, h–o = 20 μm.

11. *Pseudocercospora populina* X.Y. Li & C.L. Yang, sp. nov. Fig. 22

MycoBank number: MB900662; Facesoffungi number: FoF15924

Etymology – Refers to the host genus *Populus*, where the species collected.

Holotype – SICAU 23-0148

Associated with leaf spots on leaves of *Populus* × *beijingensis* W. Y. Hsu. Sexual morph: Not observed. Asexual morph: *Hyphomycetous*. *Mycelium* internal and external, hyphae subhyaline to pale brown, septate, smooth, branched, thin-walled, 2–3 μm width. *Caespituli* fasciculate, hypophyllous, grey to dark grey, scattered over the entire surface of lesions. *Conidiophores* 16–40 × 3–4 μm ($\bar{x}$ = 29 × 3.2 μm, n = 30), aggregated in dense fascicles, arising from the upper cells of stroma, erumpent, subcylindrical, straight to variously curved, brown, unbranched, septate, smooth, thin-walled. *Conidiogenous cells* 11–19 × 2–3 μm ($\bar{x}$ = 14 × 2.5 μm, n = 30), terminal, subhyaline to pale brown, smooth, unbranched, tapering to flat-tipped apical loci. *Conidia* 27–65 × 3–4 μm ($\bar{x}$ = 43 × 3.3 μm, n = 50), solitary, subcylindrical or narrowly obclavate, subhyaline to pale brown, 1–5-septate, slightly constricted at septa or not, straight to mildly curved, apex obtuse to subobtuse, base obconically subtruncate, thin-walled, smooth; *hila* unthickened, neither darkened nor refractive, 1.5–2 μm diameter.

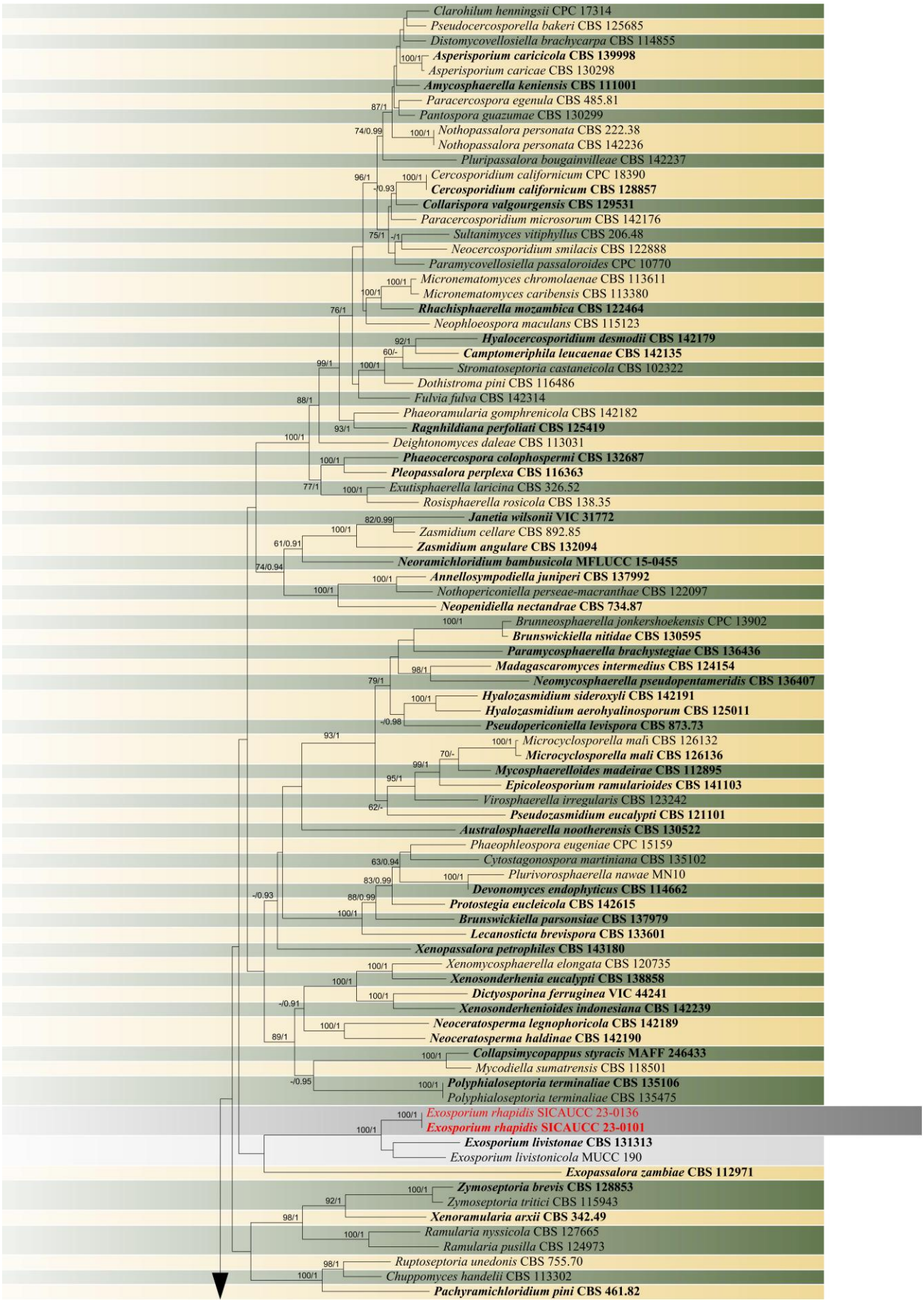

Figure 21 – Continued.

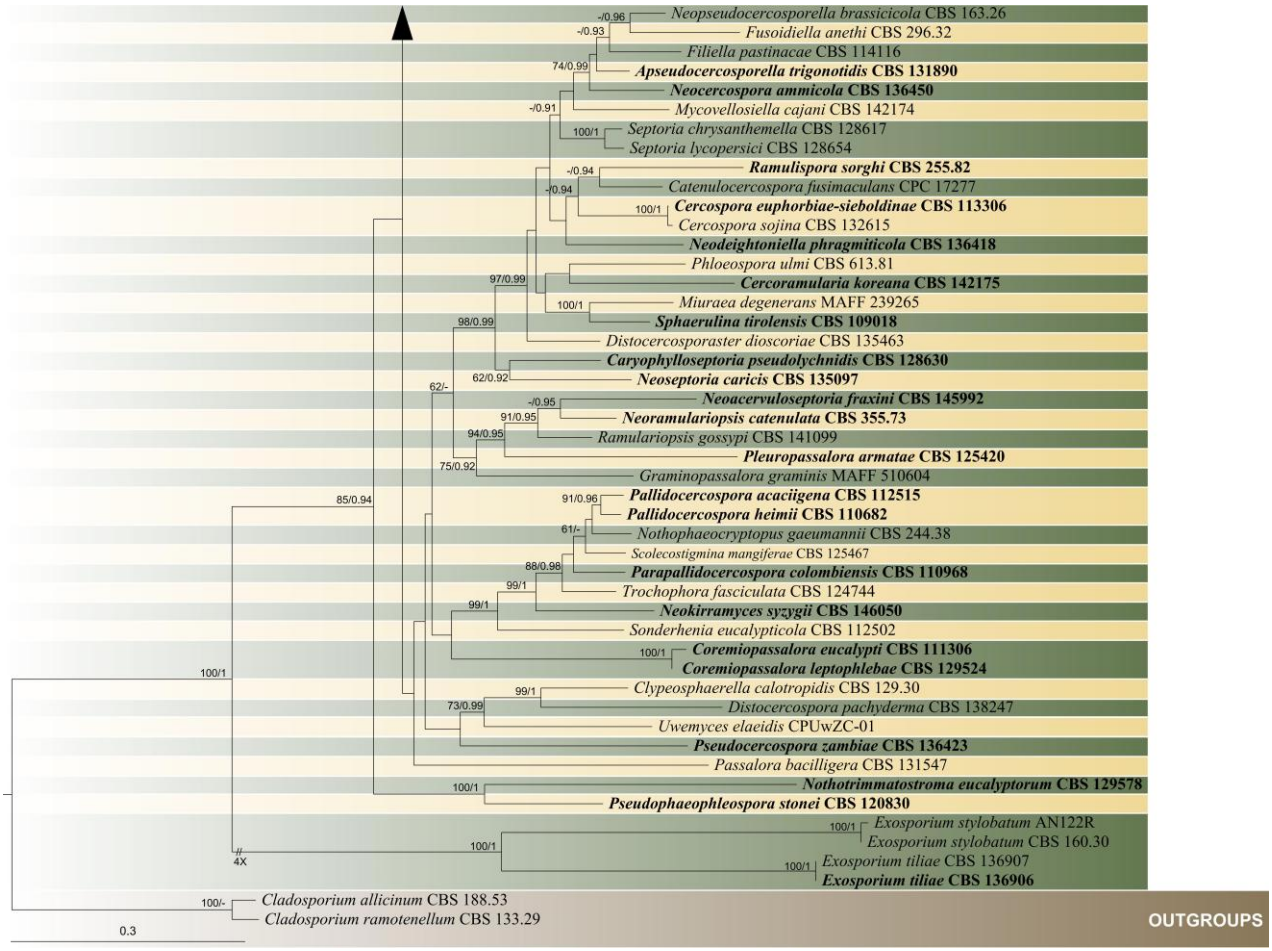

Figure 21 – Phylogram derived from maximum likelihood analyses of a combined dataset comprising ITS, *rpb*2, and LSU sequence dataset representing the species in *Ascomycota*. The dataset included one hundred and thirty-five strains and a total of 3,183 characters (ITS: 1–1,116, *rpb*2: 1,117–2,233, LSU: 2,234–3,183) after alignment. Single-gene analyses were conducted using both Maximum Likelihood (ML) and Bayesian (BY) methods, yielding similar tree topologies and ensuring consistent comparisons of clade stability. The best-scoring RAxML tree with a final likelihood value of -75,534.792396 is presented. The matrix contained 1,941 distinct alignment patterns, with 31.21% of undetermined characters or gaps. Estimated base frequencies were as follows: A = 0.246954, C = 0.251657, G = 0.286212, T = 0.215177. Substitution rates were as follows: AC = 1.804529, AG = 3.524151, AT = 1.172240, CG = 1.245322, CT = 7.902033, GT = 1.000000. Bootstrap support values (MLBS) equal or greater than 60%, and Bayesian posterior probabilities (BYPP) equal or greater than 0.90 are indicated at the nodes as MLBS / BYPP. The tree is rooted to *Cladosporium allicinum* (CBS 188.53) and *Cladosporium ramotenellum* (CBS 133.29). The ex-type strains are in bold, and the new isolates of this study are in red. Bar = 0.3 represents the estimated number of nucleotide substitution sites per branch.

Culture characteristics – *Colonies* on PDA attaining 25–30 mm diameter in 30 days, dense, subcircular, crenated, coriaceous, greyish white in the center, grey-olivaceous to olivaceous towards the margins, aerial mycelium infrequent, reverse dull green.

Material examined – China, Sichuan Province, Chengdu City, Wenjiang District, Schoolyard of Sichuan Agricultural University, 103°51′27.55″E 30°42′19.5″N, 533 m, isol. from leaves of *Populus* × *beijingensis*, 3 Nov. 2020, C.L. Yang, YCL202011002 (SICAU 23-0148, holotype), ex-type culture (SICAUCC 23-0095). *ibid.* YCL202011002-2 (SICAU 23-0155), living culture SICAUCC 23-0130.

GenBank numbers – SICAUCC 23-0095 = ITS: PP736386, LSU: PP732741, *tef*1-α: PP779587, *act*: PP782115, *rpb*2: PP782086. SICAUCC 23-0130 = ITS: PP736387, LSU: PP732742, *tef*1-α: PP779588, *act*: PP782116, *rpb*2: PP782087

Notes – Phylogenetic analyses of concatenated sequences from ITS, LSU, *rpb*2, *tef*1-α, and *act* revealed that our strain (SICAUCC 23-0095) forms a cluster with the ex-epitype strain *Pseudocercospora pini-densiflorae* (MUCC 1714) (Fig. 23). Sequence comparison in the *rpb*2, *tef*1-α, *act* and ITS regions between *P. populina* (SICAUCC 23-0095) and *P. pini-densiflorae* (MUCC 1714) revealed similarity values of 95.09% (639/672 bp, 0 gap), 96.45% (299/310 bp, 0 gap), 98.07% (203/207 bp, 0 gap), and 99.79% (476/477 bp, 0 gap), respectively. Morphologically, *P. populina* can be differentiated from *P. pini-densiflorae* by the occasional constriction of conidia at septa and the presence of straight to variably curved conidiophores (Braun et al. 2013). Therefore, we introduce our isolate as a novel species within the genus *Pseudocercospora*, supported by morphological observations and phylogenetic evidence.

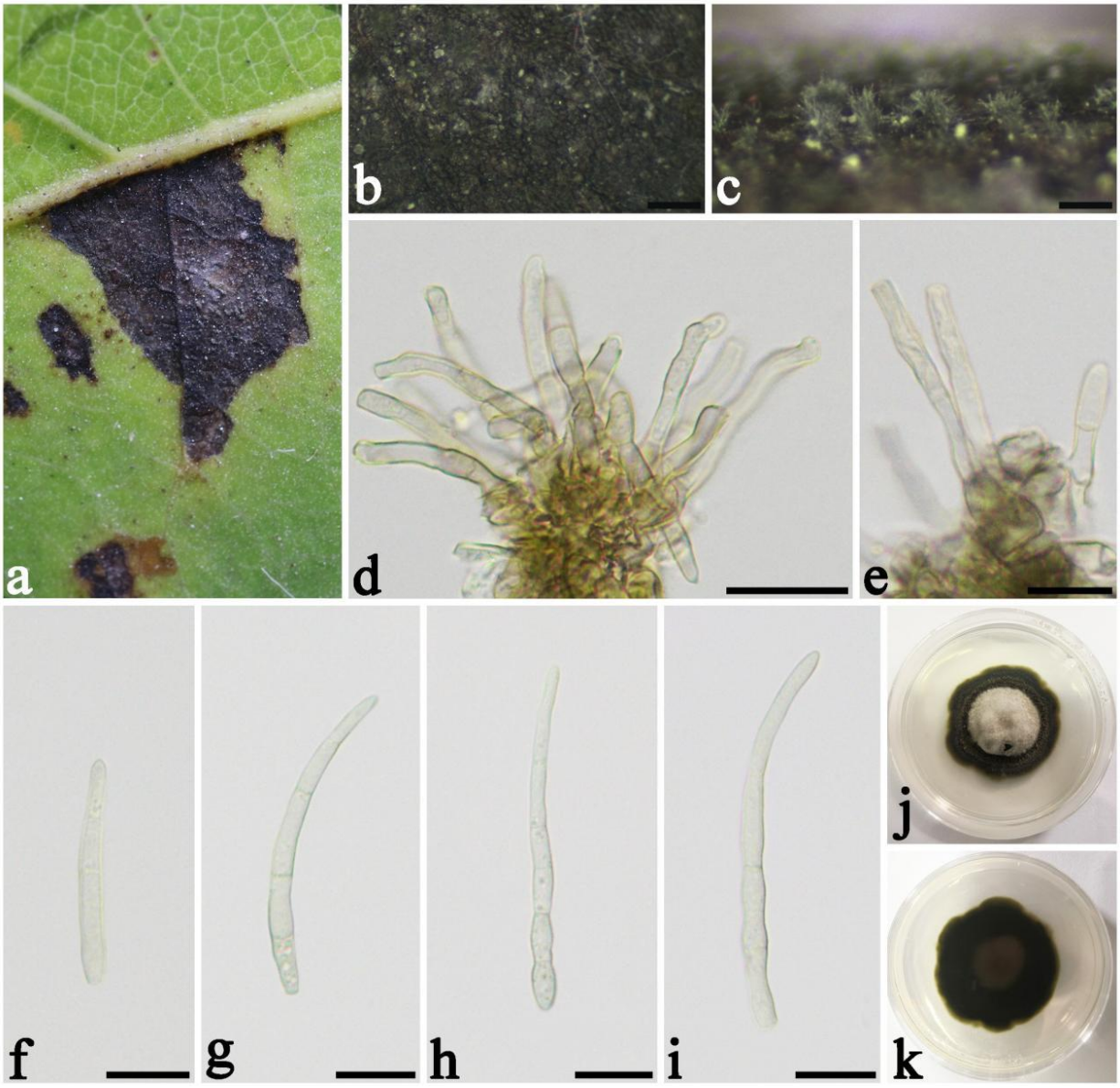

Figure 22 – *Pseudocercospora populina* (holotype, SICAU 23-0148). a Symptoms on the leaf. b, c Appearance of conidiogenesis. d, e Fascicles with conidiophores and conidiogenous cells. f–i Conidia. j Front view of colony on PDA. k Reverse view of colony on PDA. Scale bars: b = 200 µm, c = 140 µm, d–i = 10 µm.

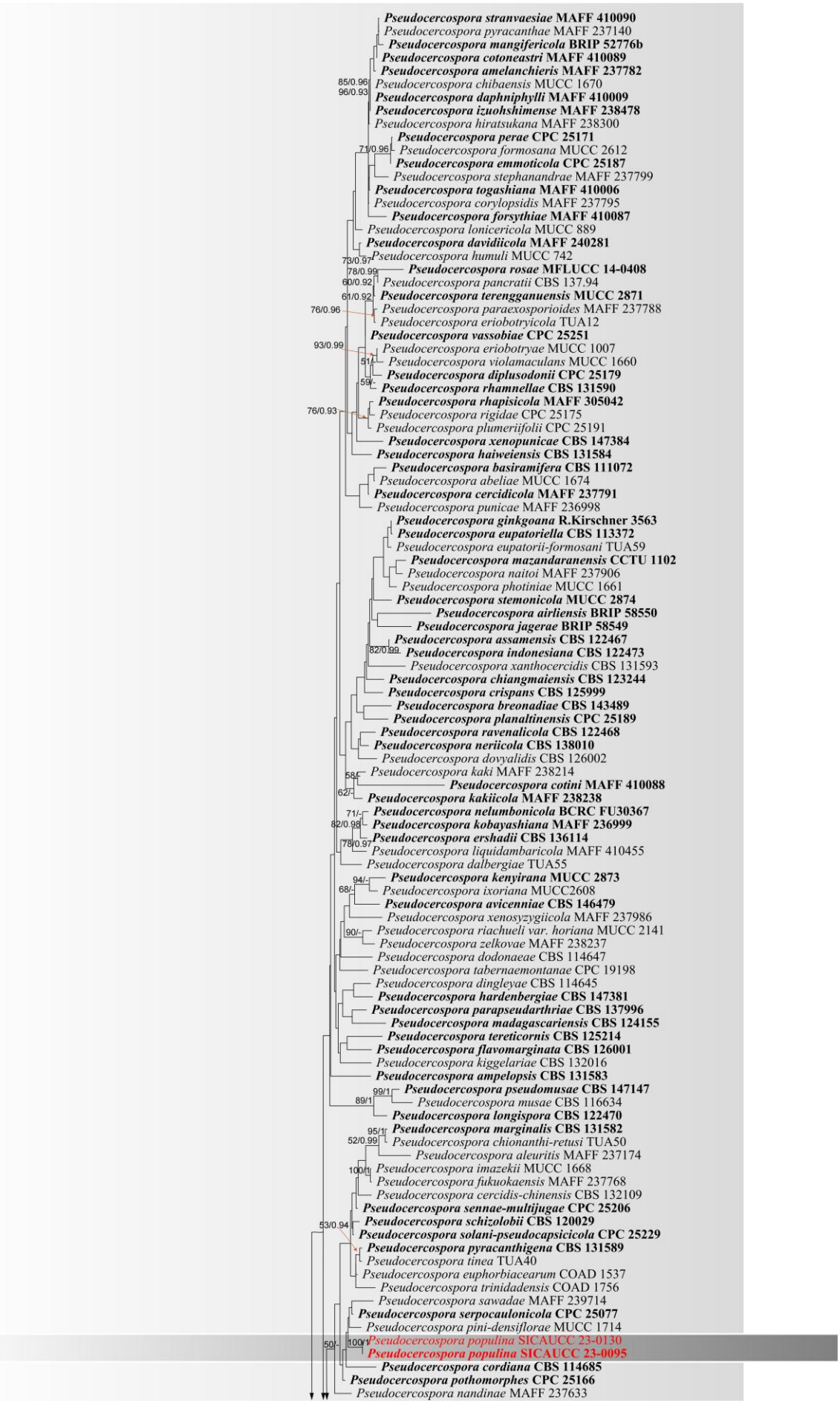

Figure 23 – Continued.

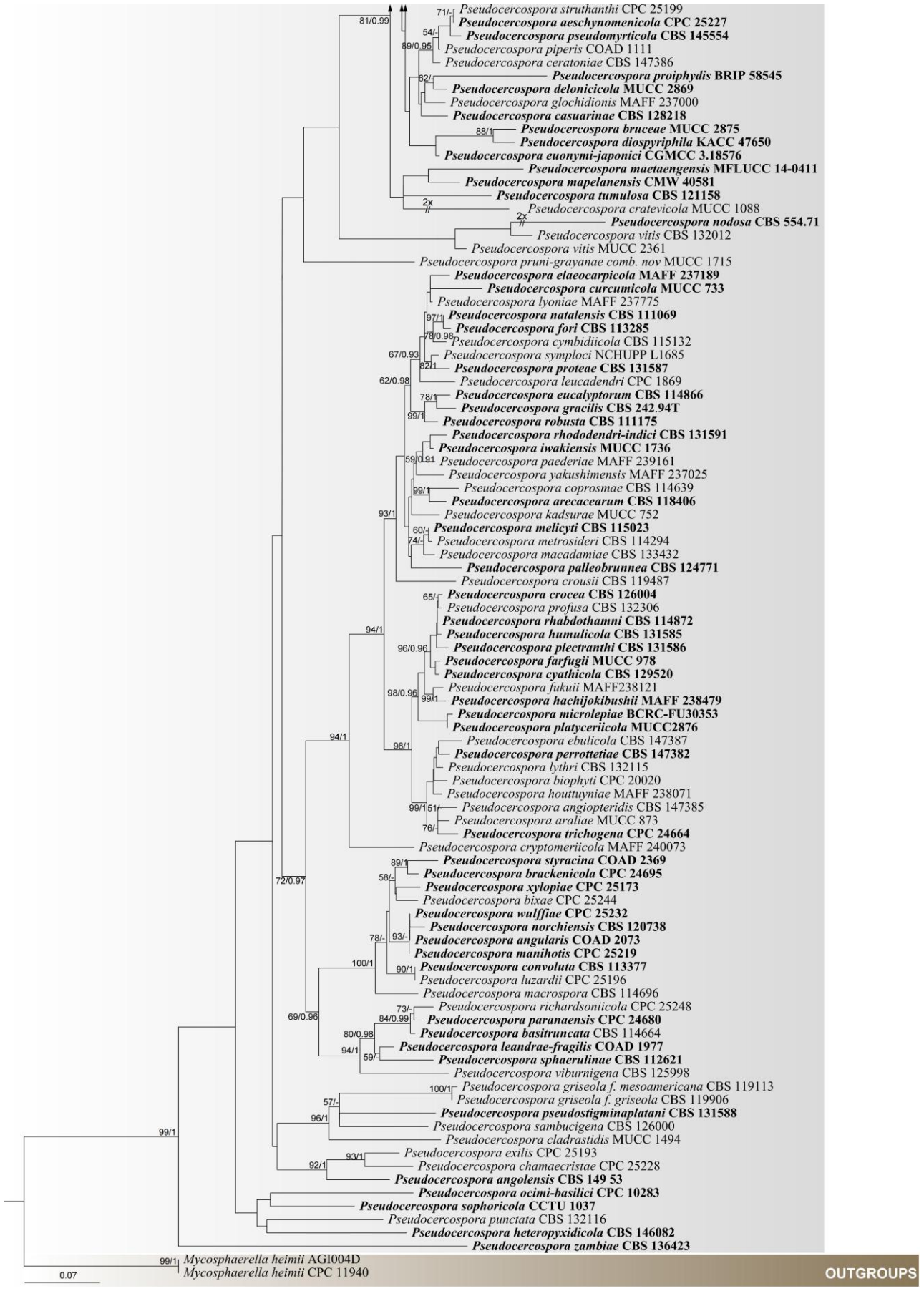

Figure 23 – Phylogram derived from maximum likelihood analyses of a combined dataset comprising ITS, LSU, *act*, *rpb*2, and *tef*1-α sequence dataset representing the species of

Pseudocercospora. The phylogenetic analysis included two hundred and one strains and a total of 4,438 characters (ITS: 1–584, LSU: 585–1,908, *act*: 1,909–2,542, *rpb*2: 2,543–3,575, *tef*1-α: 3,576–4,438) after alignment. The tree is rooted to *Mycosphaerella heimii* (AGI004D) and *Mycosphaerella heimii* (CPC 11940). Single-gene analyses were conducted, resulting in similar tree topologies between the ML and BY methods, ensuring consistent comparisons of clade stability. The best-scoring RAxML tree with a final likelihood value of -44,847.504426 is presented. The matrix had 1,978 distinct alignment patterns, with 55.04% of undetermined characters or gaps. Estimated base frequencies were as follows: A = 0.239767, C = 0.253733, G = 0.270430, T = 0.236070; substitution rates AC = 1.388896, AG = 3.503481, AT = 1.106017, CG = 0.864890, CT = 6.145958, GT = 1.000000. Bootstrap support values (MLBS) equal or exceeding 50%, and Bayesian posterior probabilities (BYPP) equal or exceeding 0.90 indicated at the nodes as MLBS / BYPP. The ex-type strains are in bold, and the new isolates of this study are in red. Bar = 0.07 represents the estimated number of nucleotide substitution sites per branch.

Myriangiales Starbäck

Notes – *Myriangiales* was introduced by Starbäck (1899) based on the type species *Myrangium duriaei* (Hyde et al. 2013). Members of *Myriangiales* are distinctively characterized by their crustose ascostromata and the presence of muriform ascospores. At present, *Myriangiales* encompasses two accepted families, *Elsinoaceae* and *Myriangeaceae*, comprising a total of 14 genera and approximately 110 documented species (Lumbsch & Huhndorf 2010, Wijayawardene et al. 2022). The divergence time of this order has been estimated with a stem age of 130 Mya by Hongsanan et al. (2020).

Elsinoaceae Höhn. ex Sacc. & Trotter

Notes – *Elsinoaceae* was introduced by Saccardo & Trotter (1913) with *Elsinoe* as the type genus. Members of *Elsinoaceae* are relatively understudied; however, they play a significant role as plant pathogens, causing issues like scab, sunken spots, and anthracnose on a variety of plants, including citrus, grapes, mangoes, peppers, legumes, herbs, and ornamental plants (Boedijn 1961, Condé et al. 1997, Hyun et al. 2001, Jayawardena et al. 2014, Hongsanan et al. 2020), and characterized by superficial stroma, asci arising at one level. Initially, *Elsinoaceae* once numbered 15 genera, but through the scrutiny of morphological characteristics and molecular analysis, the family has been refined to include only two genera: *Elsinoe* and *Molleriella* (von Arx & Müller 1975, Lumbsch & Huhndorf 2010, Li et al. 2011b, Jayawardena et al. 2014, Hongsanan et al. 2020).

Elsinoe Racib.

Notes – *Elsinoe* was erected by Raciborski (1900) with *E. canavaliae* as the type species. *Elsinoe* species are significant phytopathogens typically associated with scab and spot anthracnose diseases in economically important crops and forest plants (Fan et al. 2017, Zhao et al. 2020, Ujat et al. 2023). Members of *Elsinoe* are characterized by usually causing scab-like blemishes with multi-loculate pseudoascostromata containing 3–8 asci inside each locule, asci bitunicate, fissitunicate, saccate to globose with eight hyaline, oblong or fusiform, septate ascospores. The asexual morph takes the form of the acervular coelomycetous *Sphaceloma*, characterized by monophialidic to polyphialidic conidiogenous cells and hyaline, ellipsoid, aseptate conidia (Jayawardena et al. 2014). Currently, this genus records a total of 202 epithets (https://www.speciesfungorum.org, November 2024), out of which approximately 85 species have associated molecular data (Hongsanan et al. 2020, Pham et al. 2021, Pem et al. 2024). More species will continue to be described due to the backbone phylogeny for this genus has been constructed based on sequences from ITS, LSU, *rpb*2, and *tef*1-α genes (Fan et al. 2017, Jayawardena et al. 2019).

12. *Elsinoe araliae* W. Yamam., Sci. Rep. Hyogo Univ. Agric. 3(1): 18 (1957) Fig. 24

MycoBank number: MB627255; Facesoffungi number: FoF16128

Associated with scab disease on the leaf, petiole, rachis and fruit of *Fatsia japonica* (Thunb.) Decne. et Planch., spots subcircular to circular, elliptical to irregular, usually raised and purplish brown at margins, greyish in center, most coalescing and developing typical scab symptoms on older infected tissues, sometimes leading to the distortion of affected organ, local death of severely infected leaves. Sexual morph: Not observed. Asexual morph: *Hyphomycetous*. *Mycelium* sparse, mainly internal. *Stromata* immersed, irregular, pale brown to brown. Dense mass of cells adhering to the surface of lesions, cells swollen, spore-like, brown to dark brown. *Conidiophores* 10–36 × 3–5 μm ($\bar{x}$ = 19.2 × 4.1 μm, n = 20), arising from stromata or hyphae, erect, straight, cylindrical or ampulliform to doliiform, simple, hyaline to brown, 0–1-septate, smooth-walled. *Conidiogenous* cells integrated, terminal, monophialidic. *Conidia* 6.5–9 × 3–5 μm ($\bar{x}$ = 7.9 × 3.9 μm, n = 30), ellipsoid or oval, apex obtuse, aseptate, hyaline, smooth-walled.

Culture characteristics – *Colonies* on MEA attaining 15–20 mm diameter in 30 days, slow-growing, raised, cerebriform, compressed and granular protuberance, some pilose aerial mycelium centrally and over other parts of the colony, gelatinous clumps, pale cinnamon, reverse dark tawny, colonies composed of a combination of thickened-walled, pale tawny hyphae and tawny pseudoparenchyma with multi-septate chlamydospores, sporulation not observed. *Colonies* on OA attaining 15–20 mm diameter in 30 days, slow-growing, circular, flat, leathery, slightly furrowed towards the margin, white to greyish white hyphae centrally and other parts grow slightly, red to dark red, reverse red to bright red, colonies composed of thin-walled hyaline hyphae and some hyphae reduced to pigment-producing cells, sporulation not observed. *Colonies* on PDA attaining 15–20 mm diameter in 20 days, slow-growing, medium raised, cerebriform, comprising and wrinkling the medium, white to greyish white aerial mycelium superficially, mucilaginous drops abundant periphery when late, reverse tawny to dark tawny, colonies subcircular to irregular, composed of pale yellow to bright yellow hyphae, walls medium-thickened, sporulation abundant.

Material examined – China, Sichuan Province, Chengdu City, Wenjiang District, Schoolyard of Sichuan Agricultural University, 103°51′27.6″E 30°42′19.41″N, 526 m, isol. from leaves of *Fatsia japonica*, 28 Dec. 2019, C.L. Yang, YCL201912003 (SICAU 23-0131), culture (SICAUCC 23-0102).

GenBank numbers – SICAUCC 23-0102 = ITS: PP781968, LSU: PP719618, *tef*1-α: PQ005617, *rpb*2: PQ005610

Notes – This new isolate is genetically more closely related to *Elsinoe araliae*, strongly supported by both Maximum Likelihood (100%) and Bayesian Inference (1.00) (Fig. 25). A comparison of the ITS, LSU, *rpb*2, and *tef*1-α nucleotides between *E. araliae* (MUCC 3490) and the new strain (SICAUCC 23-0102) showed 100% (744/744, 0 gap) similarity for *rpb*2, 99.8% (531/532, 0 gap) for ITS, 99.9% (735/736, 0 gap) for LSU, and 99.5% (368/370, 0 gap) for *tef*1-α (Ujat et al. 2023). Morphologically, our new collections fit well with the description of *E. araliae* (Choi et al. 1998). In this study, we identified the newly isolated strain as a new record *E. araliae* from *Fatsia japonica*.

Pleosporales Luttr. ex M.E. Barr

Notes – The *Pleosporales*, a prolific order within the *Dothideomycetes*, harbors a considerable array of consequential species, predominantly encompassing phytopathogenic fungi that afflict a wide range of ecologically and economically significant plants, with a global presence well-documented (Zhang et al. 2012, Hongsanan et al. 2020). Currently, this order boasts a comprehensive documentation of no fewer than 6,950 taxa spanning across 91 families (Ren et al. 2022, Wijayawardene et al. 2022, Konta et al. 2023).

Didymosphaeriaceae Munk

Notes – *Didymosphaeriaceae* was proposed by Munk (1953), typified by the genus *Didymosphaeria*. *Didymosphaeriaceae* species are parasitic, endophytic, and saprobic on various hosts in terrestrial or aquatic environments (Ariyawansa et al. 2014a, Alidadi et al. 2019, Jamali

2020, Ren et al. 2022). Specifically, *Didymosphaeriaceae* was historically challenging to distinguish from *Montagnulaceae*. However, Ariyawansa et al. (2014b) merged *Montagnulaceae* into *Didymosphaeriaceae* following comprehensive phylogenetic and morphological evidence. In comparison to similar groups, members of *Didymosphaeriaceae* are distinguished by their morphologically diverse, brown, uni-septate ascospores, as well as trabeculate pseudoparaphyses that primarily anastomose above the asci (Ariyawansa et al. 2014a, Hongsanan et al. 2020). *Didymosphaeriaceae* is currently documented to encompass 33 genera comprising approximately 270 species, with *Didymosphaeria*, *Montagnula*, *Paraphaeosphaeria*, and *Spegazzinia* each containing more than 20 species (Wijayawardene et al. 2022, Devadatha et al. 2023).

Paraconiothyrium Verkley.

Notes – *Paraconiothyrium* was introduced by Verkley et al. (2004) to accommodate four new species, *P. estuarinum*, *P. Brasiliense*, *P. cyclothyrioides*, and *P. fungicola*. Currently, *Paraconiothyrium* encompasses a total of 26 recognized species (Verkley et al. 2004, Damm et al. 2008, Budziszewska et al. 2011, Verkley et al. 2014, Tennakoon et al. 2022b). The morphological characters of *Paraconiothyrium* are variable. The conidiomata within this genus can range from eustromatic to pycnidial, while the conidiogenous cells demonstrate phialidic or annelidic forms. Furthermore, the conidia display a spectrum from smooth-walled to minutely warted, transitioning from hyaline to brown in later stages of development (Verkley et al. 2004, de Gruyter et al. 2013, Tennakoon et al. 2022b).

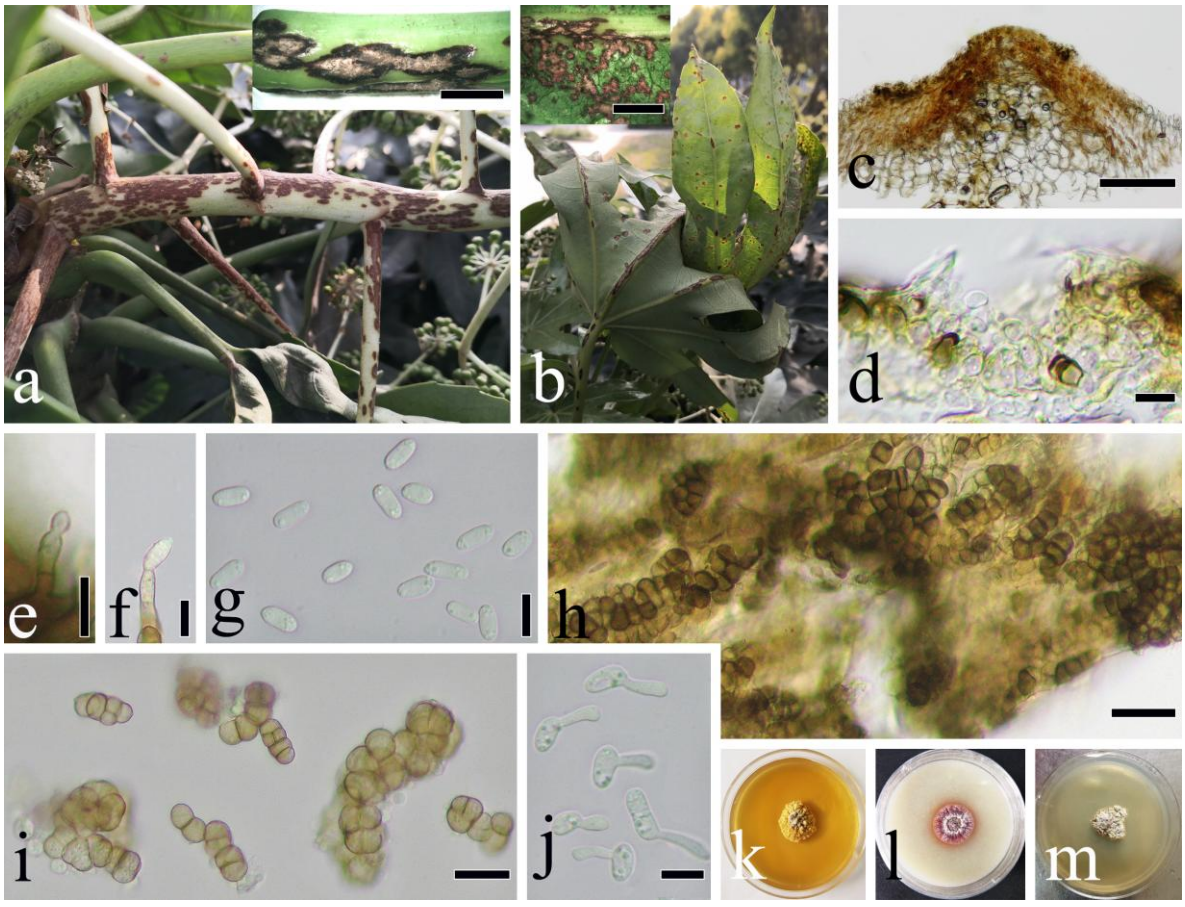

Figure 24 – *Elsinoe araliae* (holotype, SICAU 23-0131). a, b Symptoms on *Fatsia japonica.* c, d Cross-section of conidiomata. e, f Conidiogenous cells with developing conidia. g Conidia. h, i Dense mass of cells adhering to the surface of lesions. j Germinating conidia. k–m Front view of colonies on EMA, OA, and PDA. Scale bars: a, b = 5000 μm, c = 200 μm, d–g, j = 10 μm, h, i = 20 μm.

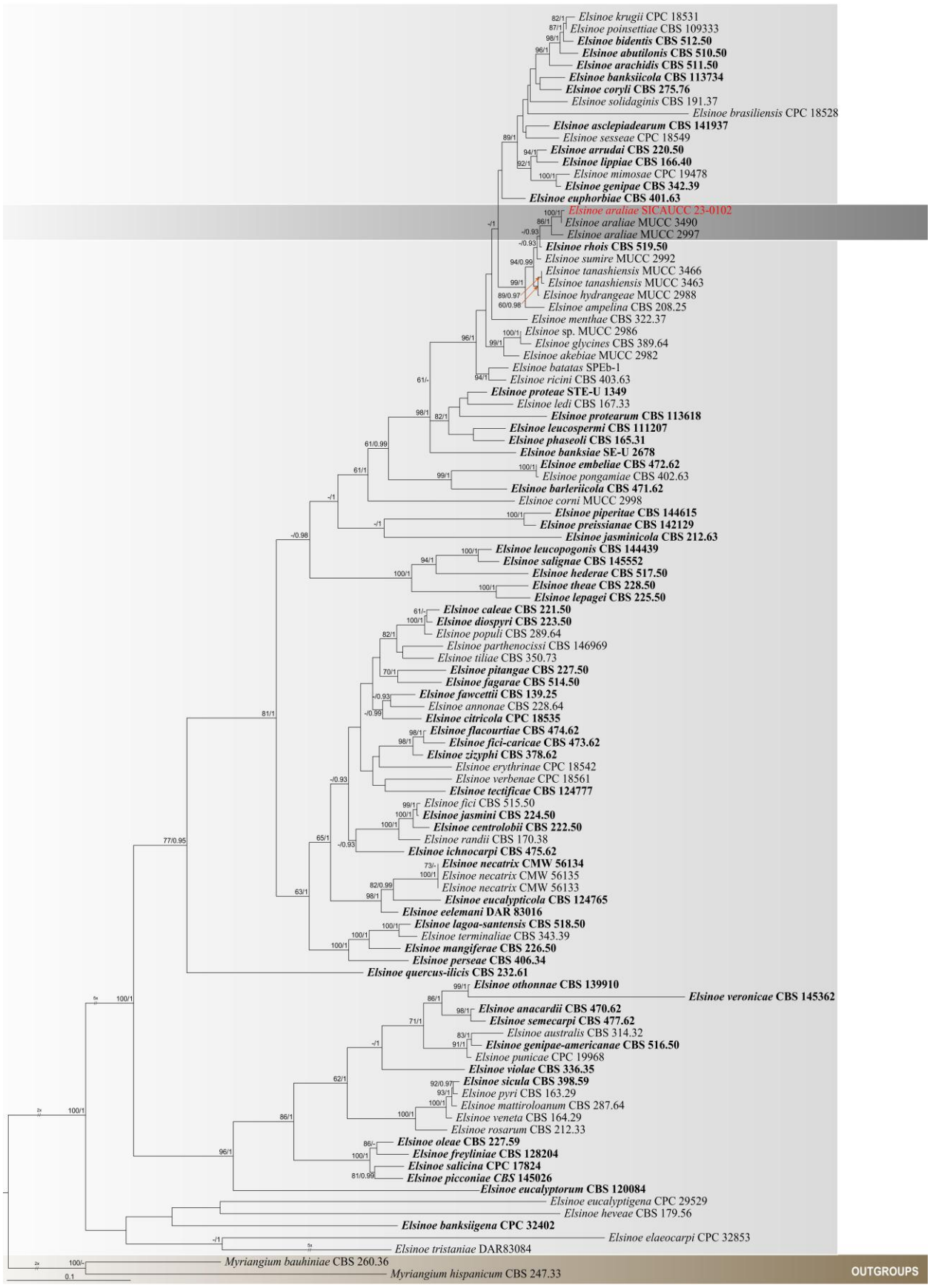

Figure 25 – Phylogram derived from maximum likelihood analyses of a combined dataset comprising ITS, LSU, *rpb*2, and *tef*1-α gene regions of *Elsinoe* and *Myriangium* genus. The alignment consisted of one hundred and five strains and 3,792 characters (ITS = 1–1,053, LSU = 1,054–2,342, *tef*1-α = 2,343–3,398, *rpb*2 = 3,399–3,792). The highest-scoring RAxML tree, with a

final likelihood value of -36,731.791960, is presented along with a matrix containing 1,490 distinct alignment patterns, of which 40.07% consist of undetermined characters or gaps. Estimated base frequencies were as follows: A = 0.238952, C = 0.263147, G = 0.286216, T = 0.211685, with substitution rates AC = 1.542790, AG = 4.299453, AT = 1.551930, CG = 1.268584, CT = 9.007765, GT = 1.00000. Maximum likelihood bootstrap support values (MLBS) greater than 60%, and Bayesian posterior probabilities (BYPP) greater than 0.9 are indicated above or below the nodes. The ex-types are bold, and the new isolates are red. The tree is rooted with *Myriangium bauhiniae* (CBS 260.36) and *Myriangium hispanicum* (CBS 247.33). Bar = 0.1 represents the estimated number of nucleotide substitution sites per branch.

13. *Paraconiothyrium brasiliense* Verkley, Stud. Mycol. 50(2): 329 (2004) Fig. 26

MycoBank number: MB500082; Facesoffungi number: FoF16126

Associated with leaf blight on leaves of *Syagrus romanzoffiana* (Cham.) Glassm. Sexual morph: Not observed. Asexual morph: *Coelomycetous*. *Conidiomata* 150–190 × 140–180 μm ($\bar{x}$ = 170 × 169 μm, n = 10), pycnidial, immersed, sometimes slightly erumpent, solitary, scattered, uniloculate, subglobose to globose, ostiolate. *Conidiomatal wall* 5–14 μm width, comprising several layers of brown to dark brown cells of *textura angularis*. *Conidiophores* reduced to conidiogenous cells. *Conidiogenous cells* 4–8 × 2–5 μm ($\bar{x}$ = 5.4 × 3.5 μm, n = 30), holoblastic, hyaline, smooth, ampulliform to doliiform, lining the conidiomatal cavity. *Conidia* 3.5–10 × 1.5–3 μm ($\bar{x}$ = 5.9 × 2.4 μm, n = 50), ellipsoid to cylindrical, initially hyaline, becoming pale brown to brown, thin-walled, smooth, 0–1-septate.

Culture characteristics – *Colonies* on PDA attaining 40–50 mm diameter in 1 week, dense, circular, entire edge, white, flocculent to fluffy, aerial mycelia developed, reverse pale yellow, becoming russetish.

Material examined – China, Sichuan Province, Chengdu City, Wenjiang District, Schoolyard of Sichuan Agricultural University, 103°51′41.24″E 30°42′17.79″N, 525 m, isol. from leaves of *Syagrus romanzoffiana*, 9 May 2020, C.L. Yang, YCL202005003 (SICAU 23-0116), culture (SICAUCC 23-0105).

GenBank numbers – SICAUCC 23-0105 = ITS: PP769688, LSU: PP719619, SSU: PP734050, *tef*1-α: PQ005618, *tub*2: PQ005625, *rpb*2: PQ005611

Notes – This new isolate demonstrates a close phylogenetic relationship (97% MLBS / 1.00 BYPP) to several strains of *Paraconiothyrium brasiliense* based on multigene analyses, which incorporate sequence data from SSU, LSU, *tub*2, *rpb*2, *tef*1-α, and ITS regions (Fig. 27). Incorporating multiple regions, the ITS, LSU, and SSU sequences of this isolate show high identity to those of the ex-type strain *Paraconiothyrium brasiliense* (CBS 100299), with matches of 99.0% (513/518, 2 gaps), 100% (890/890, 0 gap), and 99.8% (1,019/1,021, 2 gaps), respectively (Verkley et al. 2004). While the *tub*2 sequences of strains in the current study displayed more variability of 91.7% (355/387, 3 gaps), suggesting the possibility of *P. brasiliense* being a species complex, the internal branches of the multilocus phylogeny lacked sufficient support for a clear delineation (Verkley et al. 2004, 2014). This species shows a broad distribution and has been identified on various host plants such as *Coffea arabica, Ginkgo biloba, Magnolia* sp., and others (Damm et al. 2008, Verkley et al. 2014, Tennakoon et al. 2022b). Notably, this species has not been previously reported within the plant family *Arecaceae*, and here we provide the first association of this species with *Syagrus*.

Lophiostomataceae Sacc.

Notes – *Lophiostomataceae* was erected by Nitschke (1869) with *Lophiostoma* as the type genus. This family was previously referred to as "*Lophiostomeae*" and later formally established as *Lophiostomataceae* within the order *Pleosporales* by Saccardo (1883). *Lophiostomataceae* species are characterized by immersed to erumpent, carbonaceous to coriaceous ascomata with rounded or slit-like ostiole on flattened necks, mostly clavate asci, and 1 to multi-septate, hyaline to dark brown ascospores with terminal appendages or mucilaginous sheaths (Holm & Holm 1988,

Thambugala et al. 2015, Bao et al. 2019). The *Lophiostomataceae* family, with 30 genera and around 200 species, is primarily distributed across Asia and Europe (Thambugala et al. 2015, Hashimoto et al. 2018, Wanasinghe et al. 2018, Bao et al. 2019, Aluthmuhandiram et al. 2022, Wijayawardene et al. 2022). *Lophiostomataceae* members are frequently saprobic, thriving on a wide range of substrates in both terrestrial and aquatic ecosystems (Thambugala et al. 2015, Wanasinghe et al. 2016, Bao et al. 2019), but certain taxa have the potential to induce plant diseases (Han et al. 2021).

Neovaginatispora A. Hashim., K. Hiray. & Kaz. Tanaka

Notes – *Neovaginatispora*, represented by *N. fuckelii*, was introduced by Hashimoto et al. (2018), featuring a consistently thin peridium (up to 25 µm thick) composed of two zones, distinguishing it from *Vaginatispora* species. Some studies have shown that *Neovaginatispora* species share a close phylogenetic relationship with *Lentistoma* and *Vaginatispora* (Bao et al. 2019, Phukhamsakda et al. 2020). Four *Neovaginatispora* species, including *N. aquadulcis*, *N. clematidis*, *N. fuckelii*, and *N. mangiferae*, are documented as both saprobic and parasitic, typically found on plant stems or debris (Phukhamsakda et al. 2020, Han et al. 2021, Magaña-Dueñas et al. 2022, Jayawardena et al. 2023).

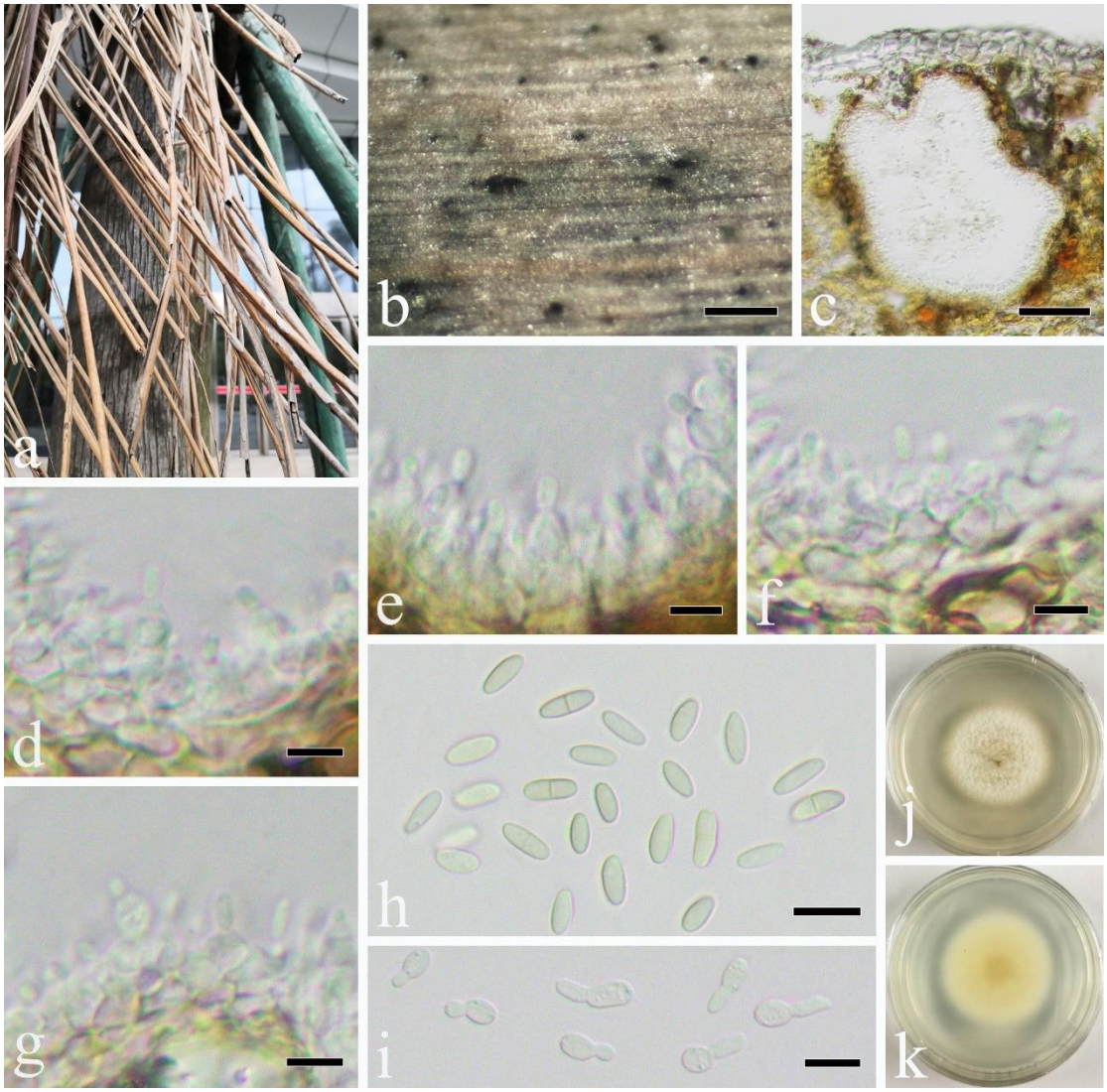

Figure 26 – *Paraconiothyrium brasiliense* (SICAU 23-0116). a Symptoms on the leaves. b Appearance of conidiomata. c Cross-section of conidioma. d–g Conidiogenous cells with developing conidia. h Conidia. i Germinating conidia. j Front view of colony on PDA. k Reverse view of colony on PDA. Scale bars: b = 300 µm, c = 50 µm, d–g = 5 µm, h, i = 10 µm.

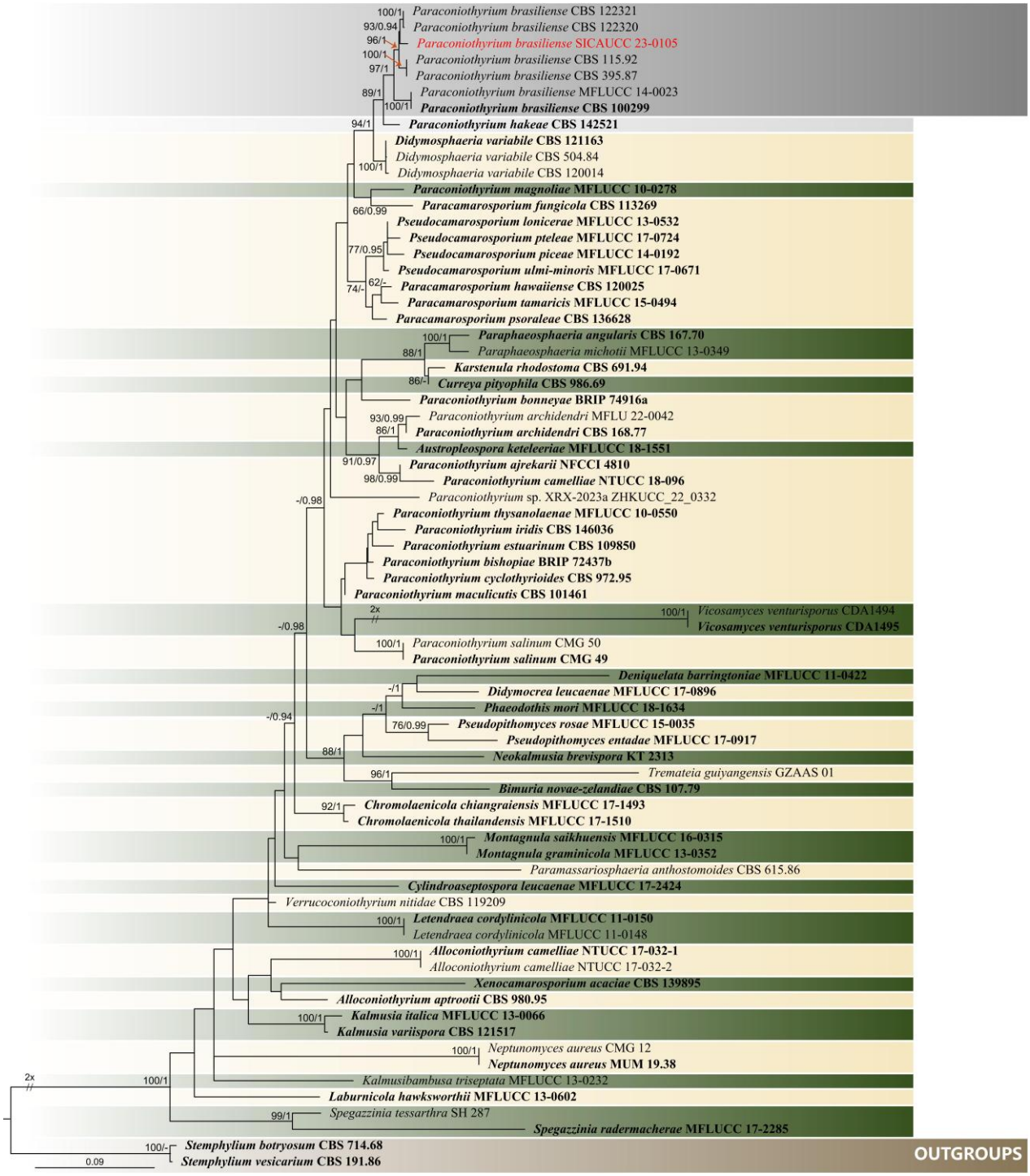

Figure 27 – Phylogram derived from maximum likelihood analyses of a combined dataset comprising ITS, LSU, SSU, *tub*2, *tef*1-α, and *rpb*2 sequence dataset representing the species in *Didymosphaeriaceae*. Seventy-two strains were included in the combined analyses, which comprised 8,348 characters (ITS: 1–1,208, LSU: 1,209–2,595, SSU: 2,596–4,692, *tub*2: 4,693–5,393, *tef*1-α: 5,394–6,360, *rpb*2: 6,361–8,348) after alignment. Single-gene analyses were conducted, resulting in similar tree topologies between the ML and BY methods, ensuring consistent comparisons of clade stability. The best-scoring RAxML tree with a final likelihood value of -36,744.301022 is presented. The matrix had 2,496 distinct alignment patterns, with 68.04% of undetermined characters or gaps. Estimated base frequencies were as follows: A = 0.240737, C = 0.248174, G = 0.270228, T = 0.240861; substitution rates AC = 1.402941, AG = 3.360186, AT = 1.509533, CG = 1.076472, CT = 7.757361, GT = 1.000000. Bootstrap support

values (MLBS) equal or greater than 60%, and Bayesian posterior probabilities (BYPP) equal or greater than 0.90 are indicated at the nodes as MLBS / BYPP. The tree is rooted to *Stemphylium botryosum* (CBS 714.68) and *Stemphylium vesicarium* (CBS 191.86). The ex-type strains are in bold, and the new isolates are in red. Bar = 0.09 represents the estimated number of nucleotide substitution sites per branch.

14. ***Neovaginatispora fuckelii*** (Sacc.) A. Hashim., K. Hiray. & Kaz. Tanaka, Stud. Mycol. 90: 188 (2018) Fig. 28

MycoBank number: MB823148; Facesoffungi number: FoF06527

Associated with leaf spots or leaf blight on leaves of *Phoenix sylvestris* Roxb. and *Syagrus romanzoffiana* (Cham.) Glassm. Sexual morph: *Ascomata* 180–310 μm high, 140–260 μm diameter ($\bar{x}$ = 241 × 206 μm, n = 10), semi-immersed to immersed, carbonaceous, black, pyriform to subglobose, ostiolate in center. *Ostiole* rounded or slit-like, variable in shape, central, unconspicuous periphysate, with a pore-like opening. *Peridium* 9–27 μm width, comprising of two strata, outer stratum comprising of brown to dark brown flattened cells arranged in a *textura angularis*, fusing and indistinguishable from the host tissues, inner stratum comprising of several layers of hyaline cells of *textura angularis*. *Hamathecium* comprising of massive, septate, hyaline, sometimes anastomosed and branched at apex, long cylindrical cellular pseudoparaphyses, usually longer than asci, 3–8 μm width at base, narrower towards to tip, 1–2.5 μm width at the tip. *Asci* 75–115 × 10–15 μm ($\bar{x}$ = 97 × 13.5 μm, n = 20), 8-spored, bitunicate, fissitunicate, cylindric-clavate, round at the apex, short pedicellate, with an indistinct ocular chamber. *Ascospores* 19–28 × 5–9 μm ($\bar{x}$ = 23 × 6.8 μm, n = 50), biseriate, overlapping, fusiform with obtuse ends, hyaline when young, pale brown to brown at maturity, mostly curved, 3-septate, strongly constricted at the middle septum, guttulate, smooth-walled, with hyaline and narrow sheath at both ends. (In samples, in most cases, immature asci and ascospores were observed in the ascomata. *Immature asci* 50–95 × 8–11.5 μm ($\bar{x}$ = 69 × 9.7 μm, n = 35), 8-spored, bitunicate, fissitunicate, cylindric-clavate, with a short, bulbous pedicel, rounded at the apex, with an indistinct ocular chamber. *Immature ascospores* 14–18.5 × 4–6.5 μm ($\bar{x}$ = 16.5 × 5.1 μm, n = 50), biseriate, fusiform with acute ends, 1-septate, strongly constricted at the septum, upper cell slightly broader than lower cell, straight or slightly curved, hyaline, guttulate, smooth-walled, frequently with globose appendages at both ends. Asexual morph: Not observed.

Culture characteristics – *Colonies* on PDA attaining 35–45 mm diameter in 3 weeks, dense, circular, flat, slightly raised, surface smooth with entire edge, zonate with different sector pale brown at the margin, dull brown to dark brown at the center, reverse same with obverse, radial cracks in all directions. No pigmentation produced in media.

Material examined – China, Sichuan Province, Chengdu City, Wenjiang District, Schoolyard of Sichuan Agricultural University, 103°51′39.26″E 30°42′17.29″N, 498 m, isol. from leaves of *Phoenix sylvestris*, 30 Nov. 2019, C.L. Yang, YCL201912002 (SICAU 23-0145), culture (SICAUCC 20-0008). China, Sichuan Province, Chengdu City, Wenjiang District, Schoolyard of Sichuan Agricultural University, 103°51′41.24″E 30°42′17.79″N, 525 m, isol. from leaves of *Syagrus romanzoffiana*, 9 May 2020, C.L. Yang, YCL202005002 (SICAU 23-0126), culture (SICAUCC 23-0120).

GenBank numbers – SICAUCC 20-0008 = ITS: PP702554, LSU: PP702580, SSU: PP702570, *tef*1-α: PP712867, *rpb*2: PP712861; SICAUCC 23-0120 = ITS: PP702555, LSU: PP702581, SSU: PP702571, *tef*1-α: PP712868, *rpb*2: PP712862

Notes – The new collections are identified as *Neovaginatispora fuckelii* based on morphology and phylogeny. Morphologically, our new collections fit well with the description of *N. fuckelii* with 8-spored, bitunicate, fissitunicate, cylindric-clavate asci, with a short, bulbous pedicel, and an indistinct ocular chamber, and 1-septate ascospores (Thambugala et al. 2015, Hashimoto et al. 2018). Remarkably, asci and ascospores described in those publications are most likely immature (Thambugala et al. 2015, Hashimoto et al. 2018, Bao et al. 2019), as we found some ascospores become darker to brown after maturity, and appendages are less noticeable. In phylogenetic

analysis, our newly collected isolates clustered with *N. fuckelii* with bootstrap support (99% MLBS / 1.00 BYPP) (Fig. 29). *Neovaginatispora fuckelii* has a wide distribution and it has been reported from terrestrial habitats in China, Japan, Germany, Sweden, Switzerland, and UK (Thambugala et al. 2015, Bao et al. 2019). In this study, we identified the new isolates as a new record *N. fuckelii* from *Syagrus romanzoffiana*.

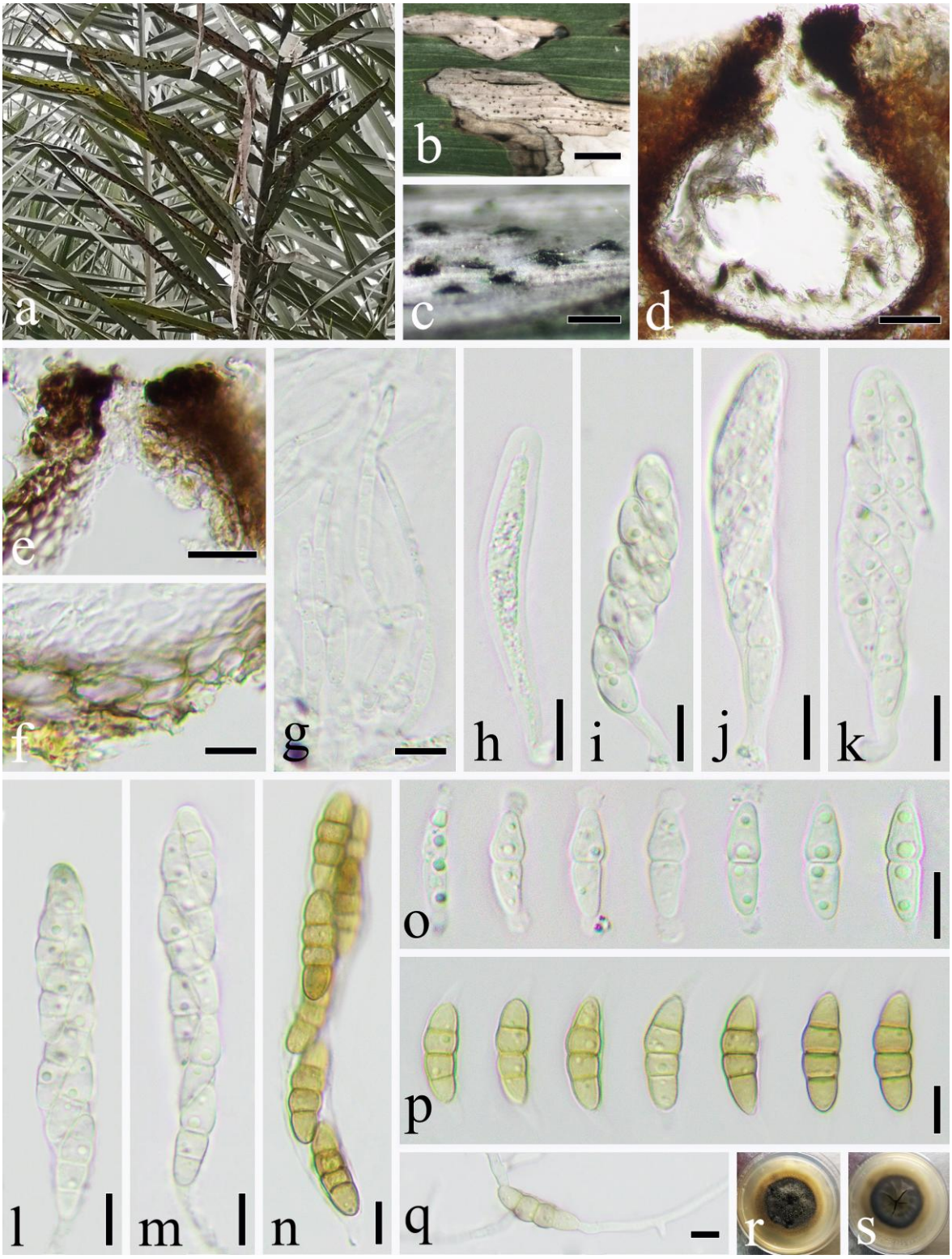

Figure 28 – *Neovaginatispora fuckelii* (SICAU 23-0145). a Symptoms on the leaves. b, c Appearance of ascomata. d Cross-section of ascoma. e Ostiole. f Peridium. g Pseudoparaphyses. h–n Asci. o Immature ascospores. p Mature ascospores. q Germinating ascospore. r Front view of

colony on PDA. s Reverse view of colony on PDA. Scale bars: b = 2500 µm, c = 300 µm, d = 50 µm, e = 20 µm, f–q = 10 µm.

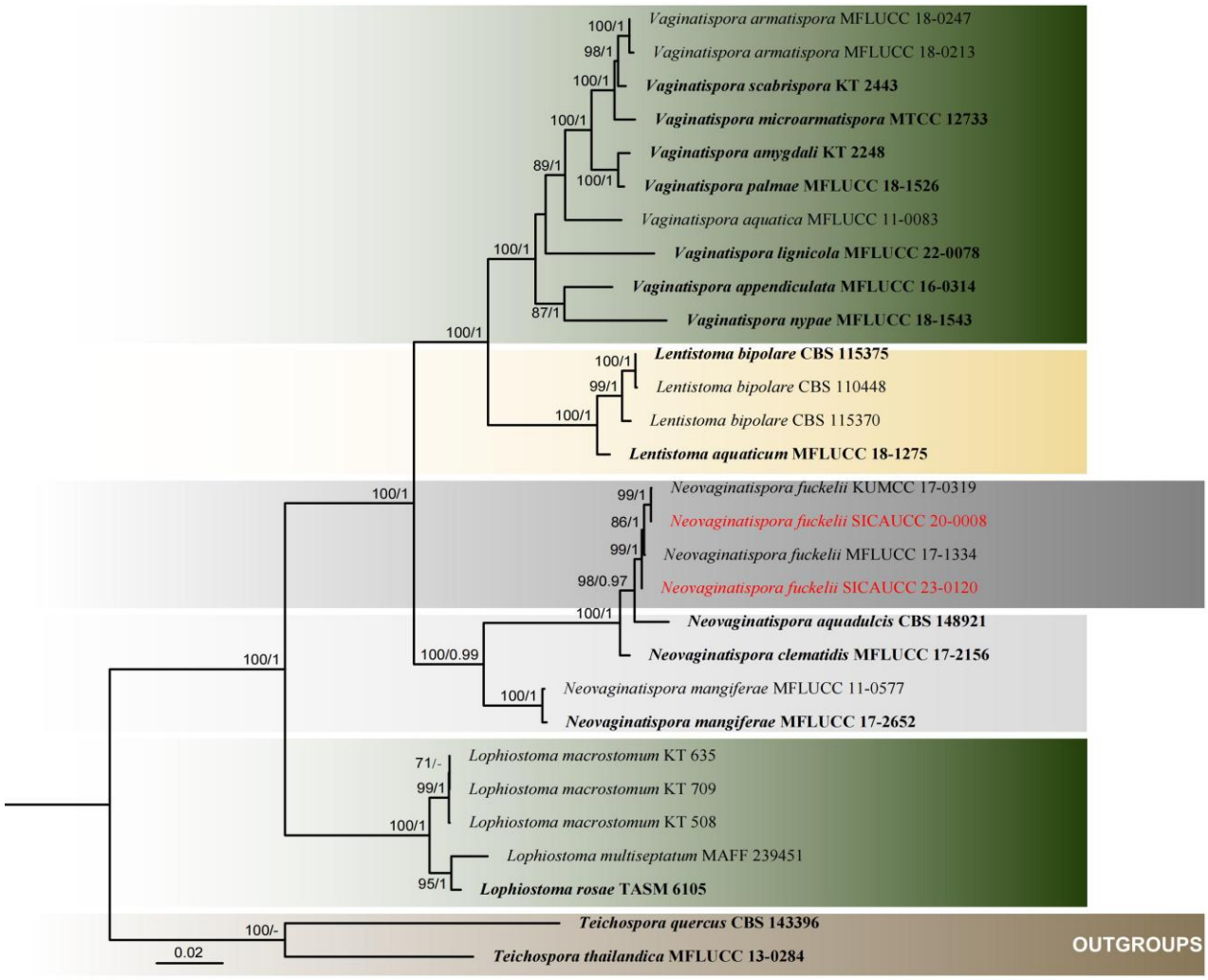

Figure 29 – Phylogram derived from maximum likelihood analyses of a combined dataset comprising ITS, LSU, SSU, *tef*1-α, and *rpb*2 sequences in partial *Lophiostomataceae* species. The alignment contained 5,282 characters (ITS: 1–831, LSU: 832–2,179, SSU: 2,180–3,210, *tef*1-α: 3,211–4,213, *rpb*2: 4,214–5,282) including gaps. The tree is rooted to *Teichospora quercus* (CBS 143396) and *T. thailandica* (MFLUCC 13-0284) in *Teichosporaceae*. Single-gene analyses were conducted, resulting in similar tree topologies between the ML and BY methods, ensuring consistent comparisons of clade stability. The best-scoring RAxML tree with a final likelihood value of -18,219.736193 is presented. The matrix had 1,379 distinct alignment patterns, with 28.37% of undetermined characters or gaps. Estimated base frequencies were as follows: A = 0.250276, C = 0.247035, G = 0.270109, T = 0.232580; substitution rates AC = 1.591291, AG = 3.390988, AT = 1.149328, CG = 1.220175, CT = 7.060542, GT = 1.000000. The gamma distribution shape parameter α = 0.180632 and the tree length = 0.705094. Bootstrap support values (MLBS) equal or exceeding 70%, and Bayesian posterior probabilities (BYPP) equal or exceeding 0.95 have been indicated above the nodes. The ex-type strains are in bold, and the new isolates are in red. The bar, set at 0.02, represents the estimated number of nucleotide substitution sites per branch.

Neomassarinaceae Mapook & K.D. Hyde

Notes – *Neomassarinaceae*, introduced by Mapook et al. (2020), shares a close phylogenetic relationship with *Sporormiaceae* and *Amorosiaceae* but can be differentiated by distinct

morphological features. Two genera (*Neomassarina*, *Pseudohelminthosporium*) comprising four species have been documented within this family, and these species are saprobic, typically found on the stems and leaves of plants (Hyde et al. 2018, Mapook et al. 2020, Phukhamsakda et al. 2020). Phylogeny, combined with morphological observations, confirm the placement of *Paramassarina* as the first coelomycetous species in *Neomassarinaceae*.

Paramassarina C.L. Yang & X.L. Xu, gen. nov.

MycoBank number: MB853709; Facesoffungi number: FoF15914

Etymology – The genus epithet reflects its morphological similarity to *Massarina* species.

Type species – *Paramassarina euonymicola* C.L. Yang & X.L. Xu

Living on *Euonymus nitidus* in terrestrial habitats. Sexual morph: Not observed. Asexual morph: *Coelomycetous*. *Conidiomata* pycnidial, initially immersed, becoming erumpent through the host epidermis, black, solitary, scattered, uni-loculate, subglobose to globose, ostiolate. *Conidiomatal wall* comprising of hyaline to brown cells of *textura angularis*. *Conidiophores* reduced to conidiogenous cells. *Conidiogenous cells* hyaline, enteroblastic, monophialidic, doliiform, smooth-walled. *Conidia* hyaline, cylindrical to ellipsoid, occasionally ovoid, thin-walled, smooth.

Notes – *Paramassarina* is established as a monotypic genus. Based on the multi-gene analysis (Fig. 31), our new collection SICAUCC 23-0121 formed a close relationship with the type species of *Pseudohelminthosporium*, *P. clematidis* (MFLUCC 17-2086), with moderate support (100% ML). However, the strain is incompatible with the concept of *Pseudohelminthosporium* in having brown to dark brown phragmosporous conidia, which is similar to *Helminthosporium* (*Massarinaceae*) (Voglmayr & Jaklitsch 2017). The asexual state of *Paramassarina* are coelomycetous with enteroblastic, monophialidic conidiogenous cells, and hyaline conidia.

15. ***Paramassarina euonymicola*** C.L. Yang & X.L. Xu, sp. nov. Fig. 30

MycoBank number: MB853710; Facesoffungi number: FoF15915

Etymology – The epithet refers to the host substrate.

Holotype – SICAU 23-0146

Associated with leaf spots on leaves of *Euonymus nitidus* Benth. Sexual morph: Not observed. Asexual morph: *Coelomycetous*. *Conidiomata* 95–130 × 70–100 μm ($\bar{x}$ = 116 × 86 μm, n = 10), pycnidial, initially immersed, becoming erumpent through the host epidermis, black, solitary, scattered, uni-loculate, subglobose to globose, ostiolate. *Conidiomatal wall* 7–17 μm width, comprising 3–4 layers of brown to dark brown cells of *textura angularis*. *Conidiophores* reduced to conidiogenous cells. *Conidiogenous cells* 3–6 × 3.5–7 μm ($\bar{x}$ = 4.2 × 5.4 μm, n = 20), hyaline, enteroblastic, monophialidic, doliiform or cone, smooth-walled. *Conidia* 4.5–8 × 2–3.5 μm ($\bar{x}$ = 5.9 × 2.7 μm, n = 50), hyaline, cylindrical to ellipsoid, occasionally ovoid, thin- and smooth-walled.

Culture characteristics – *Colonies* on PDA attaining 25–40 mm diameter in 30 days, dense, circular, entire edge, leathery, yellowish-brown centrally, creamy yellow at the margin, intermediate region distinctly radially furrowed, aerial mycelia underdeveloped, reverse creamy yellow, intermediate region with a dark concentric ring.

Material examined – China, Sichuan Province, Ya'an City, Tianquan County, Renyi Town, Lijia Village, 102°47′40.01″E 30°5′46.35″N, 820 m, isol. from leaves of *Euonymus* sp., 11 Jun. 2020, C.L. Yang, YCL202006008 (SICAU 23-0146, holotype), ex-type culture (SICAUCC 23-0121). *ibid.* YCL202006008-2 (SICAU 23-0156), living culture SICAUCC 23-0125.

GenBank numbers – SICAUCC 23-0121 = ITS: PP702561, LSU: PP702587, SSU: PP702577, *tef*1-α: PP712874, *rpb*2: PP712865. SICAUCC 23-0125 = ITS: PP702562, LSU: PP702588, SSU: PP702578, *tef*1-α: PP712875, *rpb*2: PP712866

Notes – In a BLASTn search of GenBank, the closest match for the ITS, LSU, and *rpb*2 sequence of SICAUCC 23-0121 was *Pseudohelminthosporium clematidis* MFLUCC 17-2086 (NR_170808) with 91.18%, 99.06%, and 84.10% similarity. The closest match for the SSU region was *Didymosphaeria enalia* C364 (MK347878). Phylogenetic analyses of combined ITS, LSU,

SSU, *rpb*2, and *tef*1-α sequence data of partial taxa in *Pleosporales* indicated that our new species grouped within *Neomassarinaceae*, and has a close relationship with *Pseudohelminthosporium clematidis* (Fig. 31). *Pseudohelminthosporium* is introduced as the asexual morph in *Neomassarinaceae* by Phukhamsakda et al. (2020). The asexual morph of *Pseudohelminthosporium* is hyphomycetous, while our new species is coelomycetous. Therefore, *Paramassarina* is treated as a distinct genus in *Neomassarinaceae*.

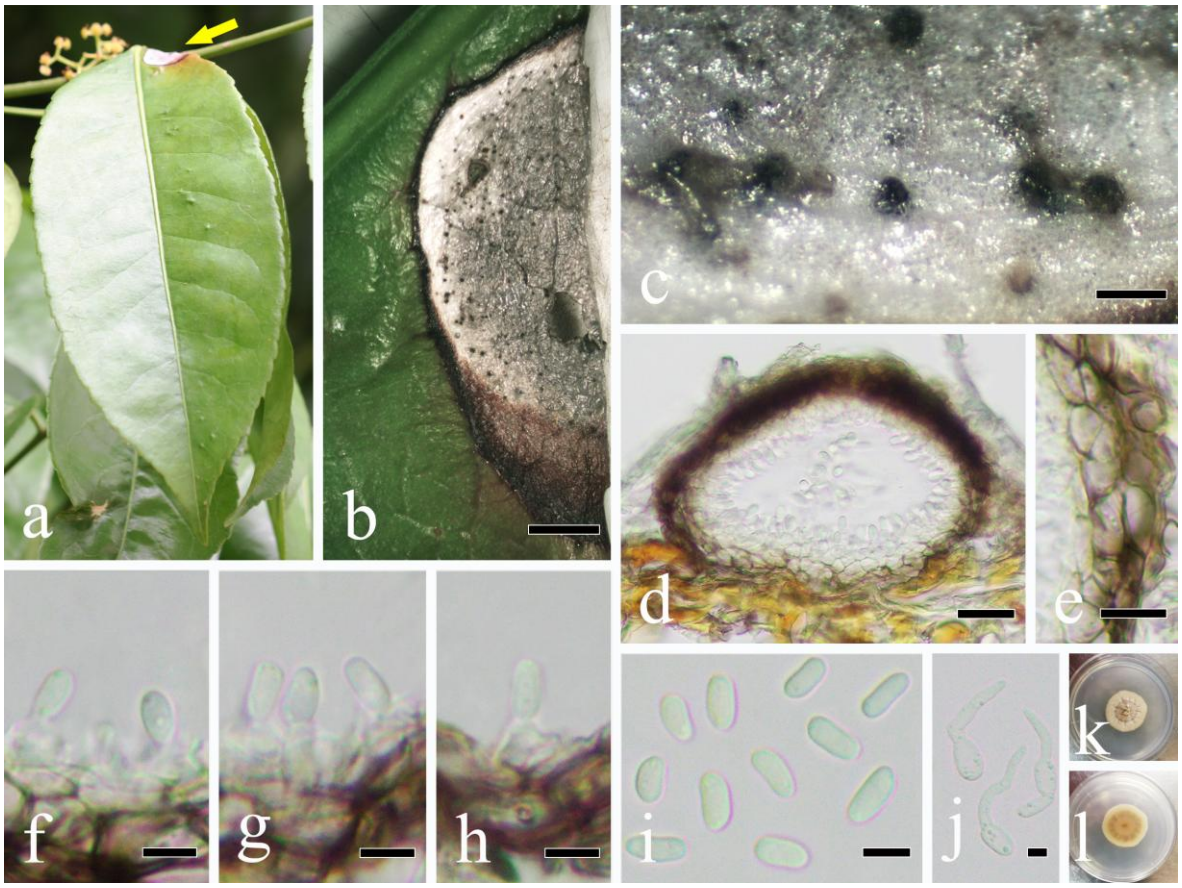

Figure 30 – *Paramassarina euonymicola* (holotype, SICAU 23-0146). a Symptoms on the leaf. b, c Appearance of conidiomata. d Cross-section of conidioma. e Conidiomatal wall. f–h Conidiogenous cells with developing conidia. i Conidia. j Germinating conidia. k Front view of colony on PDA. l Reverse view of colony on PDA. Scale bars: b = 2000 μm, c = 200 μm, d = 20 μm, e = 10 μm, f–j = 5 μm.

Phaeosphaeriaceae M.E. Barr

Notes – *Phaeosphaeriaceae*, typified by *Phaeosphaeria*, was established by Barr (1979) and has since undergone expansion and revision based on both morphological data and molecular phylogenetics (Phookamsak et al. 2014, Li et al. 2015, Karunarathna et al. 2017). *Phaeosphaeriaceae* members are distinguished by their morphologically diverse assemblage of ascomata immersed, superficial or erumpent, globose or conical, short papillate, asci bitunicate, ascospores hyaline, yellowish or brown, obovoid, septate or aseptate (Barr 1979, Zhang et al. 2012, Hyde et al. 2013, Phookamsak et al. 2014). This family, with a stem age of approximately 99 Mya, is a prominent constituent of the order *Pleosporales*, encompassing 85 genera with around 740 species (Liu et al. 2017, Wijayawardene et al. 2022, Ashrafi et al. 2023), and includes species known to cause diseases in economically important forests and crops (Quaedvlieg et al. 2013, Phookamsak et al. 2014, Zhang et al. 2018, Yang et al. 2019a, Al-Jaradi et al. 2020).

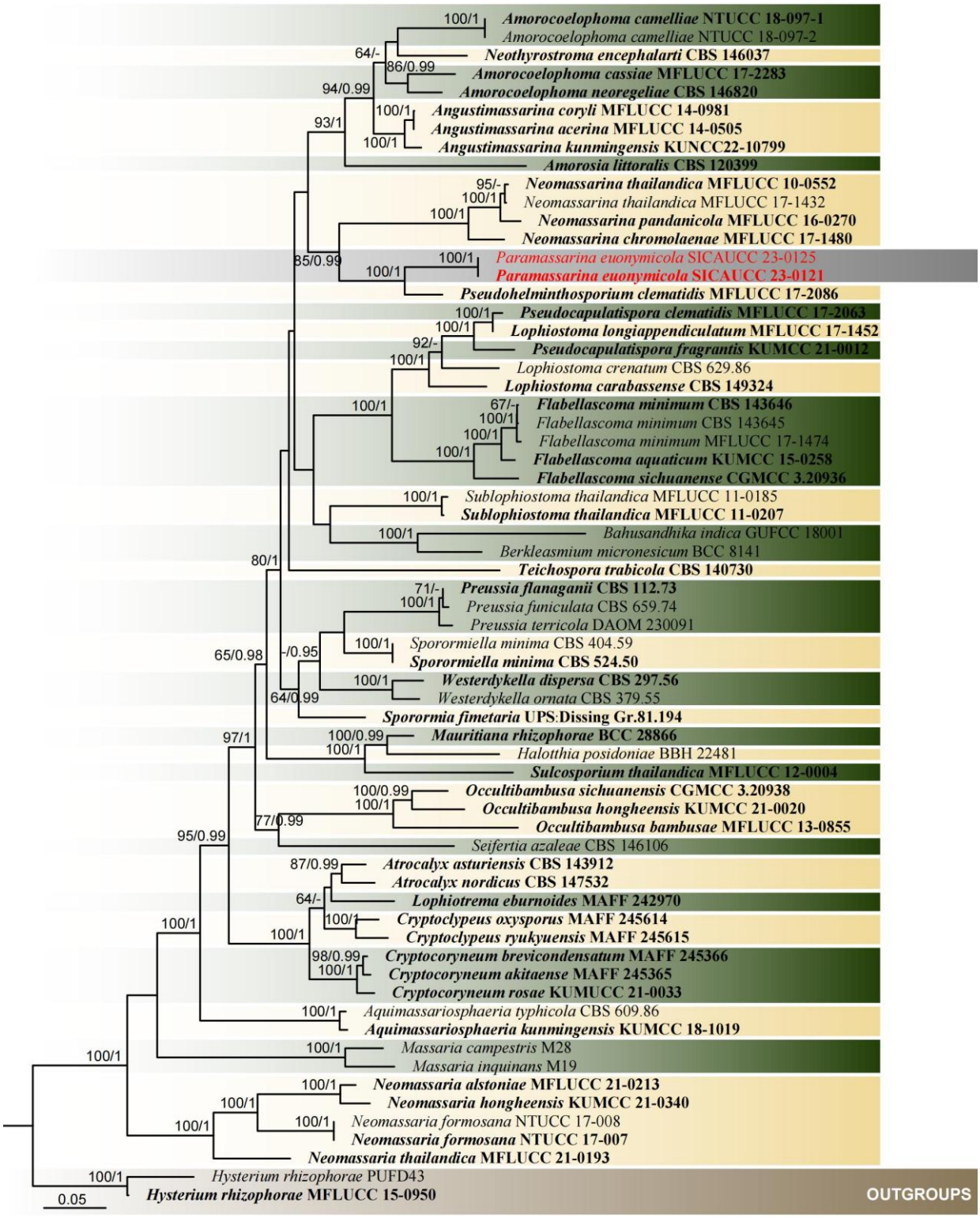

Figure 31 – Phylogram derived from maximum likelihood analyses of a combined dataset comprising ITS, LSU, SSU, *tef*1-α, and *rpb*2 sequences in *Neomassarinaceae* species. The alignment contained 6,802 characters (ITS: 1–1,809, LSU: 1,810–3,222, SSU: 3,223–4,665, *tef*1-α: 4,666–5,701, *rpb*2: 5,702–6,802) including gaps. The tree is rooted to *Hysterium rhizophorae* (MFLUCC 15-0950 and PUFD43). Single-gene analyses were conducted, resulting in similar tree topologies between the ML and BY methods, ensuring consistent comparisons of clade stability. The best-scoring RAxML tree with a final likelihood value of -48,991.475157 is presented. The matrix had 2,791 distinct alignment patterns, with 49.73% of undetermined characters or gaps. Estimated base frequencies were as follows: A = 0.249028, C = 0.249141, G = 0.268935, T =

0.232896; substitution rates AC = 1.441457, AG = 3.477746, AT = 1.577540, CG = 1.356114, CT = 7.031795, GT = 1.000000. The gamma distribution shape parameter α = 0.221152, and the tree length = 4.286046. Bootstrap support values (MLBS) equal or exceeding 60%, and Bayesian posterior probabilities (BYPP) equal or exceeding 0.95 have been indicated above the nodes. The ex-type strains are in bold, and the new isolates are in red. The bar, set at 0.05, represents the estimated number of nucleotide substitution sites per branch.

Paraphoma Morgan-Jones & J.F. White emend S.S. Xiang & C.L. Yang

Saprobic and parasitic on many substrates in aquatic or terrestrial environment. Sexual morph: Not observed. Asexual morph: *Coelomycetous*. *Conidiomata* pycnidial, solitary to aggregated, partially setae, superficial to immersed, brown to dark brown, spherical to subglobose, uniloculate. *Conidiomatal wall* composed of 2–6 layers of hyaline to brown cells of *textura angularis*. *Conidiogenous cells* formed from inner layer of conidiomatal wall, lageniform, monophalidic, translucent to somewhat translucent, discrete. *Conidia* diversified shape, oval to rod-like, 0–3 septate, smooth, hyaline. *Chlamydospores* unicellular.

Notes – *Paraphoma*, typified by *P. radicina*, was initially introduced by Morgan-Jones et al. (1983), to accommodate the species that produced numerous setae on pycnidia. However, the discovery of new specimens has demonstrated that the original genus-level characteristics are inadequate to account for the full diversity of existing species. *Paraphoma dioscoreae*, *P. melnikiae*, and *P. populi* lack setae, while the conidia of *P. melnikiae* and *P. convolvuli* are distinguished by the presence of septa (Quaedvlieg et al. 2013, Gomzhina et al. 2020). To date, this genus comprises 15 documented species, which are typically associated with root diseases and necrotic leaf spots on ornamental and herbaceous plants (Phookamsak et al. 2014, Gomzhina et al. 2020, Crous et al. 2021, Guarnaccia et al. 2022).

16. ***Paraphoma populi*** S.S. Xiang & C.L. Yang, sp. nov. Fig. 32

MycoBank number: MB901631, Facesoffungi number: FoF16126

Etymology – Refers to the host genus *Populus.*

Holotype – SICAU 23-0149

Associated with leaf spots on leaves of *Populus* × *beijingensis* W. Y. Hsu. Sexual morph: Not observed. Asexual morph: *Coelomycetous*. *Conidiomata* 109–143 × 65–128 μm ($\bar{x}$ = 120 × 87 μm, n = 10), pycnidial, long ellipsoid, semisubmerged, aggregated, dark brown. *Conidiomatal wall* composed of 2–3 layers of chartreuse *textura globulosa,* with brown cells in the outer layer and hyaline cells in the inner layer. *Conidiophores* reduced to conidiogenous cells. *Conidiogenous cells* 2.5–5 × 3–6 μm ($\bar{x}$ = 3.6 × 4.6 μm, n = 30), densely aggregated, smooth, ellipse, subulate, mostly straight, phialidic, simple, cylindrical, hyaline. *Conidia* 4–6 × 2–3 μm ($\bar{x}$ = 4.8 × 2.6 μm, n = 50), solitary, subglobose or ovoid, smooth-walled, aseptate, obtuse both ends.

Culture characteristics – Germinated conidia on PDA within 12 h and germ tubes produced from both ends. *Colonies* on PDA attaining 21–24 mm after 12 days, circular, surface with thick aerial mycelium, initially appearing white and light yellow, becoming flavovirens from the center with age, in reverse light yellow to dark brown with smooth margin, pigmentation in the center.

Material examined – China, Sichuan Province, Chengdu City, Wenjiang District, Gongping Street, Sichuan Agricultural University. 103°51′27.55″E 30°42′19.5″N, 533 m, isol. from leaves of *Populus* × *beijingensis*, 3 Nov. 2020, C.L. Yang, YCL202011001 (SICAU 23-0149, holotype) ex-type culture (SICAUCC 23-0097). *ibid.* YCL202011001-2 (SICAU 23-0157), living culture SICAUCC 23-0132.

GenBank numbers – SICAUCC 23-0097 = LSU: PP719620, SSU: PP734051, *tef*1-α: PQ005619, ITS: PP769689. SICAUCC 23-0132 = LSU: PP719625, SSU: PP734053, *tef*1-α: PQ005622, ITS: PP769693

Notes – In the phylogenetic analyses using combined ITS, LSU, SSU, and *tef*1-α sequence data, *Paraphoma populi* clusters with *P. convolvuli*, *P. dioscoreae*, *P. garibaldi*, *P. melnikiae*, and *P. salicis* (98% MLBS / 1.00 BYPP) (Fig. 33). In comparative sequence analyses, the ITS and LSU

sequences of *N. populi* show notable differences when compared with other species. For *P. convolvuli* (MF-9.222), the ITS similarity is 88.3% (424/480, 4 gaps), and LSU similarity is 99.4% (840/845, 0 gap). Compared with *P. dioscoreae* (CBS 135100, holotype), the ITS similarity is 86.9% (449/517, 6 gaps) and LSU is 99.5% (831/835, 0 gap). For *P. salicis* (CPC 38651, holotype), the ITS similarity is 90.2% (525/582, 4 gaps) and LSU is 99.6% (833/836, 0 gap). In comparison with *P. melnikiae* (MF-9.95, holotype), ITS similarity is 88.4% (428/484, 8 gaps) and LSU is 99.3% (839/845, 0 gap). For *P. garibaldi* (CBS 148459, holotype), the ITS similarity is 97.7% (414/472, 5 gaps). Morphologically, *P. populi* can be readily distinguished from *P. convolvuli* and *P. melnikiae* based on the septation and size of the conidia (*P. populi*: 0-septate, 4–6 × 2–3 µm vs. *P. convolvuli*: 2–3-septate, 15–18 µm; *P. melnikiae*: 0–2-septate, 9–22 × 2–4 µm) (Gomzhina et al. 2020). *Paraphoma populi* differs from *P. dioscoreae* by having subglobose to ovoid conidia, as opposed to the cylindrical conidia of *P. dioscoreae*, and by the absence of droplets (0 droplet vs. 2 droplets in *P. dioscoreae*) (Quaedvlieg et al. 2013). Compared with *P. garibaldi*, the conidiomata of *P. populi* are smaller (109–140 µm vs. 200–300 µm) and lack setae, and the conidia have no droplets (Guarnaccia et al. 2022). Compared with *P. salicis, P. populi* has smaller conidiomata (109–140 µm vs. 180–200 µm) and produces thicker aerial mycelia on PDA (Crous et al. 2021). The morphological characteristics and molecular phylogenetic analyses support the recognition of a new species.

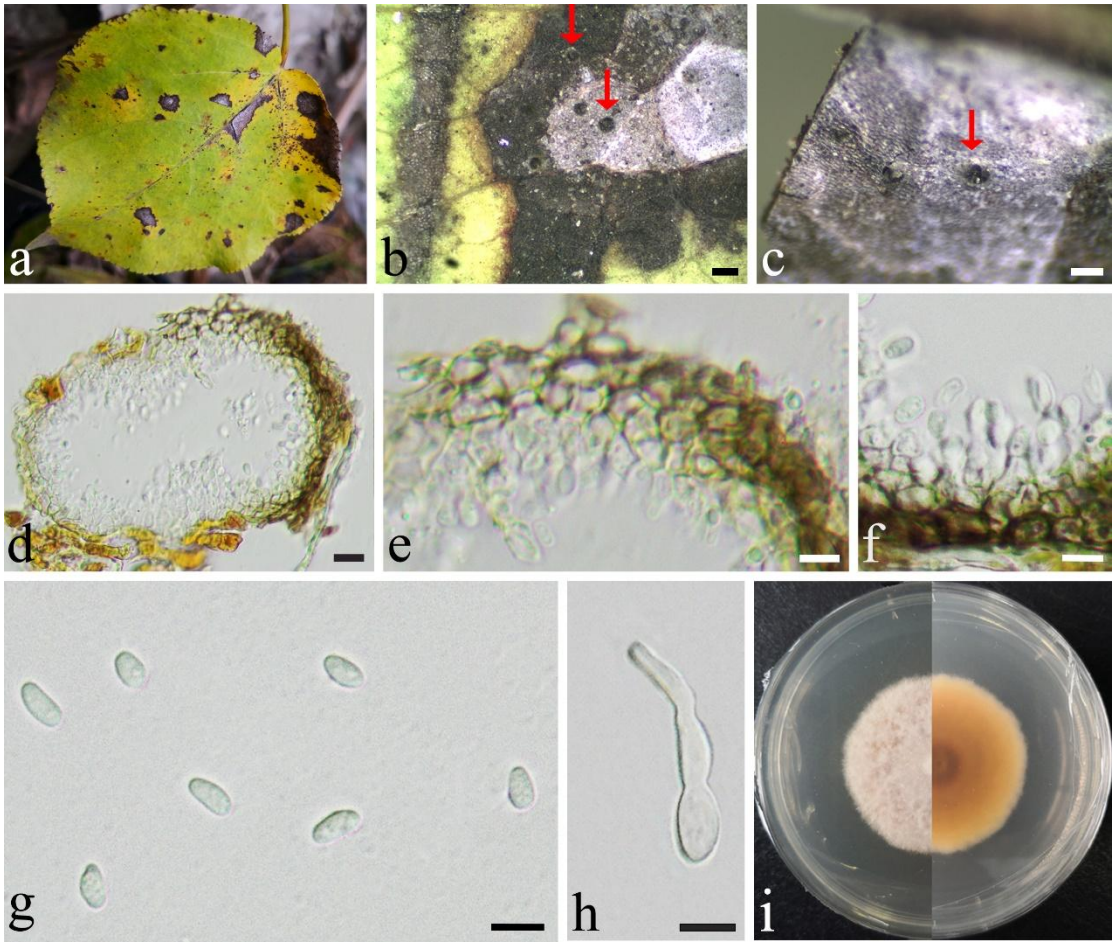

Figure 32 – *Paraphoma populi* (holotype, SICAU 23-0149). a Symptoms on the leaf. b, c Appearance of conidiomata. d Cross-section of conidioma. e Conidiomatal wall. f Conidiogenous cells with developing conidia. g Conidia. h Germinating conidium. i Front and reverse view of colonies on PDA. Scale bars: b, c = 200 µm, d, e = 10 µm, f–h = 5 µm.

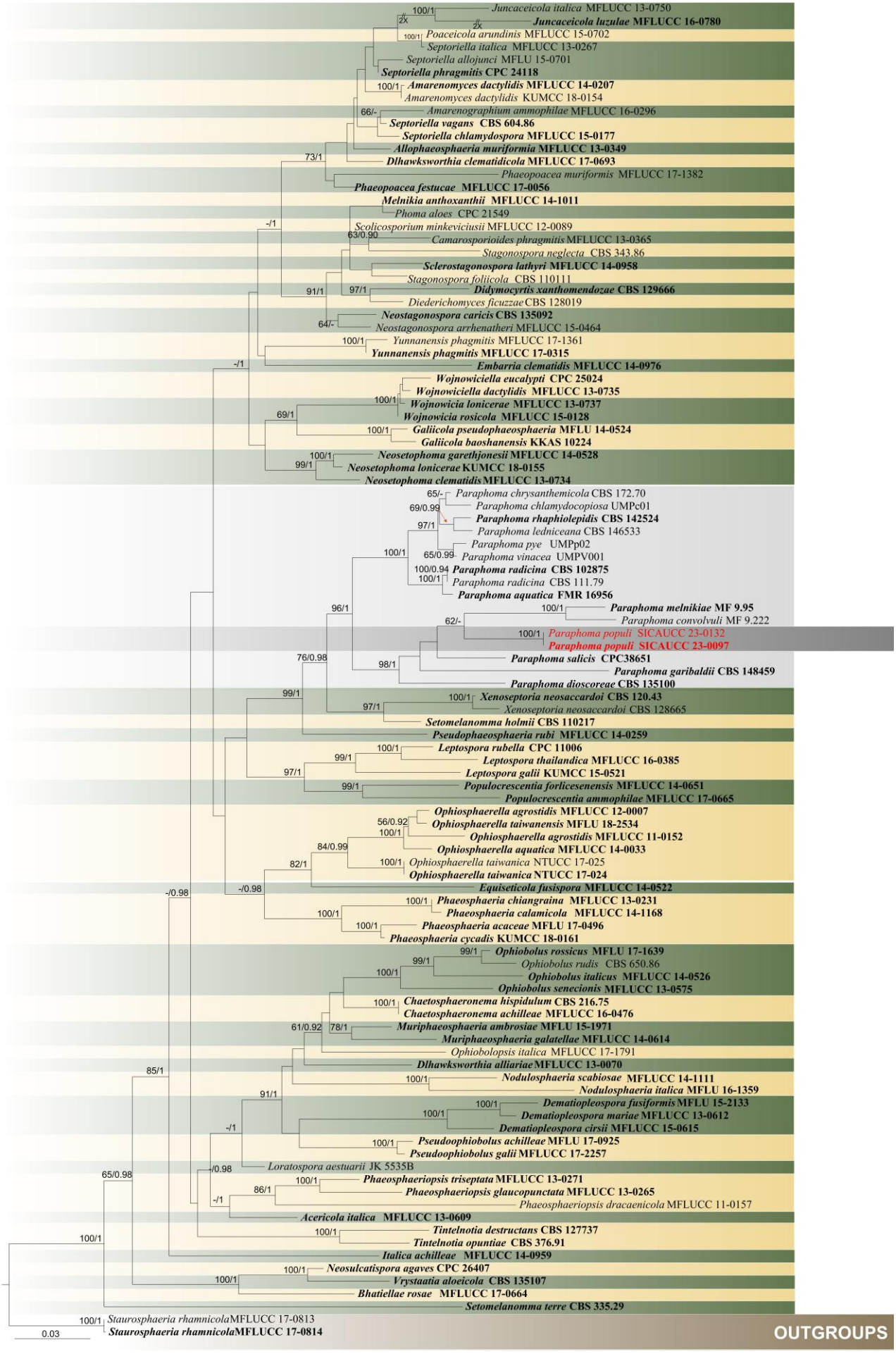
Juncaceicola italica MFLUCC 13-0750
Juncaceicola luzulae MFLUCC 16-0780
Poaceicola arundinis MFLUCC 15-0702
Septoriella italica MFLUCC 13-0267
Septoriella allojunci MFLU 15-0701
Septoriella phragmitis CPC 24118
Amarenomyces dactylidis MFLUCC 14-0207
Amarenomyces dactylidis KUMCC 18-0154
Amarenographium ammophilae MFLUCC 16-0296
Septoriella vagans CBS 604.86
Septoriella chlamydospora MFLUCC 15-0177
Allophaeosphaeria muriformia MFLUCC 13-0349
Dlhawksworthia clematidicola MFLUCC 17-0693
Phaeopoacea muriformis MFLUCC 17-1382
Phaeopoacea festucae MFLUCC 17-0056
Melnikia anthoxanthii MFLUCC 14-1011
Phoma aloes CPC 21549
Scolicosporium minkeviciusii MFLUCC 12-0089
Camarosporioides phragmitis MFLUCC 13-0365
Stagonospora neglecta CBS 343.86
Sclerostagonospora lathyri MFLUCC 14-0958
Stagonospora foliicola CBS 110111
Didymocyrtis xanthomendozae CBS 129666
Diederichomyces ficuzzae CBS 128019
Neostagonospora caricis CBS 135092
Neostagonospora arrhenatheri MFLUCC 15-0464
Yunnanensis phagmitis MFLUCC 17-1361
Yunnanensis phagmitis MFLUCC 17-0315
Embarria clematidis MFLUCC 14-0976
Wojnowiciella eucalypti CPC 25024
Wojnowiciella dactylidis MFLUCC 13-0735
Wojnowicia lonicerae MFLUCC 13-0737
Wojnowicia rosicola MFLUCC 15-0128
Galiicola pseudophaeosphaeria MFLU 14-0524
Galiicola baoshanensis KKAS 10224
Neosetophoma garethjonesii MFLUCC 14-0528
Neosetophoma lonicerae KUMCC 18-0155
Neosetophoma clematidis MFLUCC 13-0734
Paraphoma chrysanthemicola CBS 172.70
Paraphoma chlamydocopiosa UMPc01
Paraphoma rhaphiolepidis CBS 142524
Paraphoma ledniceana CBS 146533
Paraphoma pye UMPp02
Paraphoma vinacea UMPV001
Paraphoma radicina CBS 102875
Paraphoma radicina CBS 111.79
Paraphoma aquatica FMR 16956
Paraphoma melnikiae MF 9.95
Paraphoma convolvuli MF 9.222
Paraphoma populi SICAUCC 23-0132
Paraphoma populi SICAUCC 23-0097
Paraphoma salicis CPC38651
Paraphoma garibaldii CBS 148459
Paraphoma dioscoreae CBS 135100
Xenoseptoria neosaccardoi CBS 120.43
Xenoseptoria neosaccardoi CBS 128665
Setomelanomma holmii CBS 110217
Pseudophaeosphaeria rubi MFLUCC 14-0259
Leptospora rubella CPC 11006
Leptospora thailandica MFLUCC 16-0385
Leptospora galii KUMCC 15-0521
Populocrescentia forlicesenensis MFLUCC 14-0651
Populocrescentia ammophilae MFLUCC 17-0665
Ophiosphaerella agrostidis MFLUCC 12-0007
Ophiosphaerella taiwanensis MFLU 18-2534
Ophiosphaerella agrostidis MFLUCC 11-0152
Ophiosphaerella aquatica MFLUCC 14-0033
Ophiosphaerella taiwanica NTUCC 17-025
Ophiosphaerella taiwanica NTUCC 17-024
Equiseticola fusispora MFLUCC 14-0522
Phaeosphaeria chiangraina MFLUCC 13-0231
Phaeosphaeria calamicola MFLUCC 14-1168
Phaeosphaeria acaceae MFLU 17-0496
Phaeosphaeria cycadis KUMCC 18-0161
Ophiobolus rossicus MFLU 17-1639
Ophiobolus rudis CBS 650.86
Ophiobolus italicus MFLUCC 14-0526
Ophiobolus senecionis MFLUCC 13-0575
Chaetosphaeronema hispidulum CBS 216.75
Chaetosphaeronema achilleae MFLUCC 16-0476
Muriphaeosphaeria ambrosiae MFLU 15-1971
Muriphaeosphaeria galatellae MFLUCC 14-0614
Ophiobolopsis italica MFLUCC 17-1791
Dlhawksworthia alliariae MFLUCC 13-0070
Nodulosphaeria scabiosae MFLUCC 14-1111
Nodulosphaeria italica MFLU 16-1359
Dematiopleospora fusiformis MFLU 15-2133
Dematiopleospora mariae MFLUCC 13-0612
Dematiopleospora cirsii MFLUCC 15-0615
Pseudoophiobolus achilleae MFLU 17-0925
Pseudoophiobolus galii MFLUCC 17-2257
Loratospora aestuarii JK 5535B
Phaeosphaeriopsis triseptata MFLUCC 13-0271
Phaeosphaeriopsis glaucopunctata MFLUCC 13-0265
Phaeosphaeriopsis dracaenicola MFLUCC 11-0157
Acericola italica MFLUCC 13-0609
Tintelnotia destructans CBS 127737
Tintelnotia opuntiae CBS 376.91
Italica achilleae MFLUCC 14-0959
Neosulcatispora agaves CPC 26407
Vrystaatia aloeicola CBS 135107
Bhatiellae rosae MFLUCC 17-0664
Setomelanomma terre CBS 335.29
Staurosphaeria rhamnicola MFLUCC 17-0813
Staurosphaeria rhamnicola MFLUCC 17-0814
0.03
OUTGROUPS

Figure 33 – Phylogram derived from maximum likelihood analyses of a combined dataset comprising LSU, SSU, *tef*1-α, and ITS sequences, encompassing species within the *Phaeosphaeriaceae* and *Didymellaceae* family. The phylogenetic analysis included one hundred and five strains with a total of 4,224 characters (ITS: 1–759, LSU: 760–1,701, SSU: 1,702–3,207, *tef1*-α: 3208–4224) after alignment. The tree is rooted to *Staurosphaeria rhamnicola* (MFLUCC 17-0813 and MFLUCC 17-0814). Single-gene analyses were conducted, resulting in similar tree topologies between the ML and BY methods, ensuring consistent comparisons of clade stability. The best-scoring RAxML tree with a final likelihood value of -28,422.316854 is presented. The matrix had 1,454 distinct alignment patterns, with 42.46% of undetermined characters or gaps. Estimated base frequencies were as follows: A = 0.247340, C = 0.231505, G = 0.265155, T = 0.256000; substitution rates AC = 1.149685, AG = 3.067236, AT = 2.326168, CG = 0.724688, CT = 5.910596, GT = 1.000000. Bootstrap support values (MLBS) equal or exceeding 60%, and Bayesian posterior probabilities (BYPP) equal or exceeding 0.90 have been indicated above the nodes. The ex-type strains are in bold, and the new isolates are in red. The bar, set at 0.03, represents the estimated number of nucleotide substitution sites per branch.

Phaeosphaeria I. Miyake

Notes – *Phaeosphaeria* was proposed by Miyake (1909) with *P. oryzae* as the type species. This genus was previously considered a synonym within *Leptosphaeria*, later scholars reinstated it as a distinct genus due to differences in peridium structure, asexual morphs, and host characteristics (Müller 1950, Holm 1957, Munk 1957, Schoch et al. 2009, Zhang et al. 2012). *Phaeosphaeria*, registering 217 recorded epithets and 180 recognized species in Species Fungorum (https://www.speciesfungorum.org, November 2024), is a speciose genus within the family *Phaeosphaeriaceae*, widely distributed in both temperate and tropical regions, and some species can cause foliar diseases in horticultural hosts (Malkus et al. 2009, Gonçalves et al. 2013).

17. *Phaeosphaeria phormii* C.L. Yang & X.L. Xu, sp. nov. Fig. 34

MycoBank number: MB853708; Facesoffungi number: FoF15916

Etymology – The epithet "phormium" refers to the host substrate.

Holotype – SICAU 22-0087

Associated with leaf blight on leaves of *Phormium tenax* J. R. Forst et G. Forst. Sexual morph: Not observed. Asexual morph: *Coelomycetous*. *Conidiomata* 135–243 × 99–186 μm ($\bar{x}$ = 182×137, n = 20), pycnidial, solitary, black, superficial or immersed, globose to subglobose, superficial central protrusion. *Conidiomatal wall* 3–5 layered, measuring 5–14 μm thick, composed of hyaline to flavidus to brown cells of *textura angularis*. *Conidiophores* reduced to conidiogenous cells, arising from the inner cells of the conidiomata, indistinct to distinct. *Conidiogenous cells* 3–4 × 2.5–4 μm ($\bar{x}$ = 3.6×3.1, n = 20), base swells into an oily bulge or bottle, hyaline to flavidus, smooth-walled. *Conidia* 5–9 × 2–4 μm ($\bar{x}$ = 6.8×3 μm, n = 50), fusoid-ellipsoidal, flavidus to brown, smooth, aseptate or medially 1-septate, mostly straight.

Culture characteristics – *Colonies* on PDA attaining 80 mm diameter in 20 days, initially white and then white gray with some scattered black dots due to pycnidial formation after 15 days and the colony edges are clearly neat.

Material examined – China, Sichuan Province, Chengdu City, Wenjiang District, Schoolyard of Sichuan Agricultural University, 103°51′40.19″E 30°42′20.79″N, 529 m, isol. from leaves of *Phormium tenax*, 20 Dec. 2021, Y.J. Zhou, ZYJ202112001 (SICAU 22-0087, holotype), ex-type culture (SICAUCC 22-0088). *ibid.* ZYJ202112001-2 (SICAU 23-0158), living culture SICAUCC 23-0126.

GenBank numbers – SICAUCC 22-0088 = ITS: PP702556, LSU: PP702582, SSU: PP702572, *tef*1-α: PP712869, *tub*2: PP712876; SICAUCC 23-0126 = ITS: PP702557, LSU: PP702583, SSU: PP702573, *tef*1-α: PP712870, *tub*2: PP712877

Notes – In the phylogenetic analysis, *Phaeosphaeria phormii* groups sister to *P. sinensis* and *P. nodulispora* (Fig. 35), but differs morphologically by having fusoid-ellipsoidal, 1-septate and

larger conidia (5–9 × 2–4 µm vs. 3.5–4.1 × 1.9–2.4 µm) while *P. sinensis* is characterized by globose to subglobose, aseptate conidia, and with prominent guttules (Jayasiri et al. 2019). In addition, *P. nodulispora* is characterized by multi-septate conidia (1–6(–7)-septate) (Oliveira et al. 2016). A comparison of the nucleotides of *Phaeosphaeria phormii* and *P. sinensis* (MFLUCC 18-1552) reveals 98.54% (474/481, 0 gap) and 98.09% (877/894, 0 gap) similarities in ITS and *tef*1-α genes, respectively. *Phaeosphaeria phormii* and *P. nodulispora* have 97.77% (527/539, 0 gap) similarity in ITS gene. The *tef*1-α gene sequence data are not available for *P. nodulispora* in GenBank. Based on these differences, we introduce a new species of *Phaeosphaeria*.

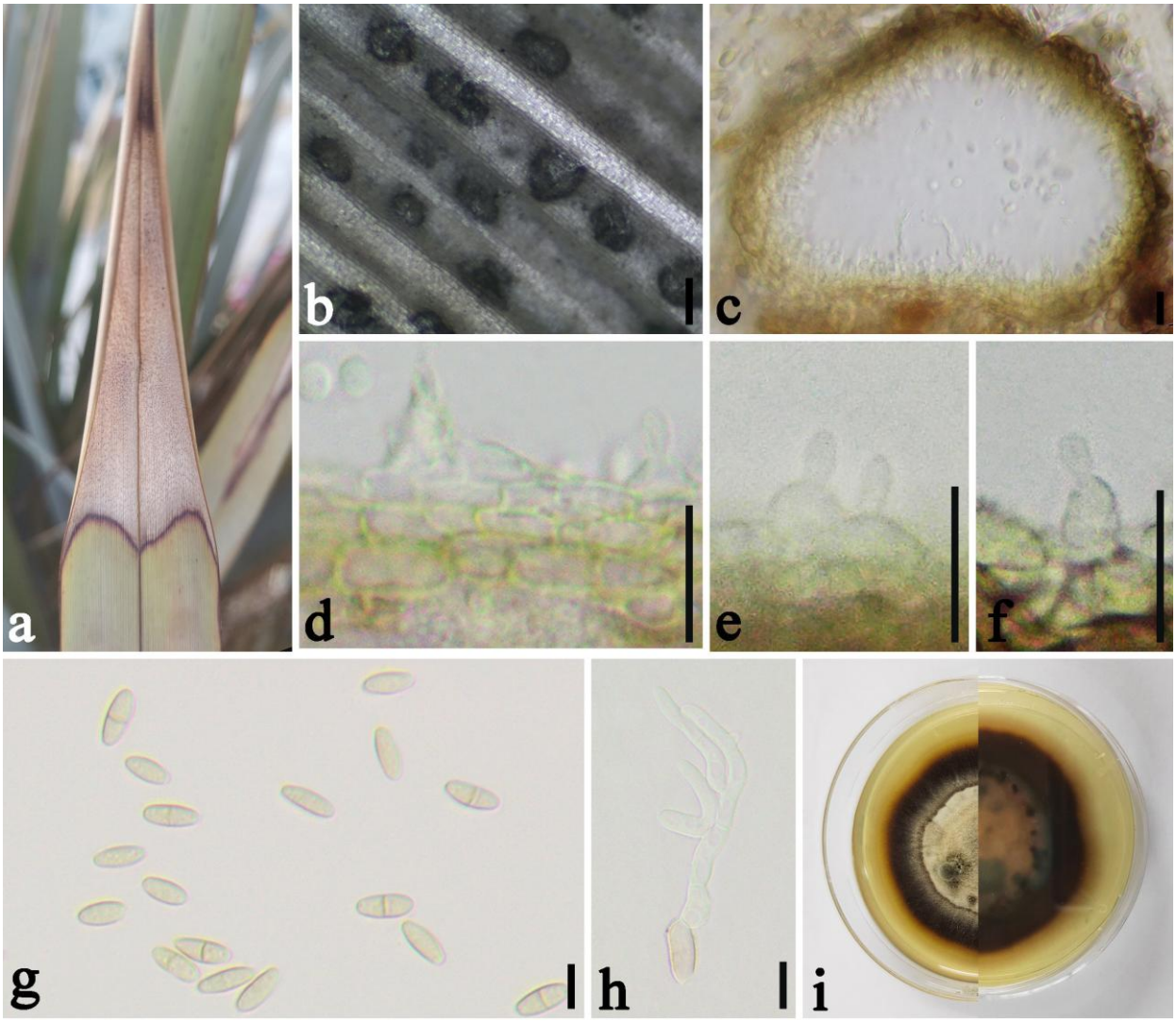

Figure 34 – *Phaeosphaeria phormii* (holotype, SICAU 22-0087). a Symptoms on the leaf. b Appearance of conidiomata. c Cross-section of conidioma. d Conidiomatal wall. e, f Conidiogenous cells with developing conidia. g Conidia. h Germinating conidium. i Front and reverse view of colonies on PDA. Scale bars: b = 200 µm, c–h = 10 µm.

Class *Leotiomycetes* O.E. Erikss. & Winka

Helotiales Nannf.

Notes – In 1932, Nannfeldt established the order *Helotiales*, which stands as the largest order within the *Leotiomycetes*, encompassing approximately 5,300 species distributed across 480 genera within 36 families (Wang & Nai 2004, Suija et al. 2020, Holien & Suija 2021, Koukol & Maciá-Vicente 2022, Wijayawardene et al. 2022, Baral et al. 2023, Iliushin & Kirtsideli 2023, Itagaki & Hosoya 2023, Jamali 2024). *Helotiales* species constitute a nutritionally diverse group,

encompassing saprophytes, endophytes, pathogens, mycorrhizal fungi, fungicolous organisms, and lichenicolous fungi (Suija et al. 2014, Tanney & Seifert 2020, Haelewaters et al. 2021).

Drepanopezizaceae Baral

Notes – *Drepanopezizaceae* was proposed by Batista & Maia (1960) without a valid basis for its definition, rendering the proposal invalid, and was validated by Johnston et al. (2019) based on multi-locus phylogeny. *Drepanopezizaceae* species exhibit phylogenetic similarities to *Ploettnerulaceae*, but they can be distinguished by stromatic structures, conidiomata acervular, conidiogenesis holoblastic, and conidia large (Johnston et al. 2019). *Drepanopezizaceae* members frequently act as parasites on the leaves and fruits of various dicotyledonous plants, resulting in the occurrence of spot diseases (Blechert & Debener 2005, Busby et al. 2013, Andersen et al. 2018, Wöhner & Emeriewen 2019). *Drepanopezizaceae* comprises nine recorded genera: *Blumeriella*, *Diplocarpon*, *Drepanopeziza*, *Felisbertia*, *Leptotrochila*, *Pseudopeziza*, *Spilopodia*, *Spilopodiella*, and *Thedgonia* (Johnston et al. 2019).

Drepanopeziza (Kleb.) Jaap.

Notes – *Drepanopeziza* is a compact and widespread genus within the *Dermateaceae* family, belonging to *Leotiales*. Noteworthy for its homogeneity, this genus exhibits a cosmopolitan distribution. Significant attention has been devoted to studying *Drepanopeziza* species, particularly those pathogenic to poplars (Rimpau et al. 1962, Gremmen et al. 1965). The taxonomic landscape of *Drepanopeziza* has seen debates and considerations, particularly regarding the synonyms of *D. brunnea*. Before 2017, this species was commonly classified within the genus *Marssonina*. However, it differs morphologically from the type species of *Marssonina*, *M. potentillae*. Rossman (2017) identified it as belonging to the genus *Drepanopeziza* (Rossman et al. 2017).

18. ***Drepanopeziza brunnea*** (Ellis & Everh.) Rossman & W.C. Allen, Mycotaxon 132(4): 952 (2017) Fig. 36

MycoBank number: MB229926; Facesoffungi number: FoF16131

Associated with leaf spots on leaves of *Populus* × *beijingensis* W. Y. Hsu. Sexual morph: Not observed. Asexual morph: *Coelomycetous*. *Conidiomata* 117–125 × 7–18 μm ($\bar{x}$ = 122 × 12 μm, n = 20), acervulus, immersed, brown to black, solitary, conical, uniloculate, glabrous, comprising 3–4 layers of thick-walled, brown cells of *textura angularis*, becoming thin-walled and hyaline towards the inner region. *Conidiophores* reduced to conidiogenous cells, arising from the inner cells of the conidiomata. *Conidiogenous cells* 4–7 × 2–4 μm ($\bar{x}$ = 5.3 × 2.9 μm, n = 30), hyaline, ampulliform or cylindrical, annellidic, separate, smooth. *Conidia* 12–18 × 6–8 μm ($\bar{x}$ = 16 × 7 μm, n = 50), solitary, oblong to ovoid, hyaline, 1-septate, slightly constricted at septa, straight to slightly curved, thin-walled, smooth.

Culture characteristics – *Colonies* on PDA attaining 20–25 mm diameter in 60 days, dense, subcircular, crenated, dark brown in the center, greyish white towards the margins, aerial mycelium infrequent, raised, reverse brown to dull brown.

Material examined – China, Sichuan Province, Chengdu City, Wenjiang District, Schoolyard of Sichuan Agricultural University, 103°51′27.55″E 30°42′19.5″N, 533 m, isol. from leaves of *Populus* × *beijingensis*, 3 Nov. 2020, C.L. Yang, YCL202011007 (SICAU 23-0142), culture SICAUCC 23-0106)

GenBank numbers – SICAUCC 23-0106 = ITS: PP769691, LSU: PP719623

Notes – This new isolate shares a close relationship with *Drepanopeziza brunnea,* with 96% MLBS and 0.97 BYPP support (Fig. 37). Moreover, sequence comparisons unequivocally establish their conspecific status, revealing a similarity of 99.0% (492/494, 0 gap) to *D. brunnea* (RHY8445A) in the ITS region (Stanosz et al. 2021). Morphologically, the isolate closely relates *D. brunnea,* showcasing 1-septate conidia and a 2-guttulate upper cell (Magnus et al. 1906), aligning with the detailed characterization provided by Magnus et al. (1906). Consequently, we formally introduce this isolate as *D. brunnea.*

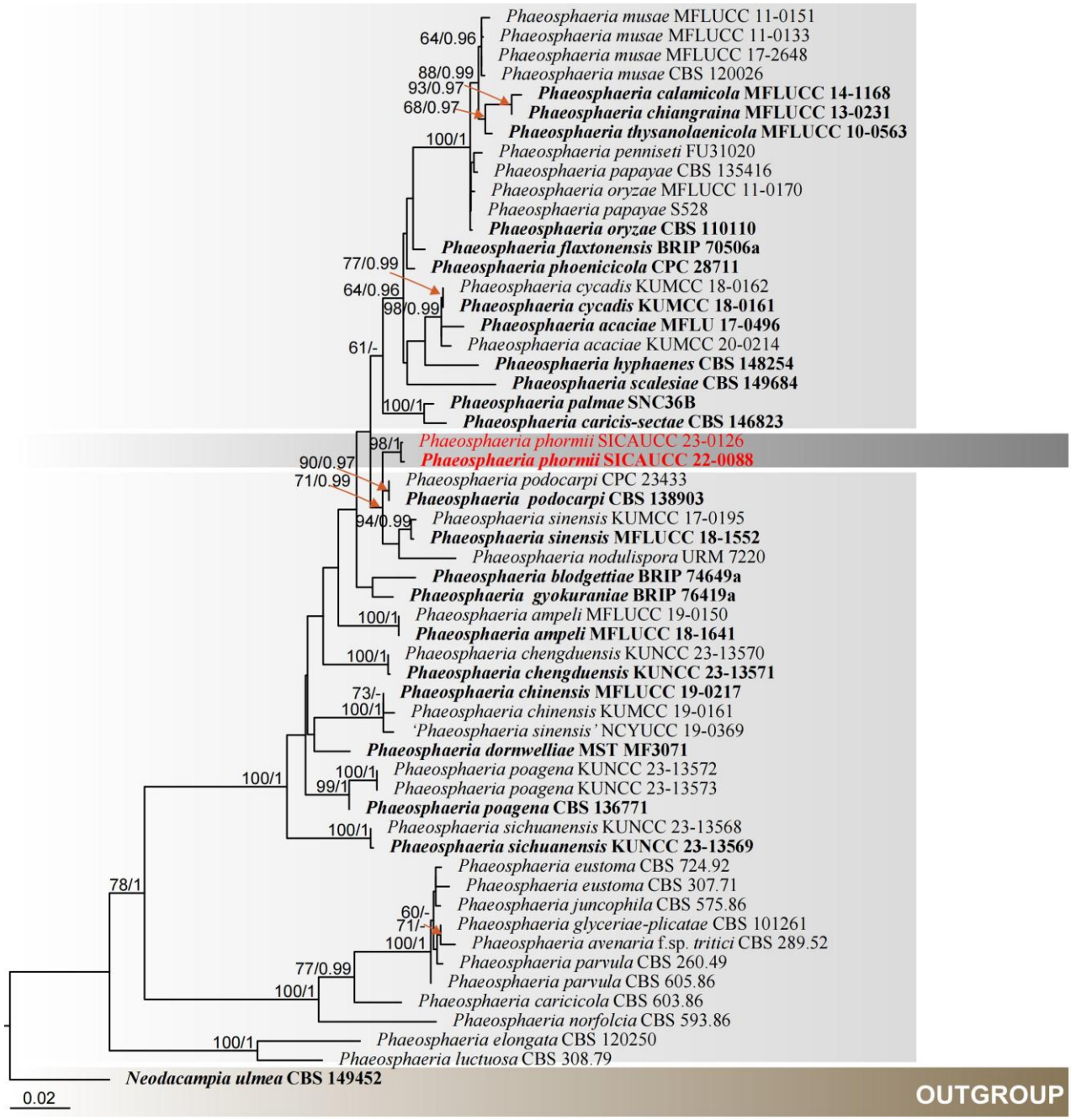

Figure 35 – Phylogram derived from maximum likelihood analyses of a combined dataset comprising ITS, LSU, SSU, *rpb*2, and *tef*1-α sequences in *Phaeosphaeria* species. The alignment contained 4,578 characters (ITS: 1–659, LSU: 660–1,583, SSU: 1,584–2,613, *rpb*2: 2,614–3,683, *tef*1-α: 3,684–4,578) including gaps. The tree is rooted to *Neodacampia ulmea* (CBS 149452). Single-gene analyses were conducted, resulting in similar tree topologies between the ML and BY methods, ensuring consistent comparisons of clade stability. The best-scoring RAxML tree with a final likelihood value of -15,786.068312 is presented. The matrix had 1,262 distinct alignment patterns, with 44.27% of undetermined characters or gaps. Estimated base frequencies were as follows: A = 0.245871, C = 0.236103, G = 0.264386, T = 0.253640; substitution rates AC = 1.125843, AG = 3.138535, AT = 1.926060, CG = 0.670887, CT = 7.055341, GT = 1.000000. The gamma distribution shape parameter α = 0.107741 and the tree length = 0.817782. Bootstrap support values (MLBS) equal or exceeding 60%, and Bayesian posterior probabilities (BYPP) equal or exceeding 0.95 have been indicated above the nodes. The ex-type strains are in bold, and

the new isolates are in red. The bar, set at 0.02, represents the estimated number of nucleotide substitution sites per branch.

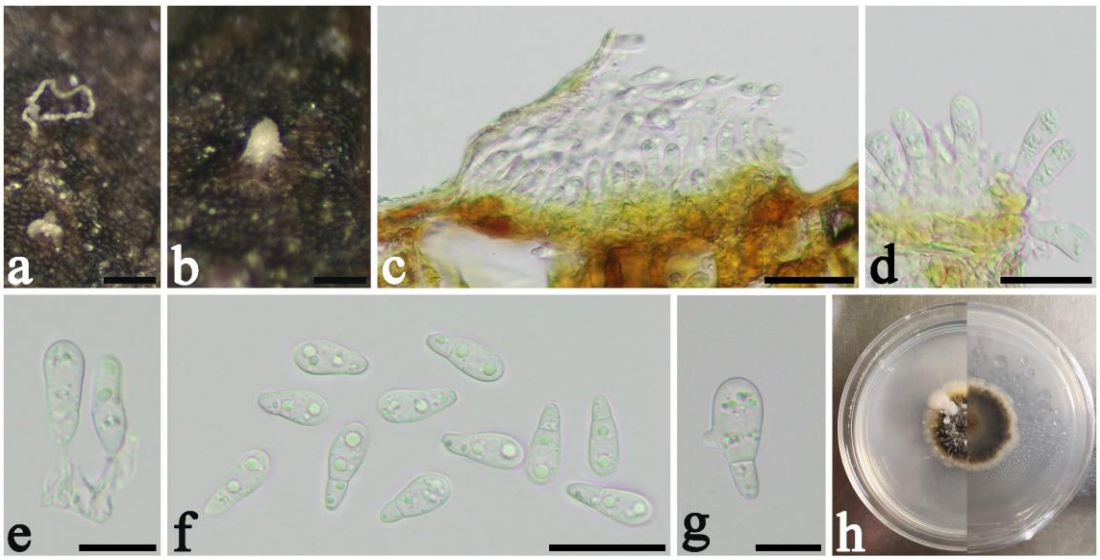

Figure 36 – *Drepanopeziza brunnea* (SICAU 23-0142). a, b Appearance of conidiomata on the leaf. c Cross-section of conidioma. d, e Conidiogenous cells with developing conidia. f Conidia. g Germinating conidium. h Front and reverse view of colonies on PDA. Scale bars: a = 150 µm, b = 200 µm, c = 20 µm, d = 20 µm, e–g = 10 µm.

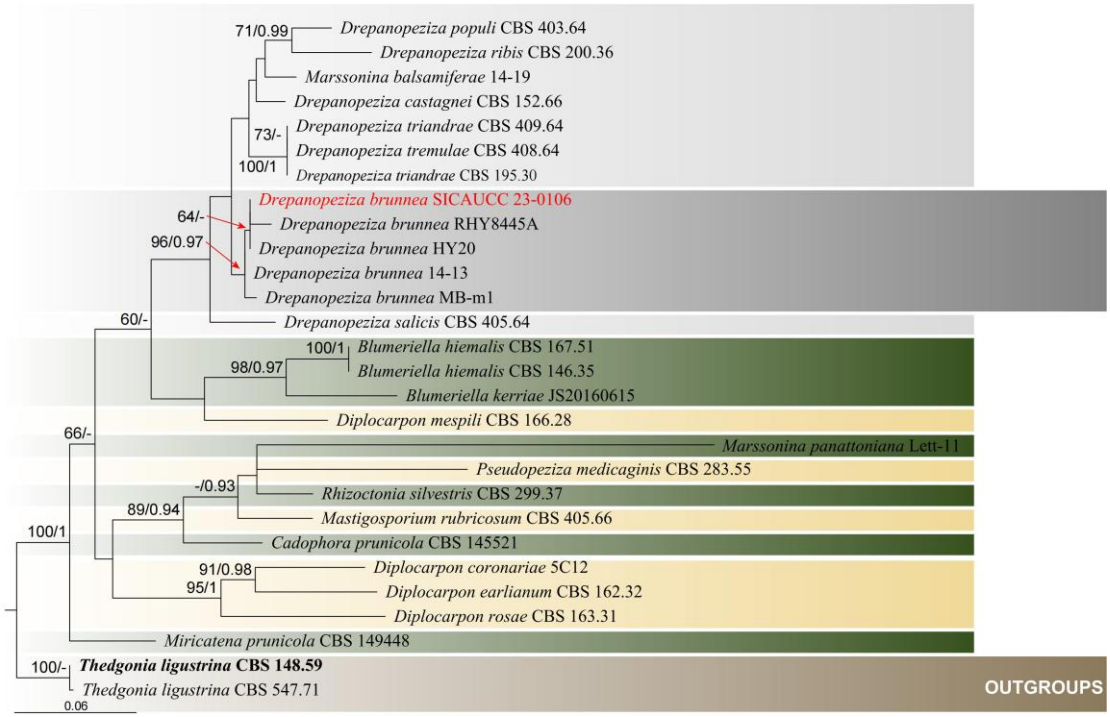

Figure 37 – Phylogram derived from maximum likelihood analyses of a combined dataset comprising ITS and LSU sequence dataset representing the species of *Ceratobasidiaceae*, *Drepanopezizaceae*, *Helotiales*, and *Ploettnerulaceae*. The analysis included 28 taxa and utilizes *Thedgonia ligustrina* (CBS 148.59 and CBS 547.71) as the root. Single-gene analyses resulted in similar tree topologies between the ML and BY methods, ensuring a reliable basis for clade stability comparisons. The alignment contained 1,832 characters (ITS = 1–840, LSU = 841–1,832). The highest-scoring RAxML tree, with a final likelihood value of -7,323.242552, is presented alongside a matrix containing 545 distinct alignment patterns, of which 40.74% are undetermined

characters or gaps. Estimated base frequencies were as follows: A = 0.233341, C = 0.257702, G = 0.287466, T = 0.221490, with substitution rates AC = 1.487423, AG = 1.913083, AT = 0.438057, CG = 1.308041, CT = 4.928679, GT = 1.00000. Bootstrap support values (MLBS, left) ≥ 60, and Bayesian posterior probabilities (BYPP, right) ≥ 0.90, are indicated at the nodes. Ex-type strains are marked in bold, and the new isolates are red. The scale bar (Bar = 0.06) represents the estimated number of nucleotide substitution sites per branch.

Erysiphaceae Tul. & C. Tul.

Notes – *Erysiphaceae*, with *Erysiphe* as the type genus, was established by Tulasne (1861). *Erysiphaceae* species are pivotal pathogens, causing powdery mildew on around 10,000 angiosperm species, including crops, fruits, forests, and ornamentals, affecting approximately 4.5% of angiosperm species recorded worldwide (Bolay et al. 2021, Darsaraei et al. 2021, Yamaguchi et al. 2021, Bradshaw et al. 2022, Gregorio-Cipriano & Gonzalez 2022, Kusch et al. 2023). This family encompasses a substantial group within the *Helotiales* order, comprising approximately 1,000 species distributed across 21 genera (Wijayawardene et al. 2022, Worobiec et al. 2023), and all documented species within it are obligate biotrophic of plants (Takamatsu 2013).

Blumeria Golovin ex Speer

Notes – *Blumeria*, typified by *B. graminis*, was initially proposed by Golovin and later retained as the valid genus name with a teleomorph-based typification, based on verification by various researchers, replacing *Oidium* (Blumer 1933, Golovin 1958, Braun 2013, Turland et al. 2018). This genus has documented eight species, including *B. americana*, *B. avenae*, *B. bromi-cathartici*, *B. bulbigera*, *B. dactylidis*, *B. graminicola*, *B. graminis*, and *B. hordei*, demonstrating a remarkably diverse host range and specialization (Liu et al. 2021). *Blumeria* species have a global distribution and can induce powdery mildew on a wide range of hosts within the *Poaceae* family (Amano 1986, Braun & Cook 2012, Adhikari 2017, Liu et al. 2021).

19. *Blumeria graminis* (DC.) Speer, Sydowia 27(1-6): 2 (1975) [1973-1974] Fig. 38

MycoBank number: MB309596; Facesoffungi number: FoF15881

Associated with powdery mildew on leaves of *Poa annua* L. Sexual morph: Not observed. Asexual morph: *Hyphomycetous*. *Mycelium* 3–7 μm width, amphigenous, hyaline, in patches or effuse, persistent, septate, thin-walled, smooth. *Hyphal appressoria* solitary, indistinct to nipple-shaped. *Conidiophores* 60–150 μm long, arising from upper surface of hyphae, erect, straight or medium curved. *Foot cells* 14–35 × 5–7 μm ($\bar{x}$ = 23.5 × 6.1 μm, n = 20), cylindrical, straight or slightly curved, base usually distinctly swollen, 10–14 μm width, followed by 3–5(–6) cells, most followed by equally long cells, basal septum at junction with hyphal mother cells or somewhat elevated, 5–8 μm. *Conidia* 22.5–43 × 10–21 μm ($\bar{x}$ = 29.8 × 16.2 μm, n = 50), catenescent, ellipsoid or limoniform, hyaline, thin-walled, smooth, base truncate or subtruncate, germ tubes subterminal, perihilar, short to moderately long, cylindrical to clavate with swollen apex.

Material examined – China, Sichuan Province, Chengdu City, Wenjiang District, Schoolyard of Sichuan Agricultural University, 103°51′34.47″E 30°42′34.67″N, 488 m, on leaves of *Poa annua*, 10 Apr. 2020, C.L. Yang, YCL202004001 (SICAU 23-0127).

GenBank numbers – SICAU 23-0127 = ITS: PP736363

Notes – The current analysis unequivocally demonstrates that our collection forms a well-supported clade with *Blumeria graminis* taxa (100% MLBS / 1.00 BYPP) (Fig. 39). Morphologically, the specimen SICAU 23-0127 exhibits identical features to those described for *B. graminis* in the work of Liu et al. (2021). Therefore, both genetically and morphologically, this species SICAU 23-0127 aligns consistently with *B. graminis*. *Blumeria graminis* is a significant pathogenic agent known for its capacity to inflict substantial damage to a wide range of plants, including economically important forests, ornamental varieties, and various crops (Inuma et al. 2007, Liu et al. 2021, Sotiropoulos et al. 2022).

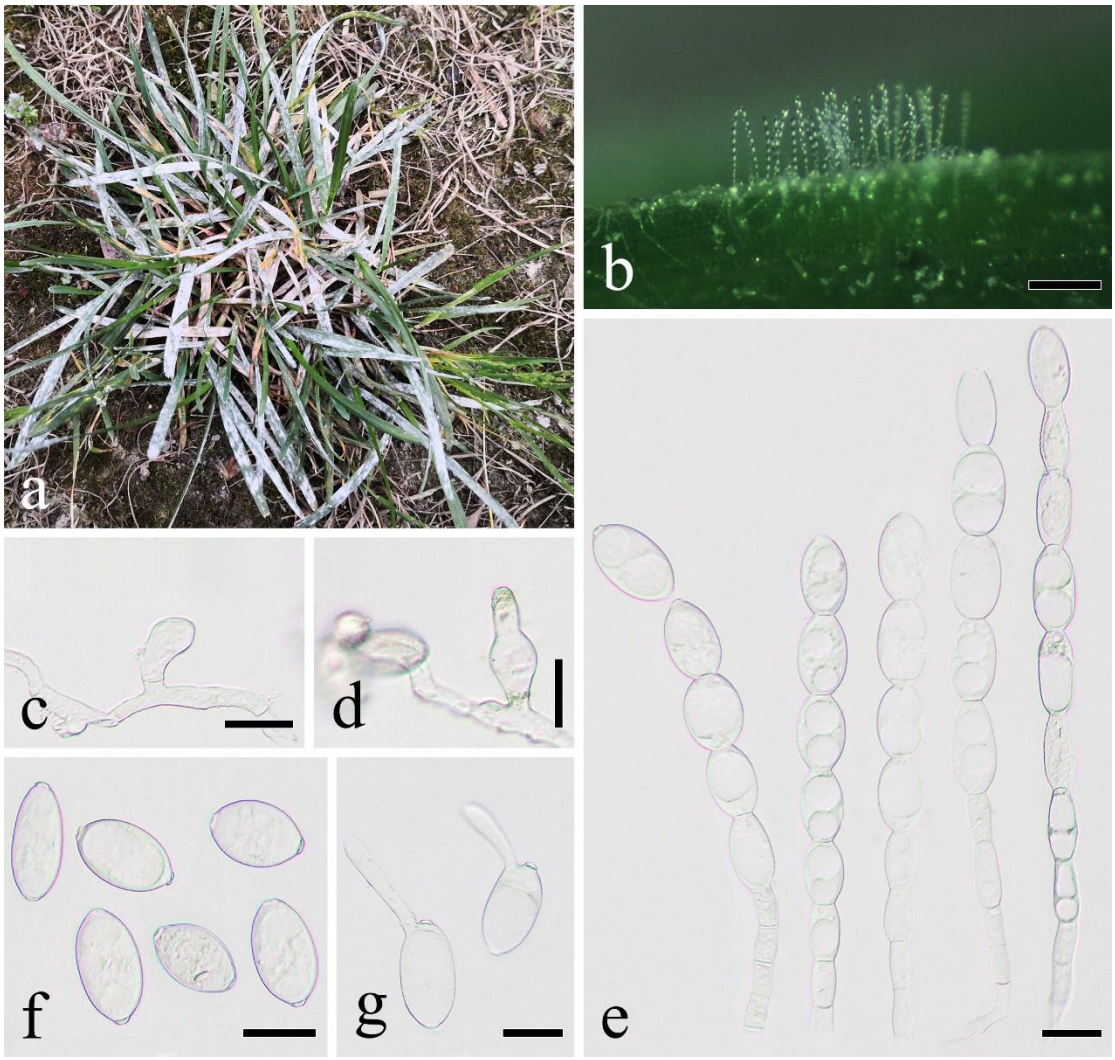

Figure 38 – *Blumeria graminis* (SICAU 23-0127). a Symptoms on the leaves. b Conidiogenesis arising from upper surface of leaf. c, d Hyphal appressoria with developing conidiophores. e Conidiophores with developing conidia. f Conidia. g Conidia with germ tube in sterilized water after 12 h. Scale bars: b = 200 μm, c–g = 20 μm.

Class *Sordariomycetes* O.E. Erikss. & Winka

Amphisphaeriales D. Hawksw. & O.E. Erikss.

Notes – *Amphisphaeriales*, initially established by Hawksworth & Eriksson (1986) with *Amphisphaeria* as the type genus, was later regarded as synonymous with *Xylariales*, then it can be differentiated from *Xylariales* through both morphological and molecular evidence (Senanayake et al. 2015, Samarakoon et al. 2016, Hongsanan et al. 2017, Daranagama et al. 2018). *Amphisphaeriales* diverged about ~181 Mya, with a crown age of around ~141 Mya (Hyde et al. 2020b, Samarakoon et al. 2021a, Chen et al. 2023a). Currently, *Amphisphaeriales* encompasses 16 families, 90 genera, and roughly 1,300 documented species (Samarakoon et al. 2021b, Jiang et al. 2022a, Liu et al. 2022a, Peng et al. 2022).

Sporocadaceae Corda

Notes – *Sporocadaceae* was introduced by Corda (1842) with *Sporodocadus* as the type genus. *Sporocadaceae* species play significant roles as pathogens affecting trunks, branches, twigs, leaves, and fruits of a wide range of horticultural plants, as well as serving as saprobes and endophytes on diverse substrates, including interactions with humans and animals (Tanaka et al. 2011, Hyde KD et al. 2020, Samarakoon et al. 2021b, Kanetis et al. 2022). This family is typically

characterized by coelomycetous fungi with conidia-bearing appendages, encompassing 35 genera and about 600 species (Jiang et al. 2023a, Sun et al. 2023).

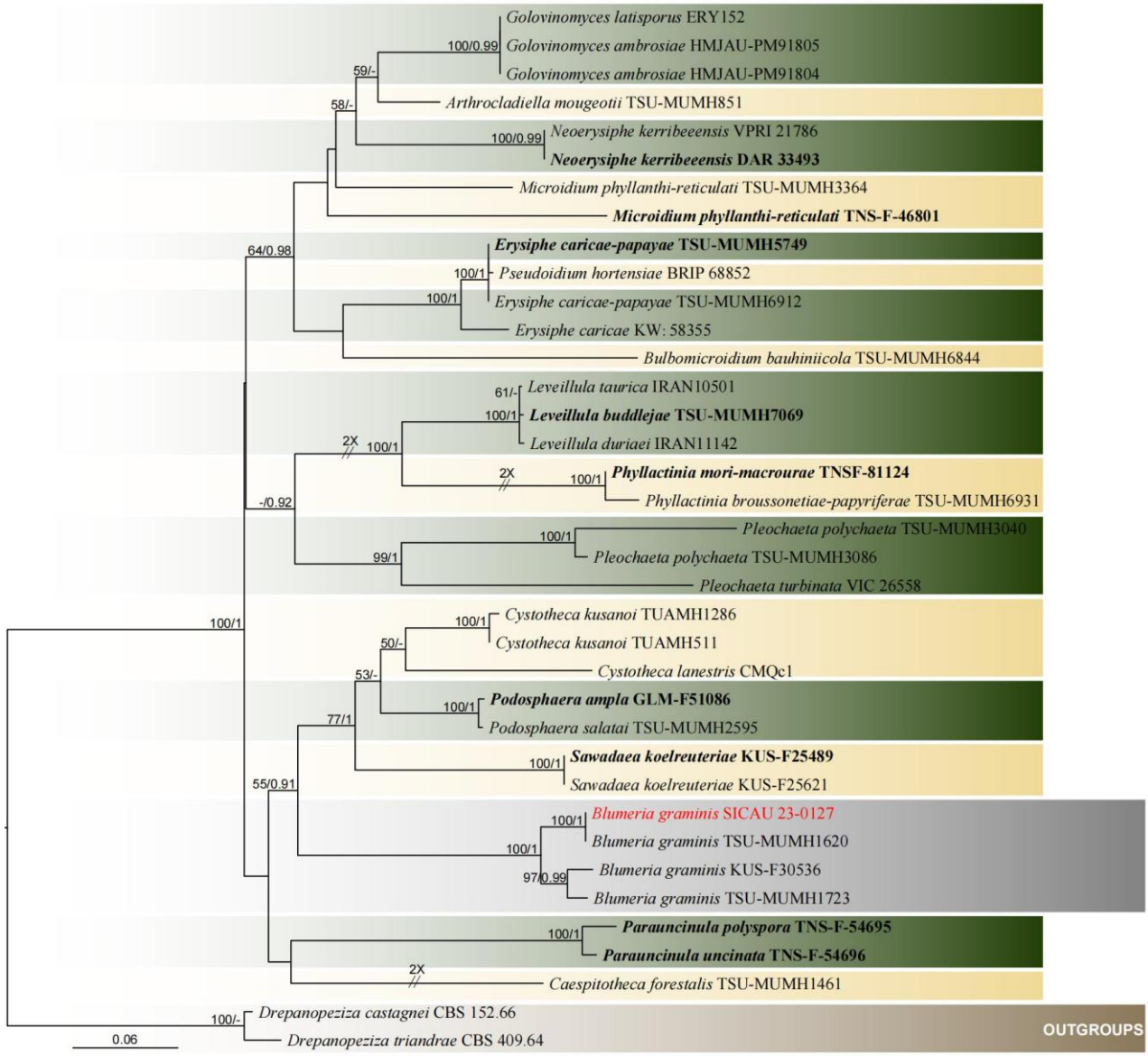

Figure 39 – Phylogram derived from maximum likelihood analyses of a combined dataset comprising ITS sequence dataset for *Erysiphaceae*, encompassing 16 genera within this family, along with two outgroup taxa (*Drepanopeziza triandrae* CBS 409.64 and *D. castagnei* CBS 152.66). A total of 37 taxa were included in this analysis, with a character set of 1,679 characters post-alignment. The best-scoring RAxML tree with a final likelihood value of -11,013.855966 is presented. The matrix had 786 distinct alignment patterns, with 50.38% of undetermined characters or gaps. Estimated base frequencies were as follows: A = 0.238621, C = 0.243870, G = 0.284897, T = 0.232612; substitution rates AC = 1.035998, AG = 1.865820, AT = 1.329795, CG = 0.698137, CT = 4.031649, GT = 1.000000. Bootstrap support values (MLBS) equal or greater than 50%, and Bayesian posterior probabilities (BYPP) greater than 0.90 are marked at the nodes. The type specimens are in bold, and the new collection of this study is in red. The scale bar of 0.06 indicates the estimated nucleotide substitutions per site per branch.

Neopestalotiopsis Maharachch., K.D. Hyde & Crous

Notes – *Neopestalotiopsis* was initially introduced by Maharachchikumbura et al. (2014), distinguished by characteristics such as the color of conidia, conidiophores, and sequence data, and

it was separated from the genera *Pestalotiopsis* and *Pseudopestalotiopsis*. *Neopestalotiopsis* species are frequently found as pathogens, capable of inducing various plant diseases, including leaf spots, wilting, root rot, fruit rot, fruit scab, canker, blight, and dieback in a wide array of horticultural plants (Ayoubi & Soleimani 2016, Maharachchikumbura et al. 2016a, Solarte et al. 2017, Jiang et al. 2018, Rodríguez-Gálvez et al. 2020, Baggio et al. 2021, Daengsuwan et al. 2021, Diogo et al. 2021, Prasannath et al. 2021), and some species as saprobes and endophytes (Kumar et al. 2019, Senanayake et al. 2020).

20. ***Neopestalotiopsis concentrica*** C. Peng & C.M. Tian, Persoonia 49: 227 (2022) Fig. 40

MycoBank number: MB843813; Facesoffungi number: FoF15917

Associated with leaf blight on leaves of *Photinia serratifolia* (Desf.) Kalkman. Sexual morph: Not observed. Asexual morph: *Coelomycetous*. *Conidiomata* 160–175 × 80–100 μm ($\bar{x}$ = 168× 88 μm, n = 20), acervulus, immersed, dark greenish brown to black, solitary, scattered, uni-loculate, globose to oblate, glabrous. *Conidiophores* indistinct. *Conidiogenous cells* 7–8 × 4–5 μm ($\bar{x}$ = 7.3 × 4.3 μm, n = 30), hyaline, ampulliform or subcylindrical, annellidic, separate, smooth-walled. *Conidia* 19–28 × 9.5–13 μm ($\bar{x}$ = 25 × 11 μm, n = 50), ellipsoidal, subcylindrical, 4-septate, slightly constricted at septa, straight or slightly curved; *three median cells* 6–10 × 3–6 μm ($\bar{x}$ = 8.2 × 4.7 μm, n = 50), doliiform, brown or olivaceous, homochromatic, with septa darker than the rest of the cell; *apical cell* hyaline, cylindrical to subcylindrical, with 2–3 tubular appendages; *apical appendages* 24–30 μm ($\bar{x}$ = 27 μm, n = 50), arising from the apical crest, unbranched, filiform; *obconical basal cell* hyaline, thin-walled; *basal appendage* single, tubular, thin-walled, unbranched, centric. *Conidiogenesis* formed on PDA. *Conidiophores* 10–27 × 1–2 μm ($\bar{x}$ = 17 × 1.4 μm, n = 20), branched or unbranched, hyaline, thin-walled. *Conidia* smaller than those on substrate, 12–16 × 3–4 μm ($\bar{x}$ = 14 × 3.7 μm, n = 50).

Culture characteristics – *Colonies* on PDA attaining 50–60 mm diameter in 5 days, cottony to fluffy, with clustered black fruiting bodies and filiform and fluffy margin, white from above and reverse.

Material examined – China, Sichuan Province, Chengdu City, Wenjiang District, Schoolyard of Sichuan Agricultural University, 103°51′29.16″E 30°42′18.97″N, 529 m, isol. from leaves of *Photinia serratifolia*, 20 Oct. 2020, S.Y. Liu, LSY202010003 (SICAU 23-0125), living culture (SICAUCC 23-0119). *ibid.* LSY202010003-2 (SICAU 23-0159), living culture SICAUCC 23-0124.

GenBank numbers – SICAUCC 23-0119 = ITS: PP702559, LSU: PP702585, SSU: PP702575, *tef*1-α: PP712872, *tub*2: PP712880. SICAUCC 23-0124 = ITS: PP702560, LSU: PP702586, SSU: PP702576, *tef*1-α: PP712873, *tub*2: PP712881

Notes – Our two collections were phylogenetically related to the ex-type of *Neopestalotiopsis concentrica* on *Rosaceae* (Peng et al. 2022) (Fig. 41). In addition, there are 97.81% (447/457, 6 gaps), 99.55% (449/451, 0 gap), and 99.80% (523/524, 0 gap) similarities between our collection (SICAUCC 23-0119) and *N. concentrica* (CFCC 55162) in the *tef*1-α, *tub*2, and ITS regions, respectively. Morphologically, compared with the ex-type culture CFCC 55162 (14–19 × 4.5–6 μm), conidia of our collection SICAUCC 23-0119 on the host plant were longer and wider (19–28 × 9.5–13 μm), while the conidia on PDA were similar in size (12–16 × 3–4.5 μm). Thus, we introduce *N. concentrica* as a new host record.

21. ***Neopestalotiopsis dimorphospora*** P. Razaghi, F. Liu & L. Cai, Stud. Mycol. 109: 155 (2024) Fig. 42

MycoBank number: MB852730; Facesoffungi number: FoF15918

Associated with leaf spots on leaves of *Eriobotrya japonica* (Thunb.) Lindl., spots subcircular to circular, or irregular shape, pale brown, with a dark brown to black border. Sexual morph: Not observed. Asexual morph: *Coelomycetous*. *In planta: Conidiomata* 95–200 × 75–140 μm ($\bar{x}$ = 142 × 117 μm, n = 10), flat stromatic, initially immersed, erumpent through the epidermis at maturity, subcircular to circular or irregular at longitudinal view, brown, glabrous. *Conidiophores* reduced to

conidiogenous cells, forming from the basal mother cells of stromata. *Conidiogenous cells* 3.5–6 × 4–5 μm ($\bar{x}$ = 4.3 × 4.4 μm, n = 20), hyaline, doliiform or lageniform, thin-walled, smooth, proliferating percurrently with one locus, collarette. *Conidia* 19–26 × 8–12.5 μm ($\bar{x}$ = 23.1 × 9.7 μm, n = 50), ellipsoid or fusiform, straight or slightly curved, simple, relatively wide at the base, 4-septate; basel cells 2.5–6 μm ($\bar{x}$ = 4 μm, n = 50) long, conic to obconic with a truncate base, hyaline to pale brown, thin-walled, smooth; *median cells* 3-cells, each 3–7 μm ($\bar{x}$ = 5 μm, n = 50) long, 4.5–6 μm ($\bar{x}$ = 5.3 μm, n = 50) long, 3.5–6 μm ($\bar{x}$ = 5.1 μm, n = 50) long, doliiform, brown to dark brown, septa and periclinal walls darker than rest of the cell, usually first cell paler than other cells, with a distinctly thickened-septum between second and third cell, versicolored, sometimes wall rugose; *apical cells* 2–7 μm ($\bar{x}$ = 3.9 μm, n = 50) long, hyaline, rarely pale brown, conic with truncate base; *apical appendages* 5.5–21 μm ($\bar{x}$ = 13.2 μm, n = 50) long, short, (1–)2–3(–4), tubular, inserted at different loci but in a crest at the apex of the apical cell, unbranched, flexuous; *basal appendages* 0–2.5 μm ($\bar{x}$ = 1.4 μm, n = 10) long, usually indistinct or lacked, single, tubular, unbranched, centric. ***In vitro:*** *Conidiogenesis* on PDA. *Conidiomata* subglobose or irregular, dark brown to black, semi-immersed on media. *Conidiophores* indistinct, often reduced to conidiogenous cells. *Conidiogenous cells* 8–24 × 2–5 μm ($\bar{x}$ = 15.4 × 3.5 μm, n = 20), discrete or integrated, cylindrical or subcylindrical, straight or curved, flexuous laterally, hyaline to pale brown, thin-walled, smooth. *Conidia* 19.5–34 × 5–7 μm ($\bar{x}$ = 26.8 × 5.9 μm, n = 50), fusiform, ellipsoid, straight or curved, occasionally flexuous, 4-septate, rarely 3-septate; *basel cells* 3.5–6 μm ($\bar{x}$ = 5.1 μm, n = 50) long, conic to obconic with a truncate base, pale brown, thin-walled, smooth; *median cells* mainly 3-cells, each 5–7 μm ($\bar{x}$ = 6 μm, n = 50) long, 3–6 μm ($\bar{x}$ = 4.9 μm, n = 50) long, 4–6.5 μm ($\bar{x}$ = 5.4 μm, n = 50) long, doliiform, brown to dark brown, concoloured, sometimes first cell paler than other cells, septa and periclinal walls darker than rest of the cell, with a distinctly thickened-septum between second and third cell, sometimes wall rugose; *apical cells* 4–8 μm ($\bar{x}$ = 5.5 μm, n = 50) long, hyaline to pale brown, conic or subcylindrical; *apical appendages* 4.5–35 μm ($\bar{x}$ = 16.9 μm, n = 50) long, (1–)2–4(–5 or –6), tubular, mainly arising from the apical crest, unbranched, straight or flexuous; *basal appendages* 1–11 μm ($\bar{x}$ = 6.2 μm, n = 50) long, single, tubular, unbranched, centric.

Culture characteristics – *Colonies* on PDA attaining 55–65 mm diameter in 1 week, fast-growing, filamentous to circular, with filiform margin, medium dense, aerial mycelium flat or raised, fluffy, white, reverse white to pale yellow, dark brown to black conidial masses formed in the late.

Material examined – China, Sichuan Province, Leshan City, Mabian County, 103°22′12″E 28°39′36″N, 3625 m, isol. from leaves of *Eriobotrya japonica*, 24 Oct. 2020, Jianlin Jizuo & C.L. Yang, JZJL202008002 (SICAU 23-0143), living culture (SICAUCC 23-0118). *ibid.* JZJL202008002-2 (SICAU 23-0160), living culture SICAUCC 23-0123.

GenBank numbers – SICAUCC 23-0118 = ITS: OK560486, LSU: OK560488, SSU: PP972334, *tef*1-α: OL310175, *tub*2: PP712878, *rpb*2: PP712863. SICAUCC 23-0123 = ITS: PP702558, LSU: PP702584, SSU: PP702574, *tef*1-α: PP712871, *tub*2: PP712879, *rpb*2: PP712864

Notes – In the phylogenetic analyses, our collections (SICAUCC 23-0118, SICAUCC 23-0123) clustered together with two strains of *Neopestalotiopsis dimorphospora* (Fig. 41), and have few sequence differences with the type strain (5 bp in *tub*2, 1 bp in *tef*1-α and 0 bp in ITS). However, based on our observation, *N. dimorphospora* shows intraspecific variation in morphological features. For instance, our collection differs from the ex-type culture CGMCC 3.23497 in the number of basal appendages (1 vs. 0–2), and thinner conidia (5–7 μm vs. 6.5–9 μm). Moreover, wide varieties in length of apical appendages (4.5–35 μm vs. 13.5–28 μm) and basal appendages (1–11 μm vs. 3–7.5 μm), and the absence of β-conidia are observed in our collections (Razaghi et al. 2024).

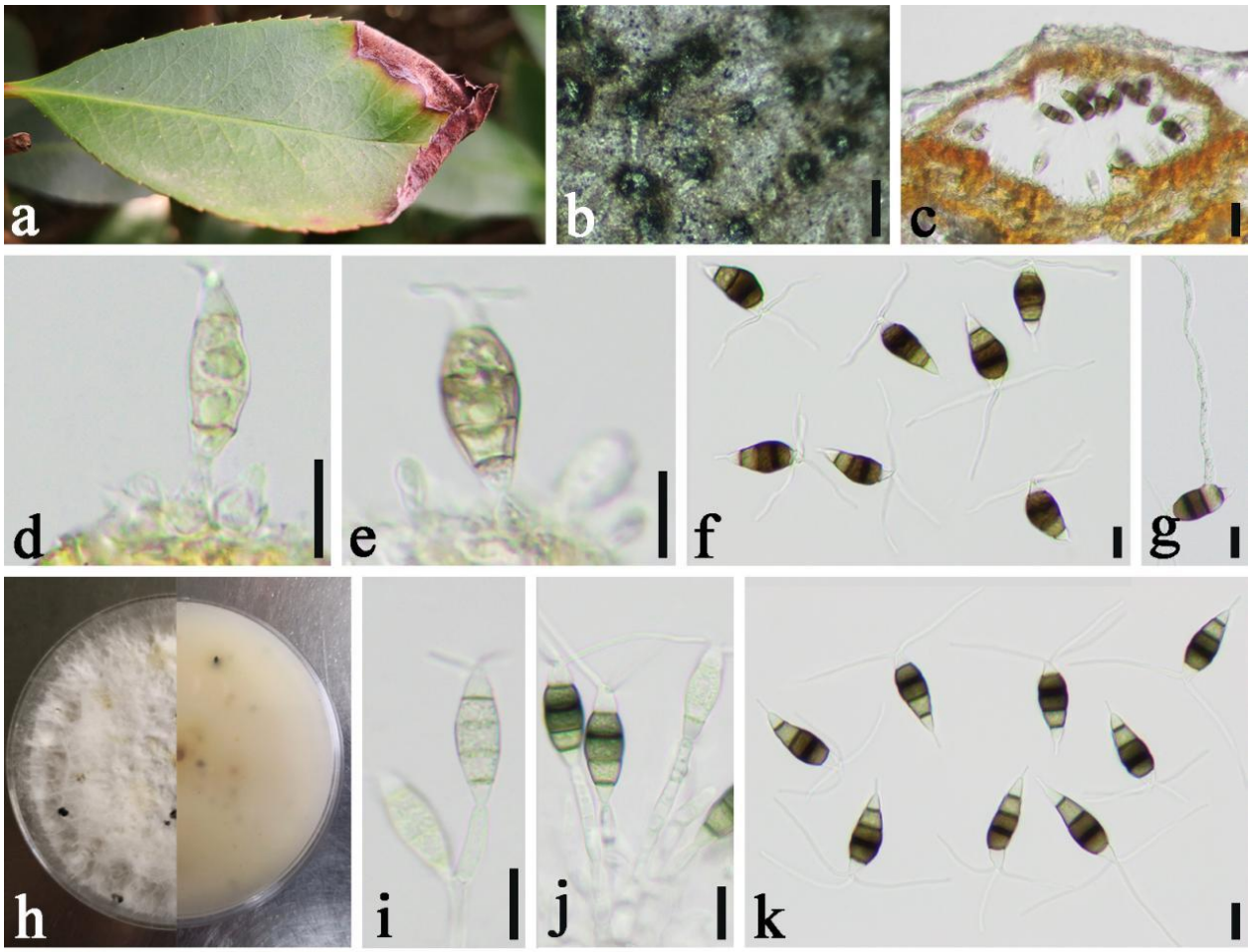

Figure 40 – *Neopestalotiopsis concentrica* (SICAU 23-0125). a Symptoms on the leaf. b Appearance of conidiomata. c Cross-section of conidioma. d, e Conidiogenous cells with developing conidia. f Conidia. g Germinating conidium. h Front and reverse view of colonies on PDA. i, j Conidiogenous cells with developing conidia on PDA. k Conidia on PDA. Scale bars: b = 200 μm, c = 20 μm, d–g = 10 μm, i–k = 10 μm.

Pestalotiopsis Steyaert

Notes – *Pestalotiopsis*, typified by *P. guepinii*, was introduced by Steyaert (1949) to encompass pestalotioid taxa characterized by 5-celled conidia (Wijayawardene et al. 2017, 2018). *Pestalotiopsis* was reclassified into two additional genera, *Neopestalotiopsis* and *Pseudopestalotiopsis*, owing to observed morphological and molecular disparities, distinguishing itself primarily in terms of conidiogenous cells and the coloration of their median conidial cells from species within the two *Pestalotiopsis*-like genera (Maharachchikumbura et al. 2014). To date, *Pestalotiopsis* includes about 110 species, with the majority of these taxa having been documented as causative agents of diseases affecting trunks, branches, twigs, leaves, and flowers across diverse host plants and environments (de Jesus et al. 2022, Hlaiem et al. 2022, Jiang et al. 2022b, Nozawa et al. 2022, Wijayawardene et al. 2022, Prasannath et al. 2023, Zhang et al. 2023a).

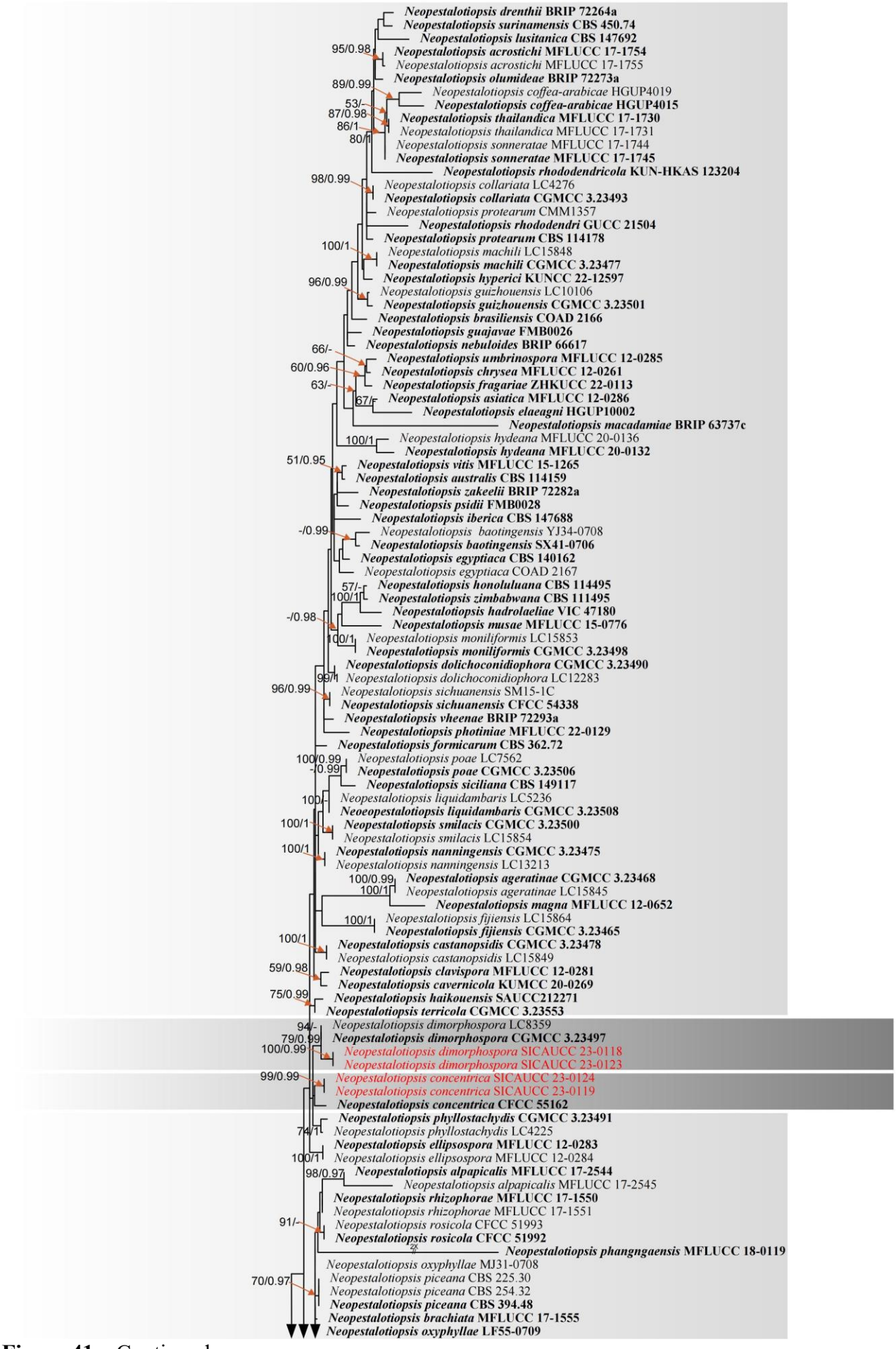

Figure 41 – Continued.

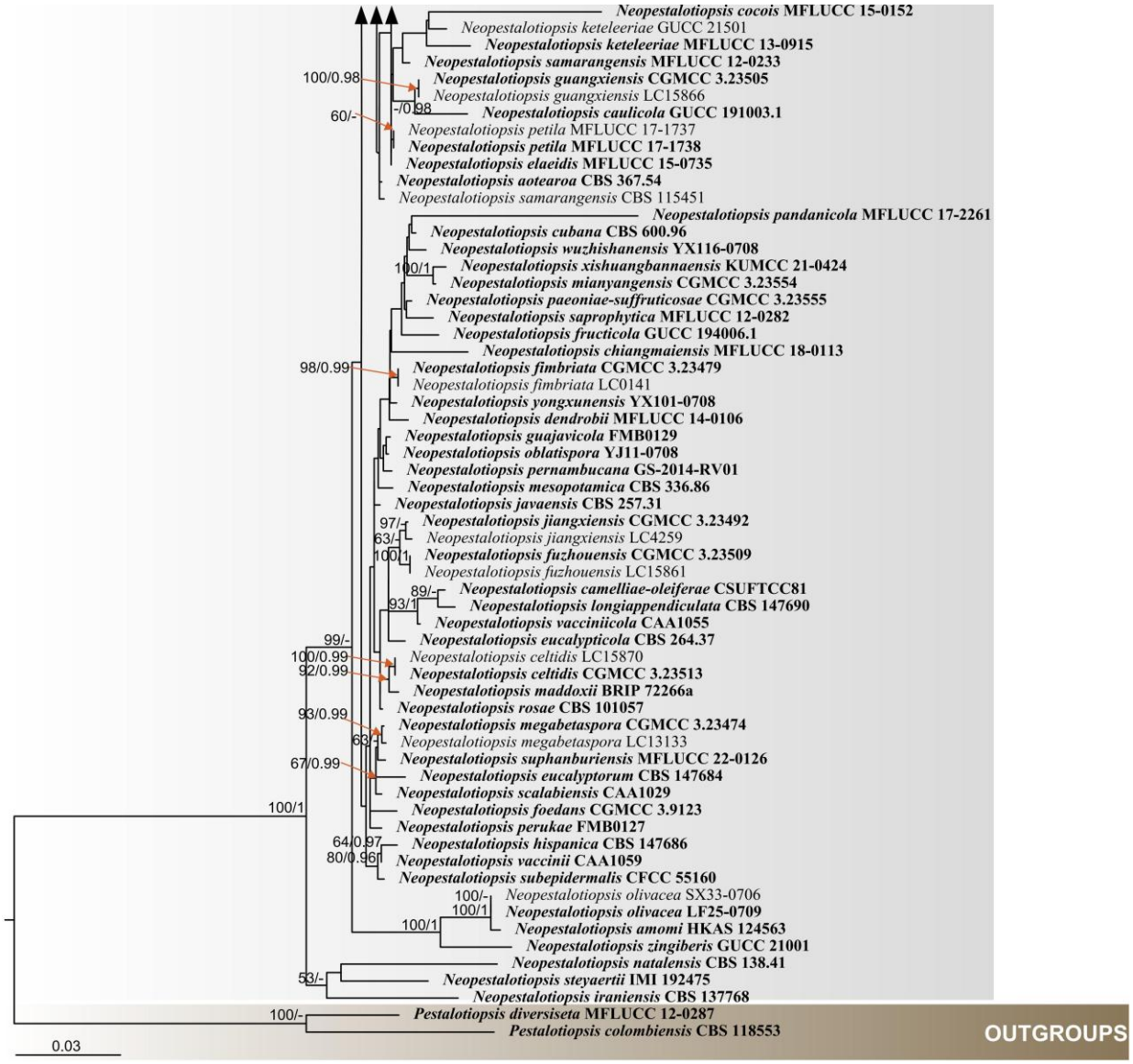

Figure 41 – Phylogram derived from maximum likelihood analyses of a combined dataset comprising ITS, *tef*1-α, and *tub*2 sequences in *Neopestalotiopsis* species. The alignment contained 2,627characters (ITS: 1–650, *tef*1-α: 651–1,767, *tub*2: 1,768–2,627) including gaps. The tree is rooted to *Pestalotiopsis diversiseta* (MFLUCC 12-0287) and *P. colombiensis* (CBS 118553). Single-gene analyses were conducted, resulting in similar tree topologies between the ML and BY methods, ensuring consistent comparisons of clade stability. The best-scoring RAxML tree with a final likelihood value of -15,109.307964 is presented. The matrix had 1,174 distinct alignment patterns, with 31.07% of undetermined characters or gaps. Estimated base frequencies were as follows: A = 0.237232, C = 0.274396, G = 0.219005, T = 0.269366; substitution rates AC = 1.106087, AG = 3.077629, AT = 1.209776, CG = 0.822114, CT = 4.233879, GT = 1.000000. The gamma distribution shape parameter α = 0.373452 and the tree length = 1.488603. Bootstrap support values (MLBS) equal or exceeding 50%, and Bayesian posterior probabilities (BYPP) equal or exceeding 0.95 have been indicated above the nodes. The ex-type strains are in bold, and the new isolates are in red. The bar, set at 0.03, represents the estimated number of nucleotide substitution sites per branch.

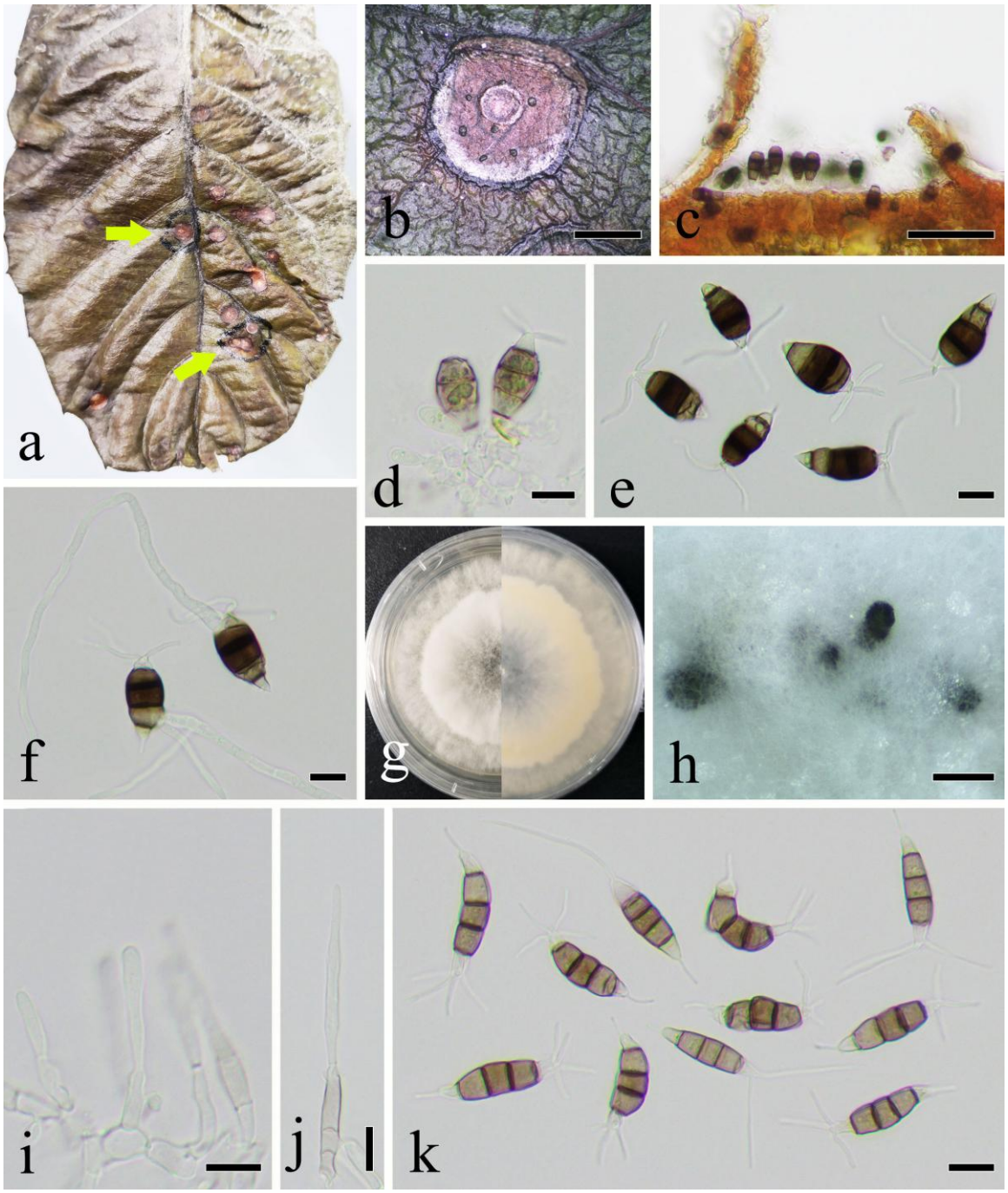

Figure 42 – *Neopestalotiopsis dimorphospora* (SICAU 23-0143). a Symptoms on the leaf. b Appearance of conidiomata. c Cross-section of conidioma. d Conidiogenous cells with developing conidia. e Conidia. f Germinating conidia. g Front and reverse view of colonies on PDA. h Conidiomata formed on PDA. i, j Conidiogenous cells produced on PDA. k Conidia produced on PDA. Scale bars: b = 1000 μm, c = 50 μm, d–f, i–k = 10 μm, h = 250 μm.

22. *Pestalotiopsis oryzae* Maharachch., K.D. Hyde & Crous, Stud. Mycol. 79: 172 (2014) Fig. 43

MycoBank number: MB809746; Facesoffungi number: FoF15923

Associated with leaf blight on leaves of *Fatsia japonica* (Thunb.) Decne. et Planch. Sexual morph: Not observed. Asexual morph: *Coelomycetous*. *Conidiomata* 80–338 × 80–295 μm (n = 30), circular to elliptical, arranged irregularly, subepidermal, disrupting outer epidermal cell wall of host. *Conidiophores* inconspicuous. *Conidiogenous cells* 4–16 × 2–7 μm ($\bar{x}$ = 8.5 × 3.8 μm, n = 35), integrated, various, cylindrical or sub-cylindrical, oval or obovate, subrotund, hyaline, smooth-walled. *Conidia* 21–31 × 6–8 μm ($\bar{x}$ = 27.4 × 6.8 μm, n = 40), fusoid to oval, straight, or slightly

curved, 4-septate; *basal cell* 3.5–8.2 µm ($\bar{x}$ = 6.0 µm, n = 40) long, cylindrical, obconic with a truncate base, hyaline, thin-walled; *three median cells* 13–20 µm ($\bar{x}$ = 17 µm, n = 40) long, doliiform or trapezoid, concolourous or the top two median cells darker than the third cell, pale brown to brown; *apical cell* 2.5–5 µm ($\bar{x}$ = 4.0 µm, n = 40) long, hyaline, sub-cylindrical or conical with a truncate or acute base, thin walled; with 1–4 tubular apical appendages, arising from apex or laterally from apical cell, unbranched, or branched at one appendage, 5–19 µm ($\bar{x}$ = 10.9 µm, n = 40) long; 1 basal appendage, when present, tubular, unbranched, centric, (1–)2–6(–13) µm ($\bar{x}$ = 3.8 µm, n = 40) long; mean conidium length/width ratio = 3.9:1.

Culture characteristics – Germinated conidia on PDA at 25–28℃ for 12 h. *Colonies* on PDA reaching 7.0 cm diameter after 5 days, medium sparse, irregular, hairy edge, white, flocculent to fluffy, aerial mycelium sparse in the middle, well developed at the margin, yellow in reverse, in the later stages of colony development, black conidiomata are formed, with a tendency to be more clustered, less dispersed, and semi-buried or buried.

Material examined – China, Sichuan Province, Chengdu City, Wenjiang District, Schoolyard of Sichuan Agricultural University, 103°51′32.11″E 30°42′26.67″N, 538 m, isol. from leaves of *Fatsia japonica*, 1 Jan. 2020, X.L. Xu, XXL202001001 (SICAU 23-0147), living culture (SICAUCC 23-0096). *ibid.* XXL202001001-2 (SICAU 23-0161), living culture SICAUCC 23-0139.

GenBank numbers – SICAUCC 23-0096 = ITS: PP736384, *tef*1-α: PP779585, *tub*2: PP782076, LSU: PP732714. SICAUCC 23-0139 = ITS: PP736385, *tef*1-α: PP779586, *tub*2: PP782077, LSU: PP732740

Notes – Multi-gene phylogenetic analysis indicated that our new collections (SICAUCC 23-0096 and SICAUCC 23-0139) formed a distinct clade sister to the clade of *Pestalotiopsis kenyana*, *P. oryzae*, *P. rhodomyrtus*, and *P. trachycarpicola* with 90% MLBS / 1.00 BYPP support (Fig. 44), and can be identified as *P. oryzae*. *Pestalotiopsis oryzae* was introduced by Maharachchikumbura et al. (2014) from seeds of *Oryza sativa*. The morphological characteristics of our collections fit well with *P. oryzae* in having dark brown to black conidial masses, straight, or slightly curved, 4-septate, fusoid conidia with 1 tubular basal appendage. To further confirm this identification, single-gene comparisons of the ITS, LSU, *tub*2, and *tef*1-α regions were conducted between SICAUCC 23-0096 and CBS 353.69. The results showed high sequence similarity, with 100% identity in ITS, LSU, and *tub*2 regions, and 98.1% (361/368, 0 gap) in *tef*1-α. Thus, we identified our new collections as *P. oryzae*.

Diaporthales Nannf.

Notes – *Diaporthales* was initially introduced by Nannfeldt (1932) to accommodate diaporthoid taxa under the circumstances. *Diaporthales* is a diverse order within the class *Sordariomycetes*, comprising pathogens, saprophytes, and endophytes inhabiting a wide range of substrates, including many economically and ecologically significant tree species (Rossman et al. 2007, Walker et al. 2012, Senanayake et al. 2017, 2018, Jiang et al. 2023b). Most *Diaporthales* species are known for their distinct features, including solitary or clustered, immersed to erumpent, orange, brown or black perithecial ascomata in various colors, short or long necks, often located within stromatic tissues or substrates, a hamathecium that may lack paraphyses, unitunicate asci with a prominent refractive ring, and diverse ascospores in terms of shape, size, and color (Barr 1978, Samuels & Blackwell 2001, Castlebury et al. 2002, Rossman et al. 2007). The asexual morphs of *Diaporthales* usually exhibit coelomycetous traits, forming acervuli, pycnidial, or synnematal conidiomata with or without a well-developed stroma. At the same time, conidiogenesis is predominantly phialidic, and conidia are typically unicellular or 1-septate (Rossman et al. 2007). The *Diaporthales* order, with a stem age of approximately 154 Mya, currently comprises 32 families, 196 genera, and around 2,020 species (Huang et al. 2022, Liu et al. 2022b, Monkai et al. 2022, Wijayawardene et al. 2022, Chen et al. 2023a, Jiang et al. 2023b, Species Fungorum 2024).

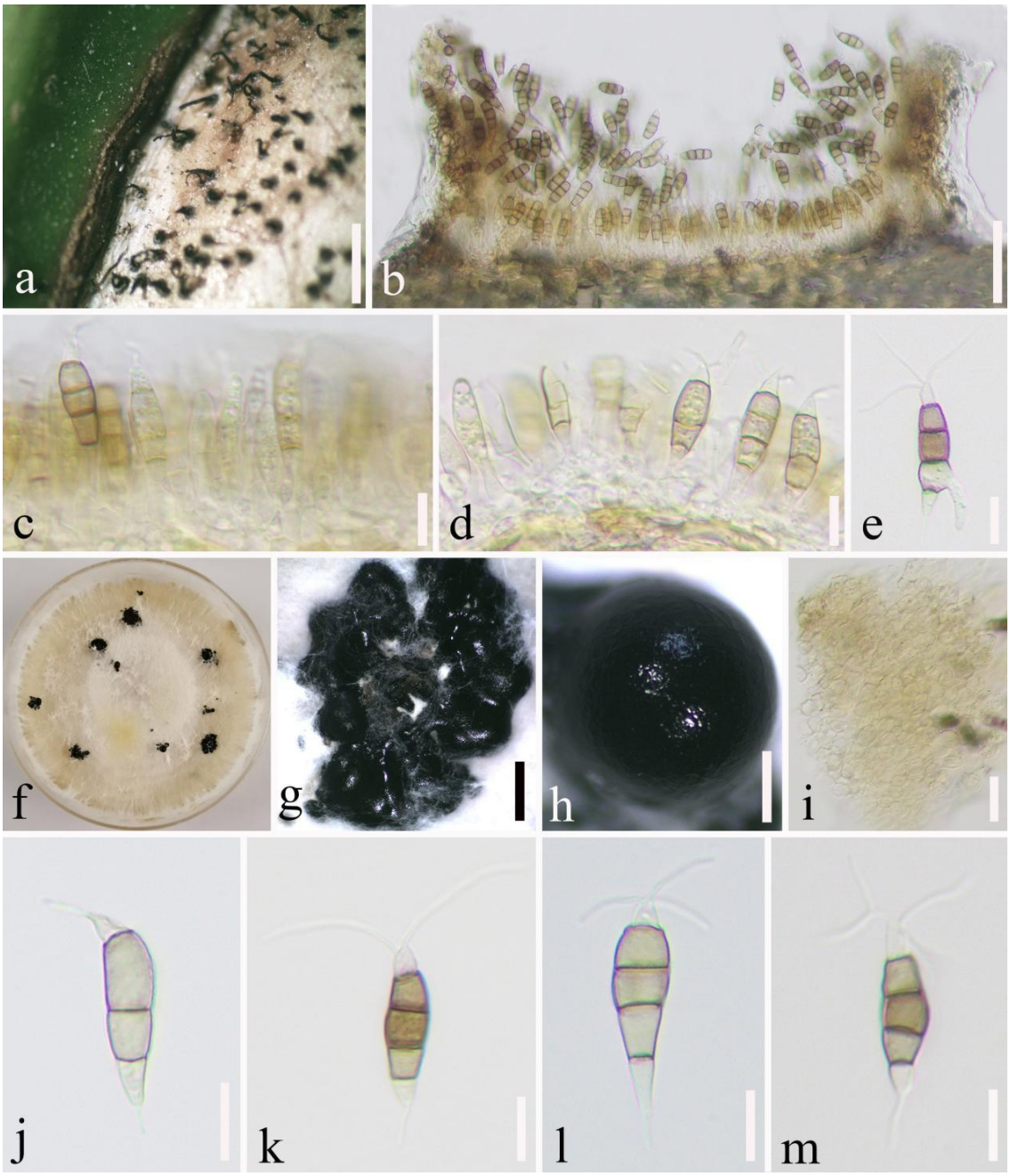

Figure 43 – *Pestalotiopsis oryzae* (SICAU 23-0147). a Appearance of conidiomata on the leaf. b Cross-section of conidioma. c, d Conidiogenous cells with developing conidia. e Germinating conidium. f Front view of colony on PDA. g, h Black conidiomata formed on PDA. i Conidiogenous cells. j–m Conidia. Scale bars: a, g = 1000 μm, b = 50 μm, c–e, j–m = 10 μm, h = 500 μm, i = 20 μm.

Cytospora Ehrenb.

Notes – *Cytospora*, typified by *C. chrysosperma*, was introduced by Ehrenberg (1818). This genus is defined by its solitary ascostromata that can be either immersed or erumpent, featuring valsoid or diatrypelloid arrangements within an ectostromatic disc, as well as ellipsoid to clavate asci with a refractive, J- apical ring, and ellipsoid to allantoid, aseptate, hyaline ascospores, while its coelomycetous asexual morph is characterized by single or labyrinthine, loculate stromata, filamentous conidiophores, enteroblastic, phialidic conidiogenous cells, and allantoid, aseptate, hyaline conidia (Maharachchikumbura et al. 2016b, Fan et al. 2020, Manawasinghe et al. 2022, Wijesinghe et al. 2023). *Cytospora* species are widely distributed worldwide and are typically recognized as saprophytes, endophytes, and phytopathogens that can affect a broad range of plants,

including monocotyledons, dicotyledons, and gymnosperms (Senanayake et al. 2018, Fan et al. 2020, Hanifeh et al. 2022). Some *Cytospora* species usually are important pathogens causing cankers or dieback on economically important trees or garden plants, which sometimes induce destructive losses (Wang et al. 2015, Lawrence et al. 2017).

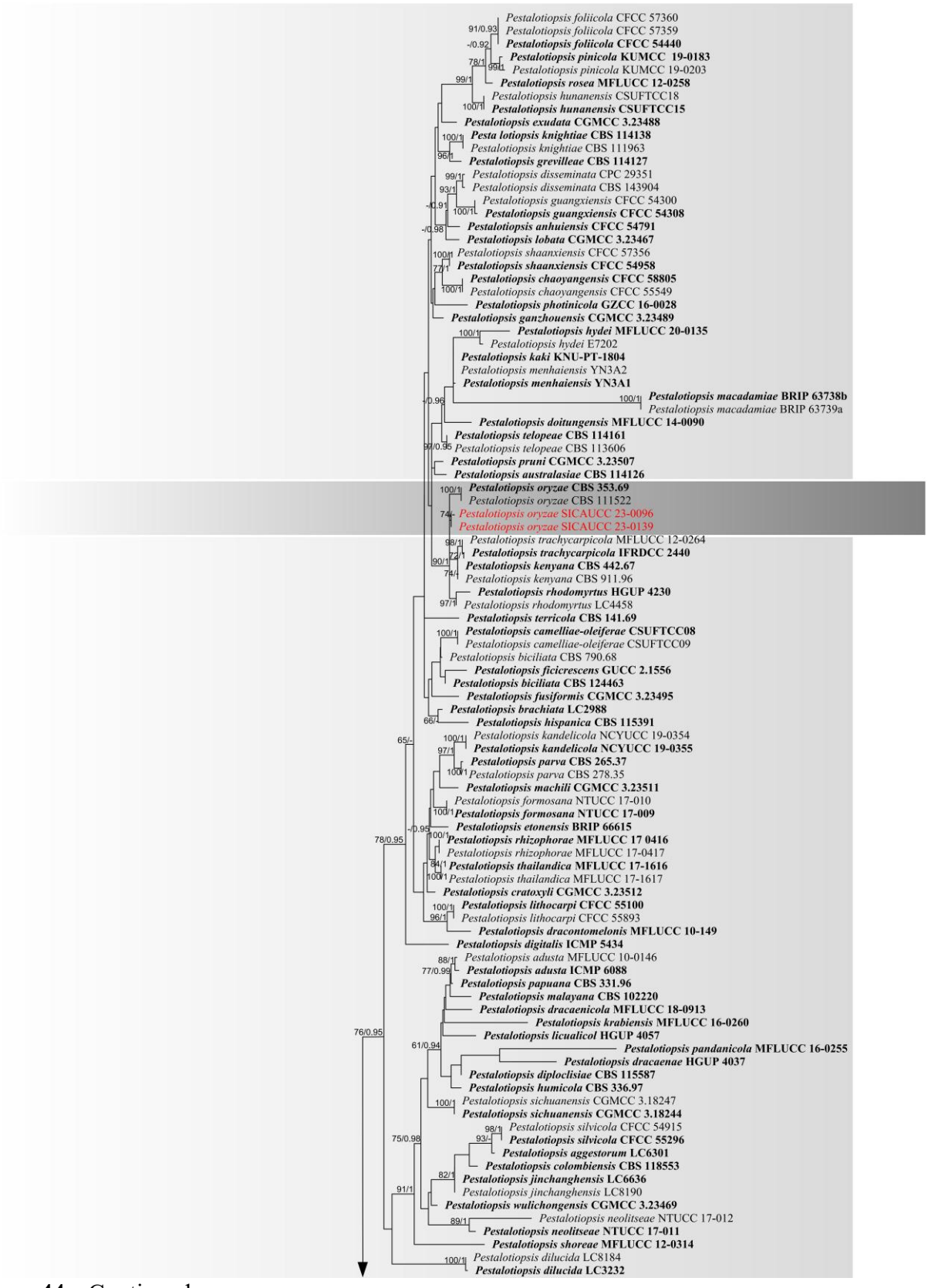

Figure 44 – Continued.

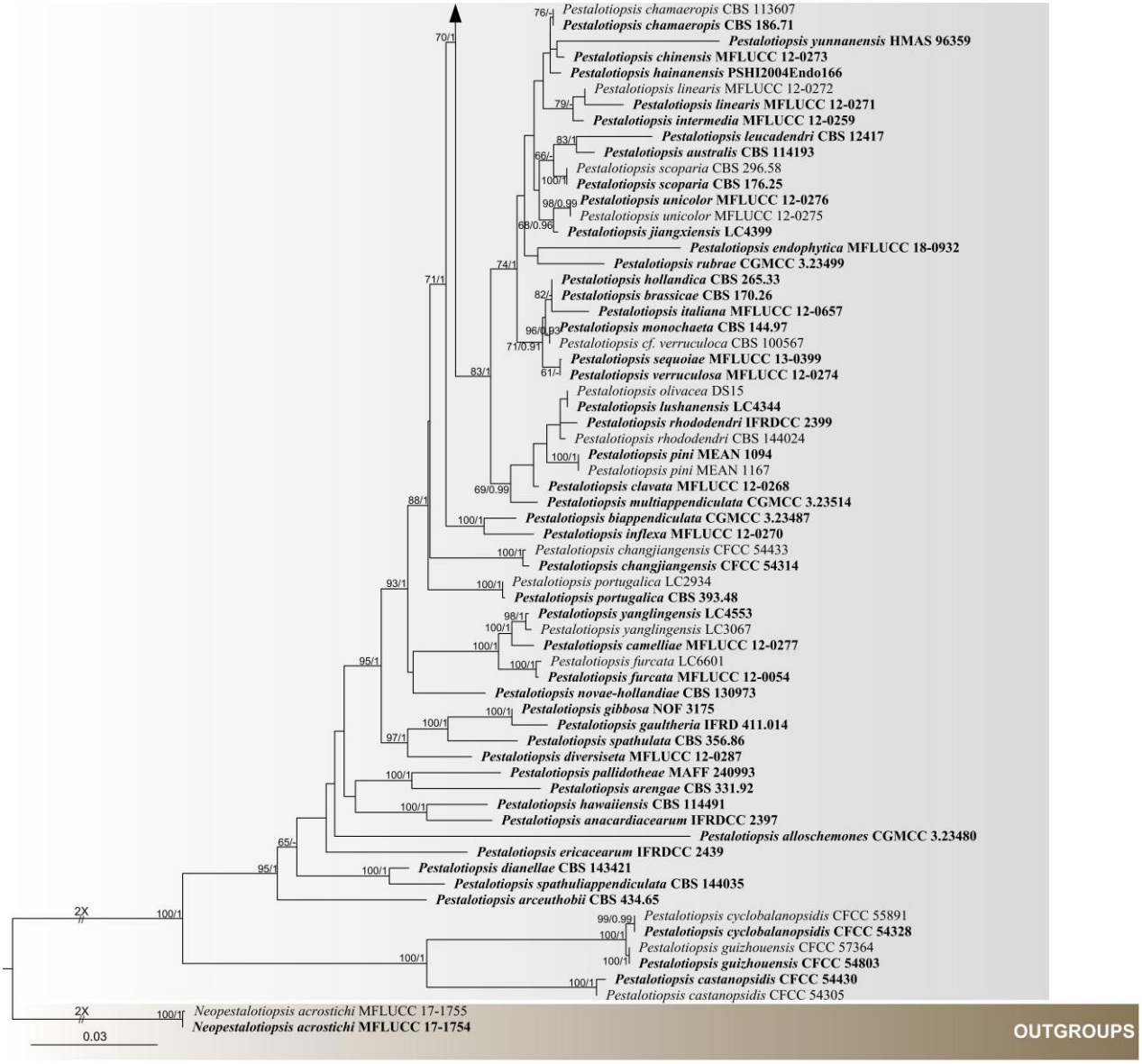

Figure 44 – Phylogram derived from maximum likelihood analyses of a combined dataset comprising ITS, *tef*1-α, *tub*2, and LSU sequences data, representing the species in *Pestalotiopsis*. The phylogenetic analysis included one hundred and sixty-two strains comprising 3,466 characters (ITS: 1–563, *tef*1-α: 564–1,630, *tub*2: 1,631–2,555, LSU: 2,556–3,466) after alignment. The tree is rooted to *Neopestalotiopsis acrostichi* (MFLUCC 17-1754 and MFLUCC 17-1755). Single-gene analyses were conducted, resulting in similar tree topologies between the ML and BY methods, ensuring consistent comparisons of clade stability. The best-scoring RAxML tree with a final likelihood value of -21,074.965683 is presented. The matrix had 1,296 distinct alignment patterns, with 43.96% of undetermined characters or gaps. Estimated base frequencies were as follows: A = 0.241606, C = 0.282168, G = 0.227579, T = 0.248647; substitution rates AC = 1.324422, AG = 3.306836, AT = 1.309613, CG = 1.158816, CT = 5.326941, GT = 1.000000. Bootstrap support values for maximum likelihood (MLBS) ≥ 60% and Bayesian posterior probabilities (BYPP) ≥ 0.90 are indicated at the nodes, respectively. The ex-type strains are in bold, and the new isolate is in red. Bar = 0.03 represents the estimated number of nucleotide substitutions of site per branch.

Cytosporaceae Fr.

Notes – *Cytosporaceae* was initially proposed by Fries (1825), later regarded as a synonym under *Valsaceae* in 1861, and ultimately reinstated as a family name by Rossman et al. (2015). This family comprises pathogens and saprobes, with the majority of its species acting as plant pathogens

responsible for cankers, diebacks, and decline syndromes in various wood-gymnosperms, angiosperms, and occasionally grasses (Lawrence et al. 2018, Senanayake et al. 2018, Pan et al. 2022, Domínguez et al. 2023). The family includes six recognized genera, totalling about 360 species, namely *Cryptascoma*, *Cytospora*, *Pachytrype*, *Paravalsa*, *Waydora*, and *Xenotypa* (Wijayawardene et al. 2022, Ilyukhin et al. 2023, Lin et al. 2023, Species Fungorum 2024).

23. *Cytospora chrysosperma* (Pers.) Fr., Syst. mycol. (Lundae) 2(2): 542 (1823) Fig. 45

=*Valsa sordida* Nitschke, Pyrenomyc. Germ. 2: 203 (1870)

MycoBank number: MB179190; Facesoffungi number: FoF15882

Associated with canker on branches and twigs of *Salix* sp. Sexual morph: Not observed. Asexual morph: *Coelomycetous*. *Conidiomata* immersed, erumpent through the surface of bark, solitary, flat to discoid, circular, with multi-locules. *Conceptacle* black. *Ectostromatic disc* 750–1050 × 750–1200 μm ($\bar{x}$ = 868 × 995 μm, n = 20), pale to dull brown, conspicuous, subcircular to circular, with one ostiole per disc. *Ostiole* 60–160 μm diameter, in the center of the disc, conspicuous, dark grey to black. *Peridium* comprising a few to several layers of cells of *textura angularis*, with pale brown to dark brown. *Locules* numerous, arranged randomly with common walls. *Conidiophores* borne along the locules, hyaline, branched at the base. *Conidiogenous cells* 5–15 × 0.5–2.5 μm ($\bar{x}$ = 10.9 × 1.9 μm, n = 50), blastic, enteroblastic, phialidic, hyaline, smooth-walled, mainly cylindrical, shorter in diameter towards the apex, hyphae-like intertwined in locule, usually longer than conidiogenous cells. *Conidia* 4.5–6 × 0.5–2 μm ($\bar{x}$ = 5.3 × 1.2 μm, n = 50), hyaline, allantoid, eguttulate, smooth, aseptate, thin-walled.

Culture characteristics: Germinated conidia formed in sterilized water after 12 h, and the germinating tube grows from one section of the spore. Colonies on PDA attaining 55–65 mm diameter in 1 week, producing dense mycelium, flat, circular, greyish white to white, lacking aerial mycelium, reverse pale yellow.

Material examined – China, Sichuan Province, Aba Prefecture, Jiuzhaigou County, Zhangzha Town, 103°42′43.24″E 33°6′55.68″N, 3110 m, isol. from branches and twigs of *Salix* sp., 31 Jul. 2020, C.L. Yang, YCL202007002 (SICAU 23-0136), culture (SICAUCC 23-0110).

GenBank numbers – SICAUCC 23-0110 = ITS: PP736366, LSU: PP732706, *act*: PP782107, *rpb*2: PP782080, *tub*2: PP782064, *tef*1-α: PP779571

Notes – *Cytospora chrysosperma*, being the designated type species of *Cytospora*, exhibits a global distribution encompassing a diverse array of hosts (Adams et al. 2006, Fan et al. 2014, 2015a, b). In the phylogenetic analyses, our novel isolate (SICAUCC 20-0000) forms a robust cluster with *C. chrysosperma*, supported by 100% MLBS / 1.00 BYPP (Fig. 46). Morphologically, the new collection closely resembles *C. chrysosperma*, exhibiting features such as immersed, flat to discoid conidiomata with large multiple locules, a subcircular to circular disc with a prominent ostiole, and allantoid, eguttulate, aseptate conidia, as described by Fan et al. (2014). Therefore, we identify the new isolate as *C. chrysosperma*.

24. *Cytospora predappioensis* Q.J. Shang, Norphanph., Camporesi & K.D. Hyde, Mycosphere 9: 376 (2018) Fig. 47

MycoBank number: MB554083; Facesoffungi number: FoF03936

Associated with canker on stems of *Ficus elastica* Roxb. ex Hornem., symptoms initially appeared as dry and shriveled on the diseased tissues, moderately raised lesions with usually a mass of conidia overflow. Sexual morph: Not observed. Asexual morph: *Coelomycetous*. *Conidiomata* 610–830 × 300–490 μm ($\bar{x}$ = 693 × 421 μm, n = 10), pycnidial, immersed in epidermis, erumpent the surface of epidermis when mature, solitary, scattered, or gathered, discoid to conical, with multi-locules. *Conceptacle* conspicuous. *Ectostromatic disc* 750–2150 × 480–970 μm ($\bar{x}$ = 1152 × 790 μm, n = 10), brown, subelliptic to elliptic, disc dark brown. *Ostiole* 60–240 μm ($\bar{x}$ = 165 μm, n = 10) diameter, conspicuous, circular, dark brown. *Locules* numerous, irregular distribution, subdivided by invaginations with common walls. *Conidiophores* hyaline, unbranched or branched at base. *Conidiogenous cells* 9–16 × 1.5–3 μm ($\bar{x}$ = 12 × 2.3 μm, n = 40), enteroblastic,

monophialidic, subcylindrical to cylindrical, straight or flexuous, hyaline. *Conidia* 4.5–8 × 1.5–2 µm ($\bar{x}$ = 6.2 × 1.9 µm, n = 60), hyaline, eguttulate, aseptate, smooth-walled, allantoid.

Culture characteristics – Germinated conidia formed in sterilized water after 3 h, and the germinating tube grows from one section of the spore.

Material examined – China, Sichuan Province, Neijiang City, Zizhong County, Huaxiang Village, 104°49′22.02″E 29°46′22.16″N, 321 m, isol. from stems of *Ficus elastica*, 4 Apr. 2021, C.L. Yang, YCL202104001 (SICAU 23-0128). *ibid.* YCL202104001-2 (SICAU 23-0168).

GenBank numbers – SICAU 23-0128 = ITS: PP736380, LSU: PP732712, *act*: PP782113, *rpb*2: PP782084, *tub*2: PP782072, *tef*1-α: PP779581. SICAU 23-0168 = ITS: PP736381, LSU: PP732713, *act*: PP782114, *rpb*2: PP782085, *tub*2: PP782073, *tef*1-α: PP779582

Notes – The newly obtained isolates (SICAU 23-0128 and SICAU 23-0168) form a sister branch with *Cytospora ceratospermopsis*, *C. ceratosperma* and *C. predappioensis* in the phylogenetic analyses with a robust statistical support (99% MLBS / 1.00 BYPP) (Fig. 46), and can be identified as *C. predappioensis*. To confirm this identification, the single gene comparison of ITS, LSU, and *rpb*2 gene regions was carried out between our strains and *C. predappioensis* (MFLUCC 18-1202), the result revealed only few nucleotide differences, and there are no base pair differences of the ITS and LSU nucleotides between our strains and *C. predappioensis* (MFLUCC 17-2458), which confirmed that the new collections are *C. predappioensis* (Hyde et al. 2018). In addition, our new collections are morphologically identical to *C. predappioensis* (MFLUCC 18-1202) (Shang et al. 2020). We, therefore, identify our isolate as *C. predappioensis*, which is the first report on *Ficus elastica*.

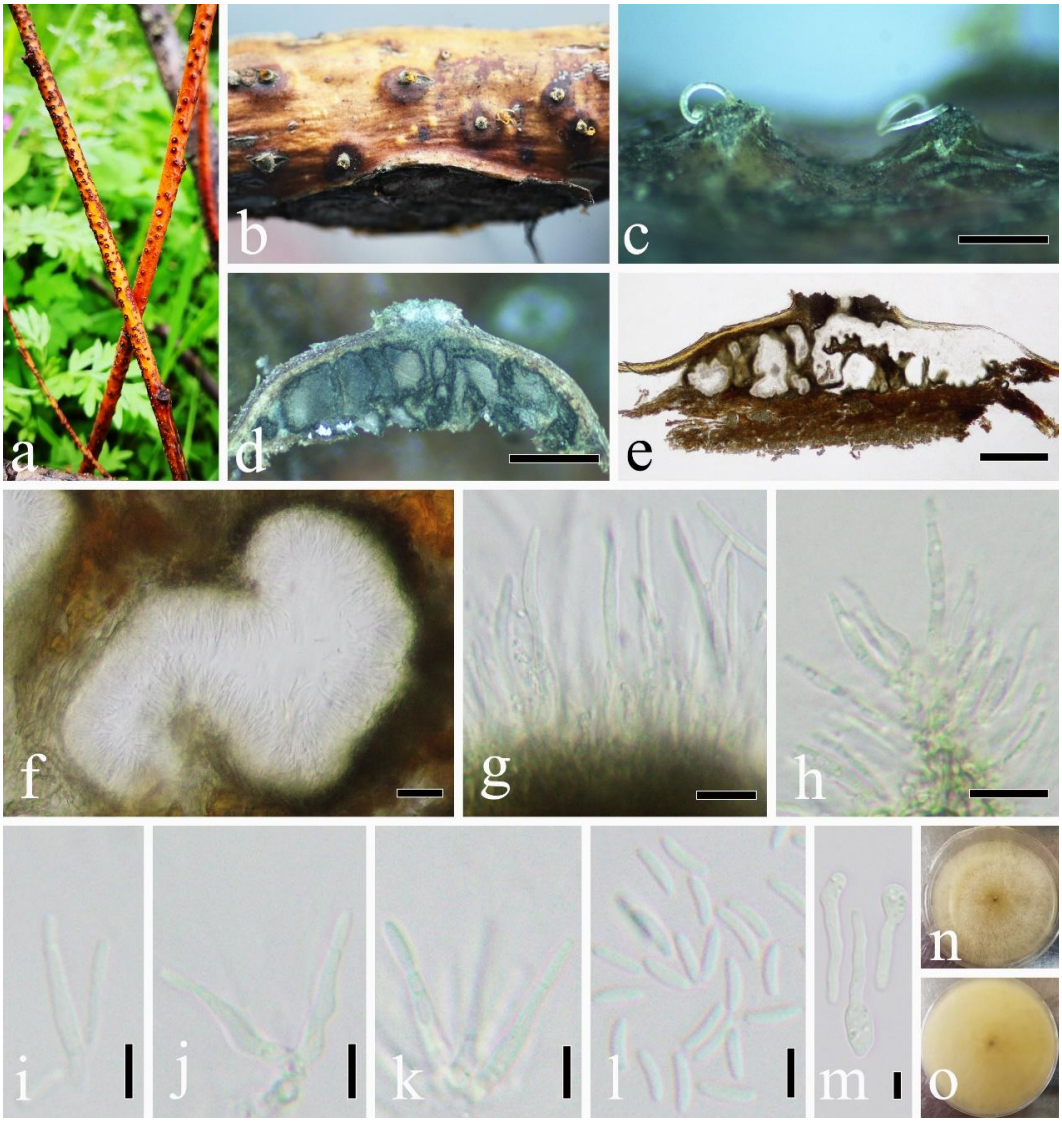

Figure 45 – *Cytospora chrysosperma* (SICAU 23-0136). a Symptoms on the branches. b, c Appearance of conidiomata. d–f Cross-section of conidiomata. g–h Conidiophores. i–k Conidiogenous cells with developing conidia. l Conidia. m Germinating conidia in sterilized water after 12 h. n Front view of colony on PDA. o Reverse view of colony on PDA. Scale bars: c–e = 500 μm, f = 20 μm, g, h = 10 μm, i–m = 5 μm.

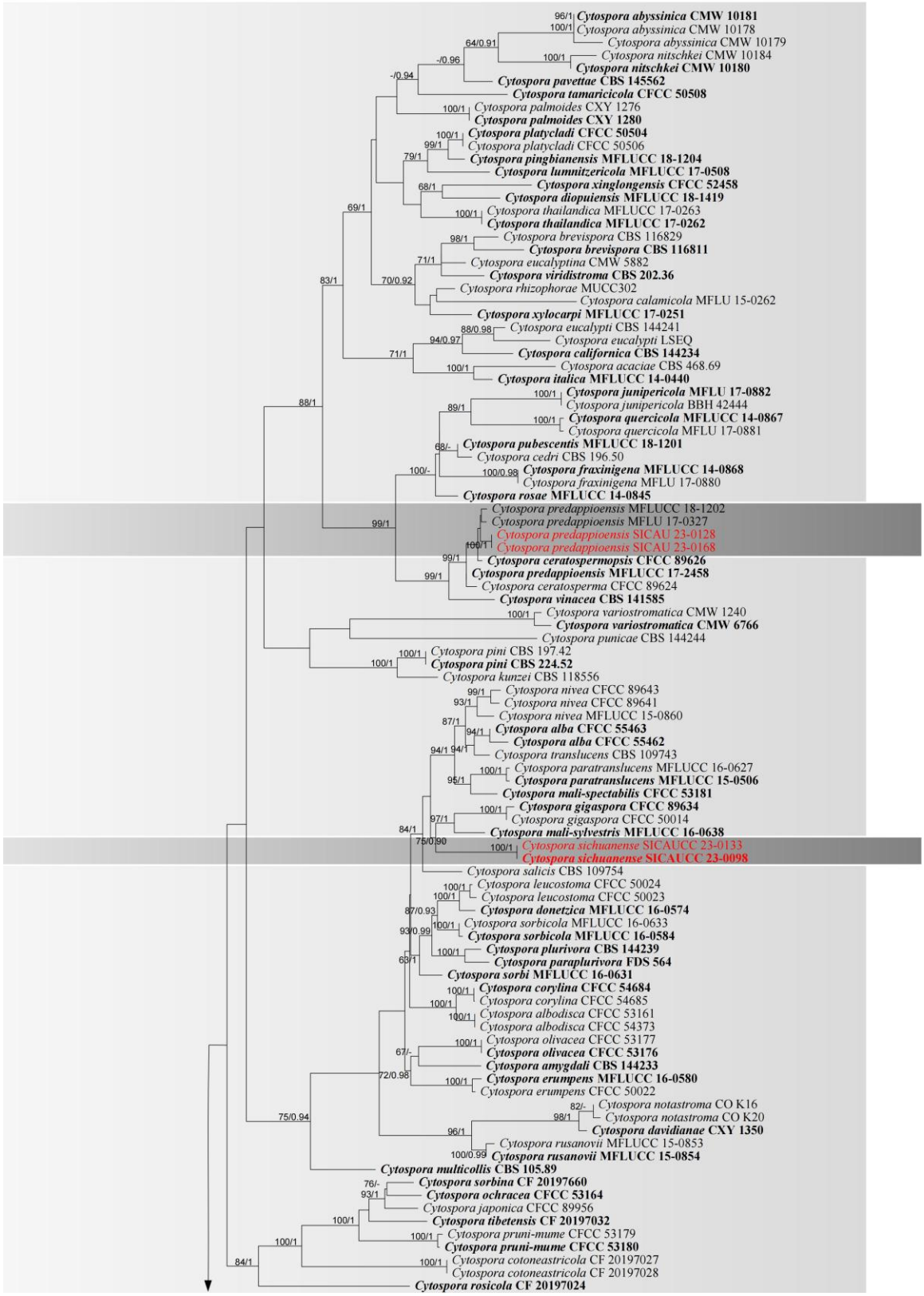

Figure 46 – Continued.

Figure 46 – Continued.

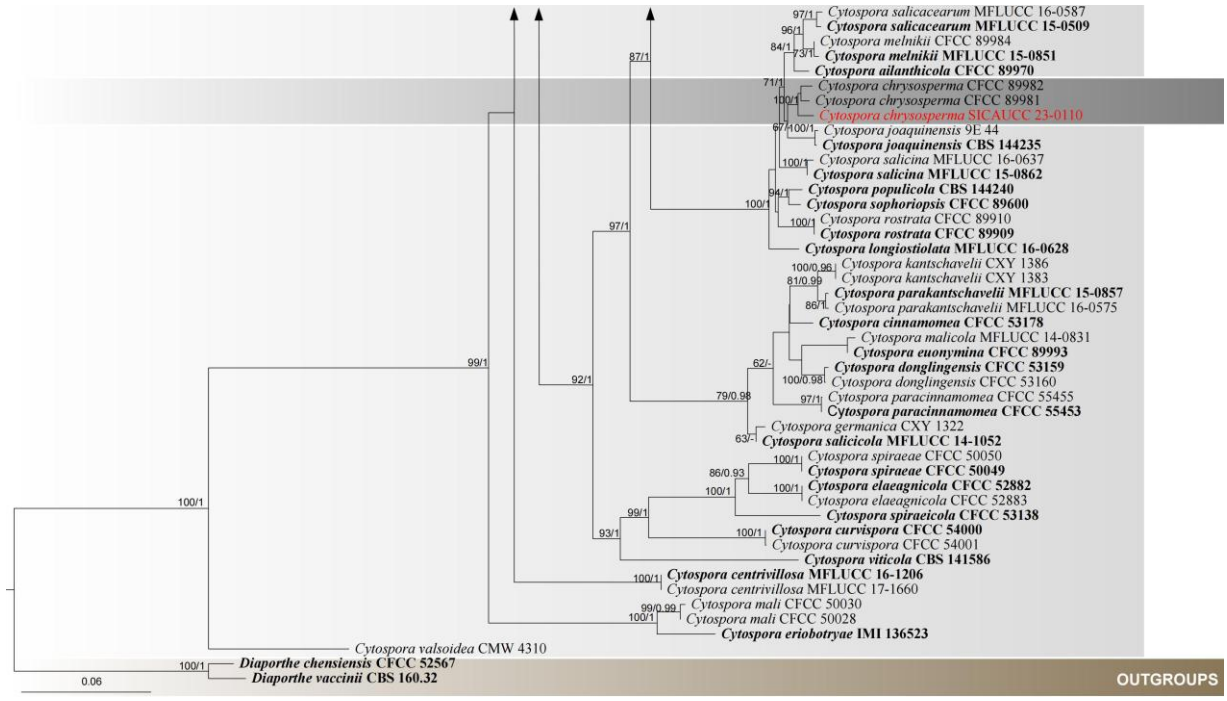

Figure 46 – Phylogram derived from maximum likelihood analyses of a combined dataset comprising ITS, LSU, *act*, *rpb*2, *tef*1-α, and *tub*2 sequences, representing the species within the *Cytospora* genus. The phylogenetic analysis included 238 strains, which comprised 6,193 characters (ITS: 1–790, LSU: 791–1,876, *act*: 1,877–2,656, *rpb*2: 2,657–3,845, *tef*1-α: 3,846–5,021, *tub*2: 5,022–6,193) after alignment. The tree is rooted to *Diaporthe chensiensis* (CFCC 52567) and *D vaccinii* (CBS 160.32). Single-gene analyses were conducted, resulting in similar tree topologies between the ML and BY methods, ensuring consistent comparisons of clade stability. The best-scoring RaxML tree with a final likelihood value of – 66,071.604115 is presented. The matrix had 3,056 distinct alignment patterns, with 65.65% of undetermined characters or gaps. Estimated base frequencies were as follows: A = 0.244597, C = 0.276519, G = 0.252652, T = 0.226232; substitution rates AC = 1.503706, AG = 3.701088, AT = 1.623222, CG = 1.063282, CT = 6.867630, GT = 1.000000. Bootstrap support values (MLBS) equal to or exceeding 60%, and Bayesian posterior probabilities (BYPP) equal to or exceeding 0.90 have been indicated above the nodes. The ex-type strains are in bold, and the new isolate is in red. Bar = 0.06 estimated number of nucleotide substitutions per site per branch.

25. *Cytospora sichuanense* X.Y. Li & C.L. Yang, sp. nov. Fig. 48

MycoBank number: MB900657; Facesoffungi number: FoF15920

Etymology – Refers to the province, where the species collected.

Holotype – SICAU 23-0137

Associated with canker on branches and twigs of *Salix* sp. Sexual morph: *Ascostromata* 1200–1500 × 500–700 µm ($\bar{x}$ = 1340 × 600 µm, n = 10), semi-immersed in host tissue, scattered, distinctly erumpent, lenticular, mostly with 1-8 locules, ostiolate with periphysis. *Conceptacle* absent. *Ectostromatic disc* 950–1710 × 550–1050 µm ($\bar{x}$ = 1260 × 779 µm, n = 30), white, usually surrounded by tightly ostiolar necks, ellipsoid, occasionally circular. *Ostioles* 45–85 µm ($\bar{x}$ = 63.3 µm, n = 30) diameter, numerous, at the same level as the disc or slightly below, concentrated, dark brown to black, arranged randomly in a disc. *Locules* 350–500 × 200–270 µm ($\bar{x}$ = 446 × 235 µm, n = 10), dark brown, arranged tightly, subspherical to spherical. *Peridium* 8.5–16 µm ($\bar{x}$ = 12.4 µm, n = 20) thickness, comprising several layers of cells of *textura angularis*, with inner most layer hyaline to pale brown, outer layer brown to dark brown. *Hamathecium* comprising long cylindrical, septate, distinctly constricted at septa, rarely branched, shorter in diameter towards the apex, hyaline, anastomosed, paraphyses. *Asci* 45.5–58 × 8–13 µm ($\bar{x}$ = 51.5 × 10.1 µm, n = 30),

unitunicate, 8-spored, clavate, with J-, apical ring, short pedicellate or sessile. *Ascospores* 16–22 × 2.5–4 μm ($\bar{x}$ = 18.5 × 3.2 μm, n = 50), bi to tri-seriate, elongate-allantoid, thin-walled, hyaline, eguttulate, aseptate. Asexual morph: Not observed.

Culture characteristics – Germinated ascospores in sterilized water within 12 h at 25°C, germ tubes produced from both upper and lower cells. *Colonies* on PDA attaining 50–70 mm diameter in 1 week, flat circular, rough margin, fimbriate, hyaline to yellowish brown, with few aerial mycelium, reverse the same as obverse.

Material examined – China, Sichuan Province, Aba Prefecture, Jiuzhaigou County, Zhangzha Town, 103°42′43.24″E 33°6′55.68″N, 3110 m, isol. From branches and twigs of *Salix* sp., 31 Jul. 2020, C.L. Yang, YCL202007003 (SICAU 23-0137, holotype), ex-type culture (SICAUCC 23-0098). *ibid.* YCL202007003-2 (SICAU 23-0162), living culture SICAUCC 23-0133.

GenBank numbers – SICAUCC 23-0098 = ITS: PP736378, LSU: PP732710, *act*: PP782111, *rpb2*: PP782082, *tub2*: PP782070, *tef*1-α: PP779579. SICAUCC 23-0133 = ITS: PP736379, LSU: PP732711, *act*: PP782112, *rpb2*: PP782083, *tub2*: PP782071, *tef*1-α: PP779580

Notes – In the phylogenetic analysis, *Cytospora sichuanense* was assigned as a novel taxon within the *Cytospora* genus, showing its closest affinity to *Cytospora gigaspora* and *Cytospora mali-sylvestris* with moderate statistical support (75% MLBS / 0.90 BYPP) (Fig. 46). Morphologically, *C. sichuanense* is distinguished from *C. mali-sylvestris* by having bigger ascostromata (1200–1500 × 500–700 μm vs. 550–600 × 400–430 μm) with more locules (1–8 vs. 1–2) and bigger ascospores (16–22 × 2.5–4 μm vs. 7–12.5 × 1.8–2.5 μm) (Hyde et al. 2017). However, comparing the morphological characteristics of our strain with those of *C. gigaspora* is not feasible, as the latter is only known by its asexual morph (Fan et al. 2015a). In addition, pairwise nucleotide comparisons revealed that *C. sichuanense* (SICAUCC 23-0098) shares 89.8% similarity (220/245 bp, 8 gaps) in *act*, 95.7% (484/506 bp, 4 gaps) in ITS, 95.2% (692/727 bp, 0 gap) in *rpb2*, 83.2% (243/292 bp, 6 gaps) in *tef*1-α, and 90.8% (366/403 bp, 1 gap) in *tub2* with *C. gigaspora* (CFCC 89634, holotype). Furthermore, it shows 88.5% similarity (193/218 bp, 6 gaps) in *act*, 96.3% (554/575 bp, 5 gaps) in ITS, and 96.1% (711/740 bp, 0 gap) in *rpb*2 with *C. mali-sylvestris* (MFLUCC 16-0638, holotype). Based on morphology and phylogenetic evidence, we introduce *C. sichuanense* as a new species.

Diaporthaceae Höhn. Ex Wehm.

Notes – *Diaporthaceae* was initially established by Von Höhnel (1917), and later, Wehmeyer (1926) revised this family. Subsequently, several researchers made a series of further revisions to the family (Kobayashi 1970, Barr 1978, 1991). *Diaporthaceae* species exhibit morphological diversity, with solitary or clustered ascomata, variable stromatic development, generally with hyaline ascospores, and diverse asexual characters (Senanayake et al. 2018). *Diaporthaceae* members are known to encompass saprobes, endophytes, zooopathogens, and phytopathogens. They infect a wide variety of plant hosts, including many common species, leading to conditions such as root rot, crown rot, fruit rot, dieback, canker, spot, blight, decay, and wilt (Lamprecht et al. 2011, Chen et al. 2014, Senanayake et al. 2018, Aiello et al. 2022). *Diaporthaceae* currently comprises 16 genera and approximately 710 species (Monkai et al. 2022, Wijayawardene et al. 2022, Jia et al. 2023b, Wan et al. 2023, Zhu et al. 2023).

Diaporthe Nitschke

Notes – *Diaporthe* was formally established by Nitschke (1867) with *D. eres* as the type species. *Diaporthe* species are characterized by stromata that often have blackened areas on the substrate, ellipsoid to fusiform ascospores, and enclosed unilocular pycnidia that contain spermatia, stylospores, and conidia (Nitschke 1867). However, this genus exhibits morphological heterogeneity due to variations in its hosts, habitats, and environments (Gao et al. 2017, Senanayake et al. 2017). *Diaporthe* members can be found worldwide and occupy various ecological niches, serving as saprobes, endophytes, and pathogens on a wide range of plant species (Gomes et al. 2013, Udayanga et al. 2014, Bhunjun et al. 2022). Many species in this genus have

the potential to cause diseases in economically important forest trees, crops and ornamental plants, typically manifesting as a wide range of symptoms, including cankers, diebacks, spots, blights, melanoses, rots, and gummosis (Dissanayake et al. 2017a,b, Norphanphoun et al. 2022).

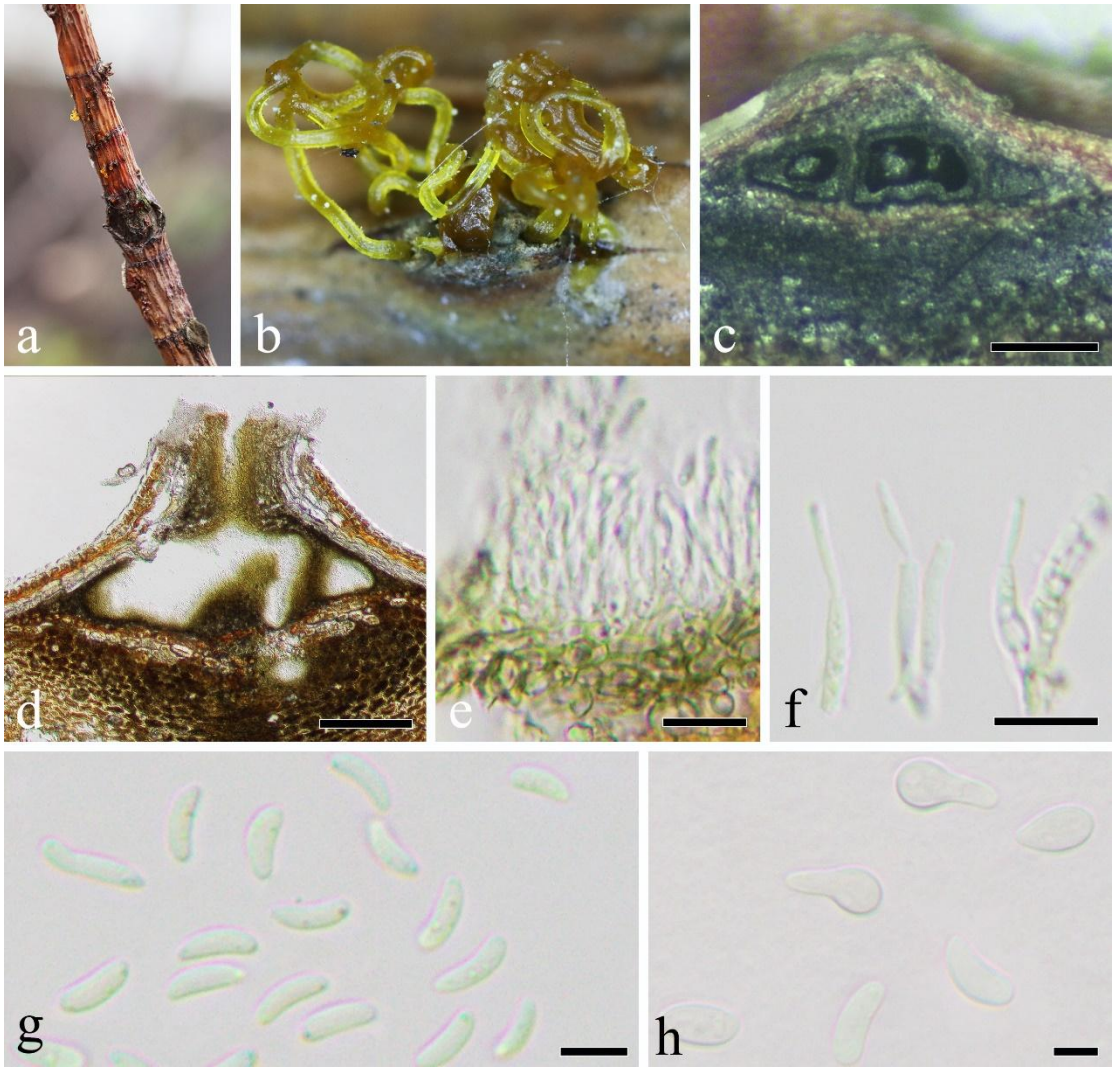

Figure 47 – *Cytospora predappioensis* (SICAU 23-0128). A Symptoms on the stem. b Appearance of conidioma. C, d Cross-section of conidiomata. E, f Conidiogenous cells with developing conidia. G Conidia. K Germinating conidia in sterilized water after 3 h. Scale bars: c, d = 200 µm, e, f = 10 µm, g, h = 5 µm.

26. *Diaporthe eres* Nitschke, Pyrenomyc. Germ. 2: 245 (1870) Fig. 49

MycoBank number: MB172054; Facesoffungi number: FoF02182

Associated with canker on stems of *Ficus elastica* Roxb. Ex Hornem., symptoms appeared as dry and shrivelled on the diseased tissues with a little conidia overflow. Sexual morph: Not observed. Asexual morph: *Coelomycetous*. *Conidiomata* 820–1050 × 330–540 µm ($\bar{x}$ = 950 × 443 µm, n = 10), pycnidial, initially immersed, erumpent at maturity, discoid to conical, or irregular, pale brown to brown, solitary, scattered, or gathered, with yellowish white conidial mass extruding from ostiole, usually unilocular. *Conceptacle* conspicuous. *Conidiomatal wall* parenchymatous consisting of multi-layers of pale brown to brown, thick-walled cells of *textura angularis* or *textura globulosa*. *Conidiophores* hyaline, smooth, straight to sinuous, branched, or unbranched at base. *Conidiogenous cells* 14.5–26 × 1.5–3 µm ($\bar{x}$ = 20.7 × 2.1 µm, n = 20) for producing alpha-conidia, 10–18 × 1–3 µm ($\bar{x}$ = 13.9 × 2.1 µm, n = 20) for producing beta-conidia, enteroblastic, monophialidic, terminal, cylindrical, slightly tapering towards the apex. *Alpha-conidia* 6–10(–12) ×

2.5–4 µm ($\bar{x}$ = 8.4 × 3.1 µm, n = 60), hyaline, aseptate, smooth, ovate to ellipsoidal, base sub-truncate, guttulate. *Beta-conidia* 21.5–40 × 1.5–2.5 µm ($\bar{x}$ = 30.6 × 1.9 µm, n = 50), hyaline, aseptate, filiform, hamate.

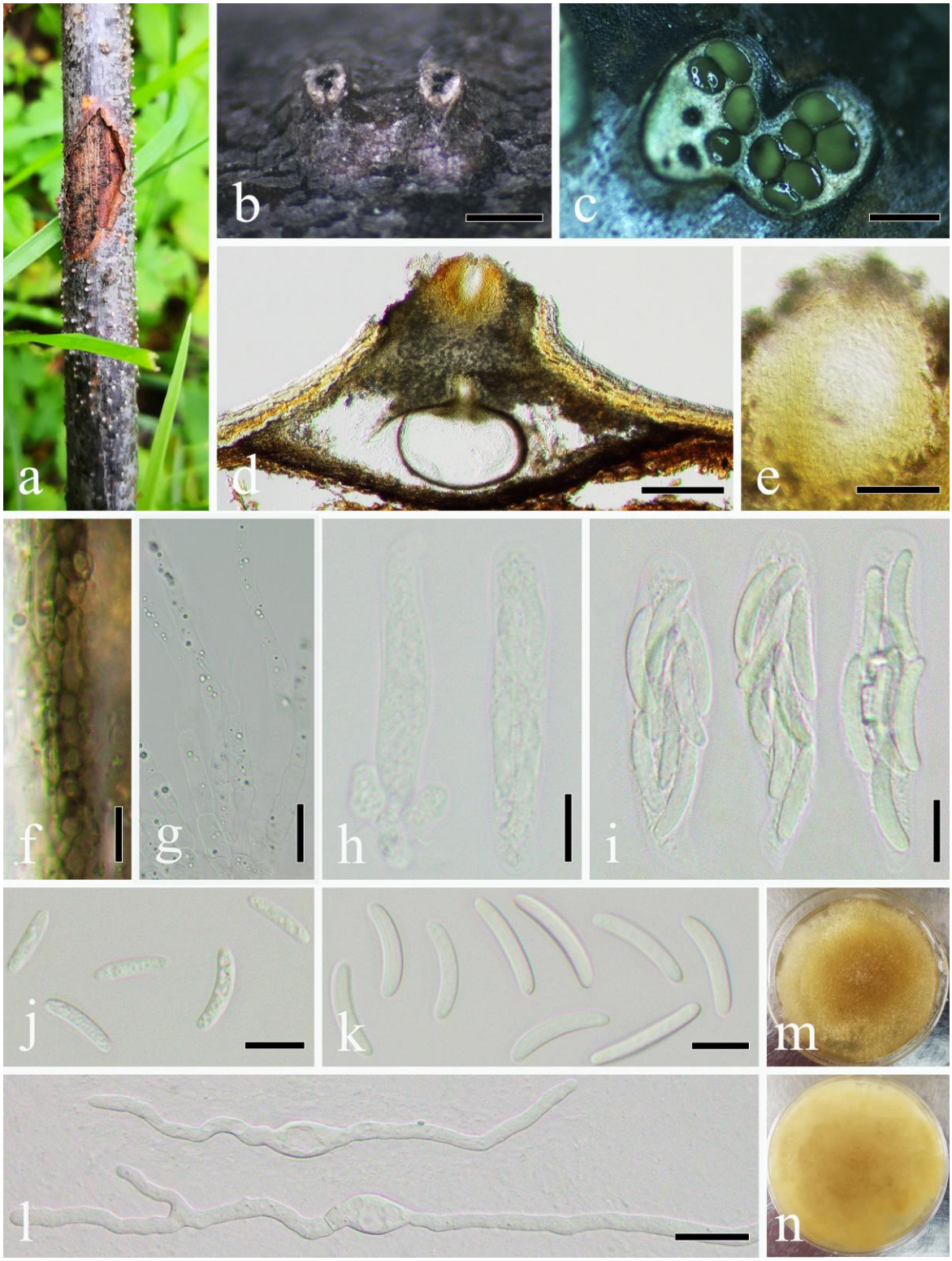

Figure 48 – *Cytospora sichuanense* (holotype, SICAU 23-0137). A Symptoms on the branch. B Appearance of ascostromata. C, d Cross-section of ascostromata. E Section of ostiole. F Peridium. G Paraphyses. H–I Asci. J–k Ascospores. L Germinating ascospores in sterilized water after 12 h. m Front view of colony on PDA. N Reverse view of colony on PDA. Scale bars: b–d = 500 µm, e = 50 µm, g = 20 µm, f, h–l = 10 µm.

Culture characteristics – Germinated alpha-conidia formed after 12 hrs, and the germinating tube grows from any part of the spore. *Colonies* on PDA initially produced white dense aerial hyphae closed to the surface of the medium, then forming dusty grey and off-white colonies, which subsequently exhibited light yellow conidial mass randomly distributed in each area of the medium.

Material examined – China, Sichuan Province, Neijiang City, Zizhong County, Huaxiang Village, 104°49′22.02″E 29°46′22.16″N, 321 m, isol. From stems of *Ficus elastica*, 4 Apr. 2021, C.L. Yang, YCL202104002 (SICAU 23-0118), culture (SICAUCC 23-0108); *ibid.* YCL202104003 (SICAU 23-0119), culture (SICAUCC 23-0109). China, Sichuan Province, Yibin City, Junlian County, 104°33′23.89″E 27°55′20.16″N, 1337 m, isol. From branches of *Phellodendron chinense* C. K. Schneid., 1 May 2024, X.Y. Li, LXY202405020 (SICAU 24-0263), culture (SICAUCC 24-0214).

GenBank numbers – SICAUCC 23-0108 = ITS: PP736369, *tef*1-α: PP779574, *tub*2: PP782067, *cal*: PP836770, *his*3: PP782127; SICAUCC 23-0109 = ITS: PP736370, *tef*1-α: PP779575, *tub*2: PP782068, *cal*: PP836771, *his*3: PP782128; SICAUCC 24-0214 = ITS: PV123955, *tef*1-α: PV133304, *tub*2: PV133305, *his*3: PV133303

Notes – *Diaporthe eres* serves as the type species of the genus *Diaporthe*, embodying its defining characteristics. A variety of hosts and distributions were reported to have been affected by the species (Dissanayake et al. 2017a, b, Guo et al. 2020, Chaisiri et al. 2021, Du et al. 2021, Hongsanan et al. 2023). In the multi-gene phylogenetic analysis, our three newly isolated strains, SICAUCC 23-0108, SICAUCC 23-0109 and SICAUCC 24-0214, were nested within Section Eres, constituting a distinctive clade closely related to the *D. eres* clade with robust support (99% MLBS / 1.00 BYPP) (Fig. 50), maintaining consistency with the morphological characteristics described in the type description (Udayanga et al. 2014, Dissanayake et al. 2024). A nucleotide comparison encompassing the ITS, *tef*1-α, *tub*2, *cal*, and *his*3 genes between SICAUCC 23-0108 and *D. eres* (AR5193) showed similarity values of 96.29% (519/539 bp, 4 gaps), 99.32% (292/294 bp, 0 gap), 98.04% (499/509 bp, 0 gap), 99.70% (335/336 bp, 0 gap), and 98.38% (426/433 bp, 0 gap), respectively. Based on the morphological characteristics and molecular evidence, the newly collected specimens are belonging to the species *D. eres*.

27. *Diaporthe erythrinae* X.Y. Li & C.L. Yang, sp. nov. Fig. 51

MycoBank number: MB900658; Facesoffungi number: FoF15922

Etymology – Refers to the host genus *Erythrina*, where the species collected.

Holotype – SICAU 23-0138

Associated with twig blight on twigs of *Erythrina crista-galli* Linn. Sexual morph: Not observed. Asexual morph: *Coelomycetous*. *Conidiomata* 123–176 × 63–148 μm ($\bar{x}$ = 150 × 92 μm, n = 20), pycnidial, semi-immersed, grey to black, gregarious, conical, globose to oblate, uniloculate, ostiolate, glabrous. *Conidiomatal wall* 7–18 μm width, comprising 4–5 layers of thick-walled, dark brown cells of *textura angularis*, becoming thin-walled and hyaline towards the inner region. *Conidiophores* 13–22 × 1–2.5 μm ($\bar{x}$ = 17 × 2 μm, n = 30), hyaline, cylindrical, smooth, unbranched, septate. *Conidiogenous cells* 5–8 × 1.5–2.5 μm ($\bar{x}$ = 6.2 × 1.9 μm, n = 30), holoblastic, hyaline, smooth, ampulliform or cylindrical, smooth. *Alpha-conidia* 6.5–9 × 1–3 μm ($\bar{x}$ = 7.7 × 2.5 μm, n = 50), fusiform, hyaline, aseptate, apex obtuse to subobtuse. *Beta-conidia* 16–20 × 0.5–1.5 μm ($\bar{x}$ = 18 × 1 μm, n = 50), filiform, hyaline, aseptate, curved, tapering towards both ends.

Culture characteristics – Germinated alpha-conidia formed after 12 h, and the germinating tube grows from one side of the spore. *Colonies* on PDA attaining 40–50 mm diameter in 5 days, medium sparse, irregular, hairy edge, white, flocculent to fluffy, aerial mycelium sparse in the middle, well developed at the margin, reverse white.

Material examined – China, Sichuan Province, Chengdu City, Wenjiang District, Schoolyard of Sichuan Agricultural University, 103°51′26.72″E 30°42′27.13″N, 552 m, isol. From twigs of *Erythrina crista-galli*, 28 Oct. 2020, C.L. Yang, YCL202010001 (SICAU 23-0138, holotype), ex-

type culture (SICAUCC 23-0094). *ibid.* YCL202010001-2 (SICAU 23-0163), living culture SICAUCC 23-0129.

GenBank numbers – SICAUCC 23-0094 = ITS: PP736382, *tef*1-α: PP779583, *tub*2: PP782074, *his*3: PP782129, *cal*: PP836772. SICAUCC 23-0129 = ITS: PP736383, *tef*1-α: PP779584, *tub*2: PP782075, *his*3: PP782130, *cal*: PP836773

Notes – In the phylogenetic analyses of combined ITS, *tub*2, *his*3, *cal*, and *tef*1-α sequence data, our new species *Diaporthe erythrinae* grouped within the section Betulicola (97% MLBS / 1.00 BYPP) (Fig. 50), while also being closely related to *D. foliicola* in this section (Dissanayake et al. 2024). However, conidiomata of *D. erythrinae* are smaller than those of *D. foliicola* (123–176 × 63–148 µm vs. 299 to 727 µm), and both its conidiogenous cells and beta-conidia are shorter than those of *D. foliicola* (5–8 × 1.5–2.5 µm vs. 9.3–16.3 × 1.6–3.1 µm, 16–20 × 0.5–1.5 µm vs. 22.7–39.5 × 1.0–1.6 µm) (Wan et al. 2023). Furthermore, a comparison of the ITS, *tef*1-α, *tub*2, *cal*, and *his*3 gene regions between SICAUCC 23-0094 and CFCC 55351 revealed sequence similarity values of 99.82% (551/552 bp, 0 gaps), 97.73% (345/353 bp, 3 gaps), 99.60% (502/504 bp, 0 gap), 98.99% (488/493 bp, 1 gap), and 99.75% (407/408 bp, 0 gap), respectively. Therefore, based on its morphological characteristics, phylogenetic analysis, nucleotide polymorphism comparison and pairwise homoplasy index (*P*-value = 1.0) test results (Fig. 52), *D. erythrinae* is described here as a new species and placed in the section Betulicola.

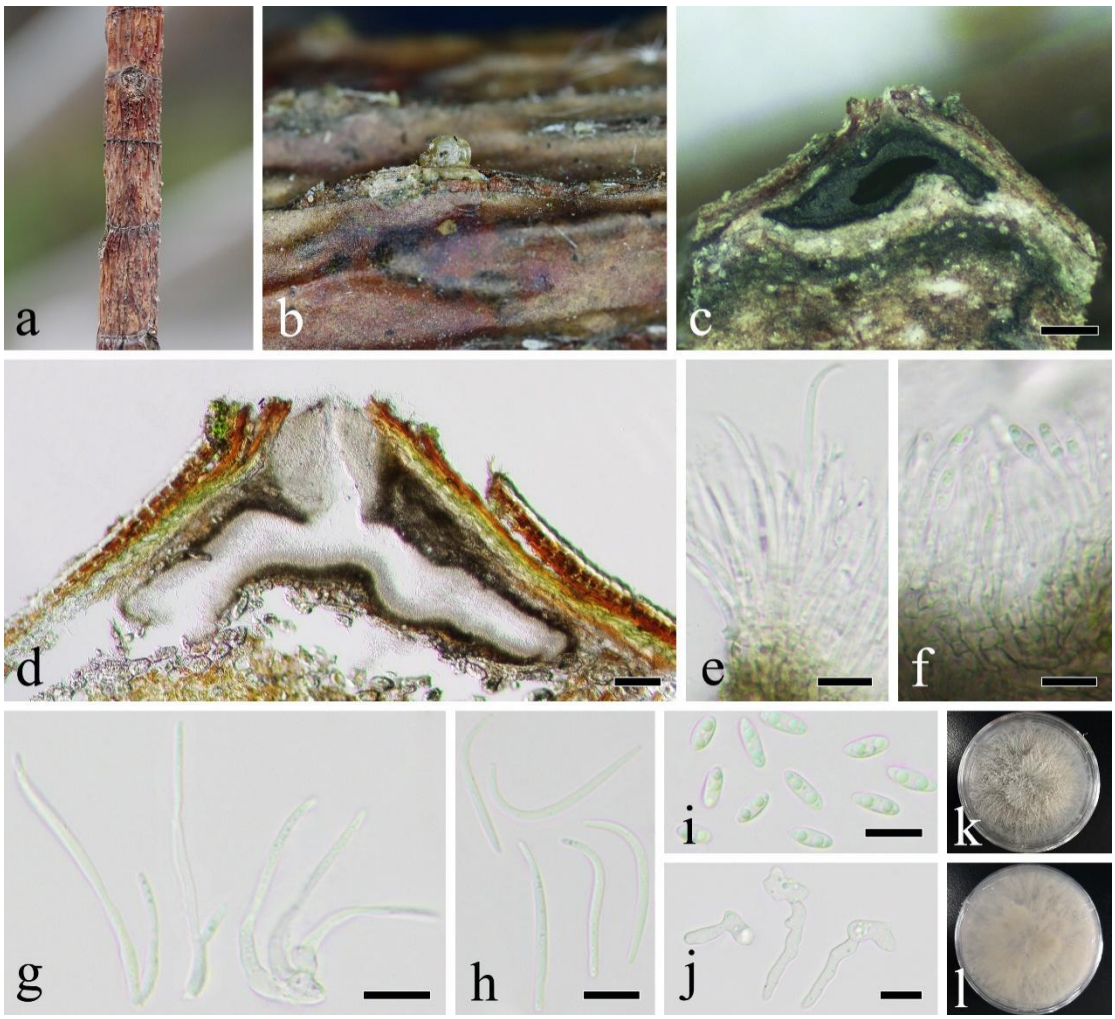

Figure 49 – *Diaporthe eres* (SICAU 23-0118). A Symptoms on the stem. b Appearance of conidiomata. C, d Cross-section of conidiomata. E, g Conidiogenous cells with developing beta-conidia. F Conidiogenous cells with developing alpha-conidia. H Beta-conidia. I Alpha-conidia. J Germinating alpha-conidia. K Front view of colony on PDA. L Reverse view of colony on PDA. Scale bars: c = 200 µm, d = 100 µm, e–j = 10 µm.

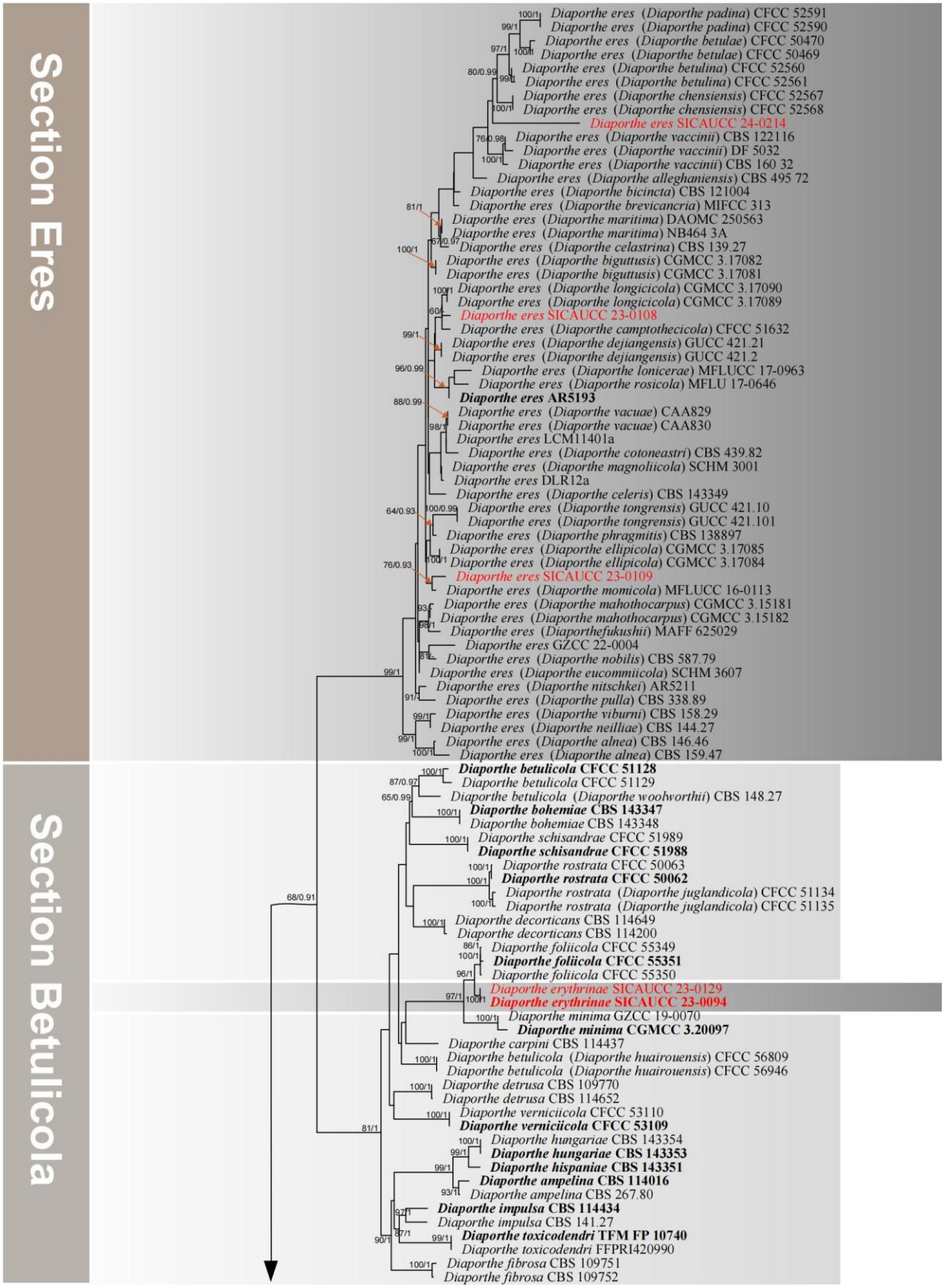

Figure 50 – Continued.

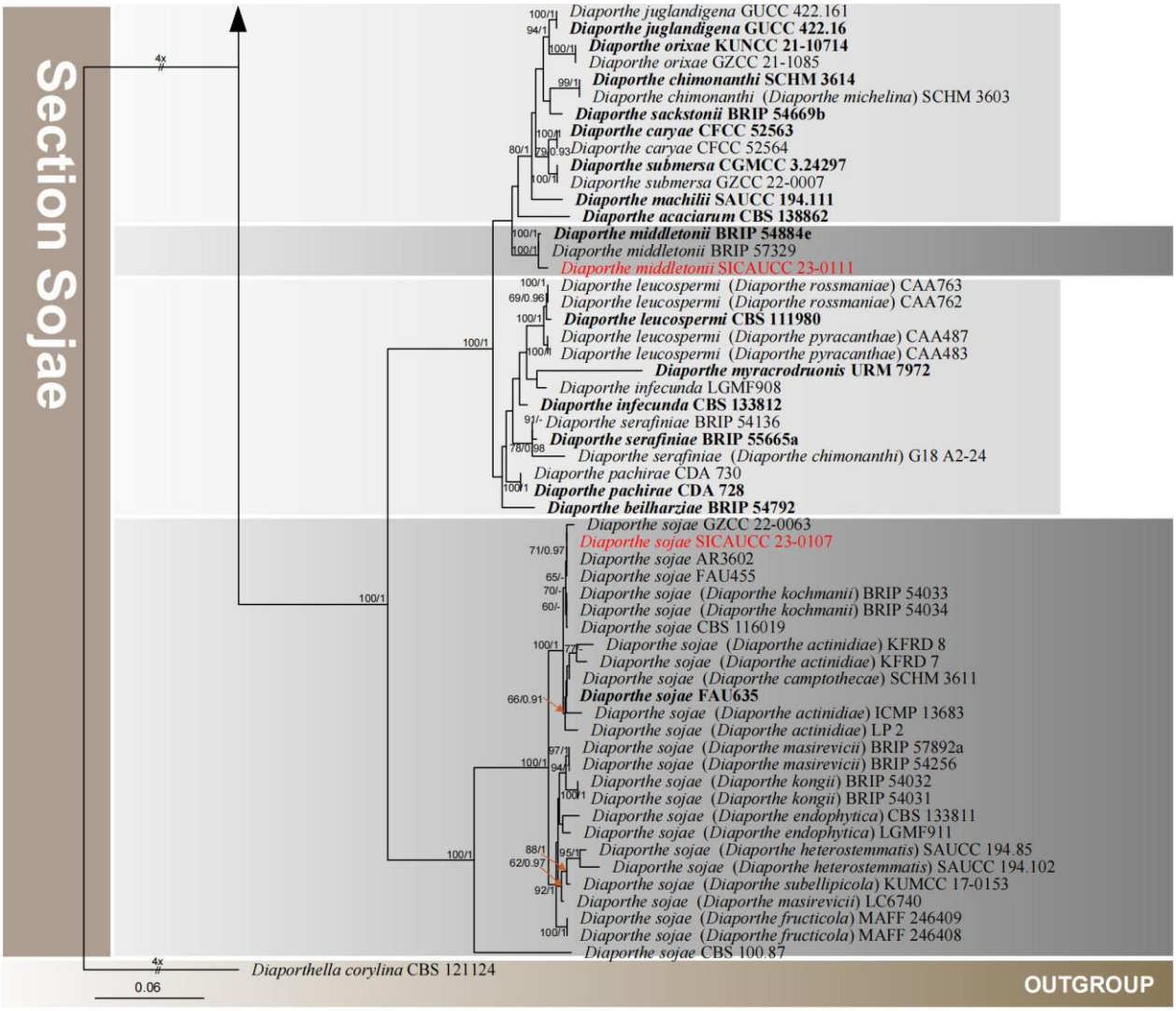

Figure 50 – Phylogram derived from maximum likelihood analyses of a combined dataset comprising ITS, *tef*1-α, *tub*2, *cal*, and *his*3 sequences dataset representing the species of *Diaporthe*. One hundred and fifty strains were included in the combined analyses, which comprised 3,936 characters (ITS: 1–670, *tef*1-α: 671–1500, *tub*2: 1,501–2,517, *cal*: 2,518–3,345, *his*3: 3,346–3,936) after alignment. The tree is rooted to *Diaporthella corylina* CBS 121124. Single-gene analyses were conducted, resulting in similar tree topologies between the ML and BY methods, ensuring consistent comparisons of clade stability. The best scoring RAxML tree with a final likelihood value of -30,141.607826 is presented. The matrix had 2,154 distinct alignment patterns, with 46.99% of undetermined characters or gaps. Estimated base frequencies were as follows: A = 0.214750, C = 0.329039, G = 0.237606, T = 0.218605; substitution rates AC = 1.044256, AG = 2.963705, AT = 1.092268, CG = 0.910357, CT = 4.275344, GT = 1.000000. Bootstrap support values (MLBS) equal to or exceeding 60% and Bayesian posterior probabilities (BYPP) equal to or exceeding 0.90 indicated at the nodes as MLBS / BYPP. The ex-type strains are in bold and the new isolates of this study are in red. Bar = 0.07 represents the estimated number of nucleotide substitutions per site per branch.

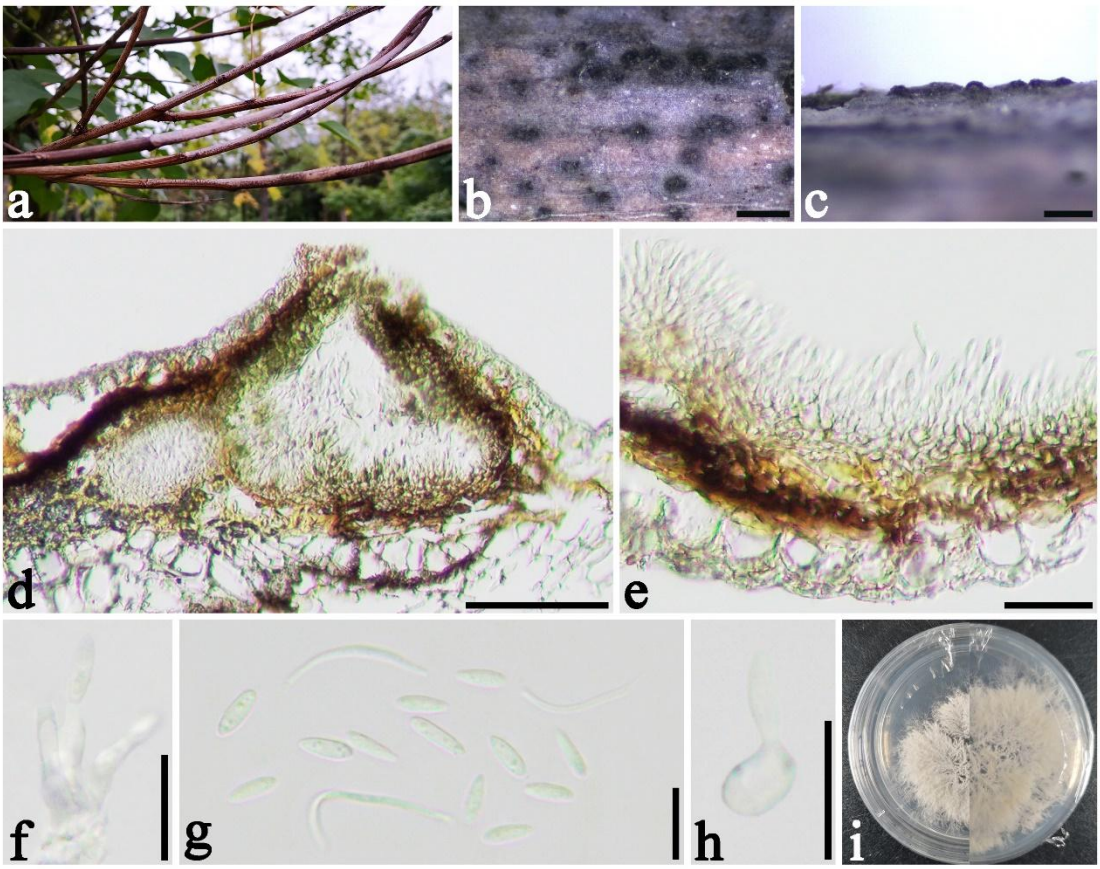

Figure 51 – *Diaporthe erythrinae* (holotype, SICAU 23-0138). a Symptoms on the twigs. b, c Appearance of conidiomata. d Cross-section of conidioma. e Conidiomatal wall. f Conidiogenous cells with developing alpha-conidia. g Conidia. h Germinating alpha-conidium. i Front and reverse view of colonies on PDA. Scale bars: b = 360 µm, c = 240 µm, d = 50 µm, e = 20 µm, f–h = 10 µm.

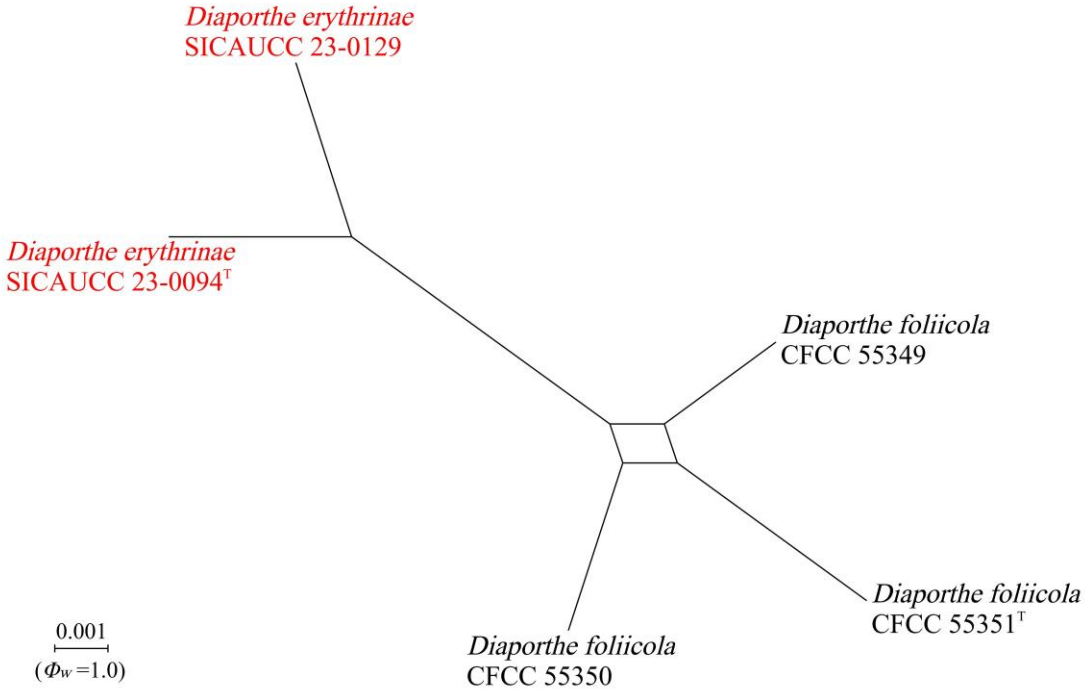

Figure 52 – The splits graph from the pairwise homoplasy index (PHI) test generated from the concatenated gene set of ITS, *tef*1-α, *tub*2, *cal*, and *his*3 sequence data of closely related species of

Diaporthe erythrinae using both LogDet transformation and splits decomposition. PHI test results $\Phi w \leq 0.05$ indicate that there is significant recombination within the dataset. The ex-type strains are denoted by "T" and the new isolates of this study are in red.

28. *Diaporthe middletonii* R.G. Shivas, L. Morin, S.M. Thomps. & Y.P. Tan, Persoonia 35: 45 (2015) Fig. 53

MycoBank number: MB808672; Facesoffungi number: FoF15883

Associated with shoot blight on branches of *Bougainvillea* sp. Sexual morph: Not observed. Asexual morph: *Coelomycetous*. *Conidiomata* 65–130 × 47–100 μm ($\bar{x}$ = 98 × 77 μm, n = 20), pycnidial, immersed to partly erumpent at maturity, brown to black, solitary, scattered, uni-loculate, ellipsoid or fusiform, ostiolate, glabrous. *Conidiomatal wall* 5–12 μm width, comprising of thick-walled, pale brown to brown cells of *textura angularis*, thickening at apical zone, 19–45 μm thick. *Conidiophores* reduced to conidiogenous cells, arising from the inner layer cells of the conidiomata. *Conidiogenous cells* 7–16 × 2–4 μm ($\bar{x}$ = 10.5 × 2.6 μm, n = 30), hyaline, enteroblastic, monophialidic, integrated, cylindrical to subcylindrical, tapered to the apices, straight or curved, with minute collarette, smooth-walled. *Alpha-conidia* 6–10 × 2.5–4 μm ($\bar{x}$ = 8.2 × 3.2 μm, n = 50), hyaline, fusiform, ellipsoid, subcylindrical, straight or slightly curved, aseptate, usually with two guttulates, thin-walled, smooth. *Beta-conidia* formed in PDA after 10 days, 25–33 × 0.5–1.5 μm ($\bar{x}$ = 29.4 × 1.1 μm, n = 30), flexuous, mostly J-shaped, hyaline, thin-walled, smooth.

Culture characteristics – Germinated alpha-conidia formed after 12 h. *Colonies* on PDA attaining 60–70 mm diameter in 4 days, fast-growing, circular, fimbriat, white, filamentous aerial mycelium superficially, reverse white.

Material examined – China, Sichuan Province, Chengdu City, Chongzhou City, Qimuhe Wetland Park, 103°37′54.92″E 30°36′15.71″N, 488 m, isol. from branches of *Bougainvillea* sp., 26 Jun. 2020, C.L. Yang, YCL202006009 (SICAU 23-0120), culture (SICAUCC 23-0111).

GenBank numbers – SICAUCC 23-0111 = ITS: PP736367, *tef1-α*: PP779572, *tub*2: PP782065, *cal*: PP836768, *his*3: PP782125

Notes – *Diaporthe middletonii* was initially documented in Australia, where it was found in the dead stem of *Rapistrum rugosum* and the living stem of *Chrysanthemoides monilifera* sub sp. *rotundata*. The morphological characteristics of our newly isolated strain, SICAUCC 23-0111, closely match the holotype of *D. middletonii* (Thompson et al. 2015). In our multi-gene phylogenetic analysis, SICAUCC 23-0111 clustered robustly with *D. middletonii* (BRIP 54884e, holotype), supported by complete bootstrap values (100% MLBS / 1.00 BYPP) within the *D. leucospermi* species complex (Fig. 50) (Dissanayake et al. 2024). The BLASTn searches of our strain (SICAUCC 23-0111) revealed sequence similarities of 100%, 99.71%, and 99.60% to *D. middletonii* (BRIP 54884e, holotype) in the ITS, *tef*1-α, and *tub*2 regions, respectively. Consequently, we identify the new collection as *D. middletonii*, marking its first documented occurrence on *Bougainvillea* sp.

29. *Diaporthe sojae* Lehman, Ann. Mo. bot. Gdn 10: 128 (1923) Fig. 54

MycoBank number: MB278338; Facesoffungi number: FoF06582

Associated with canker on leaves of *Phalaenopsis aphrodite* Rchb. F. Sexual morph: Not observed. Asexual morph: *Coelomycetous*. *Conidiomata* 300–378 μm ($\bar{x}$ = 344 μm, n = 10) diameter, immersed, pycnidial, conical, solitary, dark brown or black, multi-locules. *Conidiophores* 8–12 × 2–4 μm ($\bar{x}$ = 9.4 × 2.8 μm, n = 20), subcylindrical to cylindrical, hyaline, smooth, 1–3-celled. *Conidiogenous cells* phialidic, cylindrical, tapering towards the apex. *Alpha-conidia* 7–8.5 ×2–3 μm ($\bar{x}$ = 8 × 2.4 μm, n = 50) unicellular, ovoid, hyaline. *Beta-conidia* 16–23 ×1–2 μm ($\bar{x}$ = 19.2 × 1.8 μm, n = 50), hyaline, aseptate, filiform, bent, eguttulate, wider at the center and thinner towards the ends. *Conidia* and *ascomycospores* were observed on PDA medium. Sexual morph on PDA: *Ascomata* 150–210 μm diameter ($\bar{x}$ = 176.4 μm, n = 20), aggregated, immersed, globose to subglobose, dark brown, papillate. *Papillate* 800–1260 × 75–110 μm ($\bar{x}$ = 959.0 × 91.2 μm), conspicuous, long, unbranched seta, black, with pale yellow or brown apex. *Asci* 36–57 × 7–11 μm

($\bar{x}$ = 41.9 × 8.4 μm, n = 50), unitunicate, clavate, with refractive apical ring, 8-spored. *Ascospores* 9–12 × 3–4.5 μm ($\bar{x}$ = 10.4 × 3.8 μm, n = 50), randomly arranged, from tightly biseriate, hyaline, smooth, spheroidicity, medianly septate, always constricted at the septum, normally 4-guttulate, 2 in each cell, and the 2 central guttules, closer to the septum, are the largest. *Paraphyses* 10–12.5 μm ($\bar{x}$ = 11.9 μm, n = 10) width, colorless and transparent, segmented, always constricted at the septum. Asexual morph on PDA: *Beta-conidia* 15–30 ×1–2 μm ($\bar{x}$ = 21.0× 1.8 μm, n = 50), similar to above beta-conidia described on substrate. *Alpha-conidia* not observed.

Culture characteristics – *Colonies* on PDA moderately fast-growing, attaining a diameter of 45 mm after 10 days at 25ºC, aerial hypae often abundant, producing white mycelia with occasional greenish-yellow surface areas turning light brown with age, darkly pigmented long-necked pycnidia hairy (flask-shaped) were produced over the colony surface on PDA after about one month.

Material examined – China, Sichuan Province, Chengdu City, Wenjiang District, Gongping Street, 103°51′14.06″E 30°42′35.25″N, 537 m, isol. from leaves of *Phalaenopsis aphrodite*, 6 Nov. 2020, C.L. Yang, YCL202011004 (SICAU 23-0139), culture (SICAUCC 23-0107).

GenBank numbers – SICAUCC 23-0107 = ITS: PP736368, *tef1-α*: PP779573, *tub*2: PP782066, *cal*: PP836769, *his*3: PP782126

Notes – *Diaporthe sojae* has a wide host range and geographic distribution (Udayanga et al. 2015, Dissanayake et al. 2015, Norphanphoun et al. 2022). The sexual and asexual morphs of this species are described by Lehman (1923) and Udayanga et al. (2015). In the phylogenetic analysis of the concatenated alignment, our isolate (SICAUCC 23-0107) formed a cohesive cluster with *D. sojae*, supported by a robust 100% MLBS / 1.00 BYPP within the section Sojae (Fig. 50) (Dissanayake et al. 2024). Morphologically, the new collection exhibits characteristics closely resembling with *D. sojae*. A comparison of the ITS, *tef*1-α, *tub*2, *cal*, and *his*3 gene regions between SICAUCC 23-0107 and FAU635 revealed high sequence similarity, with similarity values of 99.64% (548/550 bp, 1 gap), 98.22% (332/338 bp, 2 gaps), 100% (440/440 bp, 0 gap), 100% (508/508 bp, 0 gap), and 99.79% (472/473 bp, 1 gap), respectively. Therefore, we identified our new collection as *D. sojae*, which is the first report on *Phalaenopsis aphrodite*.

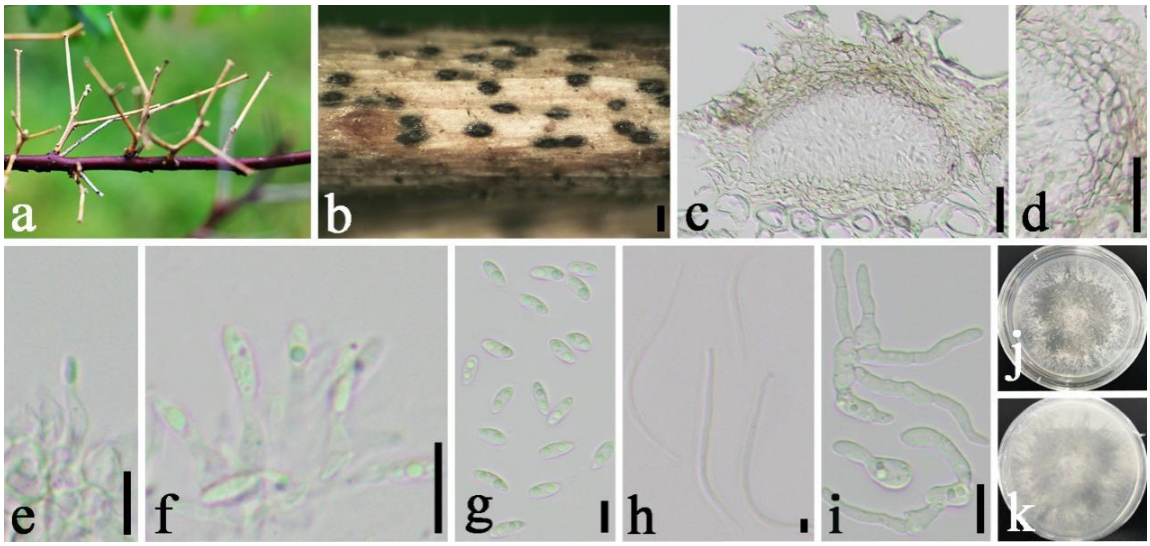

Figure 53 – *Diaporthe middletonii* (SICAU 23-0120). a Symptoms on the branches. b Appearance of conidiomata. c Cross-section of conidioma. d Conidiomatal wall. e–f Conidiogenous cells with developing alpha-conidia. g Alpha-conidia. h Beta-conidia. i Germinating alpha-conidia in sterilized water after 12 h. j Front view of colony on PDA. k Reverse view of colony on PDA. Scale bars: b = 200 μm, c–d = 20 μm, e–i = 10 μm.

Glomerellales Chadef. ex Réblová, W. Gams & Seifert

Notes – *Glomerellales* was first proposed by Chadefaud (1960), but was formally and validly published by Réblová et al. (2011). *Glomerellales* species are recognized by their darkly pigmented

ascomata, which can sometimes develop into sclerotia, multi-layered perithecial walls with periphysate ostioles, tapering paraphyses in the hamathecium, unitunicate asci with 8-spored, thin-walled ascospores featuring variable ascal apex thickness and lacking amyloid content, and ascospores that may be hyaline or pigmented, aseptate or multiseptate, alongside asexual forms displaying phialidic conidiogenesis (Réblová et al. 2011). *Glomerellales* comprises five families with about 700 species (Maharachchikumbura et al. 2016b, Tibpromma et al. 2018, Kuo et al. 2022, Wijayawardene et al. 2022, Species Fungorum 2024), which most species are associated with pathogens that affect a wide variety of plant species (Giraldo & Crous 2019, Pecchia et al. 2019, Talhinhas & Baroncelli 2021), and the stem age of *Glomerellales* dates back ~199 Mya (Hongsanan et al. 2017, Chen et al. 2023a).

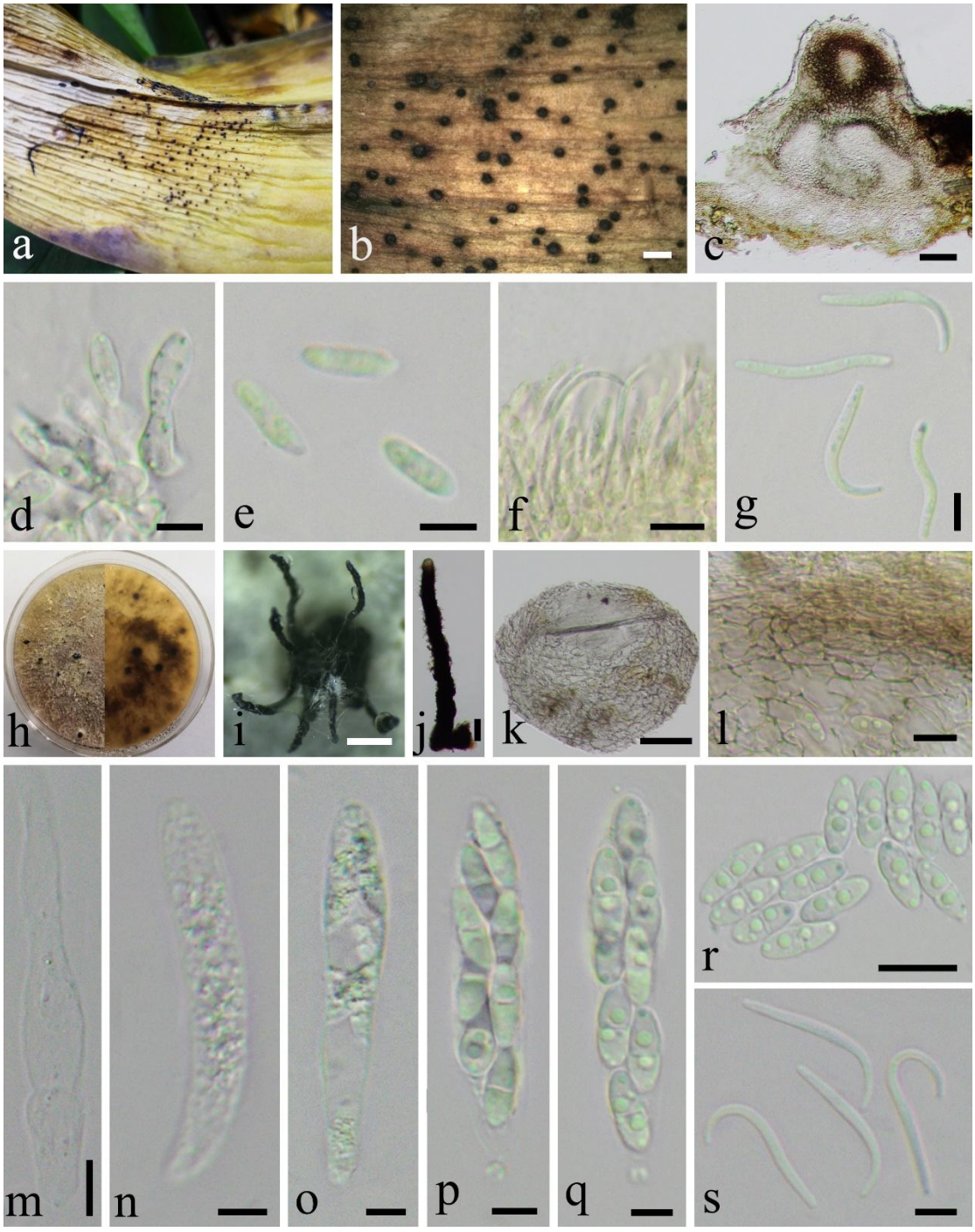

Figure 54 – *Diaporthe sojae* (SICAU 23-0139). a Symptoms on the leaf. b Appearance of conidiomata. c Cross-section of conidioma. d Conidiogenous cells with developing alpha-conidia. e

Alpha-conidia. f Conidiogenous cells with developing beta-conidia. g Beta-conidia. h Front and reverse view of colonies on PDA. i, j Papillate on PDA. k Ascoma. l Peridium. m Paraphyses. n-q Immature and mature unitunicate ascospores in asci. r Ascospores. s Beta-conidia on PDA. Scale bars: b = 1000 μm, c, k = 50 μm, d, e, g, l, r, s, = 5 μm, f, m–q = 10 μm, i = 500 μm, j = 100 μm.

Glomerellaceae Locq. ex Seifert & W. Gams

Notes – *Glomerellaceae*, exemplified by the genus *Colletotrichum* (= *Glomerella*), was initially proposed by Locquin (1984), but later validated by Zhang et al. (2006), and its phylogenetic position has been substantiated in a subsequent study by Maharachchikumbura et al. (2016). This family is monotypic and is characterized by both a *Colletotrichum* asexual morph and a *Glomerella* sexual morph (Réblová et al. 2011, Hyde et al. 2020c).

Colletotrichum Corda

Notes – *Colletotrichum* was introduced by Corda (1831) based on the species *C. lineola*. *Colletotrichum*, the exclusive genus in the *Glomerellaceae* family, encompasses a broad array of nutritional strategies and lifestyles, encompassing saprophytic, endophytic, and parasitic behaviors, affecting a wide range of hosts, including plants, soils, air, animals, and even humans (Cannon et al. 2012, Crouch et al. 2014, Ma et al. 2018, Viswanathan & Selvakumar 2020, Jayawardena et al. 2021a,b, Qiao et al. 2021, Talhinhas & Baroncelli 2021, Chen et al. 2022, Liu et al. 2022c, Tikami et al. 2023). This genus is among the world's top 10 crucial phytopathogen genera, with most species causing plant diseases like blight, wilt, dieback, rot, anthracnose, and spot on various plant parts, including seedling, stems, twigs, fruits, and leaves, in plants closely associated with humans (Warren & Nicholson 1975, Lees & Hilton 2003, Cai et al. 2009, Cannon et al. 2012, Crouch et al. 2014, Riolo et al. 2021). *Colletotrichum* currently encompasses 16 species complexes: the *C. acutatum* complex, *C. agaves* complex, *C. bambusicola* complex, *C. boninense* complex, *C. caudatum* complex, *C. dematium* complex, *C. destructivum* complex, *C. dracaenophilum* complex, *C. gigasporum* complex, *C. gloeosporioides* complex, *C. graminicola* complex, *C. magnum* complex, *C. orbiculare* complex, *C. orchidearum* complex, *C. spaethianum* complex, and *C. truncatum* complex, along with several additional singleton species (Bhunjun et al. 2021, Liu et al. 2022c). The estimated divergence times for these complexes span a range of 4.8 to 32.2 Mya (Bhunjun et al. 2021, Chen et al. 2022). In this study, there are four complexes associated, including *C. boninense* complex, *C. gloeosporioides* complex, *C. magnum* complex, and *C. orchidearum* complex.

30. ***Colletotrichum camelliae*** Massee, Bulletin of Miscellaneous Informations of the Royal Botanical Gardens Kew 1899: 91 (1899) Fig. 55

MycoBank number: MB176099; Facesoffungi number: FoF09388

Associated with anthracnose on leaves of *Camellia sinensis* (Linn.) O. Kuntze. Sexual morph: Not observed. Asexual morph: *Coelomycetous*. *Conidiomata* gregarious, immersed, globose to subglobose, dark brown to black. *Conidiogenous cells* 7.5–16 × 2–5 μm ($\bar{x}$ = 14 × 3.7 μm, n = 20), cylindrical, straight, colorless, and smooth. *Conidia* 13–18 × 4–6 μm ($\bar{x}$ = 16 × 5 μm, n = 50), cylindrical, straight or slightly curved, with both ends rounded, hyaline, smooth-walled.

Culture characteristics – *Colonies* on PDA fast-growing, reaching 8 cm in 5 days at 25°C, under 12 h light/12 h dark, circular, with even margin, floccose, white at beginning, then greyish white, reverse light olivatious.

Material examined – China, Sichuan Province, Liangshan Prefecture, Leibo County, Xilin Village, 103°34′0.12″E 28°29′29.90″N, 834 m, isol. from leaves of *Camellia sinensis*, 4 Jun. 2021, Xiaoying A-Niu, ANXY202106001 (SICAU 23-0110), culture (SICAUCC 23-0088).

GenBank numbers – SICAUCC 23-0088 = ITS: PP133651, *gapdh*: PP601242, *tub*2: PP601246, *act*: PP601245, *his*3: PP601244, *chs*-1: PP601243

Notes – *Colletotrichum camelliae* was described by Massee (1989). The strain SICAUCC 23-0088 clustered with the ex-type strain (CGMCC 3.14925) with 95% MLBS and 0.99 BYPP

bootstrap support (Fig. 56). Nucleotide comparisons of ITS, *gapdh*, *chs*-1, *his*3, *act*, and *tub*2 (SICAUCC 23-0088) showed high homology with the sequences of *C. camelliae* (CGMCC 3.14925), similarities are 100% (514/515, 0 gap), 100% (253/253, 0 gap), 100% (273/273, 0 gap), 100% (363/363, 0 gap), 100% (245/245, 0 gap), and 100% (720/720, 0 gap), respectively.

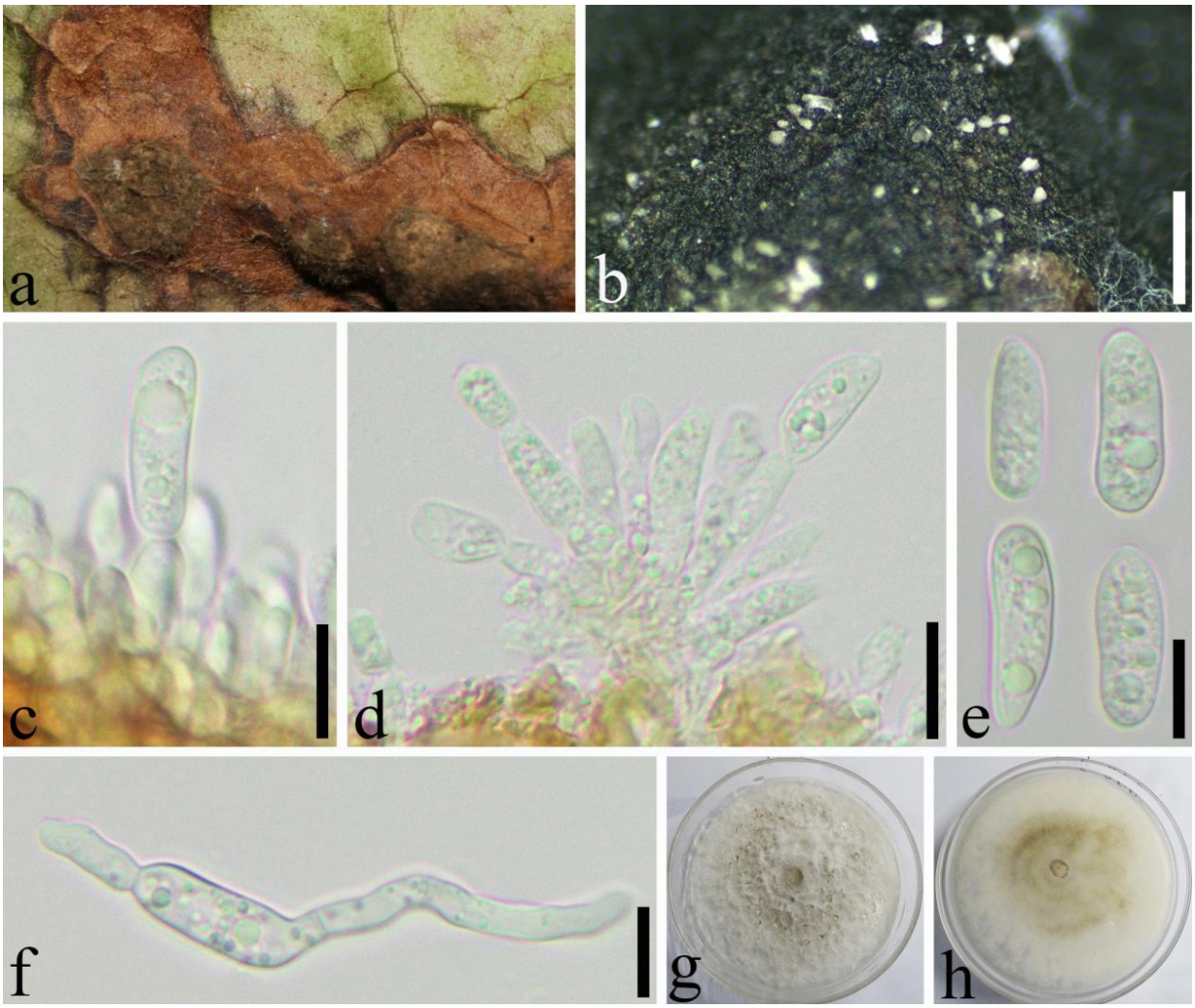

Figure 55 – *Colletotrichum camelliae* (SICAU 23-0110). a, b Appearance of conidiomata on the leaf. c, d Conidiogenous cell with developing conidia. e Conidia. f Germinating conidium. g Front view of colony on PDA. h Reverse view of colony on PDA. Scale bars: b = 500 μm, c–f = 10 μm.

31. *Colletotrichum cymbidiicola* Damm et al., Stud. Mycol. 73: 19 (2012) Fig. 57

MycoBank number: MB560740; Facesoffungi number: FoF15258

Associated with brown spots on leaves of *Cymbidium sichuanicum* Z. J. Liu & S. C. Chen. Sexual morph: See Damm et al. (2012). Asexual morph: *Coelomycetous*. *Conidiomata* 185–445 × 95–215 μm ($\bar{x}$ = 284 × 150 μm, n = 50), acervulus, blister-like, brown to dark brown, globose to subglobose, or irregular shape, submerged, solitary, gregarious, conidiophores formed on a cushion of pale brown to brown cells. *Setae* not observed. *Conidiophores* hyaline to pale brown, mostly septate, branched, developed 1–3 conidiogenous cells at apex. *Conidiogenous cells* 10–26 × 3–7 μm ($\bar{x}$ = 17.5 × 4.9 μm, n = 20), hyaline to pale brown, smooth-walled, monophialidic, cylindrical or sometimes conoid, opening 1–2 μm diameter, collarette missing. *Conidia* 9–24 × 5.5–8 μm ($\bar{x}$ = 17.5 × 6.7 μm, n = 50), hyaline, aseptate, smooth-walled, frequently cylindrical, sometimes ellipsoid or allantoid, obtusely rounded apex, guttulate. *Appressoria* 9–13 × 7–10 μm ($\bar{x}$ = 10.7 × 7.9 μm, n = 20), single, medium to dark brown, smooth-walled, navicular, elliptical, or irregular in outline, with an undulate or entire margin.

Culture characteristics – *Colonies* on PDA attaining 55–65 mm diameter in 2 weeks, aerial mycelia grey to pale brown in center, white towards the margins, reverse brown to dull brown. *Conidiomata* and *Chlamydospores* not observed.

Material examined – China, Sichuan Province, Chengdu City, Qionglai City, Pingle Ancient Town, Guandi Village, 103°19′18.38″E 30°21′11.26″N, 507 m, isol. from leaves of *Cymbidium sichuanicum*, 9 Nov. 2020, C.L. Yang, YCL202011006 (SICAU 23-0110), culture (SICAUCC 23-0091).

GenBank numbers – SICAUCC 23-0091 = ITS: PP133653, *gapdh*: PP965565, *tub*2: PP965568, *act*: PP965567, *his*3: PP965566

Notes – The sexual and asexual morphs of *Colletotrichum cymbidiicola* were reported by Damm et al. (2012). Morphologically, our observations were identical to the sexual descriptions provided by Damm et al. (2012). The strain SICAUCC 23-0091 clustered with the *C. cymbidiicola* complex (including ex-type strain IMI 347923) with 99% MLBS and 1.00 BYPP bootstrap support (Fig. 58). Nucleotide comparisons of ITS, *gapdh*, *his*3, *act*, and *tub*2 (SICAUCC 23-0091) showed high homology with the sequences of *C. cymbidiicola* (IMI 347923, ex-type), similarities are 100% (554/554, 0 gap), 100% (247/247, 0 gap), 100% (389/389, 0 gap), 100% (275/275, 0 gap), and 100% (497/497, 0 gap), respectively.

32. *Colletotrichum cymbidiumdis* C.L. Yang & Q. Zeng, sp. nov. Fig. 59

MycoBank number: MB902328; FacesofFungi number: FoF16262

Etymology – Refers to the host genus *Cymbidium*.

Holotype – SICAU 23-0111

Associated with brown spots on leaves of *Cymbidium hybrid* (Hybrid orchid, *C. faberi* Rolfe × *C. hookerianum* Rchb.f. × *C. serratum* Schltr.). Sexual morph: Not observed. Asexual morph: *Coelomycetous*. *Conidiomata* 110–220 × 68–110 μm ($\bar{x}$ = 144.6 × 91.6 μm, n = 30), blister-like, pale brown to dull brown, globose to ellipsoid, submerged, solitary, gregarious, conidiophores formed on a cushion of hyaline to pale brown cells. *Setae* not observed. *Conidiophores* hyaline to pale brown, septate, occasionally branched. *Conidiogenous cells* 10–35 × 2–8 μm ($\bar{x}$ = 21.4 × 5.1 μm, n = 30), hyaline or sometimes pale brown, smooth-walled, phialidic, cylindrical or ampulliform, usually 1-septate. *Conidia* 11.5–24 × 4–6 μm ($\bar{x}$ = 18.8 × 5.1 μm, n = 50), hyaline, aseptate, smooth-walled, allantoid, cylindrical, ellipsoid or irregular shape, obtusely rounded apex, guttulate. *Appressoria* 8–15 × 6.5–9.5 μm ($\bar{x}$ = 10.7 × 8.8 μm, n = 20), formed from conidia germination, single, pale brown to brown, aseptate, mostly globose to subglobose, rounded in margin.

Culture characteristics – *Colonies* on PDA attaining 55–65 mm diameter in 1 week, aerial mycelia white to pale brown, reverse brown to dull brown, pale yellow to white towards the margins. *Conidiomata*, conidiophores and setae formed directly on hyphae. *Setae* 36–110 × 1–5 μm ($\bar{x}$ = 79.1 × 3.9 μm, n = 30), pale brown to dull brown, more or less light in color towards the apex, smooth-walled, shorter in diameter towards the apex, cylindrical, straight or flexuous, base sometimes inflated to conical, 1–5(–7)-septate. *Conidiophores* hyaline to pale brown, smooth-walled, septate, branched. *Conidiogenous cells* 8–76(–106) × 3–6 μm ($\bar{x}$ = 31.8 × 4.2 μm, n = 50), hyaline to pale brown, smooth-walled, cylindrical to clavate, or ampuliform, or irregular shape, straight or flexuous, opening 0.5–2 μm diameter, collarette 0.5–2 μm long. *Conidia* 12–20 × 3.5–6 μm ($\bar{x}$ = 16.4 × 4.9 μm n = 50), hyaline, smooth-walled, aseptate, mainly straight, allantoid, cylindrical or ellipsoidal, rounded at both ends. *Chlamydospores* 9.5–26 × 3–8 μm ($\bar{x}$ = 16.7 × 4.7 μm, n = 30), sparse, subglobose to globose, or irregular shape, pale brown to brown, formed between hyphae.

Material examined – China, Sichuan Province, Chengdu City, Wenjiang District, Kejin Road, No. 355, 103°51′14.25″E 30°42′35.68″N, 516 m, isol. from leaves of *Cymbidium hybrid*, 6 Jul. 2020, C.L. Yang, YCL202007001 (SICAU 23-0111, holotype), ex-type culture (SICAUCC 23-0089). *ibid.* YCL202007001-2 (SICAU 23-0164), living culture SICAUCC 23-0127.

GenBank numbers – SICAUCC 23-0089 = ITS: PP133655, *gapdh*: PP965569, *chs*-1: PP965570, *his*3: PP965571, *act*: PP965572, *tub*2: PP965573. SICAUCC 23-0127 = ITS: PP732532, *gapdh*: PQ014232, *chs*-1: PP836774, *his*3: PP782131, *act*: PP782117, *tub*2: PP782078

Notes – In the multigene phylogenetic tree, our new species *Colletotrichum cymbidiumdis* forms a lineage with sister to *C. guangdongense* (Fig. 60). *Colletotrichum cymbidiumdis* differs from *C. guangdongense* (ZHKUCC 21-0105, holotype) in having shorter setae (36–110 μm, 2–4-septate vs. 60–136 μm, 1–5(–7)-septate) and conidia of a different shape (12–20 × 3.5–6 μm, allantoid, cylindrical, or ellipsoidal, as opposed to 7–12 × 5–10 μm, cylindrical). The sequence comparisons show 99.65% (562/564, 0 gap), 98.24% (223/227, 0 gap), 97.92% (283/289, 0 gap), 99.20% (371/374, 0 gap), 99.60% (252/253, 0 gap), and 99.37% (470/473, 0 gap) similarities in the ITS, *gapdh*, *chs*-1, *his*3, *act*, and *tub*2, respectively, between *C. cymbidiumdis* and the type strain of *C. guangdongense* (ZHKUCC 21-0105). The PHI test results indicate the absence of significant recombination events between *C. cymbidiumdis* and *C. guangdongense* (Fig. 61), suggesting that they are not conspecific. The morphological characteristics and molecular phylogenies support the establishment of a new species.

33. *Colletotrichum gloeosporioides* (Penz.) Penz. & Sacc., Atti Inst. Veneto Sci. lett., ed Arti, Sér. 6 2(5): 670 (1884) Fig. 62

≡*Vermicularia gloeosporioides* Penz., Michelia 2(no. 8): 450 (1882)

MycoBank number: MB158410; Facesoffungi number: FoF09424

Associated with anthracnose on stems and branches of *Citrus reticulata* Blanco (Orah mandarin). Sexual morph: Not observed. Asexual morph: *Coelomycetous*. *Conidiomata* 173–352 μm long × 129–306 μm width × 56–128 μm high ($\bar{x}$ = 273 × 198 × 91 μm, n = 30), gregarious, immersed, subglobose, dark brown to black. *Conidiogenous cells* septated, branched, cylindrical, straight, colorless, and smooth. *Conidia*15–18 × 5.5–6.5 μm ($\bar{x}$ = 17 × 6 μm, n = 50), cylindrical, straight, aseptate, rounded at both ends, hyaline, smooth-walled. *Appressoria* 8–11 × 6–7 μm ($\bar{x}$ = 9.4 × 6.7 μm, n = 20), single, medium to dark brown, smooth-walled, navicular, irregular in outline, with an undulate or entire margin.

Culture characteristics – *Colonies* on PDA fast-growing, reaching 6 cm in 5 days at 25°C, under 12 h light/12 h dark, circular, with even margin, white towards the margins, reverse brown. *Conidiomata* and *Chlamydospores* observed.

Material examined – China, Sichuan Province, Mianyang City, Zitong County, 105°9′59″E 31°37′49″N, 440 m, 20 Oct. 2021, isol. from stems and branches of *Citrus reticulata*, W.G. Cai, CWG202110002 (SICAU 23-0109), culture (SICAUCC 23-0087).

GenBank numbers – SICAUCC 23-0087 = ITS: PP133650, *gapdh*: PP957828, *chs*-1: PP957829, *his*3: PP957830, *act*: PP957831, *tub*2: PP957832

Notes – *Colletotrichum gloeosporioides* was first identified by Saccardo (1884). Our collections are identical to the descriptions of *C. gloeosporioides* provided by Cannon et al. (2008). Nucleotide comparisons of ITS, *gapdh*, *chs*-1, *his*3, *act*, and *tub*2 (SICAUCC 23-0087) showed high homology with the sequences of *C. gloeosporioides* (IMI 356878, ex-type), similarities are 100% (573/573, 0 gap), 99.6% (265/266, 0 gap), 100% (291/291, 0 gap), 99.5% (379/381, 0 gap), 100% (281/281, 0 gap), and 100% (701/701, 0 gap), respectively.

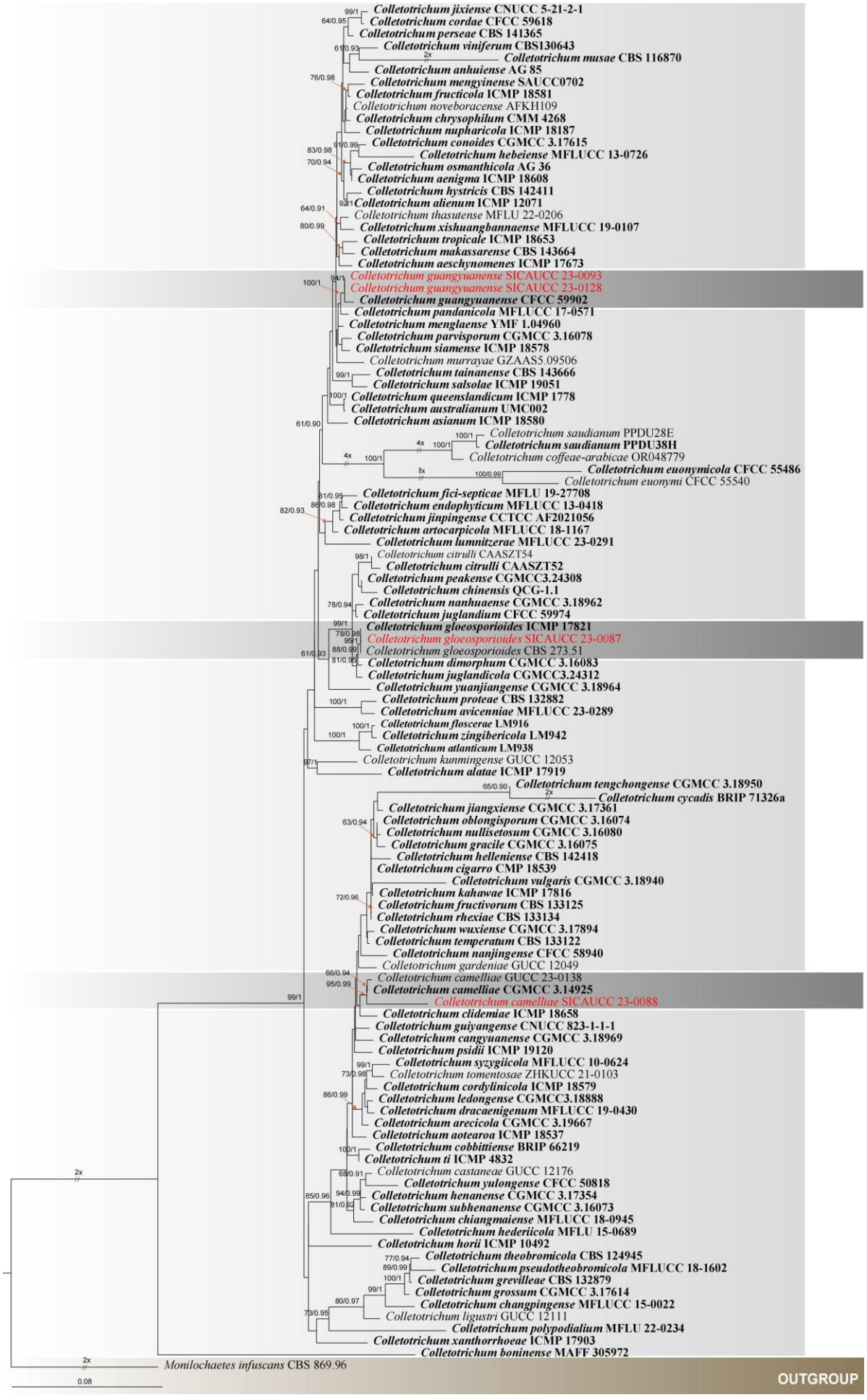
Colletotrichum jixiense CNUCC 5-21-2-1
Colletotrichum cordae CFCC 59618
Colletotrichum perseae CBS 141365
Colletotrichum viniferum CBS130643
Colletotrichum musae CBS 116870
Colletotrichum anhuiense AG 85
Colletotrichum mengyinense SAUCC0702
Colletotrichum fructicola ICMP 18581
Colletotrichum noveboracense AFKH109
Colletotrichum chrysophilum CMM 4268
Colletotrichum nupharicola ICMP 18187
Colletotrichum conoides CGMCC 3.17615
Colletotrichum hebeiense MFLUCC 13-0726
Colletotrichum osmanthicola AG 36
Colletotrichum aenigma ICMP 18608
Colletotrichum hystricis CBS 142411
Colletotrichum alienum ICMP 12071
Colletotrichum thasutense MFLU 22-0206
Colletotrichum xishuangbannaense MFLUCC 19-0107
Colletotrichum tropicale ICMP 18653
Colletotrichum makassarense CBS 143664
Colletotrichum aeschynomenes ICMP 17673
Colletotrichum guangyuanense SICAUCC 23-0093
Colletotrichum guangyuanense SICAUCC 23-0128
Colletotrichum guangyuanense CFCC 59902
Colletotrichum pandanicola MFLUCC 17-0571
Colletotrichum menglaense YMF 1.04960
Colletotrichum parvisporum CGMCC 3.16078
Colletotrichum siamense ICMP 18578
Colletotrichum murrayae GZAAS5.09506
Colletotrichum tainanense CBS 143666
Colletotrichum salsolae ICMP 19051
Colletotrichum queenslandicum ICMP 1778
Colletotrichum australianum UMC002
Colletotrichum asianum ICMP 18580
Colletotrichum saudianum PPDU28E
Colletotrichum saudianum PPDU38H
Colletotrichum coffeae-arabicae OR048779
Colletotrichum euonymicola CFCC 55486
Colletotrichum euonymi CFCC 55540
Colletotrichum fici-septicae MFLU 19-27708
Colletotrichum endophyticum MFLUCC 13-0418
Colletotrichum jinpingense CCTCC AF2021056
Colletotrichum artocarpicola MFLUCC 18-1167
Colletotrichum lumnitzerae MFLUCC 23-0291
Colletotrichum citrulli CAASZT54
Colletotrichum citrulli CAASZT52
Colletotrichum peakense CGMCC3.24308
Colletotrichum chinensis QCG-1.1
Colletotrichum nanhuaense CGMCC 3.18962
Colletotrichum juglandium CFCC 59974
Colletotrichum gloeosporioides ICMP 17821
Colletotrichum gloeosporioides SICAUCC 23-0087
Colletotrichum gloeosporioides CBS 273.51
Colletotrichum dimorphum CGMCC 3.16083
Colletotrichum juglandicola CGMCC3.24312
Colletotrichum yuanjiangense CGMCC 3.18964
Colletotrichum proteae CBS 132882
Colletotrichum avicenniae MFLUCC 23-0289
Colletotrichum floscerae LM916
Colletotrichum zingibericola LM942
Colletotrichum atlanticum LM938
Colletotrichum kunmingense GUCC 12053
Colletotrichum alatae ICMP 17919
Colletotrichum tengchongense CGMCC 3.18950
Colletotrichum cycadis BRIP 71326a
Colletotrichum jiangxiense CGMCC 3.17361
Colletotrichum oblongisporum CGMCC 3.16074
Colletotrichum nullisetosum CGMCC 3.16080
Colletotrichum gracile CGMCC 3.16075
Colletotrichum helleniense CBS 142418
Colletotrichum cigarro CMP 18539
Colletotrichum vulgaris CGMCC 3.18940
Colletotrichum kahawae ICMP 17816
Colletotrichum fructivorum CBS 133125
Colletotrichum rhexiae CBS 133134
Colletotrichum wuxiense CGMCC 3.17894
Colletotrichum temperatum CBS 133122
Colletotrichum nanjingense CFCC 58940
Colletotrichum gardeniae GUCC 12049
Colletotrichum camelliae GUCC 23-0138
Colletotrichum camelliae CGMCC 3.14925
Colletotrichum camelliae SICAUCC 23-0088
Colletotrichum clidemiae ICMP 18658
Colletotrichum guiyangense CNUCC 823-1-1-1
Colletotrichum cangyuanense CGMCC 3.18969
Colletotrichum psidii ICMP 19120
Colletotrichum syzygiicola MFLUCC 10-0624
Colletotrichum tomentosae ZHKUCC 21-0103
Colletotrichum cordylinicola ICMP 18579
Colletotrichum ledongense CGMCC3.18888
Colletotrichum dracaenigenum MFLUCC 19-0430
Colletotrichum arecicola CGMCC 3.19667
Colletotrichum aotearoa ICMP 18537
Colletotrichum cobbittiense BRIP 66219
Colletotrichum ti ICMP 4832
Colletotrichum castaneae GUCC 12176
Colletotrichum yulongense CFCC 50818
Colletotrichum henanense CGMCC 3.17354
Colletotrichum subhenanense CGMCC 3.16073
Colletotrichum chiangmaiense MFLUCC 18-0945
Colletotrichum hederiicola MFLU 15-0689
Colletotrichum horii ICMP 10492
Colletotrichum theobromicola CBS 124945
Colletotrichum pseudotheobromicola MFLUCC 18-1602
Colletotrichum grevilleae CBS 132879
Colletotrichum grossum CGMCC 3.17614
Colletotrichum changpingense MFLUCC 15-0022
Colletotrichum ligustri GUCC 12111
Colletotrichum polypodialium MFLU 22-0234
Colletotrichum xanthorrhoeae ICMP 17903
Colletotrichum boninense MAFF 305972
Monilochaetes infuscans CBS 869.96
OUTGROUP
0.08

Figure 56 – Phylogram derived from maximum likelihood analyses of a combined dataset comprising ITS, *gapdh*, *chs*-1, *act*, and *tub*2 sequence dataset, representing the species of *C. gloeosporioides* species complex. One hundred and thirteen strains were included in the combined analyses, which comprised 2,529 characters (ITS: 1–736, *gapdh*: 737–1,816, *chs*-1: 1,817–2,279, *act*: 2,280–2,603, *tub*2: 2,604–4,419) after alignment. The best scoring RAxML tree with a final likelihood value of -24,606.624592 is presented. The matrix had 1,816 distinct alignment patterns, with 57.13% of undetermined characters or gaps. Estimated base frequencies were as follows: A = 0.228634, C = 0.299726, G = 0.242512, T = 0.229128; substitution rates AC = 0.865135, AG = 2.436704, AT = 1.085508, CG = 0.863104, CT = 3.184305, GT = 1.000000. Bootstrap support values for ML equal to or greater than 60%, and BYPP equal to or greater than 0.90 are indicated at the nodes as MLBS / BYPP. *Monilochaetes infuscans* (CBS 869.96) was used as the outgroup taxa. The ex-type strains are in bold, and the new isolates in this study are in red.

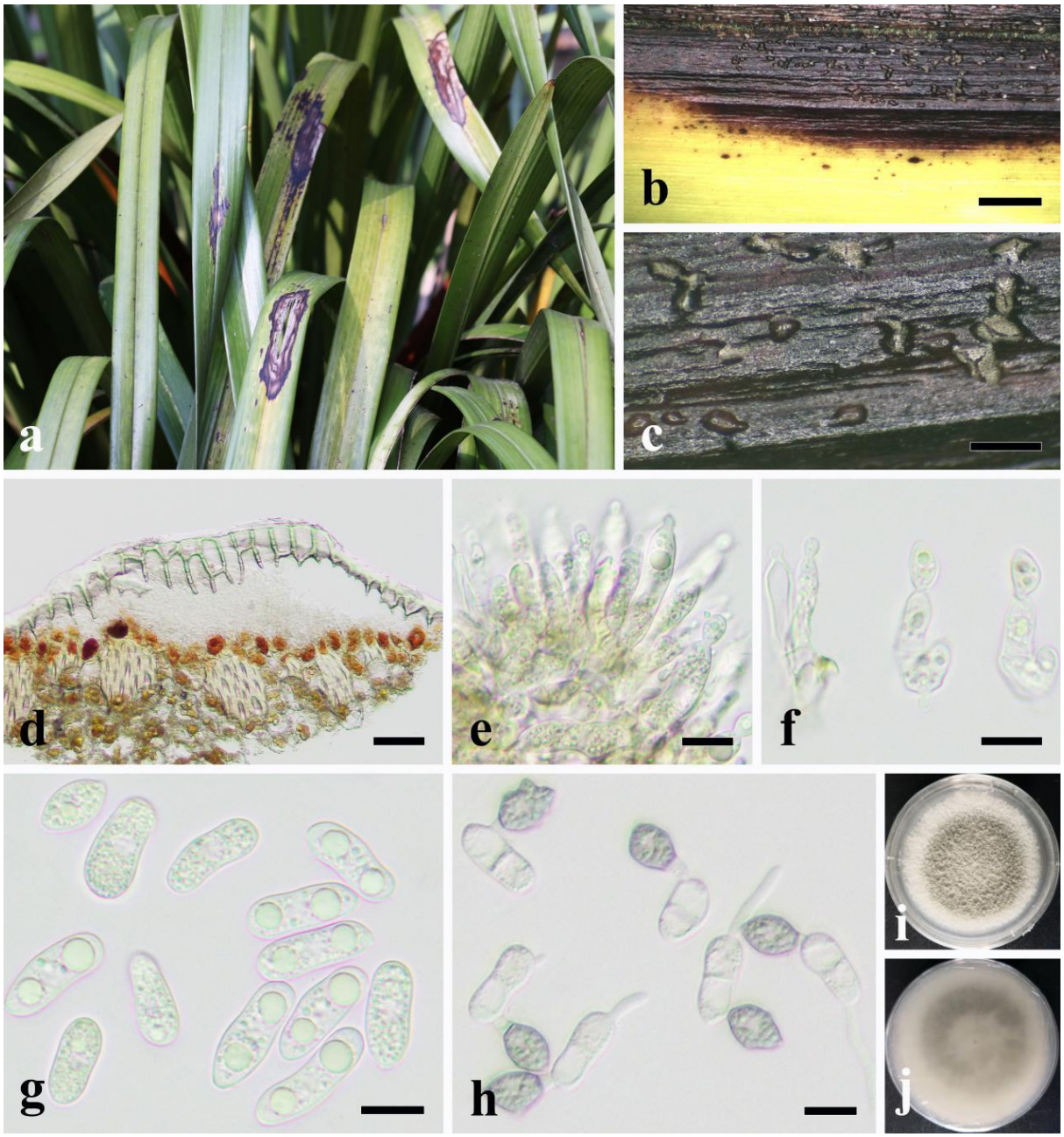

Figure 57 – *Colletotrichum cymbidiicola* (SICAU 23-0110). a Symptoms on the leaves. b, c Appearance of conidiomata. d Cross-section of conidioma. e, f Conidiogenous cells with developing conidia. g Conidia. h Germinating conidia with appressoria. i Front view of colony on

PDA. j Reverse view of colony on PDA. Scale bars: b = 2 mm, c = 500 µm, d = 50 µm, e–h = 10 µm.

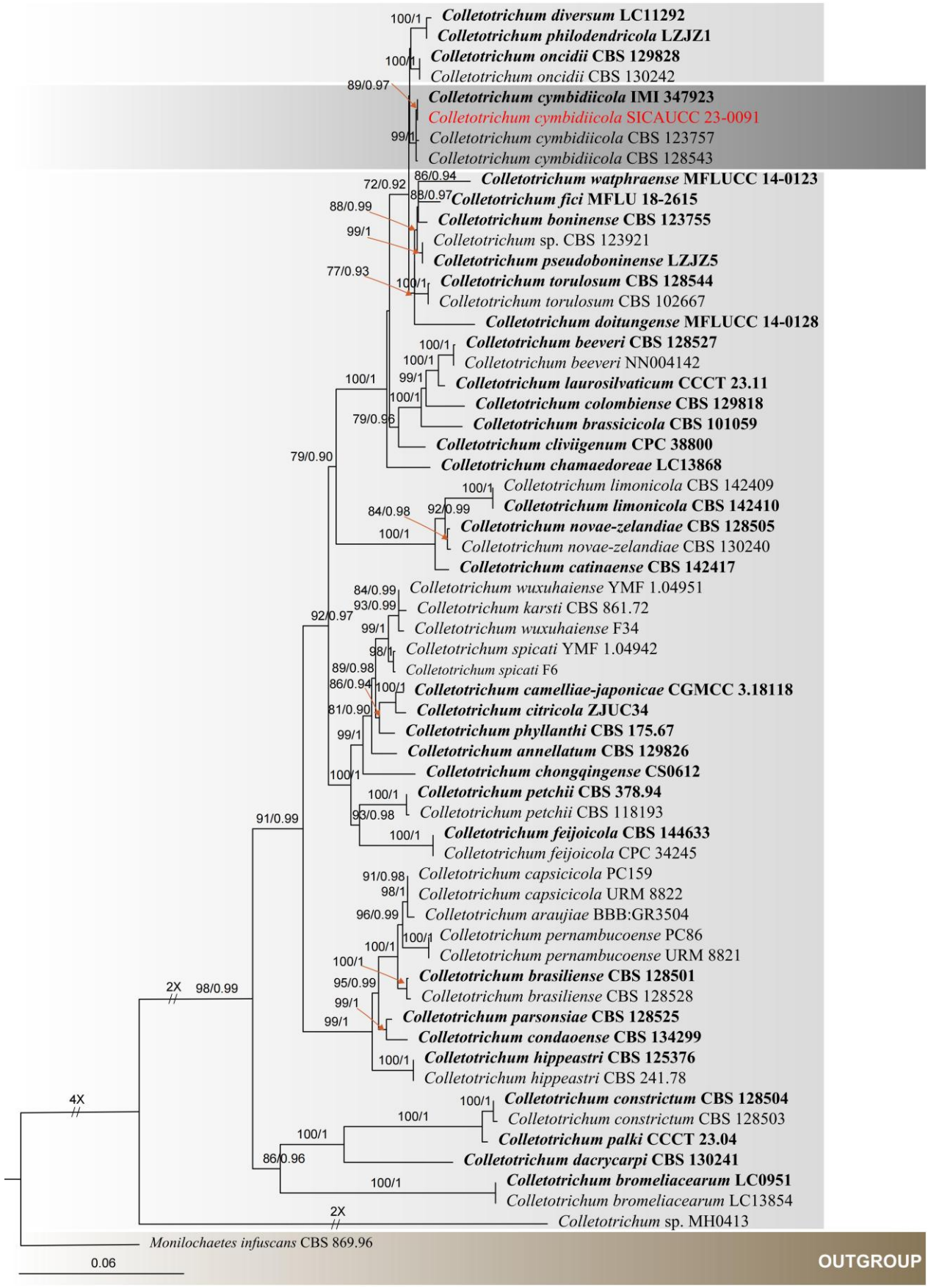

Figure 58 – Phylogram derived from maximum likelihood analyses of a combined dataset comprising ITS, *gapdh*, *chs*-1, *his*3, *act*, and *tub*2 sequence dataset, representing the species of *C. boninense* species complex. Sixty-one strains were included in the combined analyses, which comprised 2,801 characters (ITS: 1–656, *gapdh*: 657–979, *chs*-1: 980–1,283, *his*3: 1,284–1,708, *act*: 1,709–2,015, *tub*2: 2,016–2,814) after alignment. The best scoring RAxML tree with a final likelihood value of -13,822.918694 is presented. The matrix had 1,139 distinct alignment patterns, with 25.95% of undetermined characters or gaps. Estimated base frequencies were as follows: A =0.222730, C = 0.311908, G = 0.245630, T = 0.219732; substitution rates AC = 1.215377, AG = 2.751073, AT = 1.085617, CG = 0.891312, CT = 5.042882, GT = 1.000000. Bootstrap support values for ML equal to or greater than 70%, and BYPP equal to or greater than 0.90 are indicated at the nodes as MLBS / BYPP. *Monilochaetes infuscans* (CBS 869.96) was used as the outgroup taxa. The ex-type strains are in bold, and the new isolates in this study are in red.

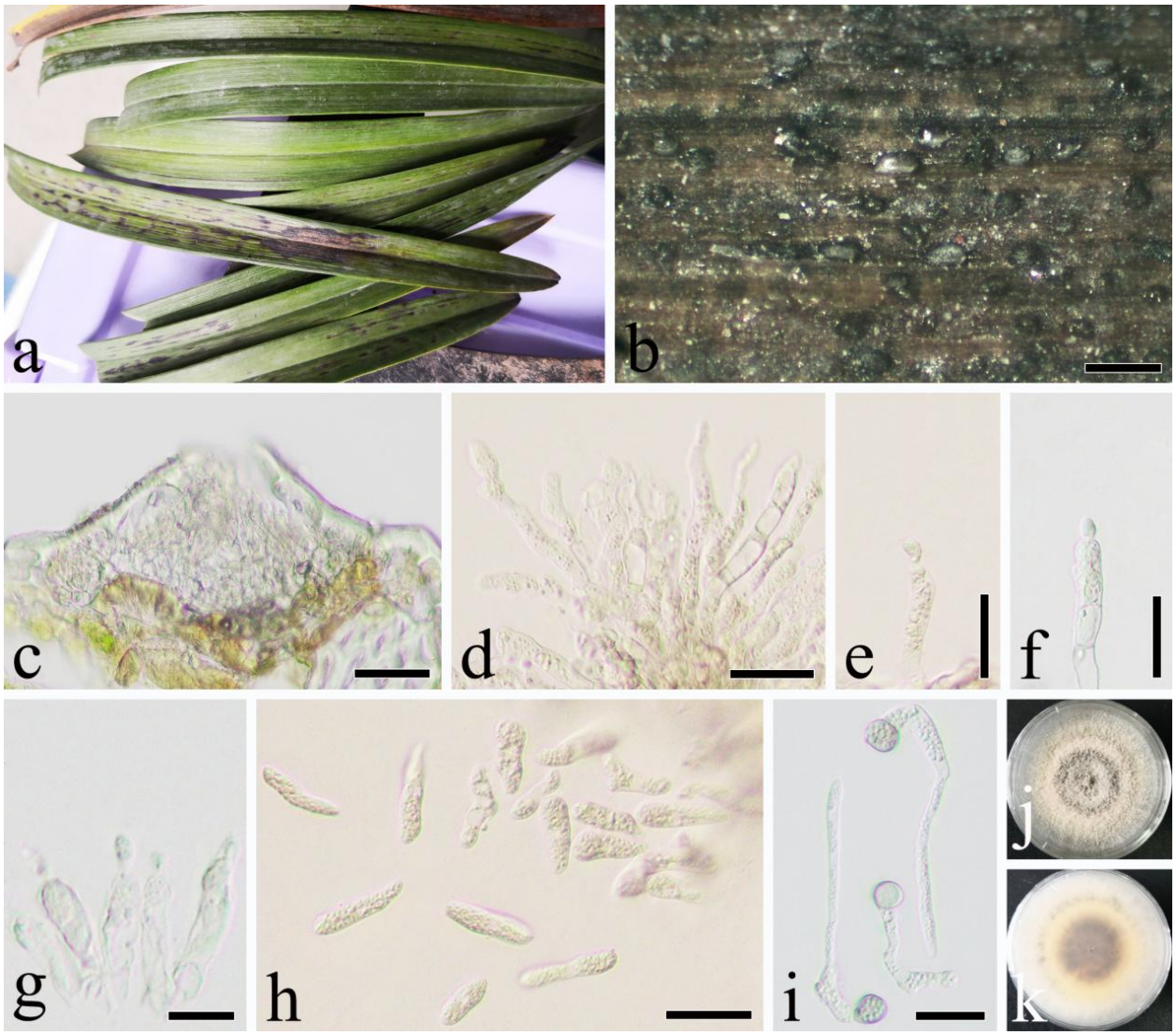

Figure 59 – *Colletotrichum cymbidiumdis* (holotype, SICAU 23-0111). a Symptoms on the leaves. b Appearance of conidiomata. c Cross-section of conidioma. d–g Conidiogenous cells with developing conidia. h Conidia. i Germinating conidia with appressoria. j Front view of colony on PDA. k Reverse view of colony on PDA. Scale bars: b = 300 µm, c = 30 µm, d–f, h, i = 20 µm, g = 10 µm.

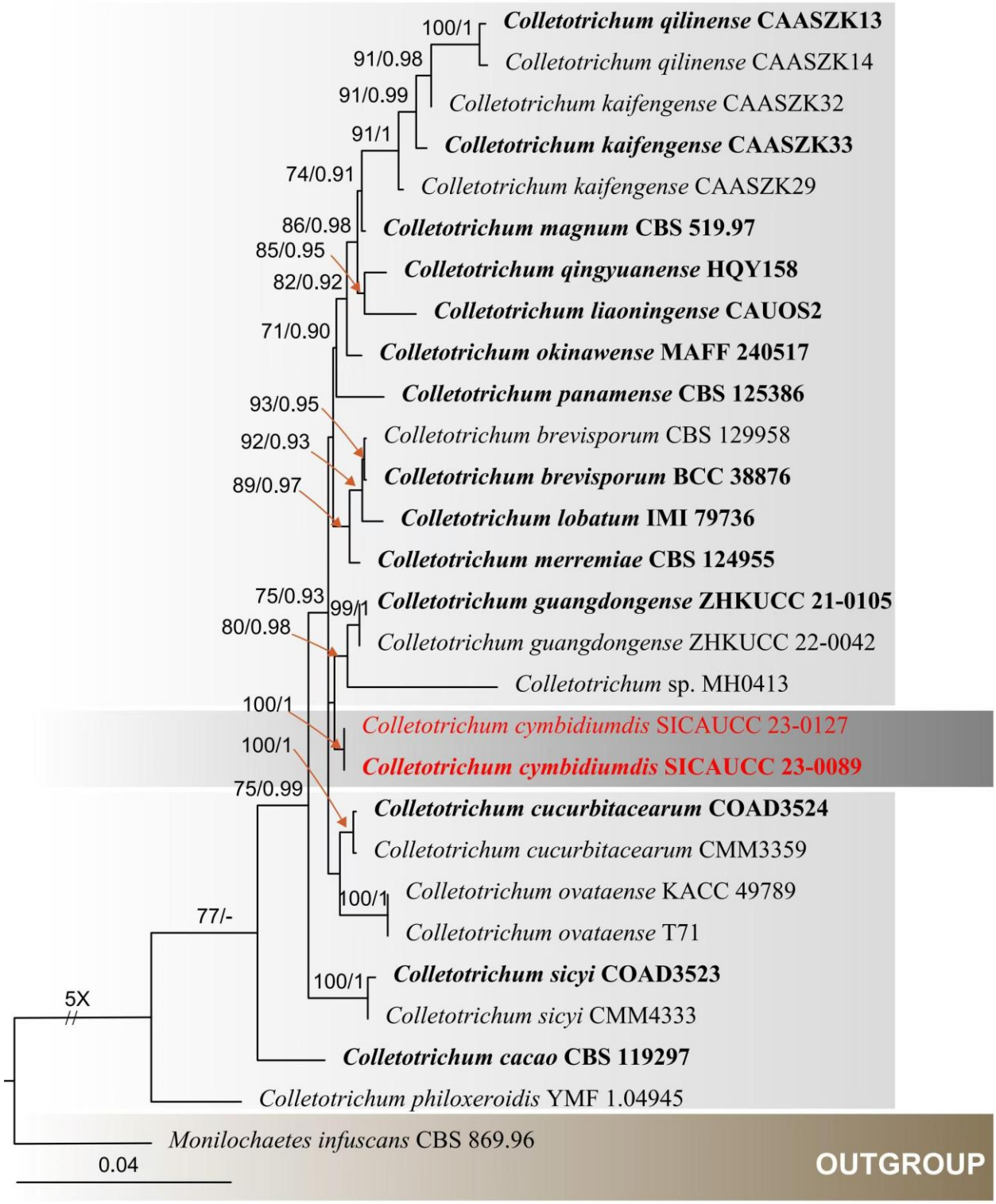

Figure 60 – Phylogram derived from maximum likelihood analyses of a combined dataset comprising ITS, *gapdh*, *chs*-1, *his*3, *act*, and *tub*2 sequence dataset, representing the species of *Colletotrichum magnum* species complex. Twenty-eight strains were included in the combined analyses, which comprised 2,660 characters (ITS: 1–624, *gapdh*: 625–892, *chs*-1: 893–1,195, *his*3: 1,196– 1,610, *act*: 1,611–1,897, *tub*2: 1,898–2,660) after alignment. The best scoring RAxML tree with a final likelihood value of -8,720.346189 is presented. The matrix had 764 distinct alignment patterns, with 26.13% of undetermined characters or gaps. Estimated base frequencies were as follows: A = 0.220661, C = 0.310130, G = 0.252490, T = 0.216719; substitution rates AC = 1.037350, AG = 2.116977, AT = 1.044432, CG = 1.022237, CT = 4.304523, GT = 1.000000. Bootstrap support values for ML equal to or greater than 70%, and BYPP equal to or greater than

0.90 are indicated at the nodes as MLBS / BYPP. *Monilochaetes infuscans* (CBS 869.96) was used as the outgroup taxa. The ex-type strains are in bold, and the new isolates in this study are in red.

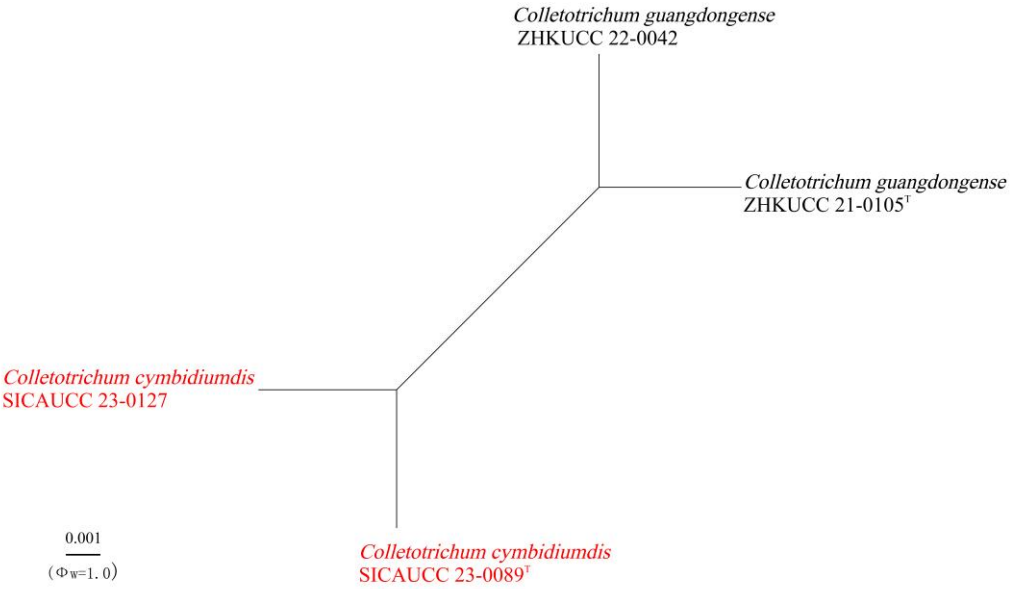

Figure 61 – The splits graph from the pairwise homoplasy index (PHI) test generated from the concatenated gene set of ITS, *gapdh*, *chs*-1, *his*3, *act*, and *tub*2 sequence data of closely related species of *Colletotrichum* using both LogDet transformation and splits decomposition. PHI test results (Φw) < 0.05 indicate significant recombination within the dataset. The ex-type strains are denoted by "T" and the new isolates of this study are in red.

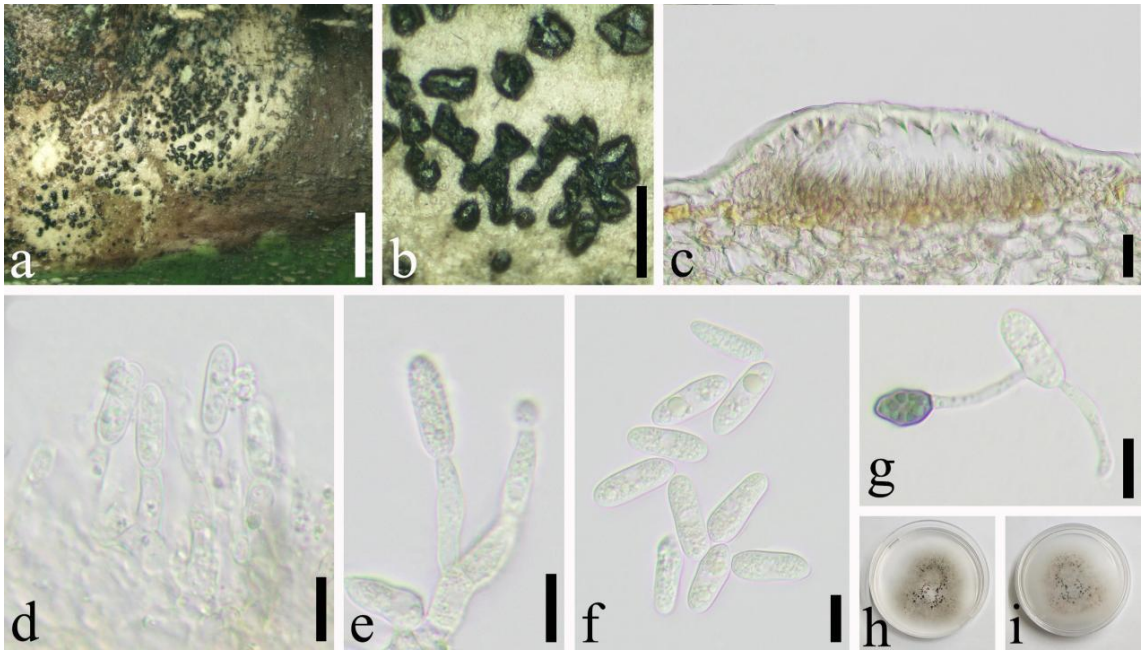

Figure 62 – *Colletotrichum gloeosporioides* (SICAU 23-0109). a, b Appearance of conidiomata on the stem. c Cross-section of conidioma. d, e Conidiogenous cells with developing conidia. f Conidia. g Germinating conidium with appressorium. h Front view of colony on PDA. i Reverse view of colony on PDA. Scale bars: a = 2 mm, b = 500 µm, c = 50 µm, d–g = 10 µm.

34. *Colletotrichum guangyuanense* Y.X. Li & X.L. Fan, MycoKeys 108: 156 (2024) Fig. 63
MycoBank number: MB852126; Facesoffungi number: FoF16261

Associated with brown spots on leaves of *Michelia* × *alba* DC. Sexual morph: Not observed. Asexual morph: *Coelomycetous*. *Conidiomata* 106–277 × 100–181 μm ($\bar{x}$ = 180 × 137 μm, n = 50) diameter, blister-like, brown to dark brown, globose to subglobose, or irregular shape, submerged, solitary, gregarious. *Conidiogenous cells* 10–18 × 3–6 μm ($\bar{x}$ = 14 × 4 μm, n = 20), hyaline to pale brown, smooth-walled, cylindrical or sometimes conoid. *Conidia* 12.5–19 × 4.5–6 μm ($\bar{x}$ = 15.6 × 5.8 μm, n = 50), hyaline, aseptate, smooth-walled, frequently cylindrical, sometimes ellipsoid. *Appressoria* 6–9 × 5–7 μm ($\bar{x}$ = 7.5 × 6.3 μm, n = 20), single, medium to dark brown, smooth-walled, elliptical, subcircular.

Culture characteristics – *Colonies* on PDA attaining 55–65 mm diameter in 2 weeks, aerial mycelia developed, villiform, white, reverse incanus to white. *Conidiomata* and *Chlamydospores* not observed. *Aerial mycelia* grey to pale brown in center, with brown concentric rings, reverse brown in center, white towards the margins.

Material examined – China, Sichuan Province, Neijiang City, Zizhong County, Huaxiang Village, 104°49′31.33″E 29°46′12.28″N, 306 m, isol. from leaves of *Michelia* × *alba*, 23 Jan. 2023, C.L. Yang, YCL202301002 (SICAU 23-0115), living culture (SICAUCC 23-0093). *ibid.* YCL202301002-2 (SICAU 23-0165), living culture SICAUCC 23-0128.

GenBank numbers – SICAUCC 23-0093 = ITS: PP133656, *gapdh*: PP970516, *chs*-1: PP970517, *his*3: PP970518, *act*: PP970519, *tub*2: PP970520. SICAUCC 23-0128 = ITS: PP732533, *gapdh*: PQ040317, *chs*-1: PP836775, *his*3: PP782132, *act*: PP782118, *tub*2: PP782079.

Notes – *Colletotrichum guangyuanense* was identified by Li et al. (2024) from leaves of *Juglans regia* L. Morphologically, our collections are identical to the descriptions of the type specimen of *C. guangyuanense* (Li et al. 2024). In the combined ITS, *gapdh*, *chs*-1, *act*, and *tub*2 analyses (Fig. 56), our two strains clustered with ex-type strain (CFCC 59902) with high bootstrap support (100% MLBS / 1.00 BYPP). Nucleotide comparisons of ITS, *gapdh*, *his*3, *act*, and *tub*2 (SICAUCC 23-0093) showed high homology with the sequences of *C. guangyuanense* (CFCC 59902, ex-type), similarities are 100% (511/511, 0 gap), 97.7% (259/265, 0 gap), 100% (289/289, 0 gap), 100% (255/255, 0 gap), and 99.8% (705/706, 0 gap), respectively. In this study, we report its occurrence on *Michelia* × *alba* for the first time.

35. *Colletotrichum plurivorum* Damm, Alizadeh & Toy. Sato, Stud. Mycol. 92: 31 (2018) Fig. 64

=*Colletotrichum sichuanensis* G.S. Gong & F.L. Liu, Scientific Reports 6(no. 32761): 6 (2016).

MycoBank number: MB824228; Facesoffungi number: FoF10691

Associated with leaf blight on leaves of *Cymbidium hybrid* (hybrid orchid, *C. faberi* Rolfe × *C. hookerianum* Rchb.f. × *C. serratum* Schltr.). Sexual morph: *Ascomata* 210–300 × 150–220 μm ($\bar{x}$ = 243 × 185 μm, n = 20), perithecia, stromatic, solitary or gregarious, superficial or immersed, multilocular, subglobose to globose, or irregular shape, ostiolate with periphysis. *Peridium* 15–68 μm thick, composed of numerous layers of brown to dull brown flattened *textura angularis*, hyaline to pale brown at inner cells. *Ascogenous hyphae* hyaline, smooth, delicate, invisible. *Interascal tissue* formed of paraphyses, 35–75 × 2.5–7 μm ($\bar{x}$ = 54.2 × 4.8 μm, n = 20), hyaline, smooth-walled, shorter in diameter towards the apex, usually flattened at the base, septate, more or less constricted at septa, disintegrating quickly, branched, J-. *Asci* 53–90 × 6–16 μm ($\bar{x}$ = 67 × 11.6 μm, n = 50), unitunicate, 8-spored, clavate to cylindrical, or broad clavate, short pedicellate, apically rounded, inamyloid. *Ascospores* 16–24 × 5–8 μm ($\bar{x}$ = 19 × 6.5 μm, n = 50), uni- or biseriately arranged, aseptate, hyaline, smooth-walled, guttulate, allantoid to fusiform, or reniform, with both ends rounded. *Appressoria* 7–15 × 7–10 μm ($\bar{x}$ = 10.6 × 8.6 μm, n = 20), formed from ascospore germination, single, pale brown to brown, aseptate, smooth-walled, mostly globose to subglobose, or irregular in outline, with an undulate, rounded margin. Asexual morph: See Damm et al. (2018).

Culture characteristics – *Colonies* on PDA attaining 50–70 mm diameter in 1 week, flat with entire margin, grey, reverse pale olivaceous grey, with random darkened spots.

Material examined – China, Sichuan Province, Chengdu City, Wenjiang District, Kejin Road, No. 355, 103°51′14.25″E 30°42′35.68″N, 516 m, isol. from leaves of *Cymbidium hybrid*, 6 Oct. 2020, C.L. Yang, YCL202008001 (SICAU 23-0112), culture (SICAUCC 23-0090).

GenBank numbers – SICAUCC 23-0090 = ITS: PP133652, *gapdh*: PP957833, *chs*-1: PP957834, *his*3: PP957835, *act*: PP957836, *tub*2: PP957837

Notes – *Colletotrichum plurivorum* was first described as *C. sichuanensis* from *Capsicum annuum* in the Sichuan Province of China (Liu et al. 2016). But no type specimen has been deposited in a fungarium, the name is therefore invalid. Later, the sexual and asexual morphs of *C. plurivorum* were reported by Damm et al. (2018). Morphologically, our observations were identical to the sexual descriptions provided by Damm et al. (2019). Nucleotide comparisons of ITS, *gapdh*, *chs*-1, *his*3, *act*, and *tub*2 (SICAUCC 23-0087) showed high homology with the sequences of *C. plurivorum* (CBS 125474, ex-type), similarities are 100% (573/573, 0 gap), 99.6% (265/266, 0 gap), 100% (291/291, 0 gap), 99.5% (379/381, 0 gap), 100% (281/281, 0 gap), and 100% (701/701, 0 gap), respectively.

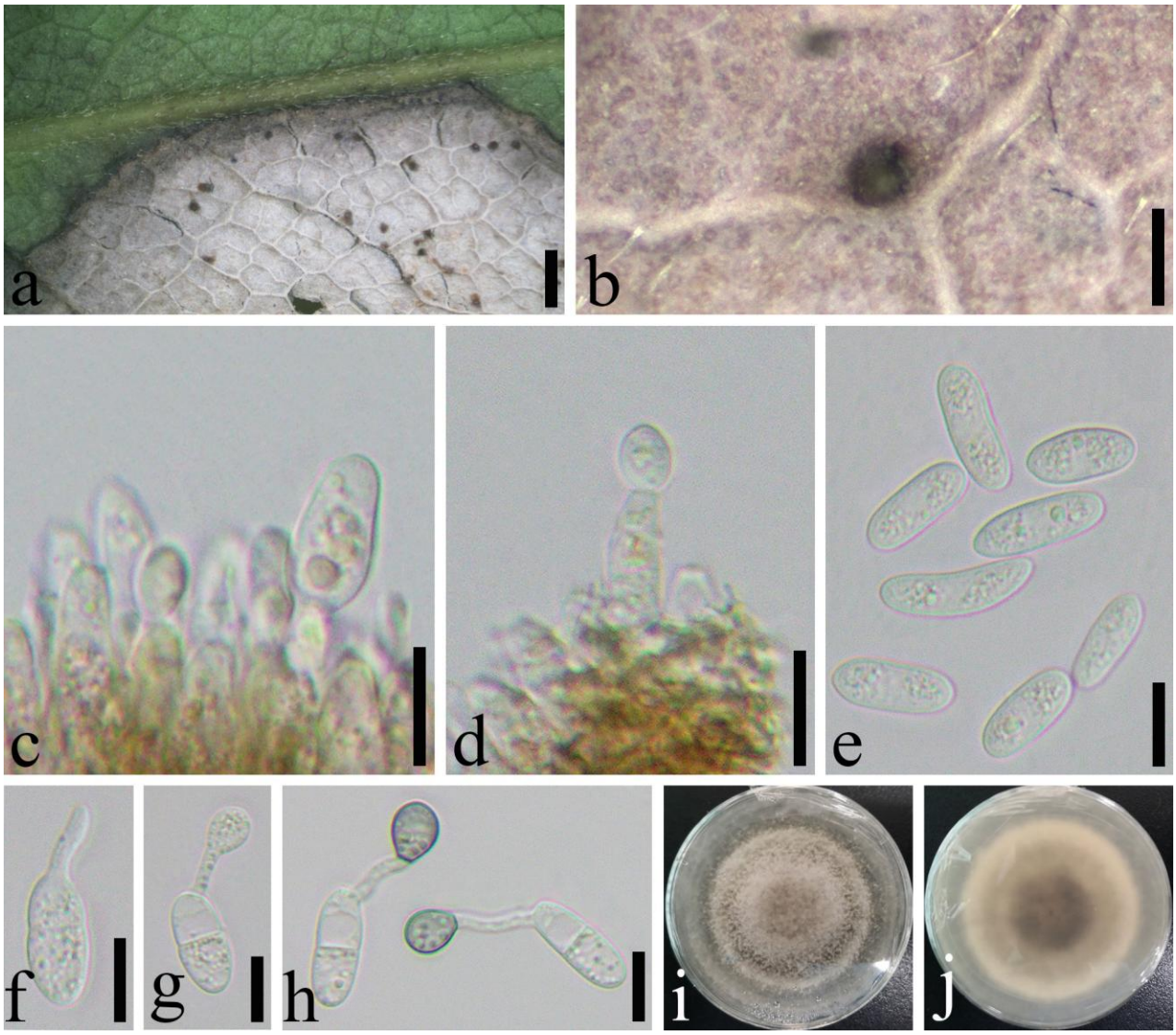

Figure 63 – *Colletotrichum guangyuanense* (SICAU 23-0115). a, b Appearance of conidiomata on the leaf. c, d Conidiogenous cells with developing conidia. e Conidia. f–h Germinating conidia with appressoria. i Front view of colony on PDA. j Reverse view of colony on PDA. Scale bars: b = 300 μm, c = 50 μm, d, e, g, h = 10 μm, f = 5 μm.

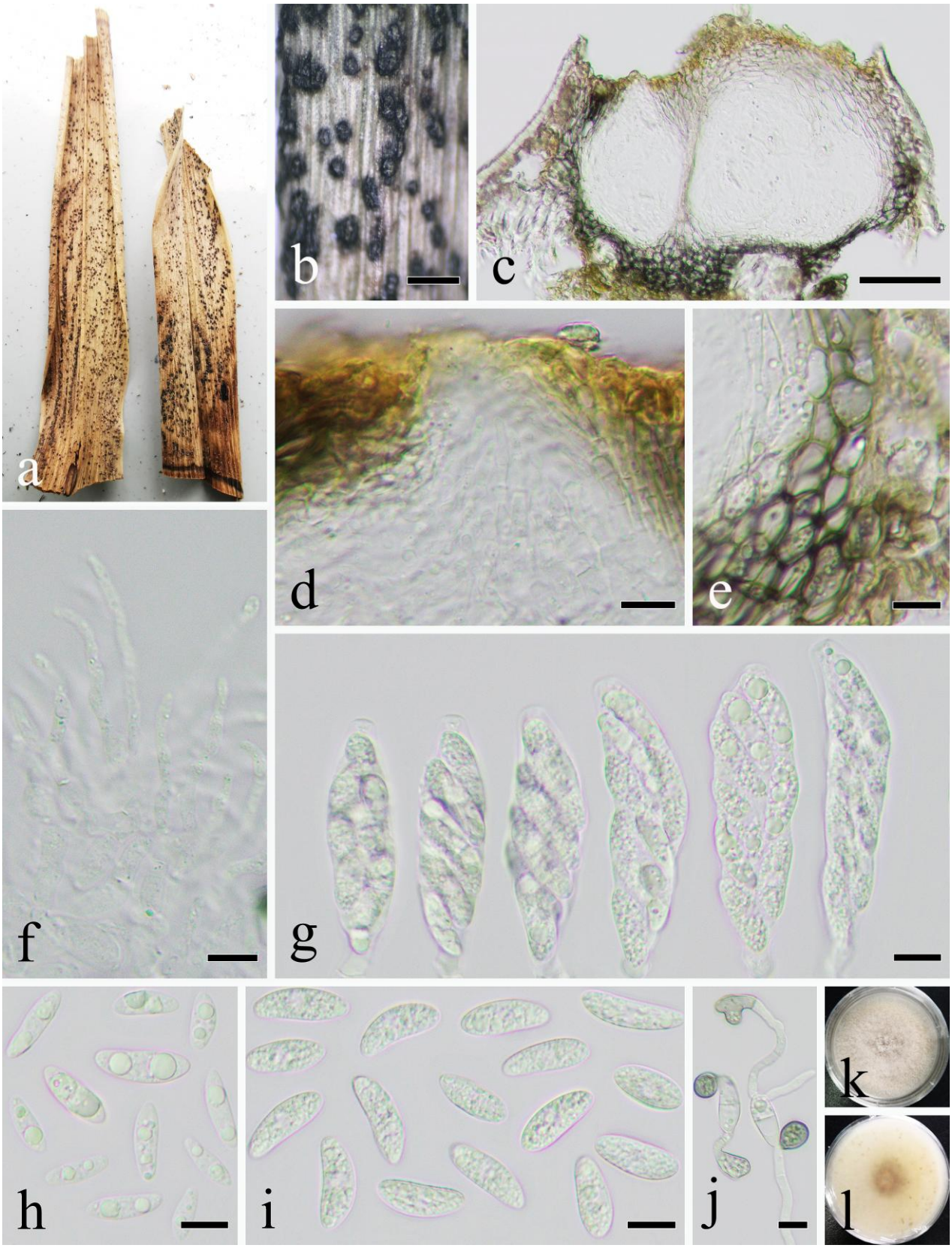

Figure 64 – *Colletotrichum plurivorum* (SICAU 23-0112). a, b Appearance of ascomata on the leaves. c Cross-section of ascoma. d Ostiole. e Peridium. f Paraphyses. g Asci. h, i Ascospores. j Germinating ascospores with appressoria. k Front view of colony on PDA. l Reverse view of colony on PDA. Scale bars: b = 500 µm, c = 50 µm, d–j = 10 µm.

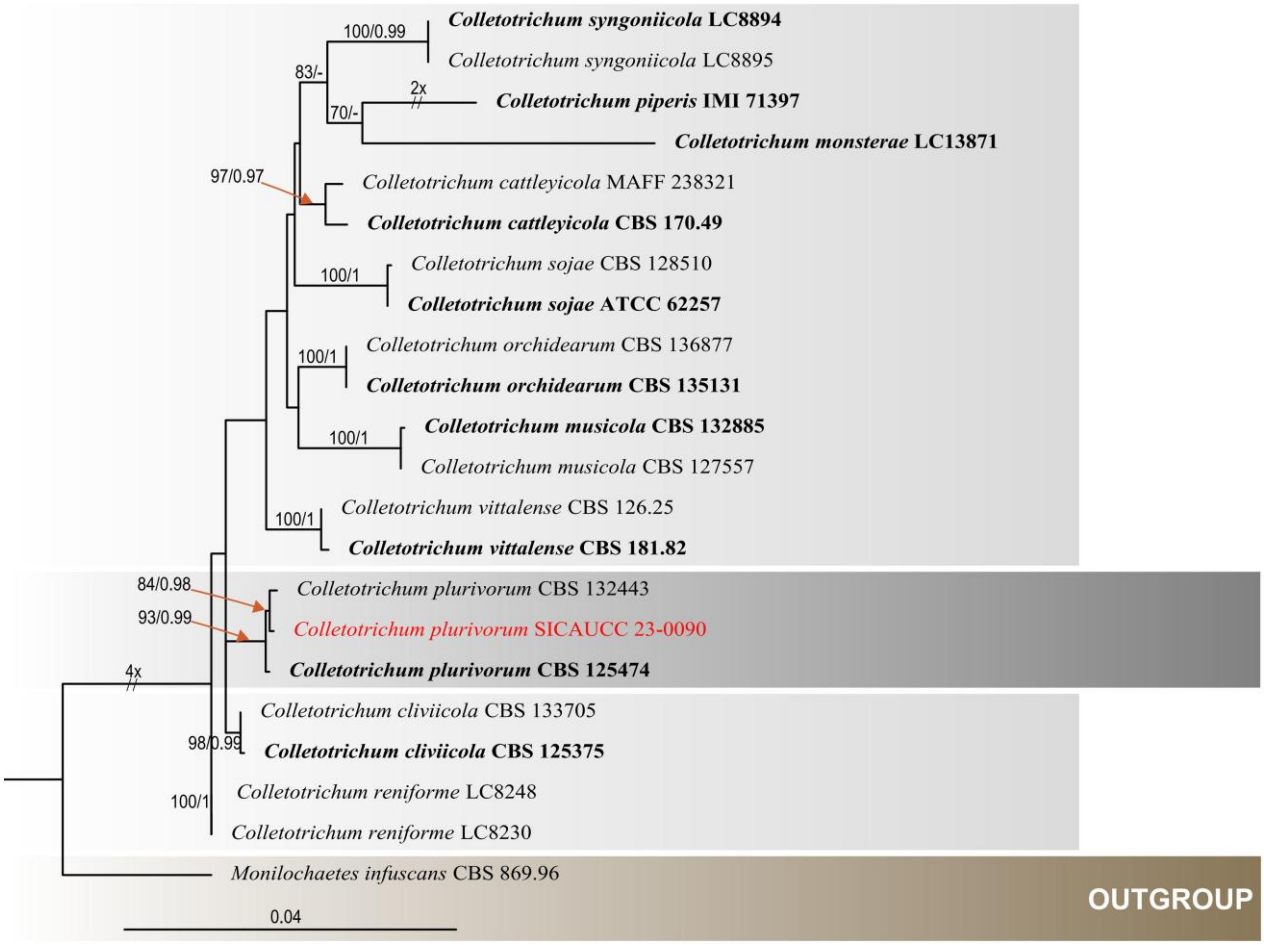

Figure 65 – Phylogram derived from maximum likelihood analyses of a combined dataset comprising ITS, *gapdh*, *chs*-1, *his*3, *act*, and *tub*2 sequence dataset, representing the species of *C. orchidearum* species complex. Twenty-two strains were included in the combined analyses, which comprised 2,627 characters (ITS: 1–606, *gapdh*: 607–872, *chs*-1: 873–1,173, *his*3: 1,174–1,591, *act*: 1,592–1,876, *tub*2: 1,877–2,627) after alignment. The best scoring RAxML tree with a final likelihood value of -7,124.271499 is presented. The matrix had 476 distinct alignment patterns, with 15.32% of undetermined characters or gaps. Estimated base frequencies were as follows: A = 0.217278, C = 0.319541, G = 0.251645, T = 0.211536; substitution rates AC = 0.906856, AG = 2.485637, AT = 0.845457, CG = 0.859750, CT = 5.037088, GT = 1.000000. Bootstrap support values for ML equal to or greater than 70%, and BYPP equal to or greater than 0.90 are indicated at the nodes as MLBS / BYPP. *Monilochaetes infuscans* (CBS 869.96) was used as the outgroup taxa. The ex-type strains are in bold, and the new isolates in this study are in red.

Hypocreales Lindau

Notes – *Hypocreales* was introduced by Lindau (1897) and typified with *Hypocrea* (*Hypocreaceae*). *Hypocreales* is one of the largest orders of the class *Sordariomycetes* with highly diverse lifestyles, currently comprising approximately 300 genera (Hyde et al. 2020b). Lifestyles vary from endophytic, fungicolous, herbicolous, corticolous, caulicolous, lichenicolous, foliicolous, entomogenous, and bryophilous (Chen et al. 2023b, Perera et al. 2023). Hyde et al. (2020d) listed 14 families under *Hypocreales*. While, Wijayawardene et al. (2022) added the family *Cylindriaceae* to the order. However, Hyde et al. (2020d) placed *Cylindriaceae* in *Xylariomycetidae*. Xiao et al. (2023) recently introduced a new family *Polycephalomycetaceae* to *Hypocreales*. Perera et al. (2023) added 3 new families including *Ijuhyaceae*, *Stromatonectriaceae* and *Xanthonectriaceae* to *Hypocreales*.

Nectriaceae Tul. & C. Tul.

Notes – *Nectriaceae* was introduced by Tulasne et al. (1865). *Nectriaceae* a highly diverse group with a worldwide distribution and it has higher diversity in warm temperate, subtropical and tropical regions (Rossman et al. 1999; Schroers et al. 2011; Hyde et al. 2014; Lombard et al. 2015). Species of *Nectriaceae* are facultative or obligate plant pathogens, soil-borne saprobes or weak to virulent, while some are facultatively fungicolous or insecticolous, even important opportunistic pathogens of humans (Rossman et al. 1999; Rossman 2000; Chaverri et al. 2011; Gräfenhan et al. 2011; Schroers et al. 2011; Guarro 2013).

Neocosmospora E.F. Sm.

Notes – *Neocosmospora* was established by Smith (1899). Currently, 155 records of *Neocosmospora* are listed in Species Fungorum (https://www.speciesfungorum.org, November 2024), and most transferred from *Fusarium solani* species complex. The genus contains saprobes, plant endophytes and pathogens of major economic significance as well as opportunistic animal pathogens (Sandoval-Denis et al. 2019; Bao et al. 2023).

36. ***Neocosmospora phalaenopsidis*** S.S. Xiang & C.L. Yang, sp. nov. Fig. 66

MycoBank number: MB900695; Facesoffungi number: FoF16130

Etymology – Refers to the host genus *Phalaenopsis*.

Holotype – SICAU 23-0140

Associated with rachis blight on the rachis of *Phalaenopsis aphrodite* Rchb. F. Sexual morph: Not observed. Asexual morph: *Hyphomycetous*. *Conidiophores* 81–124 × 2–4 μm ($\bar{x}$ = 106 × 3 μm, n = 30), aggregated in dense fascicles, arising from the upper cells of stroma, erumpent, subcylindrical, straight to variously curved, hyaline, unbranched or branched once or twice, septate, smooth, thin-walled; each branch terminating in a single phialide, tapering uniformly from base to tip, collarette of phialides thickened, not conspicuously flared. *Conidia* typically arising from conidiophore or sporodochia, hyaline, thin-walled, smooth. *Alpha-conidia* 7–18 × 4–6 μm ($\bar{x}$ = 11 × 4.9 μm, n = 50), ellipsoidal, aseptate. *Beta-conidia* 15–39 × 4–6 μm ($\bar{x}$ = 28 × 5 μm, n = 50), falcate, tapering uniformly to a subacute tip, 1–3–septate. *Chlamydospores* unicellular, ovoid to ellipsoidal, single or in chains, terminal on hyphae or intercalary, pale brown in colour, consisting of enlarged, thick-walled vegetative cells: unicellular 8–9.5 × 7–9 μm ($\bar{x}$ = 8.8 × 8.0 μm, n = 50); multicellular 13–37 × 7–12 μm ($\bar{x}$ = 20 × 8.3 μm, n = 50).

Culture characteristics – *Colonies* on MEA attaining 40–45 mm diameter in 20 days, colony surface greyish white, aerial mycelium white, cottony and more densely formed at the colony center becoming flat towards the margin, reverse yellow at the center fading to brown at the margin. Colony margin entire to undulate. *Colonies* on OA attaining 40–45 mm diameter in 70 days, colony surface white, aerial mycelium white, flocculent, reverse overall white with irregular yellow to brown pigmented areas. *Colonies* on PDA attaining 40–45 mm diameter in 20 days, medium sparse, irregular, hairy edge, colony surface white, aerial mycelium white, cottony, reverse white. *Colonies* on SNA attaining 40–45 mm diameter in 70 days, sparse, irregular, hairy edge, colony surface white, aerial mycelium white, well developed in the middle, sparse at the margin, reverse white.

Material examined – China, Sichuan Province, Chengdu City, Wenjiang District, 103°51′14.06″E 30°42′35.25″N, 537 m, isol. from the rachis of *Phalaenopsis aphrodite*, 20 Nov. 2020, C.L. Yang, YCL202011005 (SICAU 23-0140, holotype), ex-type culture (SICAUCC 23-0104). *ibid.* YCL202011005-2 (SICAU 23-0166), living culture SICAUCC 23-0138.

GenBank numbers – SICAUCC 23-0104 = ITS: PP769690, LSU: PP719622, *tef*1-α: PQ005621, *rpb*2: PQ005613, PQ005614. SICAUCC 23-0138 = ITS: PP769694, LSU: PP719627, *tef*1-α: PQ005624, *rpb*2: PQ005615, PQ005616

Notes – Our strain, as revealed by multigene analyses encompassing ITS, LSU, *rpb*2, and *tef*1-α sequence data, forms a cluster with *Neocosmospora solani*, albeit with low bootstrap support (Fig. 67). In the context of sequence comparisons with *N. solani* (CBS 140079), notable differences

emerge. The *rpb*2 fragments show similarity levels of 97.75% (781/799, 0 gap) and 98.13% (839/855, 0 gap), while the *tef*1-α fragment is 98.03% (698/712, 3 gaps), the ITS fragment is 99.12% (561/566, 1 gap), and the LSU fragment is 99.83% (598/599, 0 gap) (Schroers et al. 2016). Morphologically, *N. phalaenopsidis* is different from *N. solani* in having smaller conidia (15–39 × 4–6 µm vs. 8.5–53 × 2.5–7) and fewer conidial septa (0–3 septa vs. 0–5 septa), and the colony growth rate of *N. phalaenopsidis* is slower than that of *N. solani* (on PDA: 2.0–2.3 mm/d vs. 6.5–8.5 mm/d; on SNA: 0.6 mm/d vs. 8–9 mm/d) (Schroers et al. 2016). The PHI test also showed that no significant recombination events between *N. solani* and *N. phalaenopsidis* (Fig. 68). Therefore, we introduce *N. phalaenopsidis* as a new species.

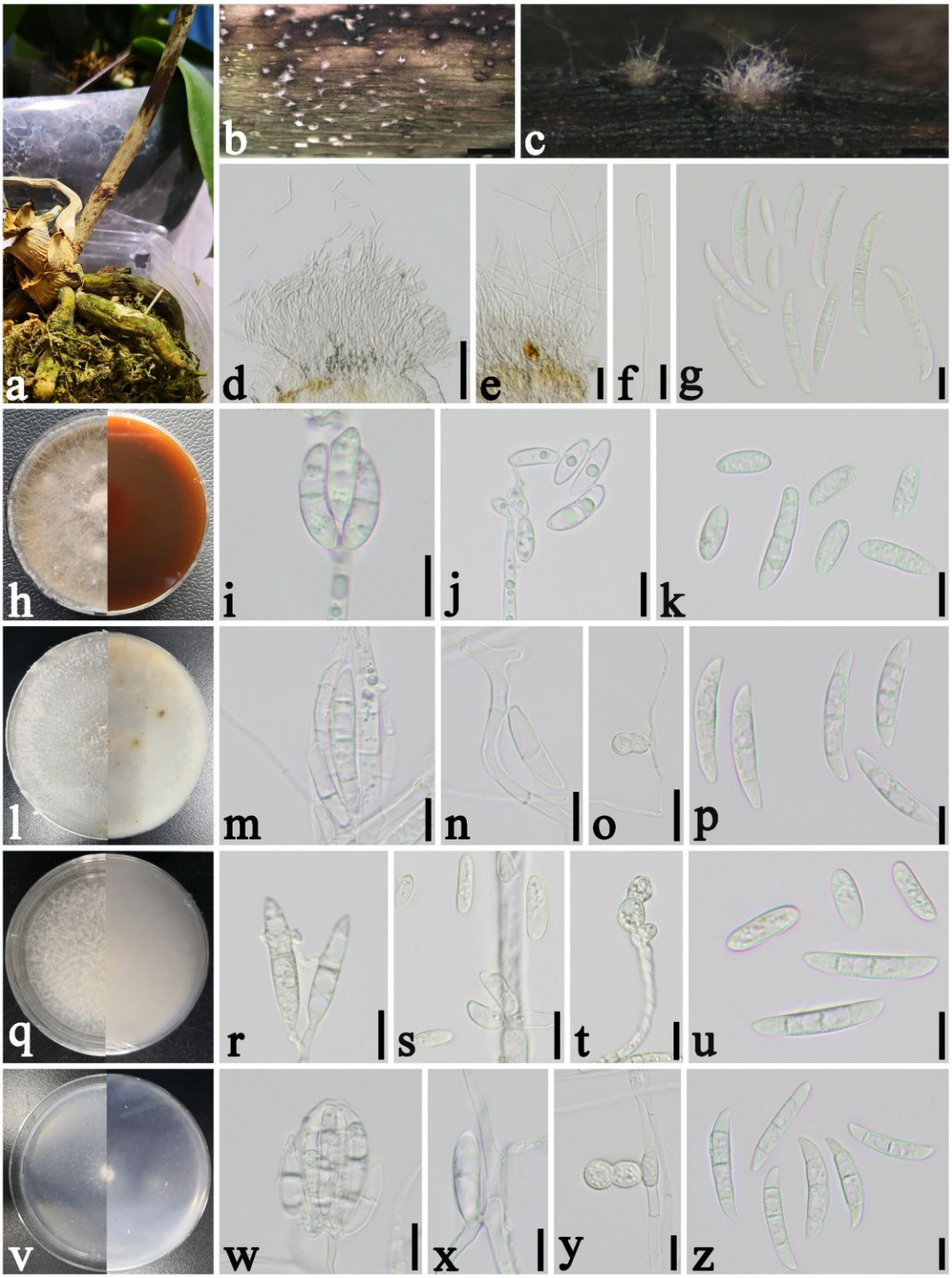

Figure 66 – *Neocosmospora phalaenopsidis* (holotype, SICAU 23-0140). a Symptoms on the rachis. b, c Appearance of conidiogenesis. d, e Fascicles with conidiophores and conidiogenous cells. f Conidiophores bearing conidia. g Conidia. h Front and reverse view of colonies on MEA. i, j Conidiophores bearing conidia on MEA. k Conidia on MEA. l Front and reverse view of colonies on OA. m, n Conidiophores bearing conidia on OA. o Chlamydospore on OA. p Conidia on OA. q Front and reverse view of colonies on PDA. r, s Conidiophores bearing conidia on PDA. t Chlamydospore on PDA. u Conidia on PDA. v Front and reverse view of colonies on SNA. w, x Conidiophores bearing conidia on SNA. t Chlamydospore on SNA. u Conidia on SNA. Scale bars: b = 190 μm, c = 40 μm, d, e = 20 μm, f–g, i–k, m–p, r–u, w–z = 10 μm.

Phyllachorales M.E. Barr

Notes – *Phyllachorales* was erected by Barr (1983) with *Phyllachoraceae* as the type family. Tar spot fungi, representing species within the *Phyllachorales* order, are known for their shiny black stromata and their ability to parasitize leaves, stems, or fruits of plants (Silva-Hanlin & Hanlin 1998, Mardones et al. 2017). *Phyllachorales* comprises five families (*Phaeochoraceae*, *Phaeochorellaceae*, *Phyllachoraceae*, *Neopolystigmataceae*, and *Telimenaceae*), encompassing approximately 1,900 species distributed across 63 genera (Guterres et al. 2022, Wijayawardene et al. 2022, Literatus et al. 2023, Species Fungorum 2024), and is distributed across diverse countries and natural plant hosts, mostly including species within *Arecaceae*, *Asclepiadaceae*, *Clethraceae*, *Erythroxylaceae*, *Fabaceae*, *Lauraceae*, *Melastomataceae*, *Moraceae*, *Myrtaceae*, *Poaceae*, *Proteaceae*, *Rosaceae*, and *Violaceae*, with some species also found growing on lichens (Zhurbenko 2008, Etayo et al. 2013, Mardones et al. 2017, 2018).

Phyllachoraceae Theiss. & H. Syd.

Notes – *Phyllachoraceae* was introduced by Theissen & Sydow (1915) with *Phyllachora* as the type genus. *Phyllachoraceae* species play a significant role as plant pathogens, primarily responsible for the development of foliar spots on a wide range of plants, especially on members of *Poaceae* (Pearce & Hyde 2001, Mardones et al. 2017). To date, this family comprises 54 genera, primarily within the order *Phyllachorales*, and these species are identified by their ascohymenial development characterized by paraphyses, thin-walled asci that may have an apical apparatus which remains unstained when treated with iodine, and ascospores that are often hyaline and unicellular (Cannon 1991, Parbery 1993, Wijayawardene et al. 2022).

Phyllachora Nitschke ex Fuckel

Notes – *Phyllachora*, typified with *P. graminis*, was initially established by Nitshke, but further refined by Fuckel (Clements & Shear 1931, Fuckel 1869). *Phyllachora* species are notable biotrophic pathogens known for inducing tar spot symptoms on a variety of forest plants and crops, with a primary affinity for *Poaceae* species while also affecting several families among both monocotyledonous and dicotyledonous plants (Cannon 1991, Mardones et al. 2017, Yang et al. 2019b, Lipps et al. 2022). *Phyllachora*, the largest genus within *Phyllachoraceae* with 1,395 epithets in Species Fungorum (https://www.speciesfungorum.org, November 2024), commonly infects mesophyll or epidermis cells, leading to the formation of black, shiny superficial tar spots, which can potentially attract or facilitate secondary infections by more virulent pathogens (Cannon 1991, dos Santos et al. 2016, Yang et al. 2019b).

37. *Phyllachora cynodontis* Niessl, Verh. nat. Ver. Brünn 14: 214 (1876) Fig. 69

MycoBank number: MB229926; Facesoffungi number: FoF15927

Associated with tarspot on leaves of *Cynodon dactylon* (L.) Pers. Sexual morph: *Stromata* 335–750 × 165–355 × 50–115 μm ($\bar{x}$ = 528 × 271 × 77 μm, n = 20), fusiform or cymbiform, domed above the leaf surface, amphigenous, scattered, sometimes gregarious, like black nevus, black and carbonaceous. *Ascomata* 100–175 × 105–198 μm ($\bar{x}$ = 134 × 144 μm, n = 20), immersed in the leaf tissue, occupying the entire leaf thickness, often developing next to adjacent ascomata and confined

by host vascular tissue, suboblate to subglobose, sometimes irregular in shape, with an indistinctive ostiole. *Peridium* 7–18 μm ($\bar{x}$ = 10.6 μm, n = 20) thick, characterized by 8–10 layers of brown to transparent ceratosporous tissue, comprising brown to dark brown cells of *textura angularis*. *Paraphyses* 1–3 μm wide, numerous, persistent, filiform, unbranched, aseptate, many guttules, slightly longer than asci. *Asci* 48–74 × 8–16 μm ($\bar{x}$ = 58.8 × 11.3 μm, n = 50), thin-walled, 8-spored, persistent, cylindrical to clavate, apex obtuse, with pedicel. *Ascospores* 9–13 × 5–8 μm ($\bar{x}$ = 11 × 6.4 μm, n = 50), uniseriate, sometimes overlapping and oblique, hyaline, frequently ellipsoidal, occasionally ovoid, one-celled, aseptate, some with one large fat globule in the center. Asexual morph: Not observed.

Material examined – China, Sichuan Province, Chengdu City, Xindu District, Xindu Manhua Manor, 104°9′12.58″E 30°46′19.75″N, alt. 477 m, on leaves of *Cynodon dactylon*, 25 Jun. 2023, Q.R. Sun, SQR202305051 (SICAU 23-0130).

GenBank numbers – SICAU 23-0130 = ITS: PP737900, LSU: PP737897, SSU: PP739515

Notes – The phylogenetic tree was classified into four lineages based on host plants, with our collection (SICAU 23-0130) grouped within Lineage I, consisting of *Phyllachora* species from the *Cynodon* in subfamily *Gramineae* (Fig. 70). Phylogenetic analysis revealed that the collection SICAU 23-0130 forms a sister clade with *P. cynodontis* complex (100% MLBS / 1.00 BYPP). Sequence comparisons with the holotype MHYAU 20133 unveiled matching ITS 100% (582/582, 0 gap) and LSU 100% (775/775, 0 gap) sequences, corroborating the morphological analysis aligning our collection with the species *P. cynodontis* as described by von Mayendorf (1876). *Phyllachora cynodontis* has a global distribution and is documented on various grass hosts within the *Poaceae* family, including species from *Bouteloua*, *Chloris*, *Cynodon*, *Distichlis*, *Elymus*, *Festuca*, and *Spartina* (Parbery 1967, French 1989, Lenné 1990).

Phylum *Basidiomycota* R.T. Moore

Class *Exobasidiomycetes* Begerow, M. Stoll & R. Bauer

Exobasidiales Henn.

Notes – *Exobasidiales*, initially described as "*Exobasidiineae*", was introduced by Hennings (1900). Members of *Exobasidiales* are relatively rare and challenging to find, yet they are significant due to the diverse morphology of their infections and specific host ranges (Begerow et al. 2001, Piepenbring et al. 2010, 2020). *Exobasidiales* species represent a parasitic group of basidiomycetes that typically induce tissue hypertrophy, gall formation, fruit teratology, witches' broom, as well as speckles on the leaves and stems of horticultural plants (Somrithipol et al. 2018, Dudka et al. 2021, Shibata et al. 2021, Shibata & Hirooka 2022). At present, *Exobasidiales* encompass five families, consisting of 21 genera and a total of around 114 species (Li et al. 2022b, Wijayawardene et al. 2022).

Graphiolaceae Clem. & Shear

Notes – *Graphiolaceae*, consisting of *Graphiola* and *Stylina*, is a relatively small fungal group with *Graphiola* as the type genus. *Graphiolaceae* species are frequently found on palm trees, leading to the development of false smut, and they produce chains of gastroid basidia within distinctive basidiocarps (Oberwinkler et al. 1982, de Sousa Poltronieri et al. 2012, Piepenbring et al. 2012). Members of *Graphiolaceae* are distinguished from other *Exobasidiales* species by their distinctive basidiocarps, basidia arranged in chains, clamped haustoria, and unique basidial morphology (Begerow et al. 2002).

Graphiola Poit.

Notes – *Graphiola* was introduced by Poiteau (1824) with *G. phoenicis* as the type species. The genus *Graphiola* primarily consists of biotrophic parasites that infest palm leaves found in tropical and subtropical regions across the globe (Mani et al. 2012, Pal 2019, Sung et al. 2022).

Graphiola species are mainly distinguished by their biotrophic parasitic relationship with palms, and the presence of black, cup-shaped basidiomata housing catenate basidia (Piepenbring et al. 2012).

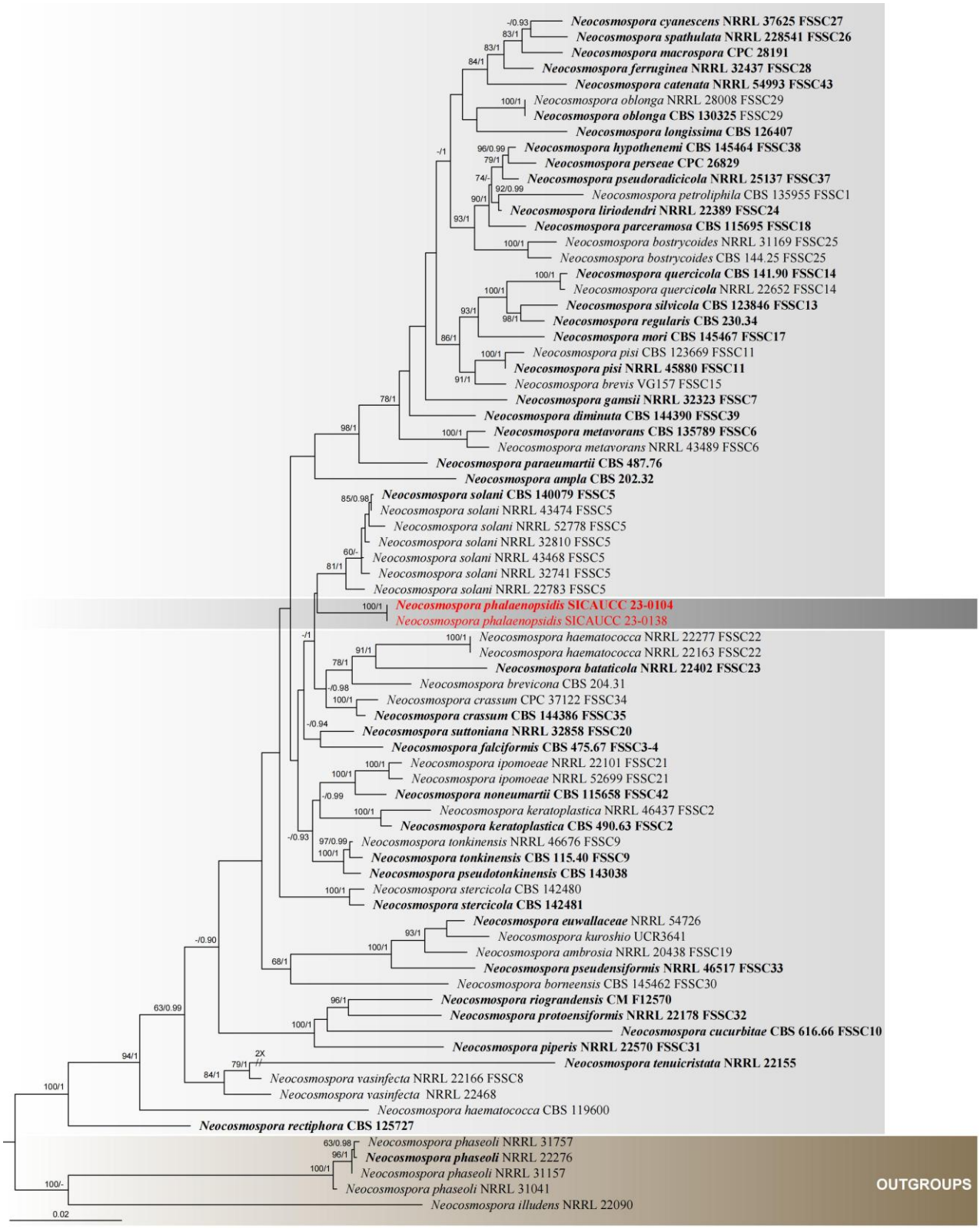

Figure 67 – Phylogram derived from maximum likelihood analyses of a combined dataset comprising ITS, LSU, *rpb*2, and *tef*1-α sequence dataset for *Neocosmospora* species. Seventy-six strains were collected in the molecular analysis, comprising 4,187 characters (ITS: 1–622, LSU: 623–1,515, *rpb*2: 1,516–3,437, *tef*1-α: 3,437–4,187), including alignment gaps. *N. illudens* (NRRL

22090) and *N. phaseoli* (NRRL 31157, NRRL 22276, NRRL 31757, and NRRL 31041) were considered as the outgroup taxa. Single-gene analyses were performed and yielded similar tree topologies between the ML and BY methods. This ensured a consistent basis for comparing the stability of clades in the analysis. The RAxML tree with the highest score, indicating a final likelihood value of -20,782.662777, is presented. The matrix employed encompasses 1,445 distinct alignment patterns, of which 24.44% consist of undetermined characters or gaps. Estimated base frequencies were as follows: A = 0.241562, C = 0.276624, G = 0.258514, T = 0.223299; substitution rates: AC = 2.298743, AG = 5.769526, AT = 2.463651, CG = 1.335603, CT = 13.660840, GT = 1.000000. Bootstrap support values (MLBS) equal or greater than 60%, and Bayesian posterior probabilities (BYPP) equal or greater than 0.90 are provided near to each branch. New isolates are highlighted in red, and strains from the holotype are indicated in bold. Bar = 0.02 represents the estimated number of nucleotide substitution sites per branch.

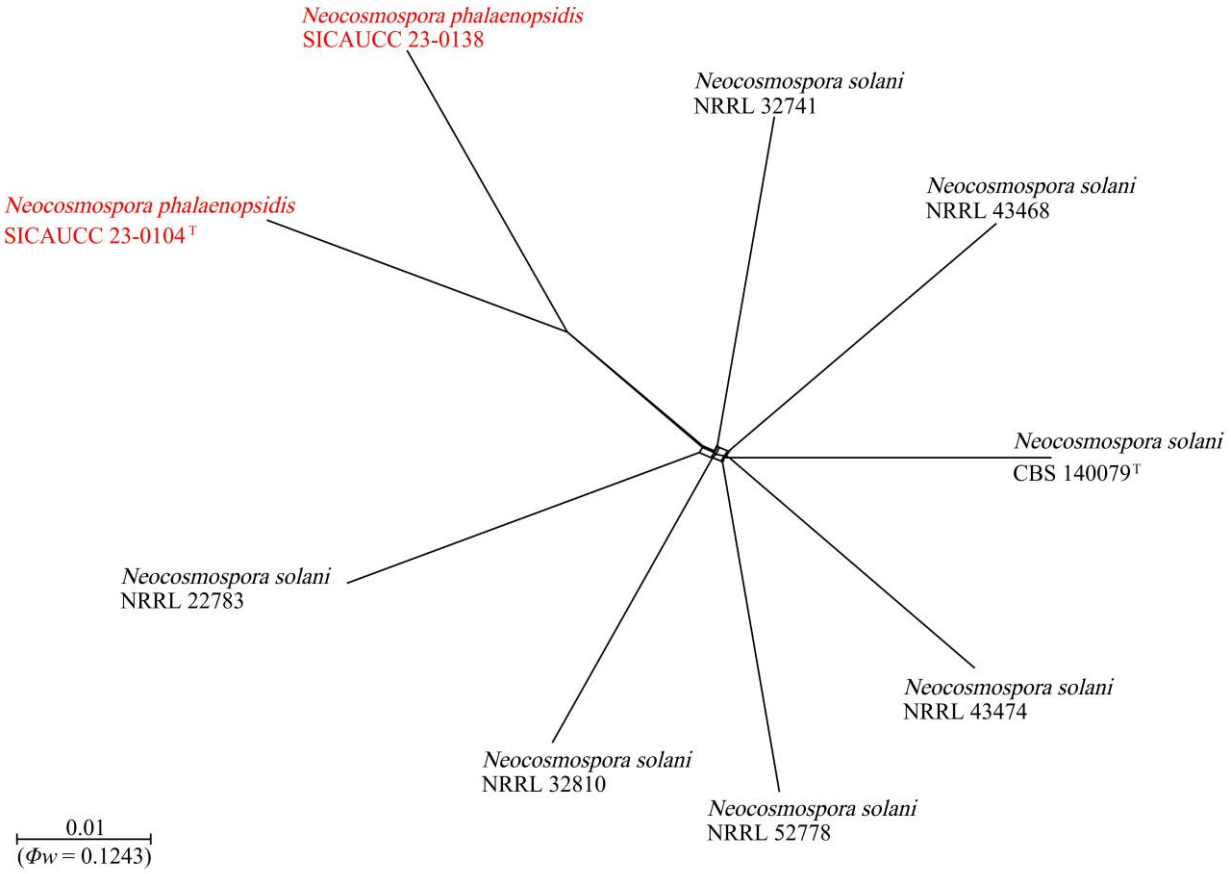

Figure 68 – The splits graph from the pairwise homoplasy index (PHI) test generated from the concatenated gene set of ITS, LSU, *rpb*2, and *tef*1-α sequence data of *N. solani* and *N. phalaenopsidis* using both LogDet transformation and splits decomposition. PHI test results $\Phi w <$ 0.05 indicate significant recombination within the dataset. The ex-type strains are denoted by "T" and the new isolates of this study are in red.

38. *Graphiola phoenicis* (Moug. ex Fr.) Poit., Ann. Sci. Nat. (Paris) 3: 473 (1824) Fig. 71

MycoBank number: MB184246; Facesoffungi number: FoF15885

Associated with false smut on foliar pinnae of leaves of *Phoenix acaulis* Roxb., symptoms initially appeared as small yellowish lesions on both sides on the leaf, then developed into brown to black globular, cylindrical or irregular sori, eminently raised basidioma with a mass of spore overflow. *Basidiomata* 430–870 µm diameter ($\bar{x}$ = 610 µm, n = 50), 360–530 µm high ($\bar{x}$ = 450 µm, n = 50), epiphyllous, adaxial and abaxial, single, sometimes adjacent ones fused, scattered, gregarious, occasionally with discolouration of surrounding host tissue, usually formed by cup-

shaped peridia with a subcircular to circular, or ovoid opening, sometimes irregular opening, central space filled with pale yellow to yellow coloured mass of basidia, spores and conspicuous elaters. *Peridia* 165–250 μm thick ($\bar{x}$ = 193 μm, n = 20) at base, black, formed by deeply pigmented cells of *textura intricate*, and hyphae closely connected and not easily separated from each other. *Elaters* significantly longer than the height of the basidioma, usually formed by above 15–20 hyphae in bundles showing 6–10 hyphae in lateral view, each cell of a hypha 2–12 μm long ($\bar{x}$ = 6.3 μm, n = 100), 1–4 μm width ($\bar{x}$ = 2.6 μm, n = 100). *Basidia* catenate, basidial cells short cylindrical, or cydariform, 1–5 μm long × 2–4 μm width ($\bar{x}$ = 2.9 × 2.9 μm, n = 50) at base, 2–5 μm long × 3–5 μm width ($\bar{x}$ = 3.4 × 3.6 μm, n = 50) when cydariform, with up to 4 or more primary spores in dispersed positions, basidia separating from the upper middle part of the chain with primary spores attached to them. *Primary spores* spherical, or ellipsoidal, separating into two secondary spores at the middle region. *Secondary spores* 3–5 μm diameter ($\bar{x}$ = 3.7 μm, n = 50), globose to bluntly angular, hyaline to pale brown, with several guttulae. *Yeast* formed on PDA, 4–7 μm long × 2–3 μm width ($\bar{x}$ = 5.6 × 2.5 μm, n = 50), hyaline, cylindrical, or ellipsoidal, aseptate, smooth-walled, occurred single, rarely in short chains.

Culture characteristics – Germinated secondary spores formed after 3 h, and the germinating tube grows from one section of the spore. *Colonies* on PDA slow-growing, circle, cheese-colored, filmy, dry, prominent ridges at center, small radiating ridges along the edges; the same in the back side. *Colonies* on YPG (0.5% yeast extract, 1% peptone, 2% glucose, 2% agar, w/v) slow-growing, circle, flesh pink, bright; the same in the backside.

Material examined – China, Sichuan Province, Chengdu City, Wenjiang District, Huiming Road 211, 103°51′36.26″E 30°42′36.27″N, 498 m, isol. from leaves of *Phoenix acaulis*, 12 Apr. 2020, C.L. Yang, YCL202004003 (SICAU 23-0122), culture (SICAUCC 23-0115); *ibid.* YCL202004004 (SICAU 23-0123), culture (SICAUCC 23-0116). China, Sichuan Province, Chengdu City, Chongzhou City, Qiquan Town, 103°39′7.28″E 30°33′43.96″N, 494 m, isol. from leaves of *Phoenix acaulis*, 28 Jun. 2020, X.L. Xu, XXL202006004 (SICAU 23-0124), culture (SICAUCC 23-0117).

GenBank numbers – SICAUCC 23-0115 = ITS: PP736371, LSU: PP732707; SICAUCC 23-0116 = ITS: PP736372, LSU: PP732708; SICAUCC 23-0117 = ITS: PP736373, LSU: PP732709

Notes – According to the current genus concept of *Graphiola*, our collections are consistent with those species that are associated with phytopathogens on palms (*Arecaceae*) (Nasr et al. 2019), and share morphological traits with *G. phoenicis* as described by Piepenbring et al. (2012). In the combined ITS + LSU analyses (Fig. 72), our three strains formed a well-supported clade that included all *G. phoenicis* species. *Graphiola phoenicis* is one of the most common, widely distributed, and well-known pathogens found exclusively on ornamental plants, particularly on palms (Mani et al. 2012, Sung et al. 2022). This fungus has been documented on over 30 plant species belonging to the *Arecaceae* family, encompassing genera such as *Arenga*, *Borassus*, *Butia*, *Chamaerops*, *Chrysalidocarpus*, *Coccothrinax*, *Cocos*, *Elaeis*, *Livistona*, *Mauritia*, *Phoenix*, *Prestoea*, *Rhopalostylis*, *Roystonea*, *Sabal*, *Syagrus*, *Thrinax*, and *Washingtonia*, and including seven species within the *Phoenix* genus, namely *P. canariensis*, *P. dactylifera*, *P. loureiroi*, *P. paludosa*, *P. reclinata*, *P. roebelenii*, and *P. sylvestris* (Piepenbring et al. 2012, Sepúlveda et al. 2017, Nasr et al. 2019). In this study, we report its occurrence on *P. acaulis* for the first time.

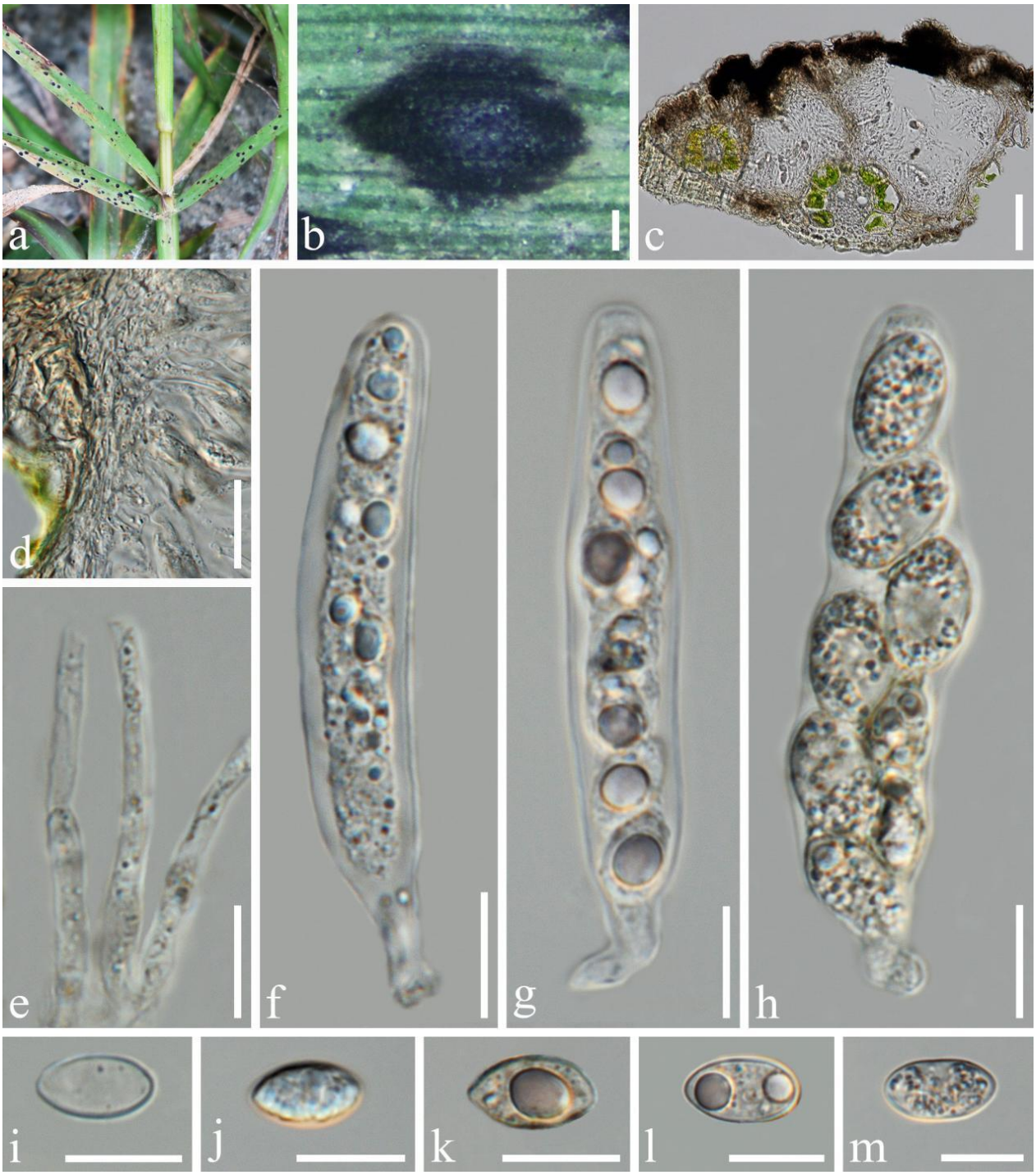

Figure 69 – *Phyllachora cynodontis* (SICAU 23-0130). a Symptoms on the leaves. b Appearance of ascoma. c Cross-section of ascoma. d Peridium. e Paraphyses. f–h Asci. i–m Ascospores. Scale bars: b = 100 µm, c = 50 µm, d–m = 10 µm.

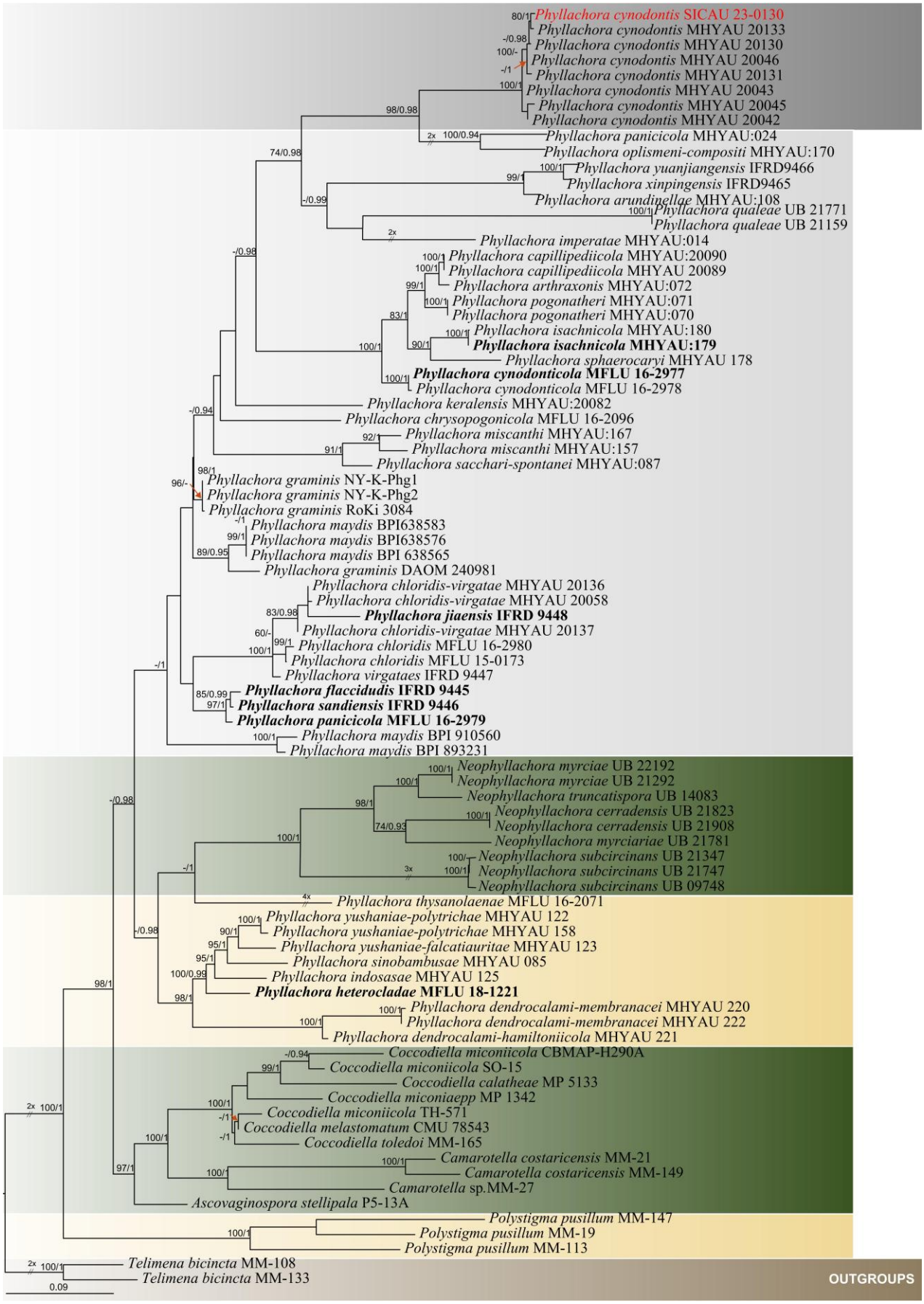

Figure 70 – Phylogram derived from maximum likelihood analyses of a combined dataset comprising LSU, ITS, and SSU, utilized 86 taxa and was rooted with *Telimena bicincta* (MM-108) and *T. bicincta* (MM-133) (*Telimenaceae*, *Phyllachorales*). The alignment contained 4,342

characters (LSU: 1–1,234, ITS: 1,235–2,451, SSU: 2,452–4,342). The highest-scoring RAxML tree, with a final likelihood value of -34,082.915, is shown alongside a matrix consisting of 2,209 distinct alignment patterns. Estimated base frequencies were as follows: A = 0.2544014, C = 0.237389, G = 0.278725, T = 0.229485, with substitution rates AC = 1.189290, AG = 2.150814, AT = 1.415275, CG = 0.838491, CT = 4.113416, GT = 1.00000. Bootstrap support values for maximum likelihood (MLBS, left) >70%, and Bayesian posterior probabilities (BYPP, right) ≥ 0.60 are indicated at the nodes, respectively. The sequences from ex-type strains are marked in bold. The newly generated sequences are written in red.

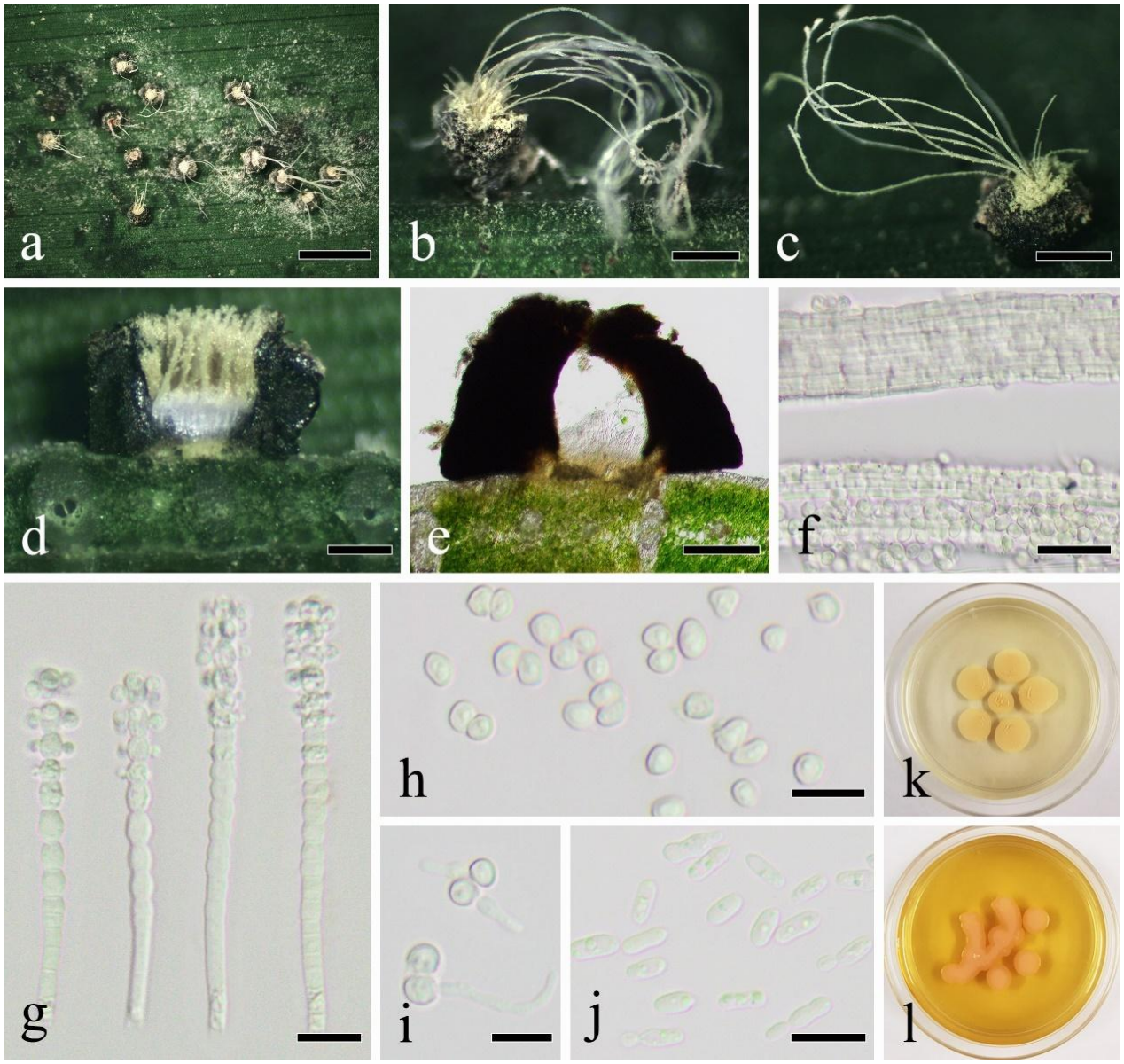

Figure 71 – *Graphiola phoenicis* (SICAU 23-0122). a Appearance of small black sori on the leaf. b, c Close-up sori with filaments protruding. d, e Cross-section of sori. f Part of elaters. g Chains of basidia with young primary spores. h Two septate primary spores and two secondary spores. i Germinating secondary spores. j Yeasts formed in PDA. k Front view of colony on PDA. l Front view of colony on YPG. Scale bars: a = 2000 μm, b, c = 500 μm, d, e = 200 μm, f = 20 μm, g–j = 10 μm.

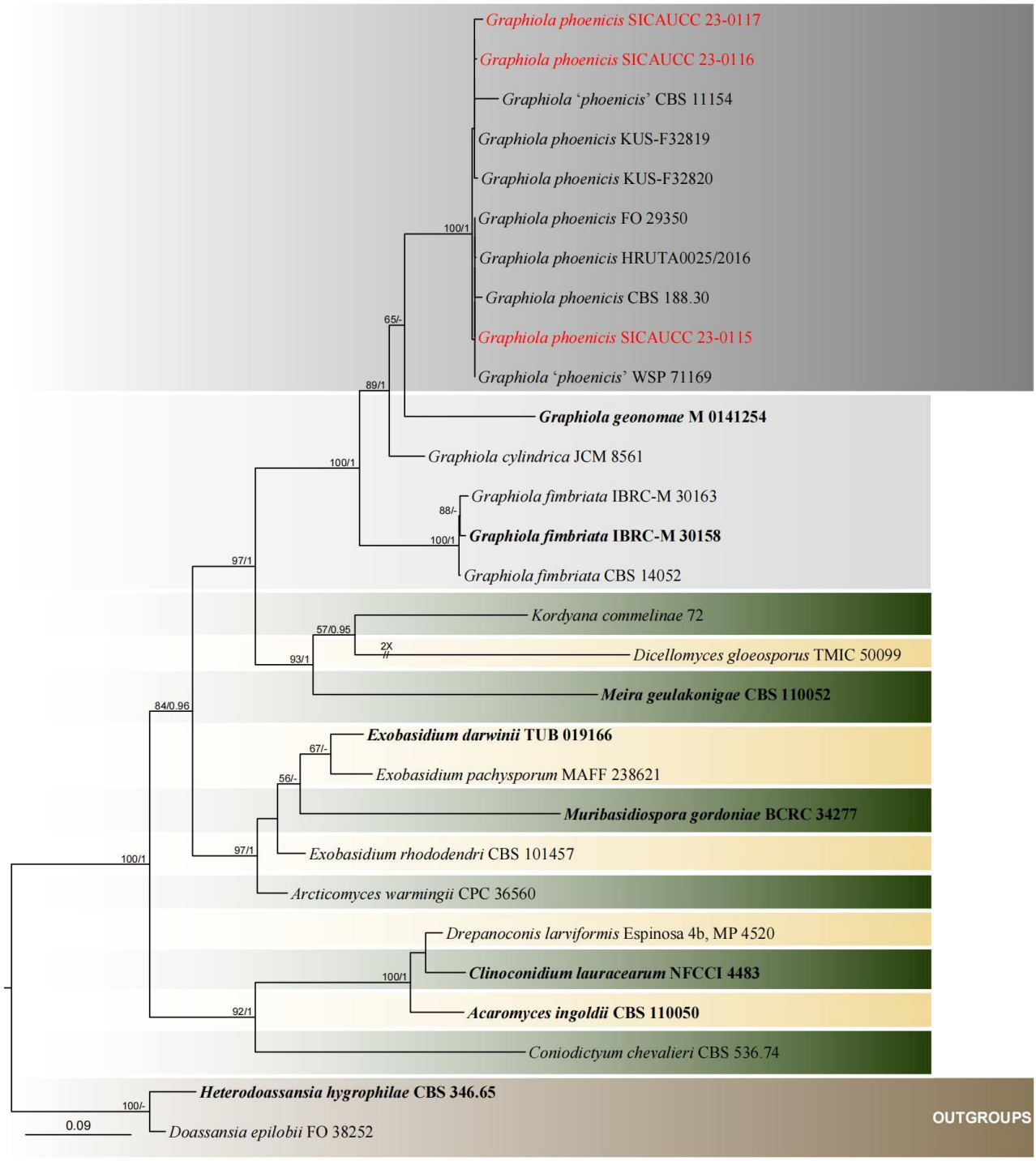

Figure 72 – Phylogram derived from maximum likelihood analyses of a combined dataset comprising ITS and LSU sequence dataset, representing the members of *Brachybasidiaceae*, *Cryptobasidiaceae*, *Exobasidiaceae*, and *Graphiolaceae*. Twenty-nine strains were included in the phylogenetic analysis, comprising 2,053 characters (ITS: 1–948, LSU: 949–2,053) after alignment. The tree is rooted with *Doassansia epilobii* (FO 38252) and *Heterodoassansia hygrophilae* (CBS 346.65). Single-gene analyses were conducted and compared with each species to assess tree topology and clade stability, revealing similarities between the ML and BY trees. The best-scoring RAxML tree with a final likelihood value of -10,925.329758 is presented. The matrix had 935 distinct alignment patterns, with 50.73% of undetermined characters or gaps. Estimated base frequencies were as follows: A = 0.272210, C = 0.198840, G = 0.260549, T = 0.268401; substitution rates AC = 1.251927, AG = 1.825244, AT = 1.499586, CG = 0.411662, CT = 4.625894, GT = 1.000000. Bootstrap support values (MLBS) equal or greater than 50%, and

Bayesian posterior probabilities (BYPP) greater than 0.90 are marked at the nodes. The ex-type strains are in bold, and the new isolates of this study are in red. Bar = 0.09 represents the estimated number of nucleotide substitution sites per branch.

DISCUSSION

This study represents the first comprehensive investigation of phytopathogens occurring on horticultural plants in the southwest region of China, and we have documented various potential fungal causal agents from a wide range of substrates in horticultural plant species. Potential pathogens associated with the stem, branch, twig, leaf, petiole, rachis, fruit, and pod of the *Araliaceae* (*Fatsia*), *Arecaceae* (*Phoenix*, *Rhapis*, *Syagrus*), *Asparagaceae* (*Polygonatum*), *Asphodelaceae* (*Phormium*), *Cactaceae* (*Hylocereus*), *Celastraceae* (*Euonymus*), *Fabaceae* (*Erythrina*, *Vicia*), *Lauraceae* (*Cinnamomum*), *Magnoliaceae* (*Michelia*), *Moraceae* (*Ficus*), *Nyctaginaceae* (*Bougainvillea*), *Orchidaceae* (*Cymbidium*, *Phalaenopsis*), *Poaceae* (*Cynodon*, *Poa*), *Rosaceae* (*Eriobotrya*, *Photinia*), *Rutaceae* (*Citrus*, *Phellodendron*), *Salicaceae* (*Populus*, *Salix*), *Sapindaceae* (*Acer*), and *Theaceae* (*Camellia*) are reported from diverse environments in southwest China. Sixty diseased plant collections were collected and comprehensively described, with their taxonomic classification determined through a combination of multi-gene analyses and morphological data.

Horticultural plants, characterized by their diverse species groups, inhabit a wide range of ecosystems in southwest China, fostering a wealth of specialized fungal resources, including parasites, saprophytes, and endophytes (Yang et al. 2017, 2019b, Ma et al. 2018, Pei et al. 2019, Guo et al. 2020, de Silva et al. 2021, Sun et al. 2023). Plant pathogenic fungi have consistent attention, particularly in relation to the development of diseases, mechanisms of infection, and methods for disease management (Gong et al. 2018, Wang et al. 2020, Liu et al. 2022d, e). However, the taxonomy of pathogenic fungi remains relatively limited and disorganized. Recently, some researchers have reported on fungi within various fungal taxa or host populations. Xu et al. (2022) and Zeng et al. (2022) conducted systematic studies, providing detailed descriptions of ascomycetes found in *Juglans* (*Juglandaceae*) and *Phyllostachys* (*Poaceae*) in the Sichuan Province, respectively. Zhao et al. (2022) and Liu et al. (2023c) elucidated species delimitation within the *Basidiomycota* fungal groups *Pucciniales* and *Polyporales*, both known to cause blister rust and brown rot in wood plants, drawing from diverse geographical sources. Zhang et al. (2023b) documented 23 *Colletotrichum* species found on medicinal plants from Guizhou, Sichuan, and Yunnan Provinces. Zhou et al. (2023) conducted a systematic study on fungal pathogens related to grapevine trunk diseases in China, reporting 13 species from Yunnan Province. Li et al. (2023) concentrated on woody oil plants in Sichuan, providing a comprehensive record of 34 species across three orders, mainly in *Pleosporales*. In recent years, research has predominantly focused on ascomycetes and basidiomycetes from economic trees and crops, specifically emphasizing ascomycetes. Nevertheless, a systematic investigation of fungal pathogens on horticultural plants remains lacking.

Fungal pathogens pose a significant threat to horticultural plants, severely impacting the sustainability of related industries by diminishing yields, ornamental appeal, and the longevity of plants (Wang et al. 2022b, Zheng et al. 2022). At present, the conventional "one pathogen-one disease" theory is increasingly being challenged by empirical evidence supporting a multi-pathogen pathogenic system, wherein diseases are often influenced by two or more pathogens, giving rise to the concept of the pathobiome (Sweet & Bulling 2017, Bass et al. 2019, Han et al. 2023). The interaction system within the pathogen microbiome is notably intricate, with uncertain roles and relationships among potential pathogens, saprophytes, and endophytes. In this study, co-infections were frequently detected across various specific diseases. For instance, *Drepanopeziza brunnea*, *Paraphoma populi*, and *Pseudocercospora populina* were all isolated from the same regions of poplar leaf spots, each capable of inducing similar leaf necrotic lesions. Canker disease of *Ficus elastica*, attributed to *Botryosphaeria dothidea*, *Cytospora predappioensis*, and *Diaporthe eres*, led to leaf detachment and stem withering, ultimately resulting in plant death. Other host plant diseases

exhibit similar symptoms caused by various pathogens, including *Citrus reticulata*, *Salix* sp., and *Syagrus romanzoffiana*. Studying the species diversity and pathogenic mechanisms of plant pathogenic microbiomes is essential for accurate disease monitoring and effective control strategies, crucial in overcoming limitations in plant disease management.

The intricate nature of diseases and the wide array of pathogens make the accurate identification of disease-causing agents in the field a formidable challenge, consequently impeding the precise prevention and control of these ailments (Han et al. 2023, Kumari et al. 2024). Considerable research is still needed in horticultural plant diseases, covering disease symptom identification, pathogen molecular markers, pathogenesis, chemical control, and forest management (Meng et al. 2023, Wang et al. 2023c, Tang et al. 2024).

In summary, this study offers new insights into the fungal diversity present in symptomatic tissues of horticultural plants, spanning a range of conditions, including cankers, blights, powdery mildew, rot, sooty mold, scabs, spots, tarspot, smut, and anthracnose, predominantly affecting stems, twigs, and leaves. This investigation revealed that *Colletotrichum* (six species) and *Diaporthe* (four species) are the most diverse genera in horticultural plants, affecting a wide range of hosts and underscoring the need for further disease management research. Although these fungi were collected from diseased plant tissues, their pathogenicity has not been tested. The classification of them as pathogens is primarily based on previous records and symptoms observed in the wild. To confirm their pathogenicity, systematic evaluation through Koch's postulates is needed in future studies. The findings underscore prevalent fungal species linked to diseases in horticultural plants, serving as a foundational platform for investigating the incidence and management strategies of these diseases in China.

ACKNOWLEDGEMENTS

Chun-Lin Yang expresses gratitude for the support provided by the Sichuan Science and Technology Program (Grant No. 2022NSFSC1011). Xiu-Lan Xu acknowledges the support from the Sichuan Science and Technology Program (Grant No. 2024NSFSC1192).

Statements and Declarations

COMPETING INTERESTS

The authors declare no conflicts of interest regarding this article.

REFERENCES

Abdollahzadeh J, Groenewald JZ, Coetzee MPA, Wingfield MJ et al. 2020 – Evolution of lifestyles in *Capnodiales*. Studies in Mycology 95, 381–414.

Adams GC, Roux J, Wingfield MJ. 2006 – *Cytospora* species (*Ascomycota*, *Diaporthales*, *Valsaceae*), introduced and native pathogens of trees in South Africa. Australasian Plant Pathology 35, 521–548.

Adesemoye AO, Eskalen A. 2011 – First report of *Spencermartinsia viticola*, *Neofusicoccum australe*, and *N. parvum* causing branch canker of citrus in California. Plant Disease 95, 770.

Adesemoye AO, Mayorquin JS, Wang DH, Twizeyimana M et al. 2014 – Identification of species of *Botryosphaeriaceae* causing bot gummosis in *Citrus* in California. Plant Disease 98, 55–61.

Adhikari MK. 2017 – Researches on the Nepalese mycoflora 3: *Erysiphales* from Nepal Kathmandu, Nepal: Kamala S. Adhikari.

Aiello D, Guarnaccia V, Costanzo MB, Leonardi GR et al. 2022 – Woody canker and shoot blight caused by *Botryosphaeriaceae* and *Diaporthaceae* on mango and litchi in Italy. Horticulturae 8, 330.

Aime MC, Miller AN, Aoki T, Bensch K et al. 2021 – How to publish a new fungal species, or name, version 3.0. IMA Fungus 12, 11.

Alidadi A, Kowsari M, Javan-Nikkhah M, Ariyawansa HA et al. 2019 – *Deniquelata quercina* sp. nov.; a new endophyte species from Persian oak in Iran. Phytotaxa 405, 187–194.
Alizadeh M, Safaie N, Shams-Bakhsh M, Mehrabadi M. 2022 – *Neoscytalidium novaehollandiae* causes dieback on *Pinus eldarica* and its potential for infection of urban forest trees. Scientific Reports 12, 9337.
Al-Jaradi AJ, Maharachchikumbura SSN, Al-Sadi AM. 2020 – *Phaeosphaeriopsis omaniana* (*Phaeosphaeriaceae*, *Pleosporales*), a novel fungus from Oman. Phytotaxa 436, 187–192.
Aloi F, Riolo M, Parlascino R, Pane A et al. 2021 – Bot gummosis of lemon (*Citrus* × *limon*) caused by *Neofusicoccum parvum*. Journal of Fungi 7, 294.
Aluthmuhandiram JVS, Wanasinghe DN, Chethana KWT, Gafforov Y et al. 2022 – *Lophiostomataceae* (*Dothideomycetes*): Introducing *Lophiostoma khanzada-kirgizbaeva* sp. nov. and *Paucispora xishanensis* sp. nov. Phytotaxa 559, 247–262.
Alves A, Crous PW, Correia A, Phillips AJL. 2008 – Morphological and molecular data reveal cryptic speciation in *Lasiodiplodia theobromae*. Fungal Diversity 28, 1–13.
Amano K. 1986 – Host range and geographical distribution of the powdery mildew fungi. Tokyo: Japan Scientific Societies Press.
Andersen KL, Sebolt AM, Sundin GW, Iezzoni AF. 2018 – Assessment of the inheritance of resistance and tolerance in cherry (*Prunus* sp.) to *Blumeriella jaapii*, the causal agent of cherry leaf spot. Plant Pathology 67, 682–691.
Anderson FE, López SPS, Sánchez RM, Fuentealba CGR et al. 2016 – *Puccinia araujiae*, a promising classical biocontrol agent for moth plant in New Zealand: Biology, host range and hyperparasitism by *Cladosporium uredinicola*. Biological Control 95, 23–30.
Ariyawansa HA, Camporesi E, Thambugala KM, Mapook A et al. 2014b – Confusion surrounding *Didymosphaeria* – phylogenetic and morphological evidence suggest *Didymosphaeriaceae* is not a distinct family. Phytotaxa 176, 102–119.
Ariyawansa HA, Tanaka K, Thambugala KM, Phookamsak R et al. 2014a – A molecular phylogenetic reappraisal of the *Didymosphaeriaceae* (= *Montagnulaceae*). Fungal Diversity 68, 69–104.
Ashrafi S, Wennrich J-P, Becker Y, Maciá-Vicente JG et al. 2023 – *Polydomus karssenii* gen. nov. sp. nov. is a dark septate endophyte with a bifunctional lifestyle parasitising eggs of plant parasitic cyst nematodes (*Heterodera* spp.). IMA Fungus 14, 6.
Ayoubi N, Soleimani MJ. 2016 – Strawberry fruit rot caused by *Neopestalotiopsis iranensis* sp. nov., and *N. mesopotamica*. Current Microbiology 72, 329–336.
Baggio JS, Forcelini BB, Wang NY, Ruschel RG. 2021 – Outbreak of leaf spot and fruit rot in florida strawberry caused by *Neopestalotiopsis* spp. Plant Disease 105, 305–315.
Bakhshi M, Arzanlou M, Babai-Ahari A, Groenewald JZ et al. 2014 – Multi-gene analysis of *Pseudocercospora* spp. from Iran. Phytotaxa 184, 245–264.
Bakhshi M, Braun U. 2022 – *Acericercospora hyrcanica* gen. et sp. nov. (*Mycosphaerellaceae*) and *Paramycocentrospora acericola* gen. et sp. nov. (*Dothidotthiaceae*) on maple trees in Hyrcanian forests. Mycological Progress 21, 71.
Bakhshizadeh M, Hashemian HR, Najafzadeh MJ, Dolatabadi S et al. 2014 – First report of rhinosinusitis caused by *Neoscytalidium dimidiatum* in Iran. Journal of Medical Microbiology 63, 1017–1019.
Bánki O, Roskov Y, Döring M, Ower G et al. 2023 – Catalogue of Life Checklist (Version 2023-08-17). Catalogue of Life. https://doi.org/10.48580/dft7
Bao DF, Hyde KD, Maharachchikumbura SSN, Perera RH et al. 2023 – Taxonomy, phylogeny and evolution of freshwater *Hypocreomycetidae* (*Sordariomycetes*). Fungal Diversity 121, 1–94.
Bao DF, Su HY, Maharachchikumbura SSN, Liu JK et al. 2019 – Lignicolous freshwater fungi from China and Thailand: Multi-gene phylogeny reveals new species and new records in *Lophiostomataceae*. Mycosphere 10, 1080–1099.

Baral H-O, Sochorová Z, Sochor M. 2023 – *Bryorutstroemia* (*Rutstroemiaceae*, *Helotiales*), a new genus to accommodate the neglected sclerotiniaceous bryoparasitic discomycete *Helotium fulvum*. Life 13, 1041.
Barber PA, Burgess TJ, Hardy GEJ, Slippers B et al. 2005 – *Botryosphaeria* species from *Eucalyptus* in Australia are pleoanamorphic, producing *Dichomera synanamorphs* in culture. Mycological Research 109, 1347–1363.
Barr ME. 1978 – The *Diaporthales* in North America with emphasis on *Gnomonia* and its segregates. Mycologia memoir 7, 1–232.
Barr ME. 1979 – A classification of *Loculoascomycetes*. Mycologia 71, 935–957.
Barr ME. 1983 – The ascomycete connection. Mycologia 75, 1–13.
Barr ME. 1991 – Revisions and additions to the *Diaporthales*. Mycotaxon 41, 287–305.
Bass D, Stentiford GD, Wang HC, Koskella B et al. 2019 – The pathobiome in animal and plant diseases. Trends in Ecology and Evolution 34, 996–1008.
Batista AC, Ciferri R. 1963 – *Capnodiales*. Saccardoa 2, 1–296.
Batista AC, Maia HS. 1960 – *Discomycetes* alienigenas (1). Saccardoa 1, 98–102.
Batista E, Lopes A, Alves A. 2021 – What do we know about *Botryosphaeriaceae*? An overview of a worldwide cured dataset. Forests 12, 313.
Begerow D, Bauer R, Oberwinkler F. 2001 – *Muribasidiospora*: *Microstromatales* or *Exobasidiales*? Mycological Research 105, 798–810.
Begerow D, Bauer R, Oberwinkler F. 2002 – The *Exobasidiales*: An evolutionary hypothesis. Mycological Progress 1, 187–199.
Bensch K, Braun U, Groenewald JZ, Crous PW. 2012 – The genus *Cladosporium*. Studies in Mycology 72, 1–401.
Bhunjun CS, Niskanen T, Suwannarach N, Wannathes N et al. 2022 – The numbers of fungi: Are the most speciose genera truly diverse? Fungal Diversity 114, 387–462.
Bhunjun CS, Phukhamsakda C, Jayawardena RS, Jeewon R et al. 2021 – Investigating species boundaries in *Colletotrichum*. Fungal Diversity 107, 107–127.
Blechert O, Debener T. 2015 – Morphological characterization of the interaction between *Diplocarpon rosae* and various rose species. Plant Pathology 54, 82–90.
Blumer S. 1933 – Die Erysiphaceen Mitteleuropas mit besonderer Berucksichtigung der Schweiz. Beiträge zur Kryptogamenflora der Schweiz., 7, 483 pp, 167 figs.
Boedijn KB. 1961 – *Myriangiales* from Indonesia. Persoonia 2, 63–75.
Bolay A, Clerc P, Braun U, Götz M et al. 2021 – New species, new records and first sequence data of powdery mildews (*Erysiphaceae*) from Europe with special emphasis on Switzerland. Austrian Journal of Mycology 28, 131–160.
Bradshaw MJ, Quijada L, Tobin PC, Braun U et al. 2022 – More than just plants: Botanical gardens are an untapped source of fungal diversity. HortScience 57, 1289–1293.
Braun U, Cook RT. 2012 – Taxonomic manual of the *Erysiphales* (powdery mildews): CBS-KNAW Fungal Biodiversity Centre Utrecht, The Nettherlands.
Braun U, Crous PW, Nakashima C. 2014 – Cercosporoid fungi (*Mycosphaerellaceae*) 2. Species on monocots (*Acoraceae* to *Xyridaceae*, excluding *Poaceae*). IMA Fungus 5, 203–390.
Braun U, Crous PW, Nakashima C. 2016 – Cercosporoid fungi (*Mycosphaerellaceae*) 5. Species on dicots (*Anacardiaceae* to *Annonaceae*). IMA Fungus 7, 161–216.
Braun U, Hill CF, Schubert K. 2006 – New species and new records of biotrophic micromycetes from Australia, Fiji, New Zealand and Thailand. Fungal Diversity 22, 13–35.
Braun U, Nakashima C, Bakhshi M, Zare R et al. 2020 – Taxonomy and phylogeny of cercosporoid ascomycetes on *Diospyros* spp. with special emphasis on *Pseudocercospora* spp. Fungal Systematics and Evolution 6, 95–127.
Braun U, Nakashima C, Crous PW. 2013 – Cercosporoid fungi (*Mycosphaerellaceae*) 1. Species on other fungi, Pteridophyta and Gymnospermae. IMA Fungus 4, 265-345.
Braun U. 1995 – A monograph of *Cercosporella*, *Ramularia* and allied genera (Phytopathogenic hyphomycetes). Eching, Germany: Ihw-Verlag.

Braun U. 2013 – Proposals to conserve the teleomorph–typified name *Blumeria* against the anamorph–typified name *Oidium* and twenty–two teleomorph–typified powdery mildew species names against competing anamorph–typified names (*Ascomycota*: *Erysiphaceae*). Taxon 62, 1328–1331.

Budziszewska J, Szypula W, Wilk M, Wrzosek M. 2011 – *Paraconiothyrium babiogorense* sp. nov., a new endophyte from fir club moss *Huperzia selago* (*Huperziaceae*). Mycotaxon 115, 457–468.

Busby PE, Zimmerman N, Weston DJ, Jawdy SS et al. 2013 – Leaf endophytes and *Populus* genotype affect severity of damage from the necrotrophic leaf pathogen, *Drepanopeziza populi*. Ecosphere 4, 1–12.

Cai L, Hyde KD, Taylor PWJ, Weir BS et al. 2009 – A polyphasic approach for studying *Colletotrichum*. Fungal Diversity 39, 183–204.

Calvillo-Medina RP, Martínez-Neria M, Mena-Portales J, Barba-Escoto L et al. 2019 – Identification and biofilm development by a new fungal keratitis aetiologic agent. Mycoses 62, 62–72.

Cannon PF, Buddie AG, Bridge PD. 2008 – The typification of *Colletotrichum gloeosporioides*. Mycotaxon 104, 189–204.

Cannon PF, Damm U, Johnston PR, Weir BS. 2012 – *Colletotrichum* – current status and future directions. Studies in Mycology 73, 181–213.

Cannon PF. 1991 – A revision of *Phyllachora* and some similar genera on the family Leguminosae. Mycological Papers 163, 1–302.

Carbone I, Kohn LM. 1999 – A method for designing primer sets for speciation studies in filamentous ascomycetes. Mycologia 91, 553–556.

Castlebury LA, Rossman AY, Jaklitsch WJ, Vasilyeva LN. 2002 – A preliminary overview of the *Diaporthales* based on large subunit nuclear ribosomal DNA sequences. Mycologia 94, 1017–1031.

Cesati V, Notaris GD. 1863 – Schema diclassificazione degli sferiacei italici aschigeri piu'o meno appartenenti al genere Sphaerianell'antico significato attribuitoglide Persoon. Commentario della Società Crittogamologica Italiana 14, 177–240.

Chadefaud M. 1960 – Les végétaux non vasculaires (Cryptogamie). In: Traité de botanique systématique. Tome I (Chadefaud M, Emberger L, eds), Masson et Cie, Paris, France.

Chaisiri C, Liu X, Lin Y, Fu Y et al. 2021 – Phylogenetic and haplotype network analyses of *Diaporthe eres* species in China based on sequences of multiple loci. Biology 10, 179.

Chaverri P, Salgado C, Hirooka Y, Rossman AY et al. 2011 – Delimitation of *Neonectria* and *Cylindrocarpon* (*Nectriaceae*, *Hypocreales*, *Ascomycota*) and related genera with *Cylindrocarpon*-like anamorphs. Studies in Mycology 68, 57–78.

Chen F, Song YF, Li XJ, Chen JH et al. 2019 – Genome sequences of horticultural plants: Past, present, and future. Horticulture Research 6, 112.

Chen SF, Morgan DP, Hasey JK, Anderson K et al. 2014 – Phylogeny, morphology, distribution, and pathogenicity of *Botryosphaeriaceae* and *Diaporthaceae* from English walnut in California. Plant Disease 98, 636–652.

Chen YP, Su PW, Hyde KD, Maharachchikumbura SSN. 2023a – Phylogenomics and diversification of *Sordariomycetes*. Mycosphere 14, 414–451.

Chen YP, Su PW, Stadler M, Xiang R et al. 2023b – Beyond observation: Genomic traits and machine learning algorithms for predicting fungal lifestyles. Mycosphere 14, 1530–1563.

Chen YP, Wu T, Tian WH, Ilyukhin E et al. 2022 – Comparative genomics provides new insights into the evolution of *Colletotrichum*. Mycosphere 13, 134–187.

Chen YY, Dissanayake AJ, Liu ZY, Liu JK. 2020 – Additions to Karst Fungi 4: *Botryosphaeria* spp. associated with woody hosts in Guizhou province, China including *B. guttulata* sp. nov. Phytotaxa 454, 186–202.

Chethana KW, Manawasinghe IS, Hurdeal VG, Bhunjun CS et al. 2021 – What are fungal species and how to delineate them? Fungal Diversity 109, 1–25.

Choi JK, Kim JJ, Chung TS. 1998 – Scab disease of Aralia elata caused by *Elsinoë araliae*. Korean Journal Plant Pathology 14, 545–547.
Chomnunti P, Hongsanan S, Aguirre-Hudson B, Tian Q et al. 2014 – The sooty moulds. Fungal Diversity 66, 1–36.
Chomnunti P, Schoch CL, Aguirre-Hudson B, KoKo TW et al. 2011 – *Capnodiaceae*. Fungal Diversity 51, 103–134.
Chung D, Kim H, Choi HS. 2019 – Fungi in salterns. Journal of Microbiology 57, 717–724.
Churchill ACL. 2011 – *Mycosphaerella fijiensis*, the black leaf streak pathogen of banana: progress towards understanding pathogen biology and detection, disease development, and the challenges of control. Molecular Plant Pathology 12, 307–328.
Clements FE, Shear CL. 1931 – The genera of fungi. The H.W. Wilson Company, New York.
Clendenin I. 1896 – *Lasiodiplodia* Ellis & Everh. n. gen. Botanical Gazette Crawfordsville 21, 92–93.
Condé BD, Pitkethley RN, Smith ESC, Kulkarni VJ et al. 1997 – Disease notes or new records: Identification of mango scab caused by *Elsinoë mangiferae* in Australia. Australasian Plant Pathology 26, 131.
Corda ACJ. 1831 – Die Pilze Deutschlands. In: Deutschlands Flora in Abbildungen nach der Natur mit Beschreibungen (Sturm, J, ed.). Sturm, Nürnberg vol. 3, Abt. 12: 33–64, tab. 21–32.
Corda ACJ. 1842 – Icones Fungorum Hucusque Cognitorum 5, 1–92.
Coutinho IBL, Cardoso JE, Lima CS, Lima JS et al. 2018 – An emended description of *Neofusicoccum brasiliense* and characterization of *Neoscytalidium* and *Pseudofusicoccum* species associated with tropical fruit plants in northeastern Brazil. Phytotaxa 358, 251–264.
Crouch J, O'Connell R, Gan P, Buiate E, Torres MF, Beirn L, Shirasu K, Vaillancourt L. The genomics of *Colletotrichum*. In: Dean AR, Lichens-Park A, Kole C, editors. Genomics of plant-associated Fungi: Monocot pathogens. Berlin, Heidelberg: Springer Berlin Heidelberg; 2014. p. 69–102.
Crous PW, Aptroot A, Kang JC, Braun U et al. 2000 – The genus *Mycosphaerella* and its anamorphs. Studies in Mycology 45, 107–121.
Crous PW, Braun U, Hunter GC, Wingfield MJ et al. 2013a – Phylogenetic lineages in *Pseudocercospora*. Studies in Mycology 75, 37–114.
Crous PW, Braun U, Wingfield MJ, Wood AR et al. 2009b – Phylogeny and taxonomy of obscure genera of microfungi. Persoonia 22, 139–161.
Crous PW, Gams W, Stalpers JA, Robert V et al. 2004a – MycoBank: An online initiative to launch mycology into the 21st century. Studies in Mycology 50, 19–22.
Crous PW, Groenewald JZ, Risède J-M, Simoneau P et al. 2004b – *Calonectria* species and their *Cylindrocladium* anamorphs: Species with sphaeropedunculate vesicles. Studies in Mycology 50, 415–430.
Crous PW, Hernández-Restrepo M, Schumacher RK, Cowan DA et al. 2021 – New and interesting fungi. 4. Fungal Systematics and Evolution 7, 255–343.
Crous PW, Quaedvlieg W, Sarpkaya K, Can C et al. 2013b – *Septoria*-like pathogens causing leaf and fruit spot of pistachio. IMA Fungus 4, 187–199.
Crous PW, Schoch CL, Hyde KD, Wood AR et al. 2009a – Phylogenetic lineages in the *Capnodiales*. Studies in Mycology 64, 17–47.
Crous PW, Slippers B, Wingfield MJ, Rheeder J et al. 2006 – Phylogenetic lineages in the *Botryosphaeriaceae*. Studies in Mycology 55, 235–253.
Crous PW, Summerell BA, Shivas RG, Romberg M et al. 2011 –Fungal Planet description sheets: 92–106. Persoonia. 27, 130–162.
Daengsuwan W, Wonglom P, Arikit S, Sunpapao A. 2021 – Morphological and molecular identification of *Neopestalotiopsis clavispora* causing flower blight on *Anthurium andraeanum* in Thailand. Horticultural Plant Journal 7, 573–578.
Damm U, Cannon PF, Woudenberg JHC, Johnston PR. 2012 – The *Colletotrichum boninense* species complex. Studies in Mycology 73, 1–36.

Damm U, Sato T, Alizadeh A, Groenewald JZ. 2019 – The *Colletotrichum dracaenophilum*, *C. magnum* and *C. orchidearum* species complexes. Studies in Mycology 92, 1–46.
Damm U, Verkley GJM, Crous PW, Fourie PH et al. 2008 – Novel *Paraconiothyrium* species on stone fruit trees and other woody hosts. Persoonia 20, 9–17.
Daranagama DA, Hyde KD, Sir EB, Thambugala KM et al. 2018 – Towards a natural classification and backbone tree for *Graphostromataceae*, *Hypoxylaceae*, *Lopadostomataceae* and *Xylariaceae*. Fungal Diversity 88, 1–165.
Darsaraei H, Khodaparast SA, Takamatsu S, Abbasi M et al. 2021 – Phylogeny and taxonomy of the *Erysiphe adunca* complex (*Erysiphaceae*, *Helotiales*) on poplars and willows. Mycological Progress 20, 517–537.
David J. 1997 – A contribution to the systematics of *Cladosporium*: Revision of the fungi previously referred to heterosporium. CAB International, Wallingford, Oxon, UK, 157 pp.
de Gruyter J, Woudenberg JHC, Aveskamp MM, Verkley GJM et al. 2013 – Redisposition of Phoma-like anamorphs in *Pleosporales*. Studies in Mycology 75, 1–36.
de Jesus JMI, Rodrigues ABL, de Paula KLM, da Cunha MG. 2022 –*Pestalotiopsis microspora* causes leaf spot on *Adenium obesum*. Journal of Phytopathology 170, 408–413.
de Silva NI, Maharachchikumbura SSN, Thambugala KM, Bhat DJ et al. 2021 – Morpho-molecular taxonomic studies reveal a high number of endophytic fungi from *Magnolia candolli* and *M. garrettii* in China and Thailand. Mycosphere 12, 163–237.
de Silva NI, Phillips AJL, Liu JK, Lumyong S et al. 2019 – Phylogeny and morphology of *Lasiodiplodia* species associated with magnolia forest plants. Scientific Reports 9, 14355.
de Sousa Poltronieri TP, Verzignassi JR, Benchimol RL, Poltronieri LS et al. 2012 – Ocorrência de *Graphiola phoenicis* em tamareira no Maranhão. Summa Phytopathologica 38, 253.
Deighton FC. 1976 – Studies on *Cercospora* and allied genera. VI. *Pseudocercospora* Speg., *Pantospora* Cif. and *Cercoseptoria* Petr. Mycological Papers 140, 1–168.
Denman S, Crous PW, Taylor JE, Kang JC et al. 2000 – An overview of the taxonomic history of Botryosphaeria and a re-evaluation of its anamorphs based on morphology and ITS rDNA phylogeny. Studies in Mycology 45, 129–140.
Devadatha B, Jones EBG, Wanasinghe DN, Bahkali AH et al. 2023 – Characterization of novel estuarine *Ascomycota* based on taxonomic and phylogenetic evaluation. Botanica Marina 66, 1–18.
Diogo E, Silva AC, Bragança H, Phillips AJL et al. 2021 – Five new species of *Neopestalotiopsis* associated with diseased *Eucalyptus* spp. in Portugal. Mycological Progress 20, 1441–1456.
Dissanayake AJ, Liu M, Zhang W, Chen Z et al. 2015 – Morphological and molecular characterization of *Diaporthe* species associated with grapevine trunk disease in China. Fungal Biology 119, 283–294.
Dissanayake AJ, Phillips AJL, Hyde KD, Yan JY et al. 2017a – The current status of species in *Diaporthe*. Mycosphere 8, 1106–1156.
Dissanayake AJ, Zhang W, Liu M, Hyde KD et al. 2017b – *Diaporthe* species associated with peach tree dieback in Hubei, China. Mycosphere 8, 533–549.
Dissanayake AJ, Zhu JT, Chen YY, Maharachchikumbura SSN et al. 2024 – A re-evaluation of *Diaporthe*: Refining the boundaries of species and species complexes. Fungal Diversity 126, 1–125.
Domínguez BIA, López-Moral A, Raya-Ortega MC, Lovera M et al. 2023 – Fungal pathogens associated with almond decline syndrome, an emerging disease complex in intensive almond crops in southern Spain. Plant Disease 107, 1716–1726.
Dos Santos MDM, de Noronha Fonseca ME, Boiteux LS, Câmara PEAS et al. 2016 – ITS phylogeny and taxonomy of *Phyllachora* species on native *Myrtaceae* from the Brazilian Cerrado. Mycologia 108, 1141–1164.
Du Y, Wang X, Guo Y, Xiao F et al. 2021 – Biological and molecular characterization of seven *Diaporthe* species associated with kiwifruit shoot blight and leaf spot in China. Phytopathologia Mediterranea 60, 177–198.

Dudka VA, Zmitrovich IV. 2021 – A critical catalogue of *Exobasidiales* (*Exobasidiomycetes*, *Basidiomycota*) of north-temperate Eurasia. Nova Hedwigia 113, 403–427.
Ehrenberg CG. 1818 – Sylvae Mycologicae Berolinenses. Formis Theophili Bruschcke, Berlin, Germany.
Ellis MB. 1961 – Dematiaceous hyphomycetes. III. Mycological Papers 82, 1–55.
Engler A, Prantl K. 1896 – Die Natürlichen Pflanzenfamilien, Teil 4, Abt. 3a; Wilhelm Engelmann: Leipzig, Gemany, pp. 302–303.
Etayo J, Flakus A, Kukwa M, Flakus PR. 2013 – *Lichenochora tertia* (*Phyllachorales*): The third species of the genus growing on *Xanthoria elegans*. Mycotaxon 113, 9–13.
Fan XL, Barreto RW, Groenewald JZ, Bezerra JDP et al. 2017 – Phylogeny and taxonomy of the scab and spot anthracnose fungus *Elsinoë* (*Myriangiales*, *Dothideomycetes*). Studies in Mycology 87, 1–41.
Fan XL, Bezerra JD, Tian CM, Crous PW. 2020 – *Cytospora* (*Diaporthales*) in China. Persoonia 45, 1–45.
Fan XL, Hyde KD, Liu M, Liang YM et al. 2015a – *Cytospora* species associated with walnut canker disease in China, with description of a new species *C. gigalocus*. Fungal Biology 119, 310–319.
Fan XL, Hyde KD, Yang Q, Liang YM et al. 2015b – *Cytospora* species associated with canker disease of three anti-desertification plants in northwestern China. Phytotaxa 197, 227–244.
Fan XL, Liang YM, Ma R, Tian CM. 2014 – Morphological and phylogenetic studies of *Cytospora* (*Valsaceae*, *Diaporthales*) isolates from Chinese scholar tree, with description of a new species. Mycoscience 55, 252–259.
Fernández-Herrera E, Moreno-Salazar SF, Rentería-Martínez ME, Arratia-Castro AA et al. 2017 – *Neoscytalidium dimidiatum*: Causal agent of dieback in *Ficus benjamina* L. in Mexico. Revista Chapingo Serie Horticultura 23, 203–210.
French AM. 1989 – California plant disease host index. California Dept. of Food and Agriculture, Sacramento. Calif.: 394.
Fries EM. 1825 – Systema orbis vegetabilis. Pars 1. Plantae homonemeae. Typographia Academica, Lund, Sweden.
Fries EM. 1832 – Systema Mycologicum 3(2): i–ii, 261–524. Sumptibus Ernesti Mauritii, Greifswald.
Fries EM. 1849 – Summa vegetabilium Scandinaviae. Typographis Academica, Uppsala.
Fu M, Crous PW, Bai Q, Zhang PF et al. 2019 – *Colletotrichum* species associated with anthracnose of *Pyrus* spp. in China. Persoonia 42, 1–35.
Fu RT, Wang J, Chen C, Ke YX et al. 2021 – Fungal disease survey and pathogen identification on *Paris polyphylla* var. *chinensis* in Sichuan. Molecular Plant Breeding 19, 209–217.
Fuckel L. 1869 – Symbolae mycologicae. Beiträge zur Kenntnis der rheinischen Pilze. Julius Niedner, Wiesbaden.
Gao Y, Liu F, Duan W, Crous PW et al. 2017 – *Diaporthe* is paraphyletic. IMA Fungus 8, 153–187.
Gao YQ, Du ST, Xiao J, Wang DC et al. 2020 – Isolation and characterization of antifungal metabolites from the *Melia azedarach*-associated fungus *Diaporthe eucalyptorum*. Journal of Agricultural and Food Chemistry 68, 2418–2425.
Giraldo A, Crous PW. 2019 – Inside *Plectosphaerellaceae*. Studies in Mycology 92, 227–286.
Glass NL, Donaldson GC. 1995 – Development of primer sets designed for use with the PCR to amplify conserved genes from filamentous ascomycetes. Applied and Environmental Microbiology 61, 1323–1330.
Glienke C, Pereira OL, Stringari D, Fabris J et al. 2011 – Endophytic and pathogenic *Phyllosticta* species, with reference to those associated with *Citrus* black spot. Persoonia 26, 47–56.
Golovin PN. 1958 – Obsor radov semejstva *Erysiphaceae*. Sborn. Rabot. Inst. Priel. Zool. Phytopathol. Leningrad, 5, 101–139.

Gomes RR, Glienke C, Videira SIR, Lombard L et al. 2013 – *Diaporthe*: A genus of endophytic, saprobic and plant pathogenic fungi. Persoonia 31, 1–41.
Gomzhina MM, Gasich1 EL, Khlopunova BL, Gannibal PB et al. 2020 – *Paraphoma* species associated with *Convolvulaceae*. Mycological Progress 19, 185–194.
Gonçalves RM, Figueiredo JEF, Pedro ES, Meirelles WF et al. 2013 – Etiology of *Phaeosphaeria* leaf spot disease of maize. Journal of Plant Pathology 95, 559–569.
Gong CW, Qin YM, Qu JS, Wang XG. 2018 – Resistance detection and mechanism of strawberry Botrytis cinerea to fludioxonil in Sichuan Province. Scientia Agricultura Sinica 51, 4277–4287.
Gräfenhan T, Schroers HJ, Nirenberg HI, Seifert KA. 2011 – An overview of the taxonomy, phylogeny, and typification of nectriaceous fungi in *Cosmospora*, *Acremonium*, *Fusarium*, *Stilbella*, and *Volutella*. Studies in Mycology 68, 79–113.
Gregorio-Cipriano R, Gonzalez D. 2022 – Molecular identification of mating types in populations of *Podosphaera xanthii* (*Erysiphaceae*) infecting cucurbits in Veracruz, Mexico. Acta Botánica Mexicana 129, e2068.
Gremmen J. 1965 – Three poplar-inhabiting *Drepanopeziza* species and their life-history. Nova Hedwigia 9, 170–176.
Guarnaccia V, Gehrmann T, Silva-Junior GJ, Fourie PH et al. 2019 – *Phyllosticta citricarpa* and sister species of global importance to *Citrus*. Molecular Plant Pathology 20, 1619–1635.
Guarnaccia V, Martino I, Tabone G, Crous PW et al. 2022 – *Paraphoma garibaldii* sp. nov. causing leaf spot disease of *Campanula rapunculoides* in Italy. Fungal Systematics and Evolution 8, 19–26.
Guarro J. 2013 – Fusariosis, a complex infection caused by a high diversity of fungal species refractory to treatment. European Journal of Clinical Microbiology & Infectious Diseases 32, 1491–1500.
Guatimosim E, Schwartsburd PB, Barreto RW, Crous PW. 2016 – Novel fungi from an ancient niche: Cercosporoid and related sexual morphs on ferns. Persoonia 37, 106–141.
Gullino ML, Daughtrey ML, Garibaldi A, Elmer WH. 2015 – *Fusarium* wilts of ornamental crops and their management. Crop Protection 73, 50–59.
Guo YS, Crous PW, Bai Q, Fu M et al. 2020 – High diversity of *Diaporthe* species associated with pear shoot canker in China. Persoonia 45, 132–162.
Guterres DC, dos Santos MdDM, Furlanetto C, Pinho DB et al. 2022 – Filling a gap in the taxonomy of phyllachoroid fungi: Proposition of *Neopolystigma*, gen. nov., and the new family *Neopolystigmataceae*. Mycologia 114, 900–913.
Haelewaters D, Park D, Johnston PR. 2021 – Multilocus phylogenetic analysis reveals that *Cyttariales* is a synonym of *Helotiales*. Mycological Progress 20, 1323–1330.
Haituk S, Suwannarach N, Hongsanan S, Senwanna C et al. 2021 – New epiphytic sooty molds: *Alloscorias syngonii* (*Readerielliopsidaceae*) from Thailand. Phytotaxa 507, 271–282.
Hall TA. 1999 – BioEdit: A user-friendly biological sequence alignment editor and analysis program for Windows 95/98/NT. Nucleic Acids Symposium Series 41, 95–98.
Hamayun M, Afzal Khan S, Ahmad N, Tang DS et al. 2009 – *Cladosporium sphaerospermum* as a new plant growth-promoting endophyte from the roots of *Glycine max* (L.) Merr. World Journal of Microbiology & Biotechnology 25, 627–632.
Han SL, Wang MM, Ma ZY, Raza M et al. 2023 – *Fusarium* diversity associated with diseased cereals in China, with an updated phylogenomic assessment of the genus. Studies in Mycology 104, 87–148.
Han YT, Chen JX, Tang J, Lv ZJ et al. 2021 – First report of *Neovaginatispora fuckelii* causing stem blight on *Rosa chinensis* in China. Journal of Plant Pathology 103, 1351–1352.
Hanifeh S, Zafari D, Soleimani MJ, Arzanlou M. 2022 – Multigene phylogeny, morphology, and pathogenicity trials reveal novel *Cytospora* species involved in perennial canker disease of apple trees in Iran. Fungal Biology 126, 707–726.

Hashimoto A, Hirayama K, Takahashi H, Matsumura M et al. 2018 – Resolving the *Lophiostoma bipolare* complex: Generic delimitations within *Lophiostomataceae*. Studies in Mycology 90, 161–189.
Hattori Y, Ando Y, Sasaki A, Uechi N et al. 2021 – Taxonomical study of noteworthy species of *Botryosphaeria* in Japan. Mycobiology 49, 122–132.
Hattori Y, Nakano L, Nakashim C. 2023 – Taxonomic re-examination of Japanese isolates of the genus *Lasiodiplodia*. Mycoscience 64, 74–82.
Hawksworth DL, David JC. 1989 – Family names: Index of Fungi supplement. Wallingford: CAB International.
He X, Zhao CL. 2022 – Diversity of wood-decaying fungi in Wuliangshan area, Yunnan Province, P.R. China. Diversity 14, 131.
Hennings P. 1900 – *Exobasidiineae*. In: Engler A, Prantl K (eds) Die natürlichen Pflanzenfamilien Verlag W. Engelman, Leipzig 1, 103–105.
Heuchert B, Braun U, Schubert K. 2005 – Morphotaxonomic revision of fungicolous *Cladosporium* species (Hyphomycetes). Schlechtendalia 13, 1–78.
Hlaiem S, Yangui I, Rocca GD, Barberini S et al. 2022 – First report of *Pestalotiopsis biciliata* causing dieback on *Quercus coccifera* and *Pistacia lentiscus* in Tunisia. Canadian Journal of Plant Pathology 44, 534–541.
Holien H, Suija A. 2021 – *Caesiodiscus populicola* gen. et sp. nov. (*Leotiomycetes*, *Helotiales*), a remarkable new corticolous ascomycete from Norway. Agarica 42, 75–90.
Holm L, Holm K. 1988 – Studies in the *Lophiostomataceae* with emphasis on the Swedish species. Symbolae Botanicae Upsalienses 28, 1–50.
Holm L. 1957 – Etudes taxonomiques sur les pléosporacées. Symb Bot Upsaliens 14, 1–188.
Hongsanan S, Hyde KD, Phookamsak R, Wanasinghe DN et al. 2020 – Refined families of *Dothideomycetes*: *Dothideomycetidae* and *Pleosporomycetidae*. Mycosphere 11, 1553–2107.
Hongsanan S, Maharachchikumbura SSN, Hyde KD, Samarakoon MC et al. 2017 – An updated phylogeny of *Sordariomycetes* based on phylogenetic and molecular clock evidence. Fungal Diversity 84, 25–41.
Hongsanan S, Norphanphoun C, Senanayake IC, Jayawardena RS et al. 2023 – Annotated notes on *Diaporthe* species. Mycosphere 14, 918–1189.
Hongsanan S, Sánchez-Ramírez S, Crous PW, Ariyawansa HA et al. 2016 – The evolution of fungal epiphytes. Mycosphere 7, 1690–1712.
Hongsanan S, Tian Q, Hyde KD, Chomnunti P. 2015 – Two new species of sooty moulds, *Capnodium coffeicola* and *Conidiocarpus plumeriae* in *Capnodiaceae*. Mycosphere 6, 814–824.
Huang HY, Huang HH, Zhao DY, Shan TJ et al. 2022 – *Pseudocryphonectria elaeocarpicola* gen. et sp. nov. (*Cryphonectriaceae*, *Diaporthales*) causing stem blight of *Elaeocarpus* spp. in China. MycoKeys 91, 67–84.
Huang SK, Tangthirasunun N, Phillips AJL, Dai DQ et al. 2016 – Morphology and phylogeny of *Neoscytalidium orchidacearum* sp. nov. (*Botryosphaeriaceae*). Mycobiology 44, 79–84.
Huda-Shakirah AR, Nor NMIM, Zakaria L, Leong YH et al. 2022 – *Lasiodiplodia theobromae* as a causal pathogen of leaf blight, stem canker, and pod rot of *Theobroma cacao* in Malaysia. Scientific Reports 12, 8966.
Hughes SJ. 1976 – Sooty moulds. Mycologia 68, 451–691, 693–820.
Huson DH, Bryant D. 2006 – Application of phylogenetic networks in evolutionary studies. Molecular Biology and Evolution 23, 254–267.
Hyde KD, Chaiwan N, Norphanphoun C, Boonmee S et al. 2018 – Mycosphere notes 169–224. Mycosphere 9, 271–430.
Hyde KD, de Silva NI, Jeewon R, Bhat DJ et al. 2020c – AJOM new records and collections of fungi: 1–100. Asian Journal of Mycology 3, 22–294.

Hyde KD, Dong Y, Phookamsak R, Jeewon R et al. 2020d – Fungal diversity notes 1151–1276: Taxonomic and phylogenetic contributions on genera and species of fungal taxa. Fungal Diversity 100, 5–277.
Hyde KD, Jeewon R, Chen YJ, Bhunjun CS et al. 2020a – The numbers of fungi: Is the descriptive curve flattening? Fungal Diversity 103, 219–271.
Hyde KD, Jones EBG, Liu JK, Ariyawansa H et al. 2013 – Families of *Dothideomycetes*. Fungal Diversity 63, 1–313.
Hyde KD, Nilsson RH, Alias SA, Ariyawansa HA et al. 2014 – One stop shop: Backbones trees for important phytopathogenic genera: I (2014). Fungal Diversity 67, 21–125.
Hyde KD, Norphanphoun C, Abreu VP, Bazzicalupo A et al. 2017 – Fungal diversity notes 603–708: taxonomic and phylogenetic notes on genera and species. Fungal Diversity 87, 1–235.
Hyde KD, Norphanphoun C, Maharachchikumbura SSN, Bhat DJ et al. 2020b – Refined families of *Sordariomycetes*. Mycosphere 11, 305–1059.
Hyun JW, Timmer LW, Lee SC, Yun SH et al. 2001 – Pathological characterization and molecular analysis of *Elsinoë* isolates causing scab diseases of *Citrus* in Jeju Island in Korea. Plant Disease 85, 1013–1017.
Iliushin VA, Kirtsideli IY. 2023 – *Pseudoxenochalara* gen. nov. (*Dermateaceae*, *Helotiales*), with *P. grumantiana* sp. nov. from the Svalbard archipelago. Botanica Serbica 47, 55–63.
Ilyukhin E, Nguyen HDT, Castle AJ, Ellouze W. 2023 – *Cytospora paraplurivora* sp. nov. isolated from orchards with fruit tree decline syndrome in Ontario, Canada. Plos One 18, e0279490.
Inuma T, Khodaparast SA, Takamatsu S. 2007 – Multilocus phylogenetic analyses within *Blumeria graminis*, a powdery mildew fungus of cereals. Molecular Phylogenetics and Evolution 44, 741–51.
Itagaki H, Hosoya T. 2023 – A new genus *Neobelonopsis* and two new species of *Trichobelonium* (*Helotiales*, *Ascomycota*) discovered mainly from poaceous grasses native to Asia in Japan. MycoKeys 99, 45–85.
Iturrieta-González I, García D, Gené J. 2021 – Novel species of *Cladosporium* from environmental sources in Spain. MycoKeys 77, 1–25.
Jaczewski AA. 1917 – Key to Fungi. Vol. II. Fungi Imperfecti. Publishing House of SL Kind, Petrograd (In Russian).
Jamali S. 2020 – First report of *Paraconiothyrium fuckelii* (*Didymosphaeriaceae*, *Pleosporales*), causing stem canker in *Rosa hybrida*, from Iran. Czech Mycology 72, 71–82.
Jamali S. 2024 – *Myxotrichum*, a new genus for the funga of Iran. Rostaniha 24, 182–186.
Janick J, Goldman IL. 2003 – Horticulture, horticultural science, and 100 years of ASHS. HortScience 38, 883–900.
Jayasiri SC, Hyde KD, Ariyawansa HA, Bhat J et al. 2015 – The Faces of Fungi database: Fungal names linked with morphology, phylogeny and human impacts. Fungal Diversity 74, 3–18.
Jayasiri SC, Hyde KD, Jones EBG, McKenzie EHC et al. 2019 – Diversity, morphology and molecular phylogeny of *Dothideomycetes* on decaying wild seed pods and fruits. Mycosphere 10, 1–186.
Jayawardena RS, Ariyawansa HA, Singtripop C, Li YM et al. 2014 – A re-assessment of *Elsinoaceae* (*Myriangiales*, *Dothideomycetes*). Phytotaxa 176, 120–138.
Jayawardena RS, Bhunjun CS, Hyde KD, Gentekaki E et al. 2021b – *Colletotrichum*: Lifestyles, biology, morpho-species, species complexes and accepted species. Mycosphere 12, 519–669.
Jayawardena RS, Hyde KD, de Farias ARG, Bhunjun CS et al. 2021a – What is a species in fungal plant pathogens? Fungal Diversity 109, 239–266.
Jayawardena RS, Hyde KD, Jeewon R, Ghobad-Nejhad M et al. 2019 – One stop shop II: Taxonomic update with molecular phylogeny for important phytopathogenic genera: 26–50 (2019). Fungal Diversity 94, 41–129.
Jayawardena RS, Hyde KD, Wang S, Sun YR et al. 2023 – Fungal diversity notes 1512–1610: Taxonomic and phylogenetic contributions on genera and species of fungal taxa. Fungal Diversity 117, 1–272.

Jeewon R, Hyde KD. 2016 – Establishing species boundaries and new taxa among fungi: Recommendations to resolve taxonomic ambiguities. Mycosphere 7, 1669–1677.
Jeger M, Bragard C, Caffier D, Candresse T et al. 2018 – Pest categorisation of *Mycodiella laricis-leptolepidis*. EFSA Journal 16, e05246.
Jia HY, Li MY, Wang CX, Ma R. 2023a – Species diversity of *Phaeobotryon* associated with tree canker and dieback diseases in Xinjiang, China. Forests 14, 864.
Jia XT, Zheng X, Damm U, Lu X et al. 2023b – *Stenocarpella chrysopogonis*, a new species causing leaf streak disease of *Chrysopogon zizanioides* in southern China. Plant Disease 107, 3674–3686.
Jiang N, Bonthond G, Fan XL, Tian CM. 2018 – *Neopestalotiopsis rosicola* sp. nov. causing stem canker of *Rosa chinensis* in China. Mycotaxon, 133, 271–283.
Jiang N, Voglmayr H, Ma CY, Xue H et al. 2022a – A new *Arthrinium*-like genus of *Amphisphaeriales* in China. MycoKeys 92, 27–43.
Jiang N, Voglmayr H, Xue H, Piao CG et al. 2022b – Morphology and phylogeny of *Pestalotiopsis* (*Sporocadaceae*, *Amphisphaeriales*) from *Fagaceae* leaves in China. Microbiology Spectrum 10, e0327222.
Jiang N, Voglmayr H, Xue H, Piao CG et al. 2023a – Diversity of *Monochaetia* species from fagaceous leaf spots in China and pathogenicity for Chinese Chestnut. Microbiology Spectrum 11, e0004223.
Jiang N, Zhu YQ, Xue H, Piao CG et al. 2023 b – *Phaeotubakia lithocarpicola* gen. et sp. nov. (*Tubakiaceae*, *Diaporthales*) from leaf spots in China. MycoKeys 95, 15–25.
Johnston PR, Quijada L, Smith CA, Baral H-O et al. 2019 – A multigene phylogeny toward a new phylogenetic classification of *Leotiomycetes*. IMA Fungus 10, 1.
Kanetis L, Taliadoros D, Makris G, Christoforou M. 2022 – A novel *Seimatosporium* and other *Sporocadaceae* species associated with grapevine trunk diseases in Cyprus. Plants 11, 2733.
Karunarathna A, Papizadeh M, Senanayake IC, Jeewon R et al. 2017 – Novel fungal species of *Phaeosphaeriaceae* with an asexual/sexual morph connection. Mycosphere 8, 1818–1834.
Katoh K, Rozewicki J, Yamada KD. 2019 – MAFFT online service: multiple sequence alignment, interactive sequence choice and visualization. Briefings in Bioinformatics 20, 1160–1166.
Kenfaoui J, Radouane N, Mennani M, Tahiri A et al. 2022 – A panoramic view on grapevine trunk diseases threats: Case of *Eutypa* dieback, *Botryosphaeria* dieback, and *Esca* disease. Journal of Fungi 8, 595.
Khodaparast SA, Pourmoghaddam MJ, Amirmijani A, Byrami F. 2020 – Phylogenetic structure of the *Iranian capnodiaceous* sooty mould fungi inferred from the sequences of rDNA regions and *TEF*1-α. Mycological Progress 19, 155–169.
Kobayashi T. 1970 – Taxonomic studies of Japanese *Diaporthaceae* with special reference to their life-histories. Bulletin of the Government Forest Experiment Station 226, 1–242.
Konta S, Tibpromma S, Karunarathna SC, Samarakoon MC et al. 2023 – Morphology and multigene phylogeny reveal ten novel taxa in *Ascomycota* from terrestrial palm substrates (*Arecaceae*) in Thailand. Mycosphere 14, 107–152.
Koukol O, Maciá-Vicente JG. 2022 – *Leptodophora* gen. nov. (*Helotiales*, *Leotiomycetes*) proposed to accommodate selected root-associated members of the genus *Cadophora*. Czech Mycology 74, 57–66.
Kumar V, Cheewangkoon R, Gentekaki E, Maharachchikumbura SSN et al. 2019 – *Neopestalotiopsis alpapicalis* sp. nov. a new endophyte from tropical mangrove trees in Krabi Province (Thailand). Phytotaxa 393, 251–262.
Kumari A, Tapwal A, Thakur N. 2024 – *Ganoderma lucidum*: Insights on host range, diagnosis, and management strategies. Journal of Basic Microbiology 64, e2300769.
Kuo C-H, Hsieh S-Y, Goh T-K. 2022 – *Wenhsuisporus taiwanensis* gen. et sp. nov., a peculiar setose hyphomycete from submerged wood in Taiwan. Mycological Progress 21, 409–426.
Kusch S, Qian JZ, Loos A, Kümmel F et al. 2023 – Long-term and rapid evolution in powdery mildew fungi. Molecular Ecology 00, 1–22.

Kushwaha P, Singh R, Chaurasia B. 2020 – *Ramularia titarpaniensis* – a new species of ramularioid complex from central India. Phytotaxa 429, 274–280.
Lamprecht SC, Crous PW, Groenewald JZ, Tewoldemedhin YT et al. 2011 – *Diaporthaceae* associated with root and crown rot of maize. IMA Fungus 2, 13–24.
Lawrence DP, Holland LA, Nouri MT, Travadon R et al. 2018 – Molecular phylogeny of *Cytospora* species associated with canker diseases of fruit and nut crops in California, with the descriptions of ten new species and one new combination. IMA Fungus 9, 333–370.
Lawrence DP, Travadon R, Pouzoulet J, Rolshausen PE et al. 2017 – Characterization of *Cytospora* isolates from wood cankers of declining grapevine in North America, with the descriptions of two new *Cytospora* species. Plant Pathology 66, 713–725.
Lee W, Kim JS, Seo CW, Lee JW et al. 2023 – Diversity of *Cladosporium* (*Cladosporiales*, *Cladosporiaceae*) species in marine environments and report on five new species. MycoKeys 98, 87–111.
Lees AK, Hilton AJ. 2003 – Black dot (*Colletotrichum coccodes*): An increasingly important disease of potato. Plant Pathology 52, 3–12.
Lehman SG. 1923 – Pod and stem blight of soybean. Annals of the Missouri Botanical Garden 10, 111–178.
Lenné JM. 1990 – A world list of fungal diseases of tropical pasture species. Phytopathological Paper No. 31, 1–162.
Li GQ, Slippers B, Wingfield MJ, Chen SF. 2020 – Variation in *Botryosphaeriaceae* from *Eucalyptus* plantations in Yunnan Province in southwestern China across a climatic gradient. IMA Fungus 11, 22.
Li SD, Miao ZQ, Gao WD. 2011a – Challenges, opportunities and obligations in management of soilborne plant diseases in China. Chinese Journal of Biological Control 27, 433–440.
Li WJ, Bhat DJ, Camporesi E, Tian Q et al. 2015 – New asexual morph taxa in *Phaeosphaeriaceae*. Mycosphere 6, 681–708.
Li WL, Dissanayake AJ, Zhang T, Maharachchikumbura SSN et al. 2022a – Identification and pathogenicity of pestalotiod fungi associated with woody oil plants in Sichuan Province, China. Journal of Fungi 8, 1175.
Li WL, Liang RR, Dissanayake AJ, Liu JK. 2023a – Botryosphaerialean fungi associated with woody oil plants cultivated in Sichuan Province, China. MycoKeys 97, 71–116.
Li WL, Liang RR, Dissanayake AJ, Liu JK. 2023b – Mycosphere Notes 413–448: *Dothideomycetes* associated with woody oil plants in China. Mycosphere 14, 1436–1529.
Li YM, Wu H, Cheng H, Hyde KD. 2011b – Morphological studies in *Doithideomycetes*: *Elsinoë* (*Elsinoaceae*), *Butleria* and three excluded genera. Mycotaxon 115, 507–520.
Li YX, Lin L, Cao J, Gan MX et al. 2024 – Three new species of *Colletotrichum* (*Glomerellales*, *Glomerellaceae*) associated with walnut (*Juglans regia*) anthracnose from China. MycoKeys 108, 147–167.
Li YY, Wang MM, Groenewald M, Li AH et al. 2022b – Proposal of two new combinations, twenty new species, four new genera, one new family, and one new order for the anamorphic basidiomycetous yeast species in *Ustilaginomycotina*. Frontiers in Microbiology 12, 777338.
Lin L, Bezerra JDP, Tian CM, Fan XL. 2023 – Re-evaluation of the fungal diversity and pathogenicity of *Cytospora* species from *Populus* in China. Plant Disease 107, 83–96.
Lindau G. 1897 – *Hypocreales*. – In – Engler HA. & Prantl, KAE, (edition.), Die natiirli chen Pflanzenfamilien. Verlag W. Engelman, Leipzig 1, 343–372.
Link JHF. 1809 – Observationes in ordines plantarum naturales. Dissertatio 1ma. Magazin der Gesellschaft Naturforschender Freunde zu Berlin 3, 3–42.
Lipps S, Smith D, Telenko D, Paul P et al. 2022 – Identification of resistance for *Phyllachora maydis* of maize in exotic-derived germplasm. Crop Science 62, 859–866.
Literatus ICE, Maharachchikumbura SSN, Withee P, Haituk S et al. 2023 – Taxonomic and phylogenetic appraisal of a new holomorphic *Neophyllachora* species from Chiang Mai, Thailand. Phytotaxa 600, 259–271.

Liu F, Bonthond G, Groenewald JZ, Cai L et al. 2018 – *Sporocadaceae*, a family of coelomycetous fungi with appendage-bearing conidia. Studies in Mycology 92, 287–415.
Liu F, Ma ZY, Hou LW, Diao YZ et al. 2022c – Updating species diversity of *Colletotrichum*, with a phylogenomic overview. Studies in Mycology 101, 1–56.
Liu F, Tang G, Zheng X, Li Y et al. 2016 – Molecular and phenotypic characterization of *Colletotrichum* species associated with anthracnose disease in peppers from Sichuan Province, China. Scientific Reports 6, 32761.
Liu JK, Hyde KD, Jeewon R, Phillips AJL et al. 2017 – Ranking higher taxa using divergence times: A case study in *Dothideomycetes*. Fungal Diversity 84, 75–99.
Liu JK, Phookamsak R, Doilom M, Wikee S et al. 2012 – Toward a natural classification of *Botryosphaeriales*. Fungal Diversity 57, 149–210.
Liu JW, Manawasinghe IS, Liao XN, Mao J et al. 2023b – Endophytic *Colletotrichum* (*Sordariomycetes*, *Glomerellaceae*) species associated with *Citrus grandis* cv. "Tomentosa" in China. MycoKeys 95, 163–188.
Liu LJ, Yang CL, Xu XL, Wang X et al. 2022d – Unlocking the changes of phyllosphere fungal communities of fishscale bamboo (*Phyllostachys heteroclada*) under rhombic-spot disease stressed conditions. Forests 13, 185.
Liu M, Braun U, Takamatsu S, Hambleton S et al. 2021 – Taxonomic revision of *Blumeria* based on multi-gene DNA sequences, host preferences and morphology. Mycoscience 62, 143–165.
Liu NG, Ariyawansa HA, Hyde KD, Maharachchikumbura SSN et al. 2016 – Perspectives into the value of genera, families and orders in classification. Mycosphere 7, 1649–1668.
Liu S, Shen LL, Xu TM, Song CG et al. 2023c – Global diversity, molecular phylogeny and divergence times of the brown-rot fungi within the *Polyporales*. Mycosphere 14, 1564–1664.
Liu SB, Liu XY, Zhang ZX, Xia JW et al. 2022a – Three new species of *Microdochium* (*Sordariomycetes*, *Amphisphaeriales*) on *Miscanthus sinensis* and *Phragmites australis* from Hainan, China. Journal of Fungi 8, 577.
Liu SB, Zhang ZX, Liu RY, Mu TC et al. 2022b – Morphological and molecular identification of *Ellipsoidisporodochium* gen. nov. (*Tubakiaceae*, *Diaporthales*) in Hainan Province, China. Phytotaxa 552, 259–266.
Liu SY, Yang CL, Zeng Q, Lv YC et al. 2022e – Biological characteristics and fungicidal control efficacy of the pathogens causing witches' broom of *Phyllostachys violascens*. Mycosystema 41, 1867–1888.
Liu YJ, Whelen S, Hall BD. 1999 – Phylogenetic relationships among ascomycetes: Evidence from an RNA polymerse II subunit. Molecular Biology and Evolution 16, 1799–1808.
Liu YQ, Sun WX, Chen XL, Huang SP et al. 2023a – Leaf spot of *Sanhua plum* caused by *Botryosphaeria wangensis* in China. Plant Disease 107, 2888.
Locquin MV. 1984 – Classification Générale des Mycota. Masson, Paris: Mycologie Générale et Structurale. p 169–175.
Lombard L, Van der Merwe NA, Groenewald JZ, Crous PW. 2015 – Generic concepts in *Nectriaceae*. Studies in Mycology 80, 189–245.
Lu Y, Bian GJ, Ji HL. 2020 – Relationship between seasonal effects of dust retention and leaf characteristics of tree species for road greening. Journal of Forest and Environment 40, 269–275.
Lu ZH, Wanasinghe DN, Madrid H, Maharachchikumbura SSN. 2022 – *Hyphocapnodia sichuanensis* gen. et sp. nov. (*Capnodiaceae*), a novel hyphomycete from Sichuan Province, China. Phytotaxa, 564, 84–94.
Lücking R, Aime MC, Robbertse B, Miller AN et al. 2021 – Fungal taxonomy and sequence-based nomenclature. Nature Microbiology 6, 540–548.
Lumbsch HT, Huhndorf SM. 2010 – Myconet volume 14. Part one. Outline of *Ascomycota* – 2009. Part two. Notes on ascomycete systematics. Nos. 4751–5113. Fieldiana Life and Earth Sciences, 1–64.

Ma XY, Nontachaiyapoom S, Jayawardena RS, Hyde KD et al. 2018 – Endophytic *Colletotrichum* species from *Dendrobium* spp. in China and northern Thailand. MycoKeys 43, 23–57.
Maddison WP, Maddison DR. 2019 – Mesquite: A modular system for evolutionary analysis. Version 3.61. http://www.mesquiteproject.org
Magaña-Dueñas V, Cano-Lira JF, Stchigel AM. 2022 – Novel freshwater ascomycetes from Spain. Journal of Fungi 8, 849.
Magnus P. 1906 – Notwendige Umänderung des Namens derPilzgattung *Marssonia* Fisch. Hedwigia 45, 88–91.
Maharachchikumbura SSN, Chen Y, Ariyawansa HA, Hyde KD et al. 2021 – Integrative approaches for species delimitation in *Ascomycota*. Fungal Diversity 109, 155–179.
Maharachchikumbura SSN, Guo LD, Cai L, Chukeatirote E et al. 2012 – A multi-locus backbone tree for *Pestalotiopsis*, with a polyphasic characterization of 14 new species. Fungal Diversity 56, 95–129.
Maharachchikumbura SSN, Hyde KD, Groenewald JZ, Xu JC et al. 2014 –*Pestalotiopsis* revisited. Studies in Mycology 79, 121–186.
Maharachchikumbura SSN, Hyde KD, Jones EBG, McKenzie EHC et al. 2016b – Families of *Sordariomycetes*. Fungal Diversity 79, 1–317.
Maharachchikumbura SSN, Larignon P, Hyde KD, Al-Sadi AM et al. 2016a – Characterization of *Neopestalotiopsis*, *Pestalotiopsis* and *Truncatella* species associated with grapevine trunk diseases in France. Phytopathologia Mediterranea 55, 380−390.
Malkus A, Song QJ, Cregan P, Arseniuk E et al. 2009 – Genetic linkage map of *Phaeosphaeria nodorum*, the causal agent of stagonospora nodorum blotch disease of wheat. European Journal of Plant Pathology 124, 681–690.
Manawasinghe IS, Calabon MS, Jones EB, Zhang YX et al. 2022 – Mycosphere notes 345–386. Mycosphere 13, 454–557.
Manawasinghe IS, Phillips AJL, Hyde KD, Chethana KWT et al. 2016 – Mycosphere Essays 14: Assessing the aggressiveness of plant pathogenic *Botryosphaeriaceae*. Mycosphere 7, 883–892.
Mani JK, Sharma SK, Singh RAJ, Shekhar C. 2012 – Role of weather parameters on graphiola leaf spot disease incidence of date palm (*Phoenix dactylifera* L.) in South Haryana. Journal of Agrometeorology 14, 117–121.
Mapook A, Hyde KD, McKenzie EHC, Jones EBG et al. 2020 – Taxonomic and phylogenetic contributions to fungi associated with the invasive weed *Chromolaena odorata* (Siam weed). Fungal Diversity 101, 1–175.
Mardones M, Trampe-Jaschik T, Hofmann TA, Mangelsdorff RD et al. 2018 – New neotropical species of *Phyllachorales* based on molecular, morphological, and ecological data. Mycologia 110, 835–859.
Mardones M, Trampe-Jaschik T, Oster S, Elliott M et al. 2017 – Phylogeny of the order *Phyllachorales* (*Ascomycota*, *Sordariomycetes*): Among and within order relationships based on five molecular loci. Persoonia 39, 74–90.
Marin-Felix Y, Groenewald JZ, Cai L, Chen Q et al. 2017 – Genera of phytopathogenic fungi: GOPHY 1. Studies in Mycology 86, 99–216.
Marsberg A, Kemler M, Jami F, Nagel JH et al. 2017 – *Botryosphaeria dothidea*: A latent pathogen of global importance to woody plant health. Molecular Plant Pathology 18, 477–488.
Martin CA, Stabler LB. 2004 – Urban horticultural ecology: Interactions between plants, people and the physical environment. Acta Horticulturae 639, 97–101.
Martinelli F, Scalenghe R, Davino S, Panno S et al. 2015 – Advanced methods of plant disease detection. A review. Agronomy for Sustainable Development 35, 1–25.
Massee, G. 1899 – Tea and coffee diseases. Bulletin of Miscellaneous Informations of the Royal Botanical Gardens Kew. 1899, 89–94.

Mayorquin JS, Wang DH, Twizeyimana M, Eskalen A. 2016 – Identification, distribution, and pathogenicity of *Diatrypaceae* and *Botryosphaeriaceae* associated with citrus branch canker in the southern California desert. Plant Disease 100, 2402–2413.
Meng HG, Wei CX, Qi WZ, Wen CY et al. 2023 – Identification and diversity analysis of fungal pathogen of jujube dry rot in different areas. Journal of Huazhong Agricultural University 42, 108–114.
Miyake I. 1909 – Studies on the parasitic fungi of rice in Japan. Bot Mag Tokyo 23, 85–97.
Mohali SR, Slippers B, Wingfield MJ. 2007 – Identification of *Botryosphaeriaceae* from *Eucalyptus*, *Acacia* and *Pinus* in Venezuela. Fungal Diversity 25, 103–125.
Monkai J, Phookamsak R, Xu S, Mortimer PE et al. 2022 –*Pseudophaeocytostroma bambusicola* gen. et sp. nov. (*Diaporthaceae*) from bamboo in Yunnan, PR China. Phytotaxa 571, 39–51.
Morgan-Jones G, White JF. 1983 – Studies in the genus *Phoma*. III. *Paraphoma*, a new genus to accommodate *Phoma radicina*. Mycotaxon 81, 57–65.
Müller E. 1950 – Die schweizerischen Arten der Gattung *Leptosphaeria* und ihrer Verwandten. Sydowia 4, 185–319.
Munk A. 1953 – The system of the *Pyrenomycetes*. A contribution to avnatural classification of the group *Sphaeriales* sensu Lindau. vDansk Bot Ark 15, 1–163.
Munk A. 1957 – Danish *Pyrenomycetes*. A preliminary flora. Dansk Bot Ark 17, 1–491.
Nakashima C, Motohashi K, Chen CY, Groenewald JZ et al. 2016 – Species diversity of *Pseudocercospora* from Far East Asia. Mycological Progress 15, 1093–1117.
Nannfeldt JA. 1932 – Studien über die Morphologie und Systematik der nichlichenisierten inoperculaten Discomyceten. Nova Acta Regiae Societatis Scientiarum Upsaliensis Series. 4, 1–368.
Nasr S, Lutz M, Amoozegar MA, Eparvier V et al. 2019 – *Graphiola fimbriata*: The first species of *Graphiolaceae* (*Exobasidiales*, *Basidiomycota*) described only based on its yeast stage. Mycological Progress 18, 359–368.
Niessl von Mayendorf G. 1876 – Notizen über neue und kritische Pyrenomyceten. Verhandlungen des Naturforschenden Vereins in Brünn. 14, 165–218.
Nitschke TRJ. 1867 – *Pyrenomycetes* Germanici. Die Kernpilze Deutschlands, Breslau 1.
Nitschke TRJ. 1869 – Grundlage eines systems der Pyrenomyceten. Verhandlungen des Naturhistorischen Vereins der Preussischen Rheinlande. Westfalens und des Regierungsbezirks Osnabrück 26, 70–77.
Norphanphoun C, Gentekaki E, Hongsanan S, Jayawardena R et al. 2022 – *Diaporthe*: Formalizing the species-group concept. Mycosphere 13, 752–819.
Nozawa S, Togawa M, Watanabe K. 2022 – Reidentification of *Pestalotiopsis* sensu lato causing gray blight of tea in Japan. Journal of General Plant Pathology 88, 293–299.
Nylander JAA. 2004 – MrModeltest 2.0. Program distributed by the author. Evolutionary Biology Centre, Uppsala University.
O'Donnell K, Cigelnik E. 1997 – Two divergent intragenomic rDNA ITS2 types within a monophyletic lineage of the fungus *Fusarium* are nonorthologous. Molecular Phylogenetics and Evolution 7, 103–116.
O'Donnell K, Kistler HC, Cigelnik E, Ploetz RC. 1998 – Multiple evolutionary origins of the fungus causing Panama disease of banana: Concordant evidence from nuclear and mitochondrial gene genealogies. The Proceedings of the National Academy of Sciences 95, 2044–2049.
Oberwinkler F. 1982 – The significance of the morphology of the basidium in the phylogeny of basidiomycetes. In Wells K, Wells EK (eds) Basidium and basidiocarp, pp. 9–35. Springer Verlag, New York, Heidelberg, Berlin.
O'Donnell K, Sarver BA, Brandt M, Chang DC et al. 2007 – Phylogenetic diversity and microsphere array-based genotyping of human pathogenic *Fusaria*, including isolates from the multistate contact lens-associated U.S. keratitis outbreaks of 2005 and 2006. Journal of Clinical Microbiology 45, 2235–2248.

Oliveira RJV, Bezerra JL, Lima TEF, Silva GA et al. 2016 – *Phaeosphaeria nodulispora*, a new endophytic coelomycete isolated from tropical palm (*Cocos nucifera*) in Brazil. Nova Hedwigia 103, 185–192.
Pal AK. 2019 – *Graphiola phoenicis* (Mong.) Poit.: An enigmatic parasitic fungus from mangrove palm of Indian Sundarbans. Journal of Mycopathological Research 57, 89–93.
Pan M, Lin L, Tian CM, Fan XL. 2022 – Identification and pathogenicity of six fungal species causing canker and dieback disease on golden rain tree in Beijing, China. Mycology 14, 37–51.
Parbery DG. 1967 – Studies on graminicolous species of *Phyllachora* Nke. in Fckl. V. A taxonomic monograph. Australian Journal of Botany 15, 271–375.
Parbery DG. 1993 – A revision of *Phyllachora* and some similar genera on the host family Leguminosae. Australasian Plant Pathology 22, 111–112.
Pearce CA, Hyde KD. 2001 – Two new genera in the *Phyllachoraceae*: *Sphaerodothella* to accommodate *Sphaerodothis danthoniae*, and *Parberya* gen. nov. Fungal Diversity 6, 83–97.
Pecchia S, Caggiano B, Lio DD, Cafà G et al. 2019 – Molecular detection of the seed-borne pathogen *Colletotrichum lupini* targeting the hyper-variable IGS region of the ribosomal cluster. Plants (Basel) 8, 222.
Pei YG, Tao QJ, Zheng XJ, Li Y et al. 2019 – Phenotypic and genetic characterization of *Botrytis cinerea* population from Kiwifruit in Sichuan Province, China. Plant Disease 103, 748–758.
Pem D, Jeewon R, Chethana KWT, Hongsanan S et al. 2021 – Species concepts of *Dothideomycetes*: Classification, phylogenetic inconsistencies and taxonomic standardization. Fungal Diversity 109, 283–319.
Pem D, Hyde KD, McKenzie EHC, Hongsanan S, et al. 2024 – A comprehensive overview of genera in *Dothideomycetes.* Mycosphere 15, 2175–4568.
Peng C, Crous PW, Jiang N, Fan XL et al. 2022 – Diversity of *Sporocadaceae* (pestalotioid fungi) from *Rosa* in China. Persoonia 49, 201–260.
Peng XJ, Wang QC, Zhang SK, Guo K et al. 2023 – *Colletotrichum* species associated with *Camellia* anthracnose in China. Mycosphere 14, 497–524.
Perera RH, Hyde KD, Jones EBG, Maharachchikumbura SSN et al. 2023 – Profle of *Bionectriaceae*, *Calcarisporiaceae*, *Hypocreaceae*, *Nectriaceae*, *Tilachlidiaceae*, *Ijuhyaceae* fam. nov., *Stromatonectriaceae* fam. nov. and *Xanthonectriaceae* fam. nov. Fungal Diversity 118, 95–271.
Pham NQ, Marincowitz S, Solís M, Duong TA et al. 2021 – *Eucalyptus* scab and shoot malformation: A new and serious foliar disease of *Eucalyptus* caused by *Elsinoe necatrix* sp. nov. Plant Pathology 70, 1230–1242.
Phillips AJL, Alves A, Abdollahzadeh J, Slippers B et al. 2013 – The *Botryosphaeriaceae*: Genera and species known from culture. Studies in Mycology 76, 51–167.
Phookamsak R, Liu JK, McKenzie EHC, Manamgoda DS et al. 2014 – Revision of *Phaeosphaeriaceae*. Fungal Diversity 68, 159–238.
Phukhamsakda C, McKenzie EHC, Phillips AJL, Jones EBG et al. 2020 – Microfungi associated with *Clematis* (*Ranunculaceae*) with an integrated approach to delimiting species boundaries. Fungal Diversity 102, 1–203.
Piepenbring M, Espinoza J, Saldaña L, Cáceres O. 2010 – New records, host plants, morphological and molecular data of *Exobasidiales* (*Basidiomycota*) from Panama. Nova Hedwigia 91, 231–242.
Piepenbring M, Hartmann M, Hofmann TA, Lutz M. 2020 – Two new species in a new genus and a critical revision of *Brachybasidiaceae* (*Exobasidiales*, *Basidiomycota*) in honor of Franz Oberwinkler. Mycological Progress 19, 351–365.
Piepenbring M, Nold F, Trampe T, Kirschner R. 2012 – Revision of the genus *Graphiola* (*Exobasidiales, Basidiomycota*). Nova Hedwigia 94, 67–96.
Poiteau PA. 1824 – Description du *Graphiola*, nouveau genre des plantes parasite de la famille des champignons. Annales des Sciences Naturelles 3, 473–476.

Prasannath K, Galea VJ, Akinsanmi OA. 2023 – Diversity and pathogenicity of species of *Botrytis*, *Cladosporium*, *Neopestalotiopsis* and *Pestalotiopsis* causing flower diseases of macadamia in Australia. Plant Pathology 72, 881–899.
Prasannath K, Shivas RG, Galea VJ, Akinsanmi OA. 2021 – *Neopestalotiopsis* species associated with flower diseases of *Macadamia integrifolia* in Australia. Journal of Fungi 7, 771.
Qiao M, Li J, Fang LL, Li JY. 2021 – Morphology, phylogeny and pathogenicity of *Colletotrichum menglaense* sp. nov., isolated from air in China. Pathogens 10, 1243.
Quaedvlieg W, Verkley GJM, Shin HD, Barreto RW et al. 2013 – Sizing up *Septoria*. Studies in Mycology 75, 307–390.
Raciborski M. 1900 – Batavia, Indonesia, Staatsdruckerei. Parasitische Algen und Pilze Javas 1, 1–39.
Rathnayaka AR, Chethana KWT, Phillips AJL, Liu JK et al. 2023 – Re-evaluating *Botryosphaeriales*: Ancestral state reconstructions of selected characters and evolution of nutritional modes. Journal of Fungi 9, 184.
Razaghi P, Raza M, Han SL, Ma ZY et al. 2024 – *Sporocadaceae* revisited. Studies in Mycology 109, 155–272.
Réblová M, Gams W, Seifert KA. 2011 – *Monilochaetes* and allied genera of the *Glomerellales*, and a reconsideration of families in the *Microascales*. Studies in Mycology 68, 163–191.
Reeb V, Lutzoni F, Roux C. 2004 – Contribution of RPB2 to multilocus phylogenetic studies of the euascomycetes (*Pezizomycotina*, Fungi) with special emphasis on the lichen-forming *Acarosporaceae* and evolution of polyspory. Molecular Phylogenetics and Evolution 32, 1036–1060.
Rehner SA, Buckley E. 2005 – A *Beauveria* phylogeny inferred from nuclear ITS and EF1-α sequences: Evidence for cryptic diversification and links to *Cordyceps* teleomorphs. Mycologia 97, 84–98.
Ren GC, Wanasinghe DN, de Farias ARG, Hyde KD et al. 2022 – Taxonomic novelties of woody litter fungi (*Didymosphaeriaceae*, *Pleosporales*) from the Greater Mekong Subregion. Biology 11, 1660.
Rimpau RH. 1962 – Untersuchungen Über die Gattung *Drepanopeziza* (Kleb.) V. H öhn.) Phytopathologische Zeitschrift 43, 257–306.
Riolo M, Aloi F, Pane A, Cara M et al. 2021 – Twig and shoot dieback of *Citrus*, a new disease caused by *Colletotrichum* species. Cells 10, 449.
Ristaino JB, Anderson PK, Bebber DP, Brauman KA et al. 2021 – The persistent threat of emerging plant disease pandemics to global food security. The Proceedings of the National Academy of Sciences 118, e2022239118.
Rodríguez-Gálvez E, Hilário S, Lopes A, Alves A. 2020 – Diversity and pathogenicity of *Lasiodiplodia* and *Neopestalotiopsis* species associated with stem blight and dieback of blueberry plants in Peru. European Journal of Plant Pathology 157, 89–102.
Rossman AY, Adams GC, Cannon PF, Castlebury LA et al. 2015 – Recommendations of generic names in *Diaporthales* competing for protection or use. IMA Fungus 6, 145–154.
Rossman AY, Allen WC, Castlebury LA, Verkley G et al. 2017 – Three new combinations in *Drepanopeziza* for species on poplar. Mycotaxon 132, 951–955.
Rossman AY, Farr DF, Castlebury LA. 2007 – A review of the phylogeny and biology of the *Diaporthales*. Mycoscience 48, 135–144.
Rossman AY, Samuels GJ, Rogerson CT, Lowen R. 1999 – Genera of *Bionectriaceae*, *Hypocreaceae* and *Nectriaceae* (*Hypocreales*, *Ascomycetes*). Studies in Mycology 42, 1–260.
Rossman AY. 2000 – Towards monophyletic genera in the holomorphic *Hypocreales*. Studies in Mycology 45, 27–34.
Saccardo PA, Trotter A. 1913 – Supplementum Universale Pars IX. Sylloge Fungorum 22, 1–1612.
Saccardo PA. 1883 – Sylloge Fungorum Omnium hucusque cognitorum: Volume 2. Padova, Italy.
Saccardo PA. 1884 – Miscellanea Mycologica I. Atti del Reale Istituto Veneto di Scienze, Lettere ed Arti. sér. 6, 2, 435–450

Samarakoon BC, Phookamsak R, Karunarathna SC, Jeewon R et al. 2021b – New host and geographic records of five pleosporalean hyphomycetes associated with *Musa* spp. (Banana). Studies in Fungi 6, 92–115.
Samarakoon MC, Hyde KD, Maharachchikumbura SSN, Stadler M et al. 2021a – Taxonomy, phylogeny, molecular dating and ancestral state reconstruction of *Xylariomycetidae* (*Sordariomycetes*). Fungal Diversity 112, 1–88.
Samarakoon MC, Hyde KD, Promputtha I, Hongsanan S et al. 2016 – Evolution of Xylariomycetidae (*Ascomycota*: *Sordariomycetes*). Mycosphere 7, 1746–1761.
Samuels GJ, Blackwell M. 2001 – *Pyrenomycetes*: Fungi with perithecia. In: McLaughlin DJ, McLaughlin EG, Lemke PA (eds) The Mycota: A comprehensive treatise on Fungi as experimental systems for basic and applied research, vol VII. Systematics and evolution: Part A. Springer, Berlin, pp 221–255.
Sandoval-Denis M, Gené J, Sutton DA, Wiederhold NP et al. 2016 – New species of *Cladosporium* associated with human and animal infections. Persoonia 36, 281–298.
Sandoval-Denis M, Lombard L, Crous PW. 2019 – Back to the roots: A reappraisal of *Neocosmospora*. Persoonia 43, 90–185.
Sandoval-Denis M, Sutton DA, Martin-Vicente A, Cano-Lira JF et al. 2015 – *Cladosporium* species recovered from clinical samples in the United States. Journal of Clinical Microbiology 53, 2990–3000.
Schoch CL, Crous PW, Groenewald JZ, Boehm EWA et al. 2009 – A class–wide phylogenetic assessment of *Dothideomycetes*. Studies in Mycology 64, 1–15.
Schoch CL, Shoemaker RA, Seifert KA, Hambleton S et al. 2006 – A multigene phylogeny of the *Dothideomycetes* using four nuclear loci. Mycologia 98, 1041–1052.
Schroers HJ, Gräfenhan T, Nirenberg HI, Seifert KA. 2011 – A revision of *Cyanonectria* and *Geejayessia* gen. nov., and related species with *Fusarium*-like anamorphs. Studies in Mycology 68, 115–138.
Schroers HJ, Samuels GJ, Zhang N, Short DPG et al. 2016 – Epitypification of *Fusisporium* (*Fusarium*) *solani* and its assignment to a common phylogenetic species in the *Fusarium solani* species complex. Mycologia 108, 806–819.
Seaver FJ. 1922 – *Phyllostictaceae*. North American Flora 6, 3–84.
Senanayake IC, Crous PW, Groenewald JZ, Maharachchikumbura SSN et al. 2017 – Families of *Diaporthales* based on morphological and phylogenetic evidence. Studies in Mycology 86, 217–296.
Senanayake IC, Jeewon R, Chomnunti P, Wanasinghe DN et al. 2018 – Taxonomic circumscription of *Diaporthales* based on multigene phylogeny and morphology. Fungal Diversity 93, 241–443.
Senanayake IC, Lian TT, Mai XM, Jeewon R et al. 2020 – *Neopestalotiopsis alpapicalis* sp. nov. a new endophyte from tropical mangrove trees in Krabi Province (Thailand). Asian Journal of Mycology 3, 512–533.
Senanayake IC, Maharachchikumbura SSN, Hyde KD, Bhat JD et al. 2015 – Towards unraveling relationships in *Xylariomycetidae* (*Sordariomycetes*). Fungal Diversity 73, 73–144.
Sepúlveda G, Arismendi M, Huanca-Mamani W, Cárdenas-Ninasivincha SC et al. 2017 – Presence of false smut (*Graphiola phoenicis* (Moug. ex Fr.) Poit.) on Canary date palm (*Phoenix canariensis*) on Easter Island, Chile. Ciencia Investigación Agraria 44, 307–311.
Shang QJ, Hyde KD, Camporesi E, Maharachchikumbura SSN et al. 2020 – Additions to the genus *Cytospora* with sexual morph in *Cytosporaceae*. Mycosphere 11, 189–224.
Shibata S, Hirooka Y. 2022 – Taxonomy and phylogeny of *Exobasidium pentasporium* causing witches' broom of *Rhododendron* species. Mycoscience 63, 254–260.
Shibata S, Ono T, Kobayashi Y, Miyagawa I et al. 2021 – First report of horn gall disease of *Cinnamomum pseudopedunculatum* caused by *Laurobasidium hachijoense* in the Bonin Islands, Japan. Journal of General Plant Pathology 87, 322–325.

Silva-Hanlin DMW, Hanlin RT. 1998 – The order *Phyllachorales*: Taxonomic review. Mycoscience 39, 97–104.
Singh A, Singh PN, Nath G, Dubey NK. 2021 – Phylogeny and taxonomy of a novel species of *Pseudocercospora* from India. Turkish Journal of Botany 45, 172–180.
Singh PN, Baghela A, Singh SK, Maurya DK. 2015 – *Exosporium gymnemae* sp. nov. from India. Mycosphere 6, 508–514.
Slippers B, Boissin E, Phillips AJL, Groenewald JZ et al. 2013 – Phylogenetic lineages in the *Botryosphaeriales*: A systematic and evolutionary framework. Studies in Mycology 76, 31–49.
Slippers B, Crous PW, Denman S, Coutinho TA et al. 2004 – Combined multiple gene genealogies and phenotypic characters differentiate several species previously identified as *Botryosphaeria dothidea*. Mycologia 96, 83–101.
Slippers B, Crous PW, Jami F, Groenewald JZ et al. 2017 – Diversity in the *Botryosphaeriales*: Looking back, looking forward. Fungal Biology 121, 307–321.
Solarte F, Muñoz CG, Maharachchikumbura SSN, Álvarez E. 2017 – Diversity of *Neopestalotiopsis* and *Pestalotiopsis* spp., causal agents of guava scab in Colombia. Plant Disease 102, 49–59.
Somrithipol S, Jones EBG, Sommai S, Suetrong S et al. 2018 – *Laurobasidiaceae* fam. nov. (*Exobasidiales*, *Basidiomycota*), a new family for fungi causing galls with aerial root-like outgrowths, with a new record from Thailand of *Laurobasidium hachijoense* on a new host, *Cinnamomum subavenium*. Phytotaxa 347, 150–164.
Sotiropoulos AG, Arango-Isaza E, Ban T, Barbieri C et al. 2022 – Global genomic analyses of wheat powdery mildew reveal association of pathogen spread with historical human migration and trade. Nature Communications 13, 4315.
Species Fungorum 2024 – http://www.speciesfungorum.org/Names/Names.asp. Accessed on November 2024.
Spegazzini C. 1910 – Mycetes Argentinenses (Series V). Anales del Museo Nacional de Historia Natural, Buenos Aires 20, 329–467.
Stamatakis A. 2014 – RAxML version 8: A tool for phylogenetic analysis and post-analysis of large phylogenies. Bioinformatics 30, 1312–1313.
Stanosz GR, Smith DR, Ramsfield TD, McMahon BG et al. 2021 – Response of balsam poplar to inoculation with *Marssonina balsamiferae* from Minnesota, USA. Forest Pathology 51, e12714.
Starbäck K. 1899 – Ascomyceten der ersten Regnellschen Expedition 1. Bihang till Kungliga Svenska Vetenskaps-Akademiens Handlingar 25, 1–68.
Steyaert RL. 1949 – Contributions à l'étude monographique de *Pestalotia* de Not. et *Monochaetia* Sacc. (*Truncatella* gen. nov. et *Pestalotiopsis* gen. nov.). Bulletin du Jardin Botanique de l'État à Bruxelles 19, 285–354.
Strange RN, Scott PR. 2005 – Plant disease: A threat to global food security. Annual Review of Phytopathology 43, 83–116.
Stukenbrock EH, Quaedvlieg W, Javan-Nikhah M, Zala M et al. 2012 – *Zymoseptoria ardabilia* and *Z. pseudotritici*, two progenitor species of the septoria tritici leaf blotch fungus *Z. tritici* (synonym: *Mycosphaerella graminicola*). Mycologia 104, 1397–1407.
Suetrong S, Schoch CL, Spatafora JW, Kohlmeyer J et al. 2009 – Molecular systematics of the marine *Dothideomycetes*. Studies in Mycology 64, 155–173.
Sui XN, Guo MJ, Zhou H, Hou CL. 2023 – Four new species of *Phyllosticta* from China based on morphological and phylogenetic characterization. Mycology 14, 190–203.
Suija A, Ertz D, Lawrey JD, Diederich P. 2014 – Multiple origin of the lichenicolous life habit in *Helotiales*, based on nuclear ribosomal sequences. Fungal Diversity 70, 55–72.
Suija A, Zhurbenko MP, Stepanchikova ISS, Himelbrant DE et al. 2020 – *Kukwaea pubescens* gen. et sp. nova (*Helotiales*, *incertae sedis*), a new lichenicolous fungus on *Cetraria islandica*, and a key to the lichenicolous fungi occurring on *Cetraria* s. str. Phytotaxa 459, 39–50.

Sun DW, Yin GF, Lu WJ, Li CH et al. 2017 – Identification and pathogenicity assessment of oat powdery mildew in Yunnan Province. Journal of Plant Protection 44, 617–622.
Sun YR, Jayawardena RS, Sun JE, Wang Y. 2023 – Pestalotioid species associated with medicinal plants in southwest China and Thailand. Microbiology Spectrum 11, e0398722.
Sung H-J, Park J-H, Lee Y-D, Shin H-D et al. 2022 – *Graphiola phoenicis* associated with false smut on Canary Island date palm (*Phoenix canariensis*) in Korea. Forest Pathology 52, e12781.
Sweet MJ, Bulling MT. 2017 – On the importance of the microbiome and pathobiome in coral health and disease. Frontiers in Marine Science 4, 1−11.
Takamatsu S. 2013 – Origin and evolution of the powdery mildews (*Ascomycota*, *Erysiphales*). Mycoscience 54, 75–86.
Talhinhas P, Baroncelli R. 2021 – *Colletotrichum* species and complexes: geographic distribution, host range and conservation status. Fungal Diversity 110, 109–198.
Tanaka K, Endo M, Hirayama K, Okane I et al. 2011 – Phylogeny of *Discosia* and *Seimatosporium*, and introduction of *Adisciso* and *Immersidiscosia* genera nova. Persoonia 26, 85–98.
Tang JL, Cheng LL, Ye L, Tan GJ. 2024 – Identification, biological characteristics and fungicide sensitivity of pathogens causing wilt disease in *Abelmoschus manihot*. Journal of Nuclear Agricultural Sciences 38, 1416–1423.
Tanney JB, Seifert KA. 2020 – *Mollisiaceae*: An overlooked lineage of diverse endophytes. Studies in Mycology 95, 293–380.
Taylor JW, Jacobson DJ, Kroken S, Kasuga T et al. 2000 – Phylogenetic species recognition and species concepts in fungi. Fungal Genetics and Biology 31, 21–32.
Temperini CV, Pardo AG, Pose GN. 2018 – Diversity of airborne *Cladosporium* species isolated from agricultural environments of northern Argentinean Patagonia: Molecular characterization and plant pathogenicity. Aerobiologia 34, 227–239.
Templeton MD, Rikkerink EHA, Solon SL, Crowhurst RN. 1992 – Cloning and molecular characterization of the glyceraldehyde-3-phosphate dehydrogenase encoding gene and cDNA from the plant pathogenic fungus *Glomerella cingulata*. Gene 122, 225–230.
Tennakoon DS, Kuo C, Maharachchikumbura SSN, Thambugala KM et al. 2021 – Taxonomic and phylogenetic contributions to *Celtis formosana*, *Ficus ampelas*, *F. septica*, *Macaranga tanarius* and *Morus australis* leaf litter inhabiting microfungi. Fungal Diversity 108, 1–215.
Tennakoon DS, Kuo C-H, Purahong W, Gentekaki E et al. 2022a – Fungal community succession on decomposing leaf litter across five phylogenetically related tree species in a subtropical forest. Fungal Diversity 115, 73–103.
Tennakoon DS, Phillips AJL, Phookamsak R, Ariyawansa HA et al. 2016 – Sexual morph of *Lasiodiplodia pseudotheobromae* (*Botryosphaeriaceae*, *Botryosphaeriales*, *Dothideomycetes*) from China. Mycosphere 7, 990–1000.
Tennakoon DS, Thambugala KM, de Silva NI, Suwannarach N et al. 2022b – A taxonomic assessment of novel and remarkable fungal species in *Didymosphaeriaceae* (*Pleosporales, Dothideomycetes*) from plant litter. Frontiers in Microbiology 13, 1016285.
Thambugala KM, Hyde KD, Tanaka K, Tian Q et al. 2015 – Towards a natural classification and backbone tree for *Lophiostomataceae*, *Floricolaceae*, and *Amorosiaceae* fam. nov. Fungal Diversity 74, 199–266.
Theissen VF, Sydow H. 1915 – Die *Dothideales*. Annales Mycologici 13, 149–430.
Theissen VF, Sydow H. 1918 – Vorentwürfe zu den *Pseudosphaeriales*. Annales Mycologici 16, 1–34.
Thompson SM, Tan YP, Shivas RG, Neate SM et al. 2015 – Green and brown bridges between weeds and crops reveal novel *Diaporthe* species in Australia. Persoonia 35, 39–49.
Tibpromma S, Hyde KD, Bhat JD, Mortimer PE et al. 2018 – Identification of endophytic fungi from leaves of *Pandanaceae* based on their morphotypes and DNA sequence data from southern Thailand. MycoKeys 33, 25–67.

Tikami Í, Boufleur TR, Prataviera F, Panciera LG et al. 2023 – Survival of *Colletotrichum truncatum* as microsclerotia in soil. Plant Disease 107, 2460–2466.
Trigiano RN, Windham MT, Windham AS. 2004 – Plant pathology: Concepts and laboratory exercises. Boca Raton: CRC Press. p. 1–600.
Tulasne LR, Tulasne C. 1865 – Selecta Fungorum Carpologia: Nectriei-Phacidiei-Pezizei. 3.
Turland NJ, Wiersema JH, Barrie FR, Greuter W et al. 2018 – International Code of Nomenclature for algae, fungi, and plants (Shenzhen Code) adopted by the Nineteenth International Botanical Congress Shenzhen, China, July 2017. Regnum Vegetabile 159. Glashütten: Koeltz Botanical Book
Udayanga D, Castlebury LA, Rossman AY, Chukeatirote E et al. 2014 – Insights into the genus *Diaporthe*: Phylogenetic species delimitation in the *D. eres* species complex. Fungal Diversity 67, 203–229.
Udayanga D, Castlebury LA, Rossman AY, Chukeatirote E et al. 2015 – The *Diaporthe sojae* species complex: Phylogenetic re-assessment of pathogens associated with soybean, cucurbits and other field crops. Fungal Biology 119, 383–407.
Ujat AH, Ono T, Hattori Y, Nakashima C. 2023 – Re-examination of several *Elsinoë* species reported from Japan. Mycobiology 51, 122–138.
Úrbez-Torres JR, Leavitt GM, Voegel TM, Gubler WD. 2006 – Identification and distribution of Botryosphaeria spp. associated with grapevine cankers in California. Plant Disease 90, 1490–1503.
Vakalounakis DJ, Ntougias S, Kavroulakis N, Protopapadakis E. 2019 – *Neofusicoccum parvum* and *Diaporthe foeniculina* associated with twig and shoot blight and branch canker of citrus in greece. Journal of Phytopathology 167, 527–537.
van der Aa HA, Vanev S. 2002 – A revision of the species described in *Phyllosticta*. Centraalbureau voor Schimmelcultures (CBS), Utrecht, The Netherlands.
van der Aa HA. 1973 – Studies in *Phyllosticta*. Studies in Mycology 5, 1–110.
Verkley GJM, Dukik K, Renfurm R, Göker M et al. 2014 – Novel genera and species of coniothyrium-like fungi in *Montagnulaceae* (*Ascomycota*). Persoonia 32, 25–51.
Verkley GJM, Silva M, Wicklow DT, Crous PW. 2004 – *Paraconiothyrium*, a new genus to accommodate the mycoparasite *Coniothyrium minitans*, anamorphs of *Paraphaeosphaeria*, and four new species. Studies in Mycology 50, 323–335.
Videira SIR, Groenewald JZ, Nakashima C, Braun U et al. 2017 – *Mycosphaerellaceae*: Chaos or clarity? Studies in Mycology 87, 257–421.
Vilgalys R, Hester M. 1990 – Rapid genetic identification and mapping of enzymatically amplified ribosomal DNA from several *Cryptococcus* species. Journal of Bacteriology 172, 4238–4246.
Viswanathan R, Selvakumar R. 2020 – Varietal breakdown to red rot in sugarcane revealed by comparing two *Colletotrichum falcatum* inoculation methods. Sugar Tech 22, 1063–1075.
Voglmayr H, Jaklitsch WM. 2017 – *Corynespora*, *Exosporium* and *Helminthosporium* revisited – New species and generic reclassification. Studies in Mycology 87, 43–76.
Von Arx JA, Müller E. 1975 – A re-evaluation of the bitunicate ascomycetes with keys to families and genera. Studies in Mycology 9, 1–159.
Von Höhnel FXR. 1910 – Fragmente zur Mykologie (Xi Mitteilung, Nr. 527 bis 573) Sitsungsber, Kaiserl. Akad Wiss Math-Naturwiss Cl Abt 1 119, 618–679.
Von Höhnel FXR. 1917 – Über die Benennung Stellung und Nebenfruchtformen von Sphaerella Fries. Berichte der Deutschen Botanischen Gesellschaft 35, 627–631.
Walker DM, Castlebury LA, Rossman AY, Mejía LC et al. 2012 – Phylogeny and taxonomy of *Ophiognomonia* (*Gnomoniaceae*, *Diaporthales*), including twenty-five new species in this highly diverse genus. Fungal Diversity 57, 85–147.
Wan Y, Li DW, Si YZ, Li M et al. 2023 – Three new species of *Diaporthe* causing leaf blight on *Acer palmatum* in China. Plant Disease 107, 849–860.

Wanasinghe DN, Jones EBG, Dissanayake AJ, Hyde KD. 2016 – Saprobic *Dothideomycetes* in Thailand: *Vaginatispora appendiculata* sp. nov. (*Lophiostomataceae*) introduced based on morphological and molecular data. Studies in Fungi 1, 56–68.
Wanasinghe DN, Phukhamsakda C, Hyde KD, Jeewon R et al. 2018 – Fungal diversity notes 709–839: Taxonomic and phylogenetic contributions to fungal taxa with an emphasis on fungi on *Rosaceae*. Fungal Diversity 89, 1–236.
Wang B, Chen G, Li C, Sun W. 2017 – Floral characteristics and pollination ecology of *Manglietia ventii* (*Magnoliaceae*), a plant species with extremely small populations (PSESP) endemic to South Yunnan of China. Plant Diversity 39, 52–59.
Wang CB, Wang TT, Ma CY, Xue H et al. 2023a – *Phyllosticta rizhaoensis* sp. nov. causing leaf blight of *Ophiopogon japonicus* in China. Fungal Systematics and Evolution 11, 43–50.
Wang CB, Yang J, Li Y, Xue H et al. 2023b – Multi-gene phylogeny and morphology of two new *Phyllosticta* (*Phyllostictaceae*, *Botryosphaeriales*) species from China. MycoKeys 95, 189–207.
Wang J, Shen XM, Liu D, Zhang M et al. 2020 – Identification of the pathogens causing anthracnose and determination of the potential infection source of *Photinia* × *fraseri* in Sichuan Province. Journal of Plant Protection 47, 637–646.
Wang K, Liu F, Cai L. 2022b – A name list of common agricultural phytopathogenic fungi in China. Mycosystema 41, 361–386.
Wang LL, Xing Z, Ma JR. 2016 – Analysis on the landscape plant in China during 2005-2014. Forest By-Product and Speciality in China 00, 86–89.
Wang Q, Nai CY. 2004 – Two new species on coelomycetes on *Dimocarpus longan*. Mycosystem 23, 461–463.
Wang SY, Wang Y, Li Y. 2022a – *Cladosporium* spp. (*Cladosporiaceae*) isolated from *Eucommia ulmoides* in China. MycoKeys 91, 151–168.
Wang XY, Li YH, Pu JA, Zhang RY et al. 2023c – Identification of pathogen causing sugarcane brown stripe in Yunnan Province. Acta Phytopathologica Sinica 53, 141–145.
Wang YL, Lu Q, Decock C, Li YX et al. 2015 – *Cytospora* species from *Populus* and *Salix* in China with *C. davidiana* sp. nov. Fungal Biology 119, 420–432.
Warren HL, Nicholson RL. 1975 – Kernel infection, seedling blight, and wilt of maize caused by *Colletotrichum graminicola*. Phytopathology 65, 620–623.
Wehmeyer LE. 1926 – A biologic and phylogenetic study of the stromatic *Sphaeriales*. American Journal of Botany 13, 575–645.
White TJ, Bruns T, Lee S, Taylor J. 1990 – Amplification and direct sequencing of fungal ribosomal RNA genes for phylogenetics. PCR protocols: A guide to methods and applications 18, 315–322.
Wijayawardene NN, Hyde KD, Dai DQ, Sanchez-Garcia M et al. 2022 – Outline of Fungi and fungus-like taxa. Mycosphere 13, 53–453.
Wijesinghe SN, Samarakoon MC, Camporesi E, Hyde KD et al. 2023 – Over the footprints of Italian mycology with emphasis on plant-associated *Ascomycota*. Current Research in Environmental & Applied Mycology (Journal of Fungal Biology) 13, 162–276.
Wikee S, Lombard L, Crous PW, Nakashima C et al. 2013b – *Phyllosticta capitalensis*, a widespread endophyte of plants. Fungal Diversity 60, 91–105.
Wikee S, Lombard L, Nakashima C, Motohashi K et al. 2013a – A phylogenetic re-evaluation of *Phyllosticta* (*Botryosphaeriales*). Studies in Mycology 76, 1–29.
Wikee S, Udayanga D, Crous PW, Chukeatirote E et al. 2011 – *Phyllosticta* – an overview of current status of species recognition. Fungal Diversity 51, 43–61.
Wöhner T, Emeriewen OF. 2019 – Apple blotch disease (*Marssonina coronaria* (Ellis & Davis) Davis) – review and research prospects. European Journal of Plant Pathology 153, 657–669.
Wonglom P, Pornsuriya C, Sunpapao A. 2023 – A new species of *Neoscytalidium hylocereum* sp. nov. causing canker on red-fleshed dragon fruit (*Hylocereus polyrhizus*) in southern Thailand. Journal of Fungi 9, 197.

Worobiec G, Piątek M, Worobiec E. 2023 – *Szaferomyces pliocenicus* nov. gen., nov. sp. from the Upper Pliocene deposits of Mizerna (Poland), a fossil fungus showing close resemblance to modern powdery mildews. Geobios.
Woronichin NN. 1925 – Über die *Capnodiales*. Annales Mycologici 23, 174–178.
Xiao YP, Wang YB, Hyde KD, Eleni G et al. 2023 – *Polycephalomycetaceae*, a new family of clavicipitoid fungi segregates from *Ophiocordycipitaceae*. Fungal Diversity 120, 1–76.
Xu XL, Wang FH, Liu C, Yang HB et al. 2022 – Morphology and phylogeny of ascomycetes associated with walnut trees (*Juglans regia*) in Sichuan Province, China. Frontiers in Microbiology 13, 1016548.
Yadav S, Singh R, Verma SK, Singh G et al. 2023 – Addition of three new lineages in *Mycosphaerellaceae*: *Neoacervuloseptoria* gen. nov., *Neocercosporella* gen. nov. and *Neoramulariopsis* gen. nov. Mycological Progress 22, 1–19.
Yadav S, Verma SK, Singh R, Singh V et al. 2022 – *Neokamalomyces indicus* gen. nov., sp. nov. (*Mycosphaerellaceae*) – *Septoria*-like genus from India. Phytotaxa 571, 141–168.
Yamaguchi Y, Meeboon J, Heluta VP, Liu SY et al. 2021 – Phylogeny and taxonomy of *Erysiphe* species (powdery mildew: *Erysiphaceae*) occurring on the ash trees (*Fraxinus* spp.). Mycoscience 62, 115–123.
Yang CL, Xu XL, Liu YG, Hyde KD et al. 2019b – A new species of *Phyllachora* (*Phyllachoraceae*, *Phyllachorales*) on *Phyllostachys heteroclada* from Sichuan, China. Phytotaxa 392, 186–196.
Yang CL, Xu XL, Wanasinghe DN, Jeewon R et al. 2019a – *Neostagonosporella sichuanensis* gen. et sp. nov. (*Phaeosphaeriaceae*, *Pleosporales*) on *Phyllostachys heteroclada* (*Poaceae*) from Sichuan Province, China. MycoKeys 46, 119–150.
Yang CL, Xu XL, Zeng Q, Liu LJ et al. 2024 – Bambusicolous mycopathogens in China with an update on taxonomic diversity, novel species, pathogenicity, and new insights. Mycosphere 15, 4788–4918.
Yang CL, Xu XL, Zhang ZG, Liu YG. 2017 – *Lirula sichuanensis* sp. nov. on *Picea likiangensis* var. *rubescens* from Sichuan, China. Mycotaxon 132, 839–847.
Yang YQ, Luo WM, Zhang WS, Mridha MAU et al. 2023 – *Cladosporium* species associated with fruit trees in Guizhou Province, China. Journal of Fungi 9, 250.
Zambelli P, Serra I, Fernandez-Arrojo L, Plou FJ et al. 2015 – Sweet-and-salty biocatalysis: Fructooligosaccharides production using *Cladosporium cladosporioides* in seawater. Process Biochemistry 50, 1086–1090.
Zeng Q, Lv YC, Xu XL, Deng Y et al. 2022 – Morpho-molecular characterization of microfungi associated with *Phyllostachys* (*Poaceae*) in Sichuan, China. Journal of Fungi 8, 702.
Zhan JS, Thrall PH, Papaïx J, Xie LH et al. 2015 – Playing on a pathogen's weakness: Using evolution to guide sustainable plant disease control strategies. Annual Review of Phytopathology 53, 19–43.
Zhang N, Castlebury LA, Miller AN, Huhndorf SM et al. 2006 – An overview of the systematics of the *Sordariomycetes* based on four-gene phylogeny. Mycologia 98, 1077–1088.
Zhang Q, Nizamani MM, Feng Y, Yang YQ et al. 2023b – Genome-scale and multi-gene phylogenetic analyses of *Colletotrichum* spp. host preference and associated with medicinal plants. Mycosphere 14, 1–106.
Zhang W, Groenewald JZ, Lombard L, Schumacher RK et al. 2021 – Evaluating species in *Botryosphaeriales*. Persoonia 46, 63–115.
Zhang Y, Crous PW, Schoch CL, Hyde KD. 2012 – *Pleosporales*. Fungal Diversity 53, 1–221.
Zhang YW, Duan TY, Nan ZB. 2018 – First report of leaf blotch caused by *Phaeosphaeria avenaria* on *Leymus chinensis* (Chinese Rye Grass) in China. Plant Disease 102, 1447.
Zhang ZX, Zhang J, Li DH, Xia JW et al. 2023a – Morphological and phylogenetic analyses reveal three new species of *Pestalotiopsis* (*Sporocadaceae*, *Amphisphaeriales*) from Hainan, China. Microorganisms 11, 1627.

Zhao GC, Zhao RL. 2012 – The higher microfungi from forests of Yunnan Province. Yunnan Science and Technology Press p. 1–572.
Zhao LJ, Xiao HJ, Ma XJ, Cheng Q. 2020 – *Elsinoë australis* causing spot anthracnose on poplar in China. Plant Disease 104, 2202–2209.
Zhao P, Crous PW, Hou LW, Duan WJ et al. 2021 – Fungi of quarantine concern for China I: *Dothideomycetes*. Persoonia 47, 45–105.
Zhao P, Liu F, Huang JE, Zhou X et al. 2022 – *Cronartium* rust (*Pucciniales*, *Cronartiaceae*): Species delineation, diversity and host alternation. Mycosphere 13, 672–723.
Zheng F, Jiao C, Xie Y, Li HY. 2022 – A checklist of pathogenic fungi on *Citrus* in China. Mycosystema 41, 387-411.
Zhou YY, Zhang W, Wu LN, Zhang J et al. 2023 – Diversity of fungal communities associated with grapevine trunk diseases in China. Mycosphere 14, 1340–1435.
Zhu YQ, Ma CY, Xue H, Piao CG et al. 2023 – Two new species of *Diaporthe* (*Diaporthaceae*, *Diaporthales*) in China. MycoKeys 95, 209–228.
Zhu ZX, Chen QB. 2020 – The research system and application of ornamental bamboo forests on human physiological and psychological response. Journal of Bamboo Research 39, 38–45.
Zhurbenko M. 2008 – *Lichenochora thorii* (*Phyllachorales*), a new lichenicolous ascomycete from Europe. Nova Hedwigia 87, 509–512.
Zlatković M, Keča N, Wingfield MJ, Jami F et al. 2016 – *Botryosphaeriaceae* associated with the die-back of ornamental trees in the Western Balkans. Antonie van Leeuwenhoek 109, 543–564.